

Principal Investigator Microgravity Services (PIMS)

**STS-107 Microgravity Environment
Summary Report**

January - February 2003

Microgravity Environment Program

Glenn Research Center

Kenol Jules
NASA Glenn Research Center

Kenneth Hrovat
ZIN Technologies, Inc.

Eric Kelly
ZIN Technologies, Inc.

Timothy Reckart
ZIN Technologies, Inc.

National Aeronautics and Space Administration
Glenn Research Center
Cleveland, Ohio



Principal Investigator Microgravity Services (PIMS)

STS-107 Microgravity Environment Summary Report

January - February 2003

Microgravity Environment Program

Glenn Research Center

Kenol Jules
NASA Glenn Research Center

Kenneth Hrovat (Vibratory Data Analysis)
ZIN Technologies, Inc.

Eric Kelly
ZIN Technologies, Inc.

Timothy Reckart
ZIN Technologies, Inc.

National Aeronautics and Space Administration
Glenn Research Center
Cleveland, Ohio



**PIMS STS-107 Mission Microgravity Environment Summary Report:
January 16 to February 1, 2003**

Table of Contents

Table of Contents	ii
List of Tables	iii
List of Figures	iii
Acknowledgements	1
Contribution	1
In Memoriam	2
Abstract	3
1 Introduction	3
2 STS-107 Mission Overview	5
2.1 Crew and Team Make-up	5
2.2 STS-107 Experiments Complement	6
3 Coordinate Systems	13
4 Acceleration Measurement System Description for STS-107	15
4.1 Orbital Acceleration Research Experiment (OARE)	15
4.2 Space Acceleration Measurement System Free Flyer (SAMS-FF)	16
5 STS-107 Experiments Support Provided by PIMS	20
5.1 Combustion Module-2 Facility Background	21
5.2 Laminar Soot Processes-2 (LSP-2)	22
5.2.1 Previous LSP-1 Results	22
5.3 Structure of Flame Balls at Low Lewis-number-2 (SOFBALL-2) Experiment	23
5.4 Water Mist Fire Suppression Experiment (MIST)	24
5.5 Mechanics of Granular Materials	25
6 Columbia Reduced Gravity Environment Description (STS-107)	27
6.1 Quasi-Steady Microgravity Environment	27
6.1.1 OARE Bias Measurements	28
6.1.2 Experiment Operations	29
6.1.2.1 Structure of Flame Balls at Low Lewis-Number (SOFBALL)	30
6.2 Vibratory Microgravity Environment	52
6.2.1 Experiment Operations	52
6.2.1.1 Enhanced Orbiter Refrigerator/Freezer (EORF)	52
6.2.1.2 Structure of Flame Balls at Low Lewis-Number	53
6.2.1.3 Water Mist Fire-Suppression Experiment (Mist)	56
6.2.1.4 Laminar Soot Processes (LSP)	57
6.2.1.5 Vapor Compression Distillation (VCD)	58
6.2.1.6 Biobox	60
6.2.1.7 Mechanics of Granular Materials (MGM)	60
6.2.2 Vehicle Operations	61
6.2.2.1 Ku-Band Antenna Dither	61
6.2.2.2 Thruster Firings	62
6.2.3 Crew Exercise	62
6.2.4 Principal Component Spectral Analysis (PCSA)	63
7 Summary of the STS-107 Mission Analysis	159

**PIMS STS-107 Mission Microgravity Environment Summary Report:
January 16 to February 1, 2003**

8	References.....	160
9	Appendix A. Acronym List and Definition	162

List of Tables

Table 2.1	Crew and Team Make-up	6
Table 2.2	STS-107 Master Experiment List (2).....	6
Table 3.1	Comparison of coordinate systems.....	13
Table 4.1	OARE Sensor Head Location and Orientation.....	16
Table 4.2	SAMS Sensor Head Locations and Orientations.....	17
Table 5.1	Principal Investigator Teams Support Requirements for the STS-107 Mission.....	20
Table 6.1	OARE and Experiment Locations	28
Table 6.2	Valid C-Range Bias Measurements.....	28
Table 6.3	C-Range Bias Fitted Values.....	29
Table 6.4	Comparison of -ZLV/-XVV Attitudes Flown on USMP-4 and STS-107.....	29
Table 6.5	Quasi-steady Vector at CM-2 Location for SOFBALL Test Points.....	30
Table 6.6	Leaky Integration of SAMS-FF For SOFBALL Test Points.....	54
Table 6.7	Leaky Integration of SAMS-FF For Mist Test Points	56
Table 6.8	Acceleration During LSP Test Points.....	58
Table 6.9	Leaky Integration of SAMS-FF For LSP Test Points.....	58
Table 6.10	ESTIMATE OF VCD Operations timeline	59
Table 6.11	VCD Operations timeline Inferred from Vibratory Measurements.....	60
Table 6.12	MGM Experiment Times.....	61
Table 6.13	MGM Interval Min/Max Results	61
Table 6.14	Crew Exercise Legend For Figure 6.115	63

List of Figures

Figure 2.1A	STS-107 SPACEHAB Research Double Module Configuration Rev-C (Bulkhead Locations)	10
Figure 2.1B	STS-107 SPACEHAB Research Double Module Configuration Rev-C (Rack Locations)	11
Figure 2.1C	SPACEHAB Research Double Module Layout and SAMS-FF locations	12
Figure 3.1	Orbiter Structural Coordinate System	14
Figure 3.2	Orbiter Body Coordinate System	14
Figure 4.1	Red Oval Showing the Location of the OARE Inside the Orbiter	18
Figure 4.2A	Location of the SAMS-FF Heads Inside The SPACEHAB — Forward Bulkhead Location	19
Figure 4.2B	Location of the SAMS-FF Heads Inside The SPACEHAB — Aft Bulkhead Location	19
Figure 5.1	Detail of the Combustion Module-2 (CM-2) Facility	26
Figure 6.1	OARE Acceleration Data Collected during the STS-107 Mission	32
Figure 6.2	SAMS-FF, TSH_11, Acceleration Data Collected during the STS-107 Mission	32
Figure 6.3	Valid C-Range Bias Measurements and Curve Fits	33

**PIMS STS-107 Mission Microgravity Environment Summary Report:
January 16 to February 1, 2003**

Figure 6.4 Time Series for –ZLV/-XVV Attitude during STS-107 Mission.....	34
Figure 6.5 Time Series for –ZLV/-XVV Attitude during USMP-4 Mission.....	35
Figure 6.6 Time Series for Gravity Gradient Transition and Free Drift.....	36
Figure 6.7 RSS for Maneuver to Gravity Gradient Attitude.....	37
Figure 6.8 Time Series for SOFBALL Test Point 14A	38
Figure 6.9 Time Series for SOFBALL Test Points 02A, 02B and 02C.....	39
Figure 6.10 Time Series for SOFBALL Test Points 08A and 08B	40
Figure 6.11 Time Series for SOFBALL Test Points 05A, 05B and 05M.....	41
Figure 6.12 Time Series for SOFBALL Test Point 09A	42
Figure 6.13 Time Series for SOFBALL Test Points 12A and 12B	43
Figure 6.14 Time Series for SOFBALL Test Points 06A, 06B, 06C and 06D.....	44
Figure 6.15 Time Series for SOFBALL Test Points 10A and 10B	45
Figure 6.16 Time Series for SOFBALL Test Points 10M, 10N and 10O	46
Figure 6.17 Time Series for SOFBALL Test Points 04A, 04B and 04C.....	47
Figure 6.18 Time Series for SOFBALL Test Points 07A and 07B	48
Figure 6.19 Time Series for SOFBALL Test Point 07C and 07D.....	49
Figure 6.20 Time Series for SOFBALL Test Points 14M and 14N	50
Figure 6.21 Time Series for SOFBALL Test Point 13A	51
Figure 6.22 Spectrogram Of EORF	64
Figure 6.23 Interval RMS Of EORF	65
Figure 6.24 Interval RMS Of Unknown Narrowband Above 25 Hz.....	66
Figure 6.25 Leaky Integration For SOFBALL Test Point 14A	67
Figure 6.26 Leaky Integration For SOFBALL Test Point 02A.....	68
Figure 6.27 Leaky Integration For SOFBALL Test Point 02B (02A Reburn).....	69
Figure 6.28 Leaky Integration For SOFBALL Test Point 02C (02B Reburn).....	70
Figure 6.29 Leaky Integration For SOFBALL Test Point 03A.....	71
Figure 6.30 Leaky Integration For SOFBALL Test Point 08A.....	72
Figure 6.31 Leaky Integration For SOFBALL Test Point 08B.....	73
Figure 6.32 Leaky Integration For SOFBALL Test Point 05A.....	74
Figure 6.33 Leaky Integration For SOFBALL Test Point 05B.....	75
Figure 6.34 Leaky Integration For SOFBALL Test Point 05M.....	76
Figure 6.35 Leaky Integration For SOFBALL Test Point 09A.....	77
Figure 6.36 Leaky Integration For SOFBALL Test Point 09B (09A Reburn).....	78
Figure 6.37 Leaky Integration For SOFBALL Test Point 12A.....	79
Figure 6.38 Leaky Integration For SOFBALL Test Point 12B.....	80
Figure 6.39 Leaky Integration For SOFBALL Test Point 06A.....	81
Figure 6.40 Leaky Integration For SOFBALL Test Point 06B.....	82
Figure 6.41 Leaky Integration For SOFBALL Test Point 06C.....	83
Figure 6.42 Leaky Integration For SOFBALL Test Point 06D.....	84
Figure 6.43 Leaky Integration For SOFBALL Test Point 11B.....	85
Figure 6.44 Leaky Integration For SOFBALL Test Point 11C.....	86
Figure 6.45 Leaky Integration For SOFBALL Test Point 10B.....	87
Figure 6.46 Leaky Integration For SOFBALL Test Point 10C.....	88
Figure 6.47 Leaky Integration For SOFBALL Test Point 10M.....	89

**PIMS STS-107 Mission Microgravity Environment Summary Report:
January 16 to February 1, 2003**

Figure 6.48 Leaky Integration For SOFBALL Test Point 10N	90
Figure 6.49 Leaky Integration For SOFBALL Test Point 10O	91
Figure 6.50 Leaky Integration For SOFBALL Test Point 04A	92
Figure 6.51 Leaky Integration For SOFBALL Test Point 04B	93
Figure 6.52 Leaky Integration For SOFBALL Test Point 04C	94
Figure 6.53 Leaky Integration For SOFBALL Test Point 07C	95
Figure 6.54 Leaky Integration For SOFBALL Test Point 07D	96
Figure 6.55 Leaky Integration For SOFBALL Test Point 14M	97
Figure 6.56 Leaky Integration For SOFBALL Test Point 14N	98
Figure 6.57 Leaky Integration For SOFBALL Test Point 13A (1 of 4)	99
Figure 6.58 Leaky Integration For SOFBALL Test Point 13A (2 of 4)	100
Figure 6.59 Leaky Integration For SOFBALL Test Point 13A (3 of 4)	101
Figure 6.60 Leaky Integration For SOFBALL Test Point 13A (4 of 4)	102
Figure 6.61 Leaky Integration For Transition Out Of Free Drift	103
Figure 6.62 Leaky Integration Of Thruster Firings For Mist Test Point 10 - 68M	104
Figure 6.63 Acceleration Magnitude Of Thruster Firings For Mist Test Point 10 - 68M	105
Figure 6.64 Cumulative RMS vs. Frequency Free Drift Comparison	106
Figure 6.65 Leaky Integration For Mist Test Point 1-61M	107
Figure 6.66 Leaky Integration For Mist Test Point 2-22M	108
Figure 6.67 Leaky Integration For Mist Test Point 3-23M	109
Figure 6.68 Leaky Integration For Mist Test Point 4-24M	110
Figure 6.69 Leaky Integration For Mist Test Point 8-01M	111
Figure 6.70 Leaky Integration For Mist Test Point 11-69M	112
Figure 6.71 Leaky Integration For Mist Test Point 13-30M	113
Figure 6.72 Leaky Integration For Mist Test Point 16-76M	114
Figure 6.73 Leaky Integration For Mist Test Point 17-41M	115
Figure 6.74 Leaky Integration For Mist Test Point 20-44M	116
Figure 6.75 Leaky Integration For Mist Test Point 22-05M	117
Figure 6.76 Leaky Integration For Mist Test Point 23-49aM	118
Figure 6.77 Leaky Integration For Mist Test Point 24-95M	119
Figure 6.78 Leaky Integration For Mist Test Point 25-97M	120
Figure 6.79 Leaky Integration For Mist Test Point 28-80M	121
Figure 6.80 Leaky Integration For Mist Test Point 29-10M	122
Figure 6.81 Leaky Integration For Mist Test Point 30-50M	123
Figure 6.82 Leaky Integration For Mist Test Point 32-49cM	124
Figure 6.83 Excerpt of As-Flown Timeline for Mist Test Point 12-34M	125
Figure 6.84 Excerpt of As-Flown Timeline for Mist Test Point 19-02M	126
Figure 6.85 Time Series For LSP Test Point 41e	127
Figure 6.86 Time Series For LSP Test Point 04e	128
Figure 6.87 Time Series For LSP Test Point 08p	129
Figure 6.88 Time Series For LSP Test Point 53e	130
Figure 6.89 Leaky Integration For LSP Test Point 41e	131
Figure 6.90 Leaky Integration For LSP Test Point 04e	132
Figure 6.91 Leaky Integration For LSP Test Point 08p	133

**PIMS STS-107 Mission Microgravity Environment Summary Report:
January 16 to February 1, 2003**

Figure 6.92 Leaky Integration For LSP Test Point 53e	134
Figure 6.93 Vapor Compression Distillation Flight Experiment (VCD FE) Facility	135
Figure 6.94 Spectrogram of VCD Spinning Up	136
Figure 6.95 Spectrogram of VCD Equipment On/Off	137
Figure 6.96 Spectrogram of VCD Equipment Operation Turn On	138
Figure 6.97 Spectrogram of VCD Equipment Operation Turn Off	139
Figure 6.98 Spectrogram of VCD Equipment Operation Turn On	140
Figure 6.99 Spectrogram of VCD Equipment Operation Turn Off	141
Figure 6.100 Spectrogram of VCD Equipment Operation On/Off	142
Figure 6.101 Spectrogram of VCD Equipment Operation Turn On	143
Figure 6.102 Spectrogram of VCD Equipment Operation Turn Off	144
Figure 6.103 Spectrogram of VCD Equipment Operation On/Off	145
Figure 6.104 Spectrogram of Weak VCD Equipment Fundamental On/Off	146
Figure 6.105 Principal Component Spectral Analysis for Biobox	147
Figure 6.106 Interval Min/Max for MGM Experiment 04-D2	148
Figure 6.107 Interval Min/Max for MGM Experiment 05-D3	149
Figure 6.108 Interval Min/Max for MGM Experiment 06-D4	150
Figure 6.109 Interval Min/Max for MGM Experiment 09-D5	151
Figure 6.110 Interval Min/Max for MGM Experiment 10-D6	152
Figure 6.111 Interval RMS of Ku-Band Antenna Dither	153
Figure 6.112 Spectrogram of 24-Hour Span with Crew Exercise Periods	154
Figure 6.113 Spectrogram of 8-Hour Span with Crew Exercise Periods	155
Figure 6.114 Interval RMS of 24-Hour Span with Crew Exercise Periods	156
Figure 6.115 Cumulative RMS vs. Frequency Of Crew Exercise Periods In 24-Hour Span	157
Figure 6.116 Principal Component Spectral Analysis	158

**PIMS STS-107 Mission Microgravity Environment Summary Report:
January 16 to February 1, 2003**

Acknowledgements

The authors would like to acknowledge the following people who contributed significantly to this report. Without their contribution, this report would have not been possible: Eugene Liberman, ZIN Technologies, developed the Principal Investigator Microgravity Services (PIMS) real-time processing and display software; Kate McGinnis, ZIN Technologies, for the SAMS-FF integration engineering support that she provided before the mission as well as for her on console support at the Johnson Space Center (NASA JSC) Payload Operation Control Center (POCC) throughout the 16-day mission; Nissim Lugasy, ZIN Technologies, for his OARE on console support at the NASA Glenn Research Center during the mission.

A special thanks to Gregory Fedor, ZIN Technologies, for his flight and ground software development for SAMS-FF. Greg also proved valuable with his diligence in monitoring the SAMS-FF data flow and kept the PIMS team informed of the need for relatively frequent software resets, which were beyond his control, throughout the 16-day mission at the JSC POCC.

The authors would like to acknowledge a number of people who provided a lot of support for the functioning of the OARE system before and during the mission: Ronald J. Sicker (NASA Glenn), William M. Foster (NASA Glenn), Thomas J. Kacpura and Nissim Lugasy, ZIN Technologies, Frank Moreno (NASA JSC), Henry Yee (Science Applications International Corporation), John Scott (NASA MSFC) and the entire INCO staff. Finally, the authors would like to acknowledge the support of Kevin McPherson, formerly NASA PIMS Project Manager, before, during and after the mission.

Contribution

The following people provided material for this report. Their contribution is herein acknowledged: Paul D. Ronney (SOFBALL), Susan Batiste (MGM) and Angel Abbud-Madrid (*Mist*).

**PIMS STS-107 Mission Microgravity Environment Summary Report:
January 16 to February 1, 2003**

In Memoriam

This report is dedicated to the hard work and to the memory of the seven crew members of the STS-107 mission who gave their lives doing what they like doing the most: Science and Exploration!

Rick D. Husband, *Commander*
William C. McCool, *Pilot*
Michael P. Anderson, *Mission Specialist*
Kalpana Chawla (KC), *Mission Specialist*
David Brown, *Mission Specialist*
Laurel Blair Salton Clark, *Mission Specialist*
Ilan Ramon, *Payload Specialist*



**PIMS STS-107 Mission Microgravity Environment Summary Report:
January 16 to February 1, 2003**

Abstract

This summary report presents the results of the processed acceleration data measured aboard the Columbia orbiter during the STS-107 microgravity mission from January 16 to February 1, 2003. Two accelerometer systems were used to measure the acceleration levels due to vehicle and science operations activities that took place during the 16-day mission. Due to lack of precise timeline information regarding some payload's operations, not all of the activities were analyzed for this report. However, a general characterization of the microgravity environment of the Columbia Space Shuttle during the 16-day mission is presented followed by a more specific characterization of the environment for some designated payloads during their operations. Some specific quasi-steady and vibratory microgravity environment characterization analyses were performed for the following payloads: Structure of Flame Balls at Low Lewis-number-2, Laminar Soot Processes-2, Mechanics of Granular Materials-3 and Water Mist Fire-Suppression Experiment.

The Physical Science Division of the National Aeronautics and Space Administration sponsors the Orbital Acceleration Research Experiment and the Space Acceleration Measurement System for Free Flyer to support microgravity science experiments, which require microgravity acceleration measurements. On January 16, 2003, both the Orbital Acceleration Research Experiment and the Space Acceleration Measurement System for Free Flyer accelerometer systems were launched on the Columbia Space Transportation System-107 from the Kennedy Space Center. The Orbital Acceleration Research Experiment supported science experiments requiring quasi-steady acceleration measurements, while the Space Acceleration Measurement System for Free Flyer unit supported experiments requiring vibratory acceleration measurement.

The Columbia reduced gravity environment analysis presented in this report uses acceleration data collected by these two sets of accelerometer systems:

1. The Orbital Acceleration Research Experiment is a low frequency sensor, which measures acceleration up to 1 Hz, but the 1 Hz acceleration data is trimmean filtered to yield much lower frequency acceleration data up to 0.01 Hz. This filtered data can be mapped to other locations for characterizing the quasi-steady environment for payloads and the vehicle.
2. The Space Acceleration Measurement System for Free Flyer measures vibratory acceleration in the range of 0.01 to 200 Hz at multiple measurement locations. The vibratory acceleration data measured by this system is used to assess the local vibratory environment for payloads as well as to measure the disturbance causes by the vehicle systems, crew exercise devices and payloads operation disturbances.

This summary report presents analysis of selected quasi-steady and vibratory activities measured by these two accelerometers during the Columbia 16-day microgravity mission from January 16 to February 1, 2003.

**PIMS STS-107 Mission Microgravity Environment Summary Report:
January 16 to February 1, 2003**

1 Introduction

The orbiter Columbia was launched on January 16, 2003 at 9:39 AM Central Standard Time (CST) from launch pad 39A of the Kennedy Space Center (KSC) for a 16-day microgravity mission known as Space Transportation System (STS)-107. The mission was a dual shift mission, meaning that the seven-member crew was divided into two groups. Each group supported a 12-hour shift working on the many experiments that were to be performed during the 16-day mission. The residual acceleration environment of an orbiting spacecraft in a low earth orbit is a complex phenomenon [1]. Many factors, such as experiment operation, life-support systems, crew activities, aerodynamic drag, gravity gradient, rotational effects and the vehicle structural resonance frequencies (structural modes) contribute to form the overall reduced gravity environment. Zero gravity is an ideal state, which cannot be achieved in practice because of the various sources of acceleration present in an orbiting spacecraft. As a result, the environment in which experiments are conducted is *not zero* gravity. Most experiments can be adversely affected by the residual acceleration because of their dependency on acceleration magnitude, frequency, orientation and duration. Therefore, experimenters must know what the environment was when their experiments were performed in order to analyze and correctly interpret the result of their experimental data. In a terrestrial laboratory, where gravity is assumed a constant, researchers are expected to know and record certain parameters such as pressure, temperature, and humidity levels in their laboratory prior to and possibly throughout their experiment. The same holds true in space, where acceleration effects emerge as an important consideration.

In order to assist the Principal Investigators (PIs) correlate their experimental results with the microgravity acceleration environment provided by the STS-107 during the 16-day mission, the National Aeronautics and Space Administration (NASA) Office of Biological and Physical Research sponsors two microgravity accelerometer systems: the Space Acceleration Measurement System for Free Flyer (SAMS-FF) and the Orbital Acceleration Research Experiment (OARE). SAMS-FF measures vibratory acceleration data in the range of 0.01 to 200 Hz for experiments that are sensitive to the vibratory regime, while OARE measures the quasi-steady acceleration data from 0.01 Hz and below for experiments that are sensitive to low frequency accelerations.

The NASA Glenn Research Center (GRC) Principal Investigator Microgravity Services (PIMS) project had the responsibility to process, analyze and interpret the SAMS-FF acceleration data in real time at the NASA Johnson Space Center (JSC) payload center in order to support the PIs during their science operations. Also, PIMS supported the PIs by providing the OARE acceleration data in near real time for their science operations decision making. Finally, PIMS was responsible for archiving the acceleration measurements, analyzing these measurements, and characterizing the reduced gravity environment in which the experiments were conducted. This report presents to the microgravity scientific community the results of some of the analyses performed by PIMS using the acceleration data measured by the two accelerometer systems that flew on the STS-107 mission during the period of January 16 to February 1, 2003 aboard the orbiter Columbia. The PIMS project is funded by the NASA Headquarters and is part of the NASA GRC's Microgravity Environment Program (MEP).

**PIMS STS-107 Mission Microgravity Environment Summary Report:
January 16 to February 1, 2003**

2 STS-107 Mission Overview

The STS-107 mission was launched on January 16, 2003 at 9:39AM CST from the KSC, pad 39A, aboard the Space Shuttle Columbia. The Space Shuttle mission STS-107, the 28th flight of the space shuttle Columbia and the 113th shuttle mission to date, gave more than 70 international scientists access to both the microgravity environment of space and seven dedicated astronaut researchers for 16 uninterrupted days [2]. Columbia's 16-day mission was dedicated to a mixed complement of competitively selected and commercially sponsored research in the space, life and physical sciences. An international crew of seven worked 24 hours a day in two alternating shifts to perform all the experiments assigned to the mission.

The mission carried out aboard the orbiter Columbia was the first flight of the SPACEHAB Research Double Module (RDM). The RDM provided a pressurized environment that was accessible to the crew while in orbit via a tunnel from the shuttle's middeck. The RDM, which has a payload capacity of 9,000 pounds, carried about 7,500 pounds of research payloads on STS-107. An additional 800 pounds of SPACEHAB integrated payloads flew on the shuttle middeck, making a total of 8,300 pounds of research payloads on STS-107 [2]. The middeck and the RDM accommodated the majority of the mission's payloads or experiments. The experiments in the RDM include nine commercial payloads involving 21 separate investigations, four payloads for the European Space Agency (ESA) with 14 investigations, one payload for the International Space Station (ISS) risk mitigation and 18 payloads supporting 23 investigations for NASA's Office of Biology and Physical Research (OBPR) [2]. The NASA's OBPR was the primary sponsor for the mission and was responsible for 30 investigations in four major divisions: Bioastronautics research, Fundamental Space Biology, Physical Sciences and Space Product Development [2]. In addition, the STS-107 carried experiments for NASA's Office of Earth Science, the European Space Agency, the commercial sectors sponsored by SPACEHAB, the U.S Air Force and other parties [3]. In summary, the primary payloads for the STS-107 mission were the SPACEHAB RDM and the Fast Reaction Experiments Enabling Science, Technology, Applications and Research (FREESTAR) external payload located in the Columbia's payload bay.

The crew successfully performed all of the experiments that flew on the mission. Unfortunately, the seven-member crew and the space shuttle Columbia were lost during reentry on the morning of February 1, 2003 due to a breach in the thermal protection system on the leading edge of the left wing, caused by a piece of insulating foam from the external tank that struck the wing during the orbiter ascent from KSC.

2.1 Crew and Team Make-up

Astronaut Rick Husband was the commander of the STS-107 mission and he was joined on Columbia's flight deck by pilot William "Willie" McCool. Mission Specialist 1 was David Brown, Mission Specialist 2 was Kalpana Chawla, Mission Specialist 3 was Michael Anderson (Payload Commander), Mission Specialist 4 was Laurel Clark and Payload Specialist was Ilan Ramon as shown in Table 2.1 below.

**PIMS STS-107 Mission Microgravity Environment Summary Report:
January 16 to February 1, 2003**

TABLE 2.1 CREW AND TEAM MAKE-UP

Crewmember	Position	Team
Rick D. Husband	Commander	Red
William C. McCool (Willie)	Pilot	Blue
David M. Brown	Mission Specialist 1	Blue
Kalpana Chawla (KC)	Mission Specialist 2	Red
Michael P. Anderson	Mission Specialist 3 (Payload Commander)	Blue
Laurel B. Clark	Mission Specialist 4	Red
Ilan Ramom	Payload Specialist	Red

2.2 STS-107 Experiments Complement

The seven crewmembers worked in two shifts throughout their 16 days in space. The seven astronauts were divided into two teams: Red and Blue. The Red team was composed of Husband, Chawla, Clark and Ramon, while the Blue team was made of McCool, Brown and Anderson. The seven astronauts worked round-the-clock to complete a multidisciplinary research program involving 32 payloads with 59 separate investigations [2]. Table 2.2 shows a list of the experiments performed during the STS-107 mission while Figures 2.1A to 2.1C show the lay-out and the locations of the payloads inside the SPACEHAB RDM during the STS-107 mission.

TABLE 2.2 STS-107 MASTER EXPERIMENT LIST (2)

Biology
Biological
Cardiovascular/cardiopulmonary
Effects of Microgravity on Total Peripheral Vascular Resistance in Humans, Peter Norsk, M.D., Ph.D., DAMEC Research, Copenhagen, Denmark, ESA
Arterial Baroreflex Control of Sinus Node during Exercise in Microgravity Conditions, Fernando Iellamo, M.D, Univ, of Rome Tor Vergata, Rome, Italy, ESA
Influence of Weightlessness on Heart Rate & Blood Pressure Regulation— Responses to Exercise & Valsalva Maneuver, Uwe Hoffmann, Ph.D., Deutsche Sport Hochschule, Cologne, Germany, ESA
Physiological Parameters that Predict Orthostatic Intolerance After Spaceflight, John Karemaker, Ph.D., Univ, of Amsterdam, Amsterdam, Netherlands, ESA
Initial Effects of Microgravity on Central Cardiovascular Variables in Humans, Regitze Videbaek, M.D., Univ, Hospital Copenhagen, Copenhagen, Denmark, ESA
Adaptation of Spontaneous Baroreflex Sensitivity to Microgravity, Marco Di Rienzo, Ph.D., Centro di Bioingegneria LaRC, Milano, Italy, ESA
Arterial Remodeling and Functional Adaptations Induced by Microgravity, Michael Delp, Ph.D., Texas A&M University, College Station, TX, NASA
Gravito-inertial sensitivity
Development of Gravity Sensitive Plant Cells in Microgravity, Fred D, Sack, Ph.D., OH State Univ., Columbus, OH, NASA
CEBAS, Fish Otolith Growth and Development of Otolith Asymmetry at Microgravity, H, Rahmann and R, Anken, Univ, of Stuttgart-Hohenheim, Stuttgart, Germany, DLR
Spatial Reorientation Following Spaceflight, William Paloski, Ph.D., NASA Johnson Space Center, Houston, TX, NASA
Anatomical Studies of Central Vestibular Adaptation, Gay R, Holstein, Ph.D., Mt, Sinai Medical Center, New York, NY, NASA
Application of Physical & Biological Techniques to study the Gravisensing and Response System of Plants, Karl H, Hasenstein, Ph.D., University of Louisiana - Lafayette, Lafayette, LA, NASA

**PIMS STS-107 Mission Microgravity Environment Summary Report:
January 16 to February 1, 2003**

TABLE 2.2 STS-107 MASTER EXPERIMENT LIST [2] (continued)

Musculo-skeletal
Cardiopulmonary & Muscular Adaptations During & After Microgravity, Dag Linnarsson, M.D., Ph.D., Karolinska Institute, Stockholm, Sweden, ESA
The Role of Bone Cells in the Response of Skeletal Tissues in Microgravity, J.P. Velduijzen, ACTA Vrije University, Amsterdam, The Netherlands, ESA
Function of the Focal Adhesion of Plaque of Connective Tissue in Microgravity, Ch.-M. Lapiere and A. Kholti, University of Liege, Liege, Belgium, ESA
Protein Turnover During Spaceflight, Arny Ferrando, Ph.D., Univ. of TX Medical Branch/Shriners Burns Institute, Galveston, TX, NASA
Calcium Kinetics During Spaceflight, Scott M. Smith, Ph.D., NASA Johnson Space Center, Houston, TX, NASA
Comparative Analysis of Osteoblastic (bone-forming) Cells at Microgravity and 1G, C. Alexandre, Paris, Paris, France, ESA
Microgravity Effects on Osteoclast (bone-removing) Driven Resorption in vitro, A. Zallone, Bari, Bari, Italy, ESA
Osteoblasts in Space, Dr. L. Vico, Mr. A. Guignandon, LBBTO, St. Etienne, France, ESA
Osteoclasts in Space, Prof. A. Zallone, Dr. Mori, Univ. of Bari, Bari, Italy, ESA
Identification of Microgravity-Related Genes in Osteoblastic Cells, R. Bouillon, Leuven, Leuven, Italy, ESA
Osteoporosis Experiment in Orbit, Dennis R. Sindrey, NPS Allelix, Mississauga, Ont., Canada, CSA
Osteoporosis Experiment in Orbit, Dr. Leticia G. Rao, St. Michael's Hospital, Toronto, Ont., Canada, CSA
Osteoporosis Experiment in Orbit, Dr. Reginald M. Gorczynski & Dr. Harvey Moldofsky, University Health Network, Toronto, Ont., Canada, CSA
Stress responses, homeostasis and integrative physiology/Educational
Ant Colony, students, G.W. Fowler High School, Syracuse, NY, Syracuse University, plus local corporate sponsors
Spiders in Space, students, Glen Waverley Secondary College, Royal Melbourne Institute of Technology, Royal Melbourne Zoo, Melbourne, Australia, RMIT, RMZ
Carpenter Bees In Space, students, Form 4a, Liechtensteinisches Gymnasium, Vaduz, Liechtenstein, Liechtensteinische VP Bank
Flight of the Medaka Fish, Maki Nihori (biology student), Ochanomizu University, Tokyo, Japan, Japan Space Utilization Promotion Center (JSUP)
Silkworm Lifecycle During Space Flight, students (initiator: 5th grade student Li Taotao), Jingshan School, Beijing, China, China Time Network Co, Ltd.
Stress responses, homeostasis and integrative physiology
Multiparametric Assessment of the Stress Response in Astronauts During Spaceflight, Massimo Pagani, M.D., Ph.D., University of Milan, Milan, Italy, ESA
Bacterial Physiology and Virulence on Earth and in Microgravity, Barry H. Pyle, Ph.D., Montana State University, Bozeman, MT, NASA
Biotechnology Cell Science Payload (Bioreactor), Leland Cheung, Emory University, Atlanta, GA, NASA
Determination of the Space Influence on Bacterial Growth Kinetics, J. van der Waarde, Bioclear B.V., University of Gronigen, Gronigen, The Netherlands, ESA
CEBAS, Immunological Investigations with <i>Xiphiphorus helleri</i> , R. Goerlich, Univ. of Dusseldorf, Dusseldorf, Germany, DLR
CEBAS, Plant Physiological Experiments with <i>Ceratophyllum demersum</i> , H. Levine, Dynamac Corp., Kennedy Space Center, FL, DLR
CEBAS, Reproductive Biological and Embryological Research in <i>Xiphiphorus helleri</i> , V. Bluem, Ruhr University, Bochum, Germany, DLR
Pharmacokinetics & Contributing Physiologic Changes During Spaceflight, Lakshmi Putcha, Ph.D., NASA Johnson Space Center, Houston, TX, NASA
Renal Stone Risk During Spaceflight: Assessment and Countermeasure Validation, Peggy A. Whitson, Ph.D., NASA Johnson Space Center, Houston, TX, NASA
Flight Induced Changes in Immune Defenses, Duane Pierson, Ph.D., NASA Johnson Space Center, Houston, TX, NASA
Spaceflight Effects on Fungal Growth, Metabolism, and Sensitivity to Antifungal Drugs, Michael R. McGinnis, Ph.D., Univ. of TX Medical Branch, Galveston, TX, NASA

**PIMS STS-107 Mission Microgravity Environment Summary Report:
January 16 to February 1, 2003**

TABLE 2.2 STS-107 MASTER EXPERIMENT LIST [2] (continued)

Sleep-Wake Actigraphy and Light Exposure During Spaceflight, Charles A. Czeisler, Ph.D., M.D., Brigham and Women's Hospital, Harvard Medical School, Cambridge, Mass., NASA
Choroidal Regulation Involved in the Cerebral Fluid Response to Altered Gravity, Jacquelin Gabrion, Ph.D., Institut des Neurosciences, Centre National de Recherche Scientifique, Paris, France, CNES
Incidence of Latent Virus Shedding During Spaceflight, Duane Pierson, Ph.D., NASA Johnson Space Center, Houston, TX, NASA
Effects of Microgravity on Microbial Physiology, Randolph W. Schweickart, Ph.D., ICOS Corp., Bothell, WA, NASA
Role of Interleukin-2 Receptor in Signal Transduction and Gravisensing Threshold in T-Lymphocytes, A. Cogoli, ETH, Zurich, Switzerland, ESA
Biological Dosimetry in Space Using Haemopoetic Stem Cell Functions, P.v. Oostveldt & A. Poffijn, Gent, Gent, Belgium, ESA
Fidelity of DNA Double-Strand Break Repair in Human Cells Under Microgravity, J. Kiefer, University of Giessen, Giessen, Germany, ESA
Bone Marrow Stromal Cells Differentiation and Mesenchymal Tissue Reconstruction in Microgravity, R. Cancedda, University of Genova, Genova, Italy, ESA
Yeast Cell Stress Under Microgravity, I. Walther, ETH, Zurich, Switzerland, ESA
Support systems
Ergometer & Advanced Respiratory Monitoring System, ESA EOR/F, Enhanced Orbiter Refrigerator/Freezer, NASA Johnson Space Center, Houston, TX, NASA
Thermoelectric Holding Module, NASA Johnson Space Center, Houston, TX, NASA
Earth and Space Sciences
Atmospheric
Mediterranean Isreali Dust Experiment, Joachim H. Joseph, Ph.D., Tel Aviv Univ., Tel Aviv, Israel, NASA
Shuttle Ionospheric Modification with Pulsed Local Exhaust Experiment, USA, Space Test Program, Kirtland AFB, Albuquerque, NM, USAF
Shuttle Ozone Limb Sounding Experiment, Dr. Ernest Hilsenrath and Dr. Richard McPeters, NASA Goddard Space Flight Center, Greenbelt, MD, USA, NASA
Solar
Solar Constant Experiment, Dr. Alexandre Joukoff, Royal Meteorological Institute of Belgium, Brussels, Belgium, NASA
Physical Sciences
Crystallography and Molecular Structure/Educational
The Chemical Garden, 35 @ 8th-grade students, ORT Kiryat Motzkin Middle School (teacher: Dr. Birnbaum), Technion University (Prof. Eliezer Kolodne), Kiryat Motzkin, Israel, Technion University, Haifa
Crystallography and Molecular Structure
Advanced Protein Crystallization Facility, Crystal Structure Analysis of the Outer Surface Glycoprotein of the Hyperthermophile Methanothermus Fervidus, J.P. Declercq, University of Louvain, Louvain, Belgium, ESA
Crystallization of Enzyme and Substrate-Analog Complexes for Highest Resolution Data Collection and Refinement, C. Betzel, University of Hamburg, Hamburg, Germany, ESA
Crystallization of Photosystem I under Microgravity, P. Fromme, University of Berlin, Berlin, Germany, ESA
Effect of Different Conditions on the Quality of Thaumatin and AspartyltRNA Synthetase Crystals Grown in Microgravity, R. Giege & N. Lorber, Institut de Biologie Moleculaire et Cellulaire du CNRS, Paris, France, ESA
Solution Flows and Molecular Disorder of Protein Crystals Growth of Ferritin Crystals, S. Weinkauff, University of Munich, Munich, Germany, ESA
Testing New Trends in Microgravity Protein Crystallization: Comparison of Long Chambers With and Without Capillaries, J.M. Garcia-Ruiz & S. Weinkauff, University of Granada & University of Munich, Granda & Munich, Spain & Germany, ESA
Testing New Trends in Microgravity Protein Crystallisation: Solution Flows and Molecular Disorder of Protein Crystals - Growth of High-quality Crystals and Motions of Lumazine Crystals, J.M. Garcia-Ruiz & S. Weinkauff, University of Granada & University of Munich, Granda & Munich, Spain & Germany, ESA
X-Ray Crystallography at Atomic Resolution, Molecular Mechanism of Ca/Mg Exchange with the EF-Hand Parvalbumin, J.P. Declercq, Univeristy of Louvain, Louvain, Belgium, ESA
Physical processes
Critical Viscosity of Xenon-2, Robert F. Berg, Ph.D., National Institute of Standards and Technology, Gaithersburg, MD, NASA

**PIMS STS-107 Mission Microgravity Environment Summary Report:
January 16 to February 1, 2003**

TABLE 2.2 STS-107 MASTER EXPERIMENT LIST [2] (continued)

Adsorption Dynamics and Transfer at Liquid/liquid Interfaces, L. Liggieri, ICFAM-CNR, Genova, Italy, ESA
Dilational Properties of Interfaces, R. Miller +2, MPI-KG, Berlin, Germany, ESA
Interfacial Rheology and the Effects of Vibrations on Interfacial Properties, G. Loglio +2, UFIR-DCO & IROE-CNR, Firenze, Italy, ESA
Laminar Soot Processes, G.M. Faeth, Ph.D., Univ. of Michigan, Ann Arbor, MI, NASA
Mechanics of Granular Materials, Stein Sture, Ph.D., Dept. of Civil, Environmental and Architectural Engineering, Univ. of Colorado at Boulder, Boulder, Colorado, NASA
Structure of Flame Balls at Low Lewis-number, Paul D. Ronney, Ph.D., University of Southern CA, Los Angeles, CA, NASA
Support systems
SAMS-FF, Space Acceleration Measurement System Free Flyer, Kenol Jules and Ronald J. Sicker, NASA Glenn Research Center. Cleveland, OH, NASA OARE, Orbiter Acceleration Research Experiment, Kenol Jules and Ronald J. Sicker, NASA Glenn Research Center. Cleveland, OH, NASA
Space Product Development
Biological processes
Astroculture™ 10/2, Gene Transfer Experiment, Dr. Weija Zhou, Wisconsin Center for Space Automation and Robotics, College of Engineering, Univ. of Wisconsin, Madison, Madison, WI, NASA
Crystallography and Molecular Structure
Commercial ITA Biological Experiments-2, Bence Jones Protein Crystal Growth Project, Dr. Allen Edmundson, Oklahoma Medical Research Foundation, Oklahoma City, OK, NASA
Commercial ITA Biological Experiments-2, Urokinase Protein Crystal Growth Project, ITA, Instrumentation Technology Associates, Inc., Exton, PA, NASA
Commercial Macromolecular Protein Crystal Growth, L. DeLucas, Ph.D., University of AL-Birmingham and seven others, Birmingham, AL, NASA
Commercial Protein Crystal Growth-Protein Crystal Facility, Larry DeLucas, Ph.D., Center for Biophysical Sciences and Engineering (CBSE), University of AL-Birmingham, Birmingham, AL, NASA
Drug Delivery
Commercial ITA Biological Experiments-2, Microencapsulation of Drugs, Dr. Denis Morrison, NASA Johnson Space Center, Institute for Research, Inc., and ITA Inc., Houston, TX, and Exton, PA, NASA
Physical processes
Water Mist Fire-Suppression Experiment, J. Thomas McKinnon, Ph.D., Center for Commercial Applications of Combustion in Space (CCACS), Colorado School of Mines, Golden, Colorado, NASA
Zeolite Crystal Growth Furnace, Albert Sacco, Ph.D., Center for Advanced Microgravity Materials Processing (CAMMP), Northeastern Univ., Boston, MA, NASA
Technology Development
Attitude Control
Star Navigation, Texas A&M University, College Station, TX, CSCE / SPACEHAB
Communications
Low Power Transmitter, NASA Goddard Space Flight Center, Greebelt, MD, NASA
Miniature Satellite Threat Reporting System, Patrick Serna, Air Force Research Laboratory, Albuquerque, NM, U.S. Air Force
Educational
Space Experiment Module, 11 elementary and middle schools, Houston, TX, NASA
Environmental control, VCD, Vapor Compression Distillation Flight Experiment, NASA Johnson Space Center, Houston, TX, NASA
Combined Two-Phase Loop Experiment, Reinhard Schlitt, OHB, GmBH, Bremen, Germany, ESA
Satellite sensor calibration
Ram Burn Observation, USAF Space and Missile Center, Los Angeles, CA, U.S. Air Force

PIMS STS-107 Mission Microgravity Environment Summary Report: January 16 to February 1, 2003

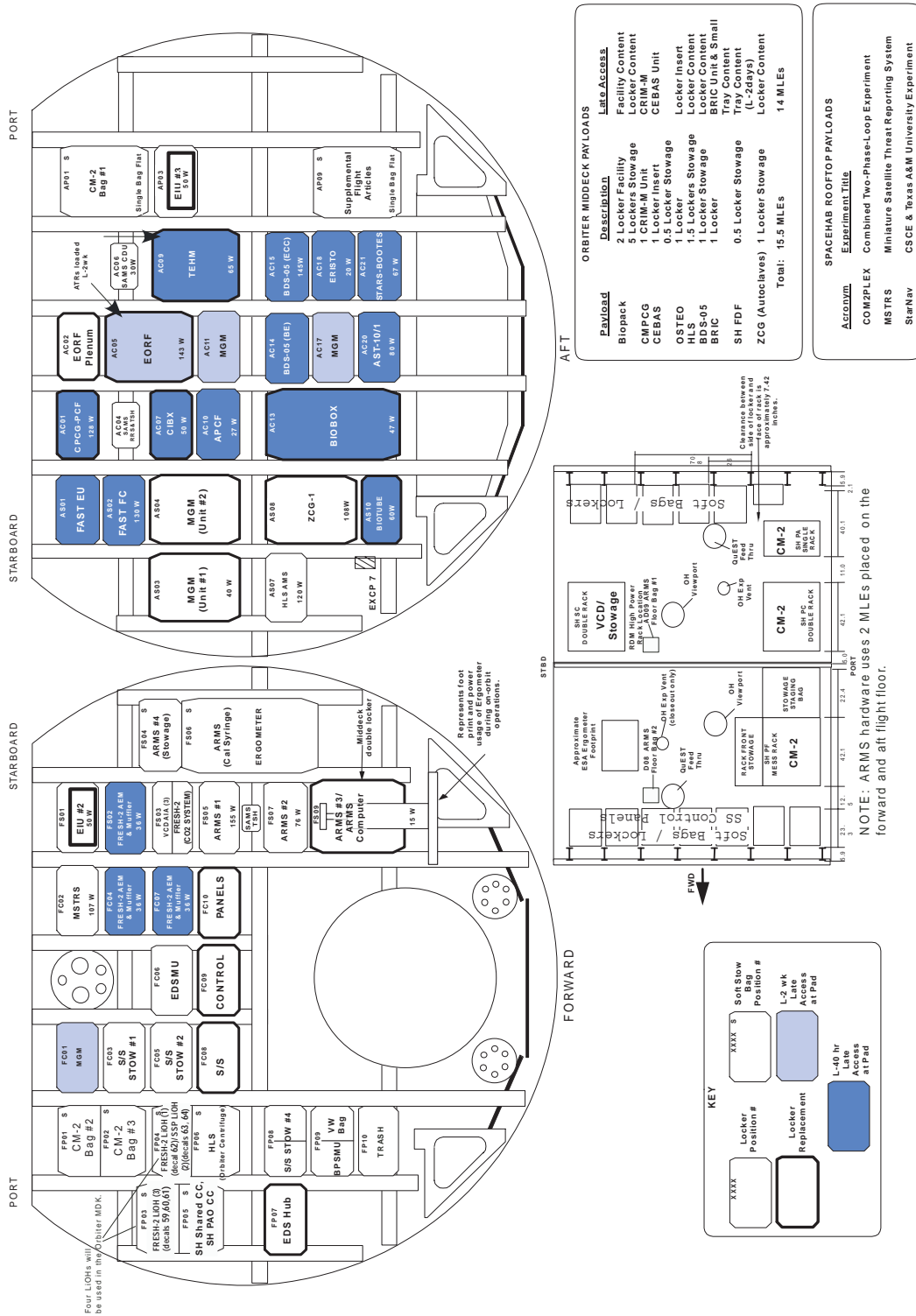


Figure 2.1A STS-107 SPACEHAB Research Double Module Configuration Rev-C (Bulkhead Locations)

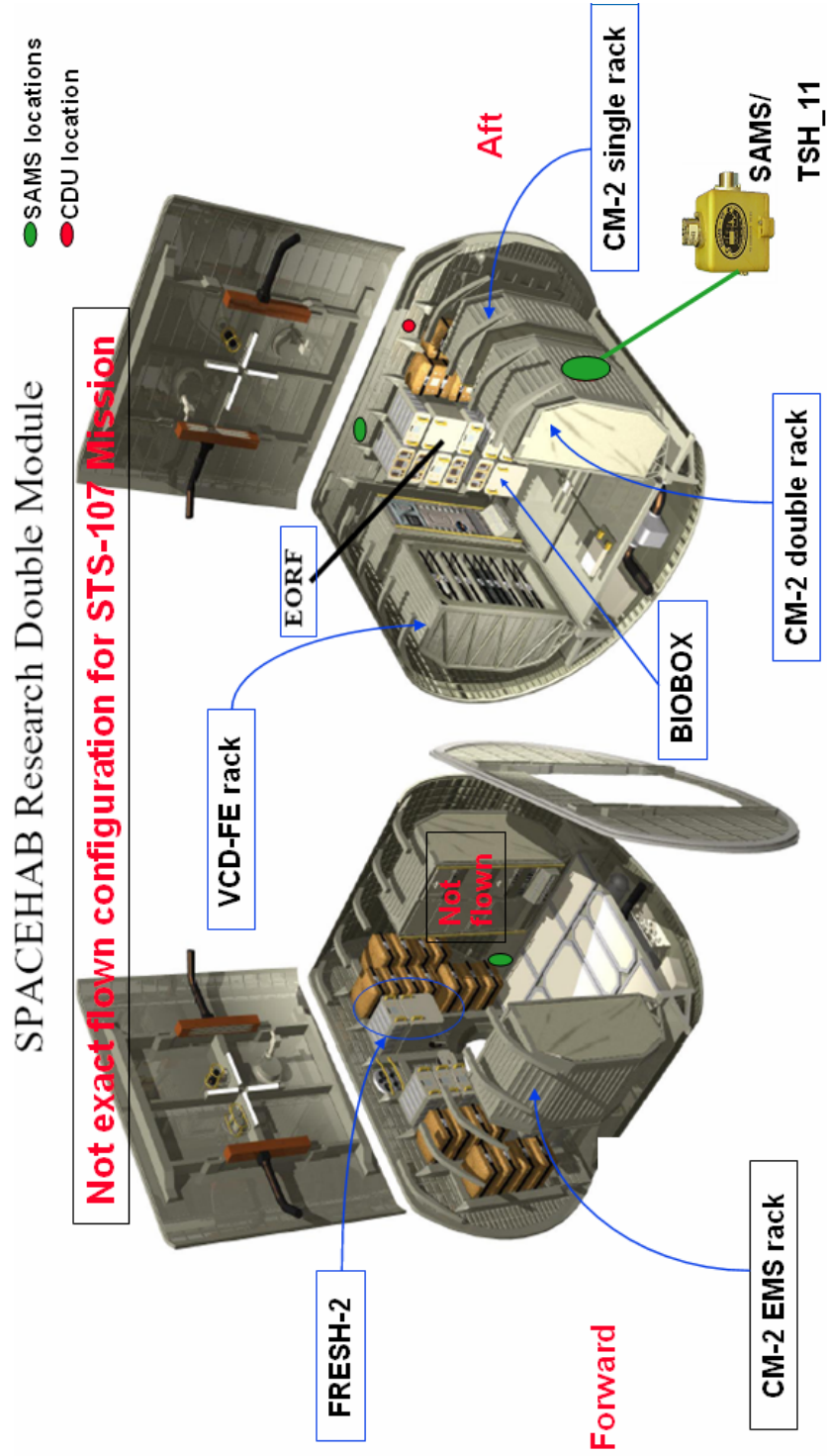


Figure 2.1C SPACEHAB Research Double Module Layout and SAMS-FF locations

**PIMS STS-107 Mission Microgravity Environment Summary Report:
January 16 to February 1, 2003**

3 Coordinate Systems

Four coordinate systems are discussed in this report: Columbia’s structural and body, OARE sensor and SAMS-FF sensor. In the Orbiter Columbia’s structural coordinate system (X_o , Y_o , Z_o), the direction from nose to tail of the Orbiter is $+X_o$, the direction from port wing to starboard wing is $+Y_o$, and the direction from the Orbiter belly to the top of the Orbiter fuselage is $+Z_o$. The origin of this coordinate system is at the tip of the external fuel tank, as illustrated in Figure 3.1. This coordinate system is usually used to specify the location of equipment inside the Orbiter [4].

In the Orbiter body coordinate system (X_b , Y_b , Z_b), the direction from tail to nose of the Orbiter is $+X_b$, the direction from port wing to starboard wing is $+Y_b$, and the direction from the top of the fuselage to the Orbiter belly is $+Z_b$. The origin of this coordinate system is at the Orbiter’s center of gravity, and is typically used as the navigational reference frame. The Orbiter body coordinate system is shown in Figure 3.2 [4].

In the OARE coordinate system (X_{OARE} , Y_{OARE} , Z_{OARE}), the direction from tail to nose of the Orbiter is $+X_{OARE}$, the direction from the Orbiter belly to the top of the Orbiter fuselage is $+Y_{OARE}$, and the direction from port wing to starboard wing is $+Z_{OARE}$. The origin of the OARE coordinate system is at the OARE sensor proofmass centroid. A description of the OARE accelerometer is given in section 4.

The SAMS-FF sensor coordinate system is specific for each sensor head. This results in three possible coordinate systems for the SAMS-FF data. SAMS-FF sensor head notation is denoted with a capital axis, a subscript “h” (to denote head), and a two-digit number to denote to which sensor head reference is made.

Table 3.1 shows a compilation of the various coordinate systems. For this report only one SAMS-FF (Triaxial Sensor Head-(TSH) Head 11) coordinate system will be used along with the OARE and the Orbiter coordinate systems because all of the data collected for the other two SAMS-FF TSH heads was lost during the Columbia accident.

TABLE 3.1 COMPARISON OF COORDINATE SYSTEMS

Orbiter Structural	Orbiter Body	OARE Sensor	SAMS-FF TSH Head 11	SAMS-FF TSH Head 12	SAMS-FF TSH Head 13
$+ X_o$	$- X_b$	$- X_{OARE}$	$- Z_{h11}$	$+ X_{h12}$	$- X_{h13}$
$+ Y_o$	$+ Y_b$	$+ Z_{OARE}$	$- X_{h11}$	$+ Z_{h12}$	$+ Y_{h13}$
$+ Z_o$	$- Z_b$	$+ Y_{OARE}$	$- Y_{h11}$	$+ Y_{h12}$	$+ Z_{h13}$

**PIMS STS-107 Mission Microgravity Environment Summary Report:
January 16 to February 1, 2003**

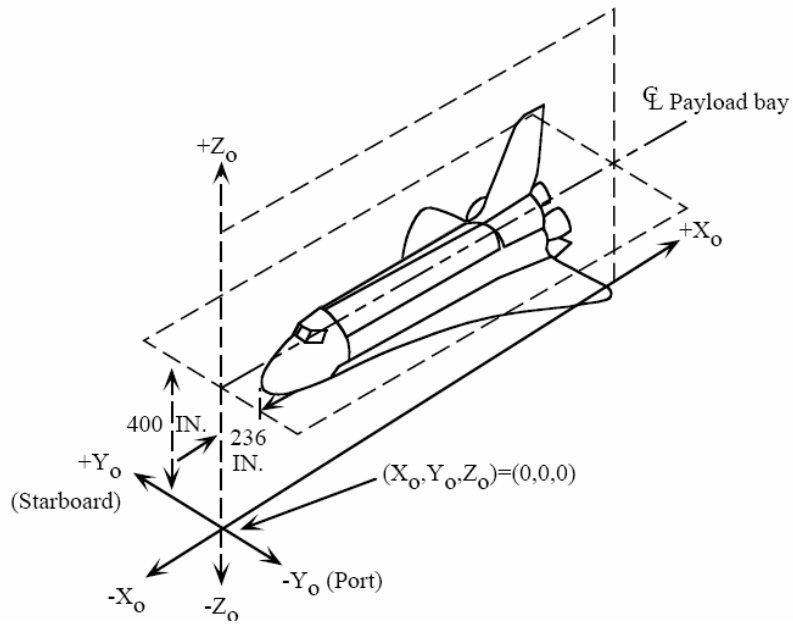


Figure 3.1 Orbiter Structural Coordinate System

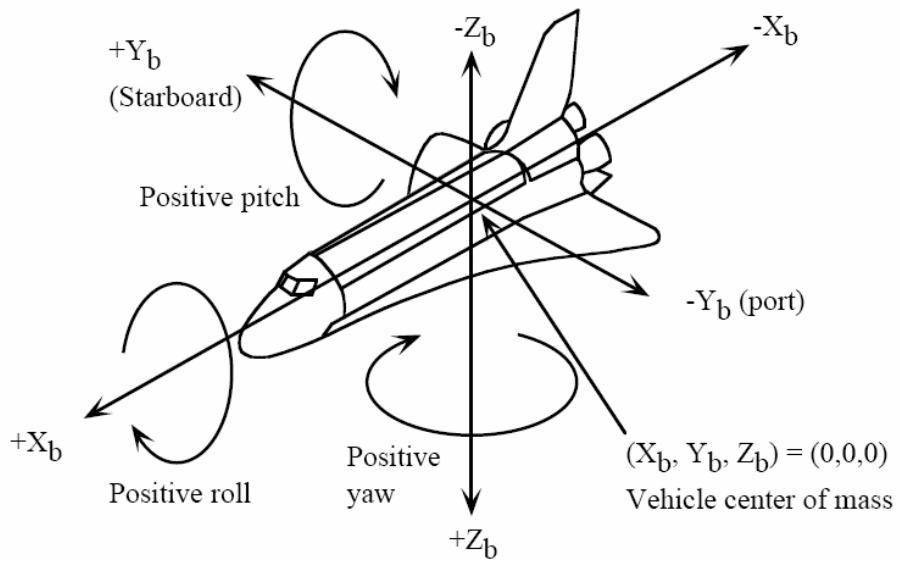


Figure 3.2 Orbiter Body Coordinate System

**PIMS STS-107 Mission Microgravity Environment Summary Report:
January 16 to February 1, 2003**

4 Acceleration Measurement System Description for STS-107

One of the major goals of a microgravity science mission is to provide a quiescent reduced gravity environment to perform fundamental scientific research. However, small disturbances aboard the Orbiter impact the overall environment in which experiments are being performed. Such small disturbances need to be measured in order to assess their potential impact on experiments.

Two accelerometer systems measured the microgravity and vibration environment of the Orbiter Columbia during the STS-107 mission: OARE and the SAMS-FF.

4.1 Orbital Acceleration Research Experiment (OARE)

The OARE contains a tri-axial accelerometer which uses a single free-floating (non-pendulous) electrostatically suspended cylindrical proofmass. The accelerometer sensor assembly is mounted on a dual-gimbal platform which is controlled by a microprocessor in order to perform in-flight calibrations [5]. The sensor's output acceleration signal was filtered using a Bessel filter with a cutoff frequency of 1 Hz for the X_{OARE} axis, and 0.1 Hz for the Y_{OARE} and Z_{OARE} axes. The output signal was discretized at 10 samples per second. The data was processed and digitally filtered with an adaptive trimmean filter (TMF) prior to electronic storage onboard the instrument. Simultaneously, the unprocessed (raw) data was recorded on the Orbiter's Payload Data Recorder (PDR) and routed to the SPACEHAB High Rate Multiplexer (HRM). Using the HRM interface, the unprocessed OARE data was downlinked from the Orbiter, and sent to the Marshall Space Flight Center (MSFC), where the data was made available to the PIMS analyst from a server after reverse playback of the PDR data packets was done by MSFC in order to correctly resequence the data packets. The PIMS analyst at the GRC processed the OARE data and then made it available on the PIMS' web site for the PIs located at the JSC Payload Operation Control Center (POCC) to retrieve the OARE acceleration data in near real time (that is soon after the data was downlinked from the Orbiter's PDR) for correlation with their science data.

OARE's objectives for the STS-107 mission were to measure the quasi-steady accelerations, to make high resolution low-frequency acceleration measurements in support of the microgravity community, and to measure Orbiter aerodynamic performance on orbit. There are several features that make the OARE well suited for making highly accurate, low-frequency acceleration measurements. OARE is a high resolution, high accuracy accelerometer flight design which has the capability to perform both bias and scale factor calibrations on orbit. Another design feature is the OARE sensor electrostatic suspension which has much less bias temperature sensitivity than pendulous accelerometers. Given the nature of the OARE sensor and its in-flight calibration capability, OARE has the ability to characterize the low-frequency environment of the Orbiter with better than 10 nano-g resolution and approximately 50 nano-g on-orbit accuracy [5].

**PIMS STS-107 Mission Microgravity Environment Summary Report:
January 16 to February 1, 2003**

The OARE accelerometer was in a power on configuration, soon after Columbia's orbit insertion, throughout the 16-day STS-107 mission. However, the Columbia's PDR was operated in an on/off mode because there were limited Ku band communication windows available for downlink and many of the experiments needed to use the Ku band communication for their science data downlink. Therefore, the PDR was turned on only when an experiment that needed OARE in "near real time" was operating. And once the Ku band became available, usually soon after the test point was finished, the OARE data recorded on the PDR was downlinked for processing and analysis.

The OARE accelerometer was mounted to the floor of Columbia's cargo bay (bay 11) on a keel bridge, close to the Orbiter's center of gravity. The location and orientation of the sensor with respect to the Orbiter structural coordinate system are given in Table 3.1 and Table 4.1 and shown graphically in Figure 4.1. In this report, the OARE data are presented in Orbiter body coordinates.

TABLE 4.1 OARE SENSOR HEAD LOCATION AND ORIENTATION

Sensor: OARE		Sampling Rate: 10 samples/second
Location: Orbiter Cargo Bay Keel Bridge (bay 11)		Frequency : 1 Hz
ORIENTATION		LOCATION
Orbiter Structural Axis	Sensor Axis	Structural Coordinates
X_o	$-X_{OARE}$	$X_o = 1153.32$ in
Y_o	$+Z_{OARE}$	$Y_o = -1.32$ in
Z_o	$+Y_{OARE}$	$Z_o = 317.76$ in

4.2 Space Acceleration Measurement System Free Flyer (SAMS-FF)

The primary means for microgravity scientists to learn how the vibratory environment of the Columbia STS-107 is affecting their research is from the SAMS-FF. SAMS-FF was provided by the Microgravity Environment Program (MEP) at the NASA Glenn Research Center. The MEP produces a variety of microgravity measurement hardware for on-orbit spacecraft (the *International Space Station (ISS)* and the Space Shuttle) and ground-based flights (drop towers, parabolic aircraft, and sounding rockets). The various SAMS (SAMS, SAMS-FF, and SAMS-II) have supported 22 shuttle missions, the Mir space station, and provide long-term support on the ISS. For the STS-107 mission, the SAMS-FF accelerometer system was used. STS-107 is the second Shuttle microgravity mission supported by SAMS-FF. SAMS-FF uses industrial grade components to provide a flexible, modular system that is easily customized for each particular mission [2].

The SAMS-FF configuration used to support the STS-107 mission consisted of a control and data acquisition unit (CDU), three remote acceleration sensor heads, and a fiber optic gyroscope (FOG). The CDU is similar to a desktop computer packaged to meet the rigors of spaceflight. It controls the operation from the ground and processes data from the sensors through a telemetry data stream, which is monitored via a computer display at the JSC POCC during the mission.

**PIMS STS-107 Mission Microgravity Environment Summary Report:
January 16 to February 1, 2003**

This allowed experimenters to have access to the measured data in near real time during the mission. The SAMS-FF TSH head that downlinked acceleration data in real time at the JSC POCC consisted of data recorded at 100 samples per second over the nominal frequency range of 0.1 to 25 Hz.

Three accelerometers are precisely mounted at right angles to form a TSH. This allows the sensor head to simultaneously detect vibrations in three different directions of movement: what would be on Earth up and down, forward and backward and side-to-side (called X, Y and Z axes). The TSH is a microcontroller-based data acquisition system capable of measuring the microgravity accelerations of the Shuttle. Sensitive inertial grade accelerometers are used to resolve the very low forces experienced during quiet periods and have the dynamic range to measure the larger vibration disturbances.

A new sensor, as part of the SAMS-FF system, that also flew on STS-107 was a fiber-optic gyroscope (FOG). To fully capture the motion of the vehicle, not only are the acceleration examined in three linear directions, but also the rotation of the vehicle is measured to understand the torque forces. FOG has no moving parts and was used to measure precisely the roll, pitch, and yaw of the shuttle.

The CDU of the SAMS-FF was located in the aft bulkhead of the SPACEHAB module. The locations of the SAMS-FF unit and its sensor heads are shown in Figures 4.2A and 4.2B.

The acceleration data was simultaneously downlinked and recorded onboard the shuttle. In this report, the SAMS-FF data is presented in terms of the Orbiter structural coordinate system. The locations of the SAMS-FF heads with respect to the Orbiter structural coordinate system are given in Table 4.2. Again, due to the Columbia accident on re-entry, only the SAMS-FF TSH head 11 that downlinked data during the mission to the JSC POCC is available. All data recorded onboard for later retrieval and processing was lost.

TABLE 4.2 SAMS SENSOR HEAD LOCATIONS AND ORIENTATIONS

Sensor: SAMS-FF TSH, Head 11		Sampling Rate: 100 samples/second
Location: SPACEHAB--CM-2 Double Rack		Frequency : 25 Hz
ORIENTATION		LOCATION
Orbiter Structural Axis	Sensor Axis	Structural Coordinates
X_o	- Z_{h11}	$X_o = 928.03$ in
Y_o	- X_{h11}	$Y_o = -53.56$ in
Z_o	- Y_{h11}	$Z_o = 409.71$ in

**PIMS STS-107 Mission Microgravity Environment Summary Report:
January 16 to February 1, 2003**

TABLE 4.2 SAMS SENSOR HEAD LOCATIONS AND ORIENTATIONS (continued)

Sensor: SAMS-FF TSH, Head 12		Sampling Rate: 10 samples/second
Location: SPACEHAB--Forward Bulkhead		Frequency : 2.5 Hz
ORIENTATION		LOCATION
Orbiter Structural Axis	Sensor Axis	Structural Coordinates (Not Known)
X_o	$+ X_{h12}$	$X_o =$ (On T-Beam, between FS05 and FS07)
Y_o	$+ Z_{h12}$	$Y_o =$
Z_o	$+ Y_{h12}$	$Z_o =$

Sensor: SAMS-FF TSH, Head 13		Sampling Rate: 100 samples/second
Location: SPACEHAB-- Aft Bulkhead (MGM)		Frequency : 25 Hz
ORIENTATION		LOCATION
Orbiter Structural Axis	Sensor Axis	Structural Coordinates(Not Known)
X_o	$- X_{h13}$	$X_o =$ (Located on T-Beam near MGM at AS04)
Y_o	$+ Y_{h13}$	$Y_o =$
Z_o	$+ Z_{h13}$	$Z_o =$

The PIMS project makes the acceleration data for the STS-107 mission available on its web site for easy access and usage by the microgravity scientific community. The data for both the OARE and the SAMS-FF accelerometer systems can be downloaded at:

<ftp://pims.grc.nasa.gov/sts107>

The SAMS-FF acceleration data is stored in the orbiter structural coordinate system, while the OARE data is stored in the body coordinate system. For more detail on these two coordinate systems, please refer to section 3.

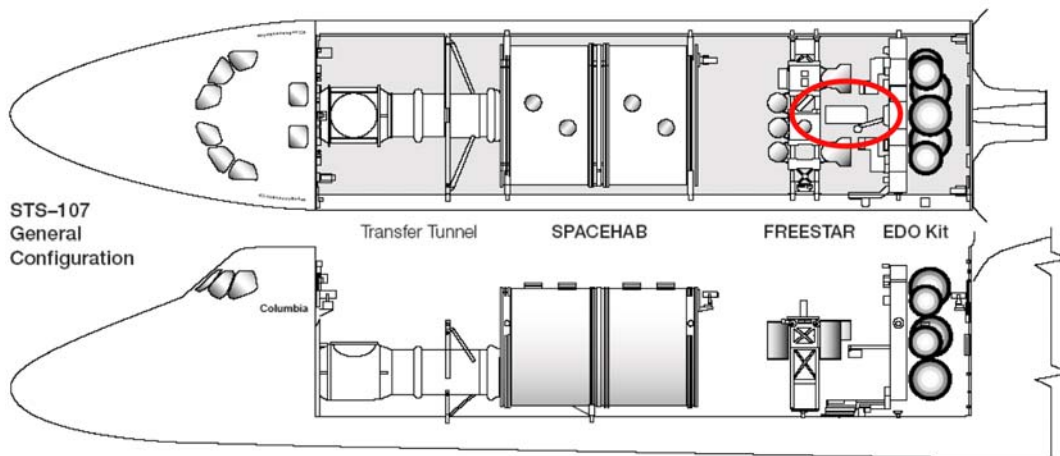


Figure 4.1 Red Oval Showing the Location of the OARE Inside the Orbiter

**PIMS STS-107 Mission Microgravity Environment Summary Report:
January 16 to February 1, 2003**

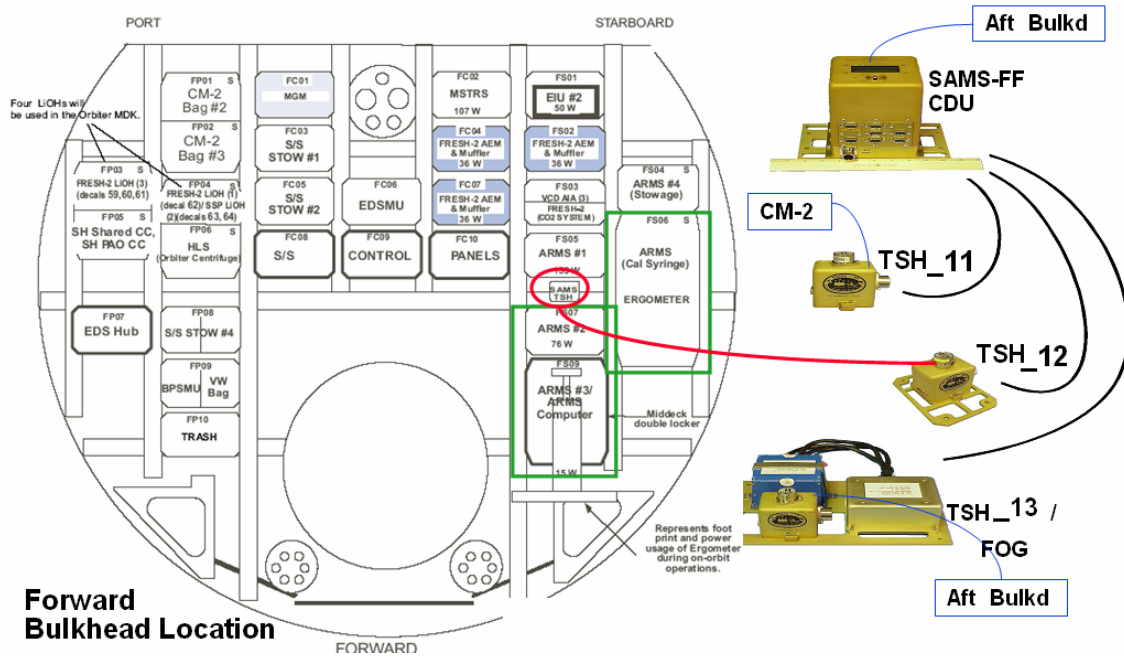


Figure 4.2A Location of the SAMS-FF Heads Inside The SPACEHAB — Forward Bulkhead Location

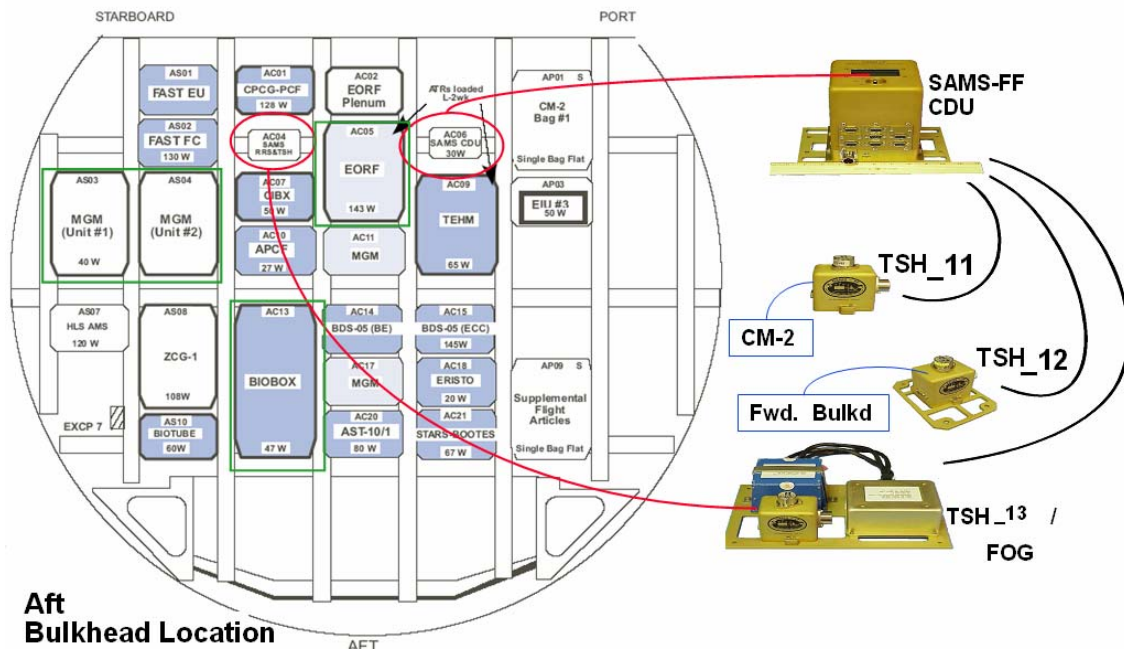


Figure 4.2B Location of the SAMS-FF Heads Inside The SPACEHAB — Aft Bulkhead Location

**PIMS STS-107 Mission Microgravity Environment Summary Report:
January 16 to February 1, 2003**

5 STS-107 Experiment Support Provided by PIMS

Prior to flight, PIMS worked with the science teams for the Combustion Module-2 (CM-2) and the Mechanics of Granular Materials (MGM) to determine their acceleration data measurement needs. This assessment included their acceleration system needs, accelerometer cutoff frequency setting and the appropriate microgravity acceleration data support (i.e., real time, near real time and post analysis data display support). As a result of the many discussions with the science teams, the PIMS project agreed to support the Principal Investigators (PIs) as follows (taking into account available resources):

1. To receive, process, analyze and interpret the accelerometer data to characterize the microgravity environment for the CM-2 investigative teams during the STS-107 mission
2. To monitor the microgravity environment in real time in support of CM-2 operations
3. To provide real time custom display plots to the CM-2 teams
4. To record and archive the acceleration data for post mission analysis
5. To provide the PIs with specific analyses and data plots

The support required from the PIs was captured as shown in Table 5.1 below.

TABLE 5.1 PRINCIPAL INVESTIGATOR TEAMS SUPPORT REQUIREMENTS FOR THE STS-107 MISSION

	EXPERIMENTS				
	LSP	SOFBALL	WATER MIST	MGM	VCD-FE
SAMS-FF (REAL-TIME)		✓			
SAMS-FF (POST MISSION)	✓	✓	✓	✓	✓
OARE (NEAR REAL-TIME)		✓			
OARE (POST MISSION)		✓	✓		
$f_c = 25$ Hz	✓	✓	✓	✓	
AOS	✓	✓	✓	✓	
SPECIALIZED DATA PLOTS	NR	✓	NR	NR	
LOS	NA	NA	NA	NA	
TOTAL POWER ON	~ 72 hrs	~ 96 hrs	~ 60 hrs	~ 55 hrs	



**PIMS STS-107 Mission Microgravity Environment Summary Report:
January 16 to February 1, 2003**

Many teleconference discussions and on-site visits were held with the science teams to discuss acceleration data display designs, and feedback was obtained from the PIs to make sure their requirements were met. In particular, PIMS had the opportunity to work closely with the Structure of Flame Balls at Low Lewis-number (SOFBALL) and the Water Mist Fire-Suppression Experiment (*Mist*). The SAMS-FF real-time displays at JSC POCC included acceleration versus time plots and a color spectrogram for the root-sum-of-squares (RSS) combination of the three axes. The color spectrogram served as an overview of the recent microgravity environment. That display allowed the PIMS team monitoring the console at the JSC POCC to determine exercise activity and other experiment start-ups in order to warn PIs with sensitive experiments in near real time of such activities. The real-time feedback allowed PIs to minimize the impact of the acceleration disturbances on their experiment whenever that was a possible course of action.

In addition to the nominal SAMS-FF displays described above, a customized analysis display was developed for SOFBALL, requested by Dr. Paul Ronney, and also used by the MIST experiment. This customized analysis display was a leaky integrator with a not-to-exceed threshold of 50 $\mu\text{g}\cdot\text{second}$. For more detail on this customized display, see the vibratory section of this report. In addition to these displays, raw (10 samples per second) OARE data was processed throughout the mission in support of the SOFBALL experiment.

5.1 Combustion Module-2 Facility Background

The CM-2 was a state-of-the-art space laboratory that allowed a wide range of users to perform combustion experiments in space. Until 1997, combustion experiments were developed for individual experiments. This was time-consuming and costly. NASA decided that a better and less expensive approach was a reusable, modular combustion facility that could accommodate diverse experiments with the same support hardware and unique Experiment Mounting Structures (EMS). This approach led to the CM [2]. CM-1 flew on STS-83 and 94 with two experiments as part of the Microgravity Sciences Laboratory 1 in 1997.

Most of the CM-2 subsystems were in a double rack and a single rack standing side-by-side in the SPACEHAB module. Flight spares and EMS's were carried in a Maximum Envelope Stowage System that is the same size as a double rack. Central to CM-2, in the double rack, was the Experiment Package, a 90-liter combustion chamber with six ports for three intensified near-infrared cameras, one color camera, and three black and white cameras; a gas chromatograph; crew switches; and thermistors. The Fluid Supply Package, in the single rack, is a complex gas control and distribution system containing 20 composite overwrapped compressed gas bottles. The Exhaust Vent Package includes a blower, canister, and other fluid components for cleanup and evacuation of chamber gases. The Dedicated Experiment Processor Package is the main processor for experiment command and control, and connects to the crew laptop (the CM-2 human interface). The EMS was experiment-unique chamber inserts. Each contained an ignition system and special sensors, Figure 5.1 [2].

**PIMS STS-107 Mission Microgravity Environment Summary Report:
January 16 to February 1, 2003**

The CM-2 experiment timeline spanned the entire mission. The CM-2 facility supported three experiments: The Laminar Soot Processes-2 (LSP-2), SOFBALL and *Mist*. The LSP experiment included 15 burns lasting about five minutes each, with active participation by the crew to adjust test conditions during the burn. The 15 SOFBALL burns ranged from 25 to 167 minutes, during which the Shuttle was placed in free drift with no attitude control so that the flame balls floated freely inside the combustion chamber. The 36 *Mist* burns were each very short ranging from less than one second to several seconds in duration. *Mist* included six tests run by the crew and 30 tests run by the ground team using commands sent directly to CM-2's on-board computer [2].

During the 16-day mission of the Columbia STS-107, the PIMS project actively supported the following experiments: LSP, SOFBALL, *Mist* and MGM. Below is a brief description of these four experiments.

5.2 Laminar Soot Processes-2 (LSP-2)

Microgravity provides an unprecedented opportunity to investigate soot processes relevant to practical flames. The chemical pathways that form soot are highly controversial in the science community. When the flame temperature falls below about 1300 °K (1900 °F), no soot is formed. Above that, hydrocarbon fuels pyrolyze or break down, even as most of the reactions form carbon dioxide and water vapor. These molecular fragments produce other molecules, including polycyclic aromatic hydrocarbons (PAH's) that coalesce into solid carbonaceous particles — soot — that are linked to human cancers in a number of studies. The LSP-2 investigation observed soot processes within laminar jet diffusion flames where a hydrocarbon jet burned in still air. Microgravity produces nonbuoyant laminar jet flames which allow observations of soot processes that cannot be duplicated on Earth. Normal gravity generates buoyant motion due to the large variations of gas densities in flames. These motions introduce soot particle motions that do not represent most practical flame environments where local effects of buoyancy are small [2].

LSP-2 experiment was conducted inside the Combustion Module-2 (CM-2) facility. Diagnostic instruments for LSP included a color camera, a soot volume fraction system (using the dimming of a laser shining through the flame), and a soot temperature measurement system. An EMS provided a large volume to allow laminar flames to form on one of two burners with diameters of 0.4 mm (0.016 in.) and 0.8 mm (0.0315 in). They produced a flame 20 to 60 mm long (0.8 to 2.4 in). Soot samplers (for six test points) snapped through the flame to capture particles for post-flight analysis. LSP-2 science operations lasted almost 42 hours and covered 15 test points using ethylene or propane fuel in air [2].

5.2.1 Previous LSP-1 Results

On the Microgravity Sciences Lab-1 mission in 1997, LSP yielded several surprises. The LSP team discovered a new mechanism of flame extinction caused by radiation from soot. The mechanism is unusual because the flame quenches near its tip, unlike conventional extinction of buoyant flames where the flame quenches near its base. This phenomenon has significant

**PIMS STS-107 Mission Microgravity Environment Summary Report:
January 16 to February 1, 2003**

implications for spacecraft fire safety and for selecting test conditions for future studies of nonbuoyant soot containing flames. The team also made the first observations of steady soot containing nonbuoyant flames both with and without soot emissions. These provided textbook examples of soot formation processes in practical flames that are invaluable for developing methods for controlling the emissions of pollutant soot [2].

5.3 Structure of Flame Balls at Low Lewis-number-2 (SOFBALL-2) Experiment

SOFBALL burns extremely lean fuel-air mixtures that are near the lower limit of combustion. The mixtures are ignited by an electrical spark. Because the mixture is lean and has a low Lewis-number, the flame does not spread across the mixture. Instead, the flame forms a spherical shell filled with combustion products and supported by fuel and oxygen diffusing inward while heat and combustion products diffuse outwards. This diffusion-controlled combustion process provides the weakest known flames and provides a means to study the limits of lean combustion. This is possibly only in a microgravity environment, where buoyant flow is absent [6].

The Lewis-number part of SOFBALL is a measure of the rate of diffusion of fuel into the flame ball relative to rate of diffusion of heat away from the flame ball. Hydrogen and methane are the only fuels that provide low enough Lewis-numbers to produce stable flame balls, and even then only for very weak, barely flammable mixtures. Nevertheless, these flame balls give scientists the chance to test combustion models in an ideal environment [6].

The biggest discovery from the first SOFBALL flights (MSL-1 and 1R) was the long life of flame balls. Scientists expected that flame balls would extinguish or drift into the chamber walls in a few minutes. Instead, most could have burned for many minutes had they not been automatically terminated at 500 seconds. The experiments also provided conclusive evidence about the limitations of existing computer models of lean combustion, and demonstrated the effects of flames reabsorbing their own radiation, which can also affect large engines and industrial boilers [2].

The objective of the SOFBALL-2 space flight experiment was to study weakly burning flames in hydrogen-oxygen-inert and methane-oxygen-inert mixtures in a configuration called “flame balls” that were originally predicted by Zeldovich in 1944 but not seen experimentally until over 40 years later in short-duration drop tower experiments [7]. Because flame balls are steady, convection-free, spherically symmetric and occur in fuels with simple chemistry, they represent the simplest possible interaction of chemistry and transport in flames. In this sense flame balls bear a similar relationship to combustion research that the fruit fly does to genetics research.

On STS-107 a total of 39 tests were performed in 15 different mixtures, resulting in a total of 55 flame balls, of which 33 were named by the crew. Most tests (by design) produced only 1 flame ball, though one test intentionally designed to produce a large number of flame balls resulted in 9 balls. The total burn time for all flames was 6 ¹/₄ hours. Since flame balls are extremely sensitive to gravitational acceleration, all tests were conducted during orbiter free drift periods.

**PIMS STS-107 Mission Microgravity Environment Summary Report:
January 16 to February 1, 2003**

Several totally new results were found, including oscillating flame balls that were predicted theoretically [8], but heretofore never observed experimentally. It is not been established whether the mechanism outlined in [8] is responsible for the observed oscillations. For some tests, particularly in methane-oxygen-sulfur hexafluoride mixtures, flame ball drift not related to gravitational disturbances nor interactions with other balls or walls. This was a completely unexpected and as yet unexplained result.

Several issues not resolved during the previous space flight experiments on STS-83 and STS-94 in 1997 [9] were addressed by this experiment on STS-107: *Can flame balls last much longer than the 500 sec maximum test time on STS-83 and STS-94 if free drift (no thruster firings) can be maintained for the entire test?* Answer: not usually - some type of flame ball motion, not related to microgravity disturbances, causes flame balls to drift to walls within ≈ 1500 seconds. The only exception to this was the very last test in which 9 flame balls formed initially and extinguished one by one until only one (name "Kelly" by the crew) remained. Unexpectedly, Kelly survived 81 minutes, seemingly immune to drift, until it was intentionally extinguished due to operational limitations (it was still burning at the time). The mechanism responsible for the drift of isolated flame balls has not yet been identified, though some mechanisms have been proposed [10]. The shorter-than-expected test times on most tests meant enough time for multiple reburns of each mixture within the flight timeline. *Can oscillating flame balls be observed in long-duration, free-drift conditions?* Answer: Probably, but it is still necessary to determine if flame ball motion rather than inherent oscillations of stationary flame balls may have caused the observed oscillations). *Are higher Lewis number flame balls (e.g. $H_2-O_2-He-CO_2$, $Le \approx 0.8$) more likely to oscillate, as predicted theoretically [8]?* Answer: No. These flames were extremely stable. Do the flame balls using methane ($CH_4-O_2-SF_6$ mixtures) behave differently from those in hydrogen fuel (e.g. $H_2-O_2-SF_6$ mixtures)? Answer: Yes. They frequently drifted in corkscrew patterns, though again the mechanism responsible for this drift is not clear.

5.4 Water Mist Fire-Suppression Experiment (*Mist*)

Space may be the ideal place to examine how water interacts with flame. On Earth, gravity causes lighter, hotter air to rise -- creating air currents that make it difficult to study the combustion process and fire-fighting techniques. In microgravity -- the low-gravity environment created as the space shuttle orbits Earth-- these currents are reduced or eliminated. This allows scientists to study exactly what happens in the combustion process.

For this experiment, scientists observed how water droplets, like those in a fine fog, interact with a flame and extinguish it. These observations will help industry determine the optimum water concentration and water droplet size needed to suppress fires. The information can be used to improve models for designing the next generation of environmentally friendly, low-cost fire-fighting systems.

**PIMS STS-107 Mission Microgravity Environment Summary Report:
January 16 to February 1, 2003**

The *Mist* experiment studied how different sizes and concentrations of droplets affect a thin layer of flame, known as a laminar flame. The water droplets were between 20 to 40 microns in size, as opposed to droplets from conventional sprinklers that are larger than 1 millimeter. The flame was produced by igniting a mixture of propane and air inside a transparent tube in the CM-2 [2].

Mist performed 32 out of the 34 tests planned and preliminary results showed the suppression effects of two droplet sizes (with mean diameters of 20 and 30 microns) and a variety of water concentrations (mass fractions ranging from 0 to 50%) on the burning velocity of lean, stoichiometric, and rich premixed flames. Total flame extinguishment was also observed in a few cases and a characterization study of the behavior of water mist in microgravity was also performed. STS-107 was the first space flight of the *Mist* experiment.

5.5 Mechanics of Granular Materials

To understand how granular materials behave under low stresses, NASA sponsored the Mechanics of Granular Materials (MGM) experiment to flight on the STS-107 mission. In space, MGM used the weightless environment to test soil under very low confining pressures. The results will further advance the understanding of the behavior of granular materials and will improve analytical modeling. The knowledge gained from this experiment will be used to improve the foundations of buildings, manage undeveloped land as well as the handling of powdered and granular materials in chemical, agricultural, and other industries.

MGM flew twice before on the space shuttle (STS-79 and -89), involving nine dry sand specimens. Several significant finds emerged from these flights and are helping scientists test a number of hypotheses about soil behavior. For example, results showed strength properties two to three times greater and stiffness properties 10 times greater than conventional theory predicted.

On STS-107, scientists investigated conditions with water-saturated sand resembling soil on Earth. Three sand specimens were used in nine experiments. The heart of the experiment was a column of sand held in a latex sleeve and compressed between tungsten metal plates. Each cell used about 1.3 kilograms (2.8 pounds) of Ottawa F-75 banding sand, 7.5 centimeters in diameter by 15 centimeter wide (3 x 6 inches). Ottawa sand, natural quartz sand with fine grains, is widely used in civil engineering experiments. The specimen assembly was contained in a water-filled Lexan jacket. A load cell measured force, and three CCD cameras videotaped the experiment. The system occupied the volume of four middeck lockers in the SPACEHAB module [2].

During the STS-107 mission, MGM did obtain some very exciting findings. Earthquake liquefaction was successfully simulated through two separate sets of experiments, and other experiments detailed constitutive behavior of low density specimens at low confining stresses. In addition, a new technique for reforming specimens in low gravity was first performed on STS-107 with success. The reforming technique allows for both an increase in the number of experiments that can be tested using one sample as well as a wider range of densities which can be tested.

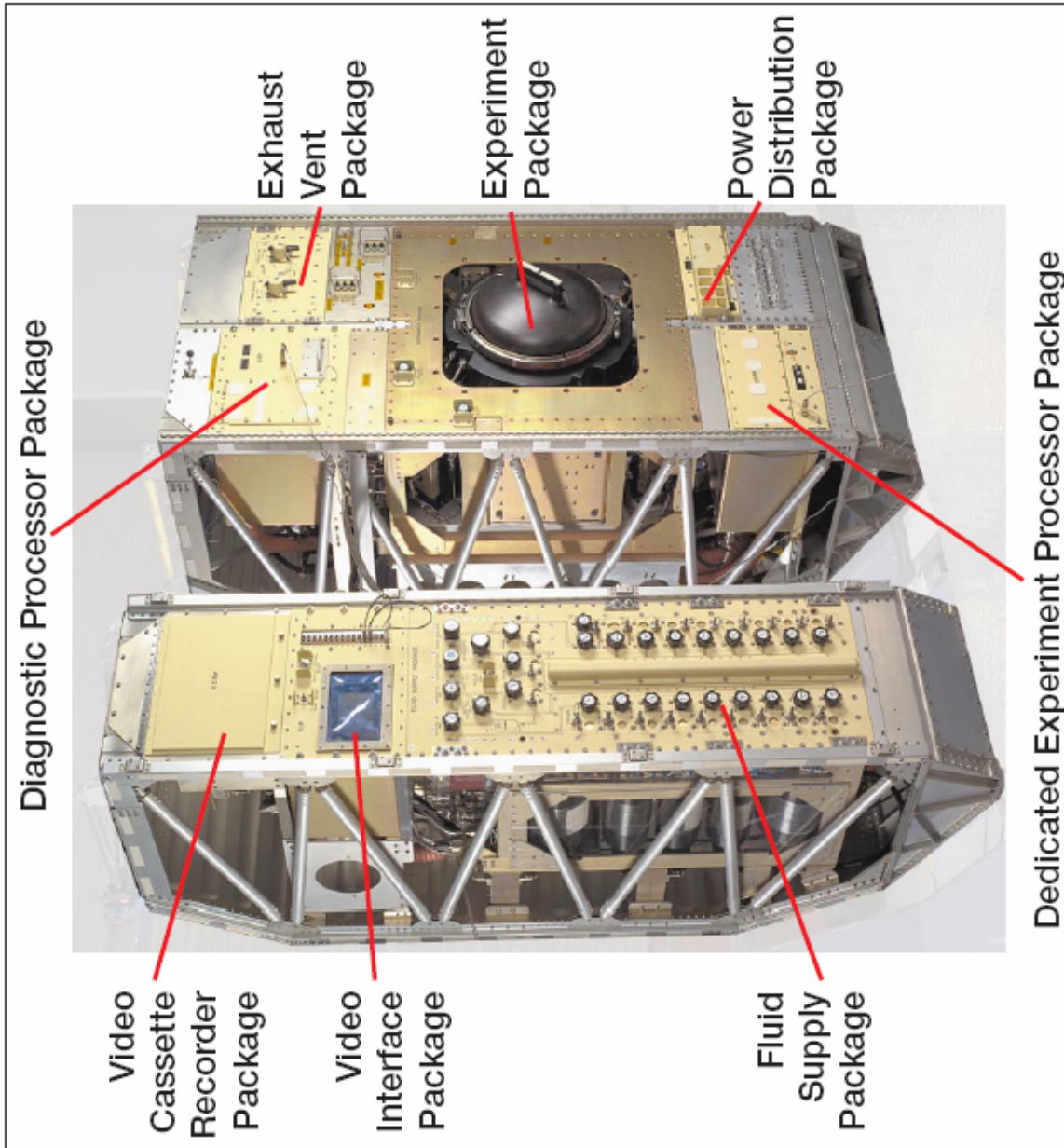


Figure 5.1 Detail of the Combustion Module-2 (CM-2) Facility – Front View

**PIMS STS-107 Mission Microgravity Environment Summary Report:
January 16 to February 1, 2003**

6 Columbia Reduced Gravity Environment Description (STS-107)

The microgravity environment of an orbiting space laboratory such as the Space Shuttle has many components. The quasi-steady microgravity environment is related to orbital phenomena such as aerodynamic drag, rotational motion, and gravity gradient effects based upon the location of interest's distance from the Orbiter's center of gravity. In addition to these quasi-steady accelerations, all on-going operations of crew life-support systems and activities, and operations of the Orbiter, crew, carrier, and experiments have transient and vibratory components that contribute to the overall acceleration environment.

The remainder of this section discusses the acceleration environment recorded during the STS-107 flight of Columbia, including accelerations related to Orbiter attitude, Orbiter venting operations, a variety of experiment-specific fans, pumps, and compressors, crew exercise, and crew quiet periods.

In order to readily preview the availability of the acceleration data for a particular sensor for a particular time period, Figure 6.1 and Figure 6.2 were generated. Figure 6.1 and Figure 6.2 show the available acceleration data for the OARE sensors and the SAMS-FF TSH head 11 over the entire STS-107 16-day mission. The data can be accessed via the PIMS ftp site at:

<http://pims.grc.nasa.gov/ftp/sts107/year2003/>

6.1 Quasi-Steady Microgravity Environment

The quasi-steady regime is comprised of accelerations with frequency content below 0.01 Hz and magnitudes expected to be on the order of 5 μg or less. These low-frequency accelerations are associated with phenomena related to the orbital rate such as aerodynamic drag, gravity gradient, and rotational effects. Another source of acceleration to consider in this regime is venting of air or water from the spacecraft, which results in a nearly constant, low-level propulsive force. The different quasi-steady environment characteristics seen during the STS-107 mission are primarily related to attitude of the shuttle. Different attitudes will affect the drag component due to the variation of the frontal cross-sectional area of the shuttle with respect to the velocity vector. The gravity gradient and rotational components variations are primarily due to the sensor or experiment's location relative to the vehicle center-of-mass (CM).

In this report, OARE data is presented in Orbiter Body coordinates. The sign convention used is consistent with an inertial frame of reference, meaning a forward thrust of the Orbiter is recorded as a positive X_b acceleration. The OARE instrument was mounted to a keel bridge in the Columbia's cargo bay, close to the Orbiter CM. OARE data may be mathematically "mapped" to an experiment location using rigid body assumptions and Orbiter telemetry data obtained from the Operational Data Reduction Complex (ODRC). Plots containing mapped data are indicated in the upper left corner ancillary text of the plot. The locations of OARE and CM-2 relative to the Orbiter center of mass are found in Table 6.1.

**PIMS STS-107 Mission Microgravity Environment Summary Report:
January 16 to February 1, 2003**

TABLE 6.1 OARE AND EXPERIMENT LOCATIONS

Location	Structural Coordinates (feet)			Distance from CM (feet)		
	X	Y	Z	X	Y	Z
OARE	96.11	-0.11	26.48	5.53	-0.08	-4.56
CM-2	76.65	-3.62	32.99	-13.92	-3.59	1.94
Center of Mass	90.57	-0.03	31.05	-	-	-

6.1.1 OARE Bias Measurements

The OARE quasi-steady sensor operated in one of three ranges, A, B or C, with C being the most sensitive to changes in the microgravity environment. The OARE required periodic calibration on a per-axis, per-range basis to calculate and remove instrument bias. During the free drift periods of the SOFBALL run, the OARE sensor was predominantly operating in the C-range. For this reason, although all three ranges were calibrated, only C-range bias measurements were considered.

A typical 16 day mission, with bias measurements every 4 hours, would result in approximately 90 valid bias points per axis, giving a high degree of confidence to the accuracy of the bias compensation, and thus accuracy of the data. A curve fitting algorithm is applied to the entire mission's worth of bias points on a per-axis basis to take into account temperature variations and the dielectric charging seen early in the mission. Unfortunately, due to the low data recovery for STS-107, the data set contains only 7 valid bias measurements for C-range.

Table 6.2 and Table 6.3 show the measured and curve fitted C-range bias values, temperature and estimated error for each axis (OARE coordinates). The data is plotted in Figure 6.3. The data is compensated with the fitted bias value with the greatest time that is less than that of the data point. Note that data between hours 0 and 0.62 was compensated with the fitted point at t = 0.62 hours.

TABLE 6.2 VALID C-RANGE BIAS MEASUREMENTS

Time (hours)	Xmeas (μg)	YMeas (μg)	ZMeas (μg)	Temperature ($^{\circ}\text{C}$)
0.62	1.11	-1.11	-6.43	32.58
3.31	0.52	-0.83	-6.27	31.93
20.34	0.84	-0.22	-6.79	53.45
27.73	1.05	-0.78	-6.12	37.28
64.67	1.30	-1.34	-5.67	24.14
79.45	1.35	-0.92	-6.50	30.87
86.84	1.78	-1.33	-5.85	15.93

Time is relative to a start time of 22-Jan-2003, 022/11:22:31.782

**PIMS STS-107 Mission Microgravity Environment Summary Report:
January 16 to February 1, 2003**

TABLE 6.3 C-RANGE BIAS FITTED VALUES

Time (hours)	XFit (μg)	YFit (μg)	ZFit (μg)	XError (μg)	YError (μg)	ZError (μg)
0.62	1.11	-1.11	-6.43	0.35	0.15	0.27
3.31	0.52	-0.83	-6.27	0.35	0.15	0.27
20.34	0.84	-0.22	-6.79	0.43	0.18	0.32
27.73	1.05	-0.78	-6.12	0.36	0.15	0.27
64.67	1.30	-1.34	-5.67	0.36	0.15	0.28
79.45	1.35	-0.92	-6.50	0.35	0.15	0.27
86.84	1.78	-1.33	-5.85	0.40	0.17	0.30

Time is relative to a start time of 22-Jan-2003, 022/11:22:31.782

These error values are higher than those for OARE in past missions (0.020 – 0.060 μg), primarily due to the small number of data points. For added insight into the reliability of the OARE data collected on STS-107, it is useful to compare similar attitudes between flights. Figure 6.4 shows OARE data from STS-107 while the orbiter was in an attitude with the $-Z_B$ -axis pointed nadir and the $-X_B$ -axis maintained in the velocity vector ($-ZLV/-XVV$). This same $-ZLV/-XVV$ attitude was flown in the USMP-4 mission at MET 001/18:00. OARE data collected during that time period can be seen in Figure 6.5. Table 6.4 summarizes the difference in mean values between each axis (OARE coordinates).

TABLE 6.4 COMPARISON OF $-ZLV/-XVV$ ATTITUDES FLOWN ON USMP-4 AND STS-107

Flight	Acceleration (μg)			Distance from CM (feet)		
	X	Y	Z	X	Y	Z
STS-107	0.61	0.44	0.06	5.53	-0.08	-4.56
USMP-4	0.41	0.46	0.40	5.40	-0.12	-4.71
Delta	0.20	-0.02	-0.34	0.13	-0.04	-0.25

The difference in distance to center of mass between the two flights would result in a calculated maximum of 0.03 μg difference in the Z-axis due to gravity gradient and rotational components. Similar differences in the other axes are not considered to be significant due to the cancellation effect in the X-axis and the very short differences in distance in the Y-axis. The difference in these acceleration values fall within the estimated error, except for the Z-axis (0.34 μg).

6.1.2 Experiment Operations

This section discusses experiment operations related to SOFBALL. Due to low recovery of OARE data during the operation of the Water Mist Fire-Suppression Experiment, an analysis of the quasi-steady vector during these time periods was not performed.

**PIMS STS-107 Mission Microgravity Environment Summary Report:
January 16 to February 1, 2003**

6.1.2.1 Structure of Flame Balls at Low Lewis-Number (SOFBALL)

During experiment runs, or “test points”, the principal investigator for SOFBALL, Dr. Paul Ronney, requested that the vehicle be in “free drift” to eliminate vehicle thruster firings as a disturbance source. Prior to a set of test points, the vehicle would maneuver to the gravity gradient attitude (Bias -XLV -YVV) and then enter into free drift for an extended period of time. Figure 6.6 shows a transition to gravity gradient attitude on GMT 26-Jan-03, 026/18:24 to 18:30 and the subsequent free drift from 18:40 to 20:35. The attitude maneuver introduces a disturbance in primarily the X and Z axes. As seen in the RSS plot of Figure 6.7, the mean magnitude of the disturbance is 11.3 μg , with peaks of 34.0 μg and 37.6 μg , as the maneuver begins and ends respectively. Also seen on the Y-axis at 20:00 is a disturbance that peaks at -4.15 μg and tapers off and returns to the original baseline established during freedrift approximately 30 minutes later. This unidentified disturbance has the appearance of a venting operation. However, no waste or water dumps appear on the timeline as occurring during this time period.

Available trimmean filtered OARE data was mapped to the CM-2 location and plotted for each free drift period and the mean acceleration per axis was calculated for the time span of each SOFBALL test point. Table 6.5 shows the results of these calculations and references to the time series figure in which the data for test point is plotted. The values found in the magnitude column were calculated from a time series of the root sum square (RSS) of the individual axes. The RSS time series plots are not included in this report. In some cases, not enough data was recovered in order to perform an analysis.

TABLE 6.5 QUASI-STEADY VECTOR AT CM-2 LOCATION FOR SOFBALL TEST POINTS

Test Point Done	GMT Start	GMT End	Mean Acceleration (μg)				See
			X	Y	Z	Mag	
14A	23-Jan-2003,02:09:36	23-Jan-2003,02:29:00	0.84	-0.53	-0.66	1.23	Figure 6.8
14B	23-Jan-2003,02:57:41	23-Jan-2003,02:57:52	Insufficient Data				No Plot
02A	23-Jan-2003,07:17:49	23-Jan-2003,07:30:38	-0.65	-0.37	-0.68	1.03	Figure 6.9
02B	23-Jan-2003,08:13:59	23-Jan-2003,08:21:06	0.62	-0.63	-0.89	1.29	Figure 6.9
02C	23-Jan-2003,08:42:27	23-Jan-2003,08:45:57	0.22	-3.53	-1.26	3.76	Figure 6.9
03A	23-Jan-2003,14:33:07	23-Jan-2003,14:37:19	Insufficient Data				No Plot
08A	23-Jan-2003,18:33:55	23-Jan-2003,18:40:09	0.13	-0.62	-0.69	0.97	Figure 6.10
08B	23-Jan-2003,19:24:19	23-Jan-2003,19:31:33	-0.24	-2.96	-0.28	2.99	Figure 6.10
05A	23-Jan-2003,23:40:15	24-Jan-2003,00:01:29	-0.07	-1.94	0.43	2.38	Figure 6.11
05B	24-Jan-2003,00:52:14	24-Jan-2003,01:08:41	0.22	-0.13	-0.30	1.23	Figure 6.11
05M	24-Jan-2003,02:07:22	24-Jan-2003,02:11:33	-0.37	1.38	-0.16	1.45	Figure 6.11
09A	24-Jan-2003,12:04:10	24-Jan-2003,12:12:24	-1.47	-3.42	-1.83	4.20	Figure 6.12
09B	24-Jan-2003,13:07:12	24-Jan-2003,13:11:26	Insufficient Data				No Plot
12A	24-Jan-2003,17:09:50	24-Jan-2003,17:15:04	-0.13	-1.30	-0.89	1.59	Figure 6.13
12B	24-Jan-2003,18:10:13	24-Jan-2003,18:18:26	0.49	-0.99	-0.29	1.16	Figure 6.13
12O	24-Jan-2003,19:18:58	24-Jan-2003,19:19:42	Insufficient Data				No Plot
06A	25-Jan-2003,01:02:05	25-Jan-2003,01:10:26	-0.46	-0.34	-0.33	1.06	Figure 6.14

**PIMS STS-107 Mission Microgravity Environment Summary Report:
January 16 to February 1, 2003**

TABLE 6.5 QUASI-STEADY VECTOR AT CM-2 LOCATION FOR SOFBALL TEST POINTS

Test Point Done	GMT Start	GMT End	Mean Acceleration (μg)				See
			X	Y	Z	Mag	
06B	25-Jan-2003,02:12:32	25-Jan-2003,02:29:12	0.56	0.57	1.25	1.79	Figure 6.14
06C	25-Jan-2003,03:03:18	25-Jan-2003,03:28:17	0.26	1.33	0.37	1.56	Figure 6.14
06D	25-Jan-2003,04:06:42	25-Jan-2003,04:16:27	-1.38	0.69	0.31	1.77	Figure 6.14
11B	25-Jan-2003,11:54:16	25-Jan-2003,12:06:01	Insufficient Data				No Plot
11C	25-Jan-2003,12:59:12	25-Jan-2003,13:07:32	Insufficient Data				No Plot
10A	25-Jan-2003,17:47:43	25-Jan-2003,17:47:47	Insufficient Data				No Plot
10B	25-Jan-2003,19:03:38	25-Jan-2003,19:19:38	-0.64	-0.90	-0.35	1.18	Figure 6.15
10C	25-Jan-2003,20:09:23	25-Jan-2003,20:16:13	-0.34	-0.68	-0.95	1.26	Figure 6.15
10M	26-Jan-2003,00:29:55	26-Jan-2003,00:33:20	0.10	1.17	-0.02	1.19	Figure 6.16
10N	26-Jan-2003,01:23:10	26-Jan-2003,01:26:10	1.32	-0.01	0.38	1.38	Figure 6.16
10O	26-Jan-2003,02:09:57	26-Jan-2003,02:11:47	-0.53	1.53	0.95	1.89	Figure 6.16
04A	26-Jan-2003,05:38:49	26-Jan-2003,05:49:49	-0.59	-0.81	0.86	1.61	Figure 6.17
04B	26-Jan-2003,06:46:03	26-Jan-2003,06:52:13	0.22	-0.44	0.79	1.11	Figure 6.17
04C	26-Jan-2003,07:11:09	26-Jan-2003,07:17:54	-1.48	0.64	0.70	1.50	Figure 6.17
07A	26-Jan-2003,11:08:55	26-Jan-2003,11:09:55	-1.45	0.63	0.05	1.60	Figure 6.18
07B	26-Jan-2003,11:56:46	26-Jan-2003,11:57:26	0.65	-2.59	-1.30	2.97	Figure 6.18
07C	26-Jan-2003,12:43:30	26-Jan-2003,12:45:00	-0.58	0.50	0.59	1.04	Figure 6.19
07D	26-Jan-2003,13:43:45	26-Jan-2003,13:45:45	0.09	1.21	0.04	1.23	Figure 6.19
07E	26-Jan-2003,14:03:50	26-Jan-2003,14:04:00	Insufficient Data				No Plot
14M	26-Jan-2003,18:34:08	26-Jan-2003,18:47:23	0.10	-0.58	-1.34	1.51	Figure 6.20
14N	26-Jan-2003,19:32:00	26-Jan-2003,19:42:00	0.93	-0.40	-0.90	1.38	Figure 6.20
13A	27-Jan-2003,01:45:27	27-Jan-2003,02:05:27	-0.52	-1.94	-2.33	3.23	Figure 6.21

**PIMS STS-107 Mission Microgravity Environment Summary Report:
January 16 to February 1, 2003**

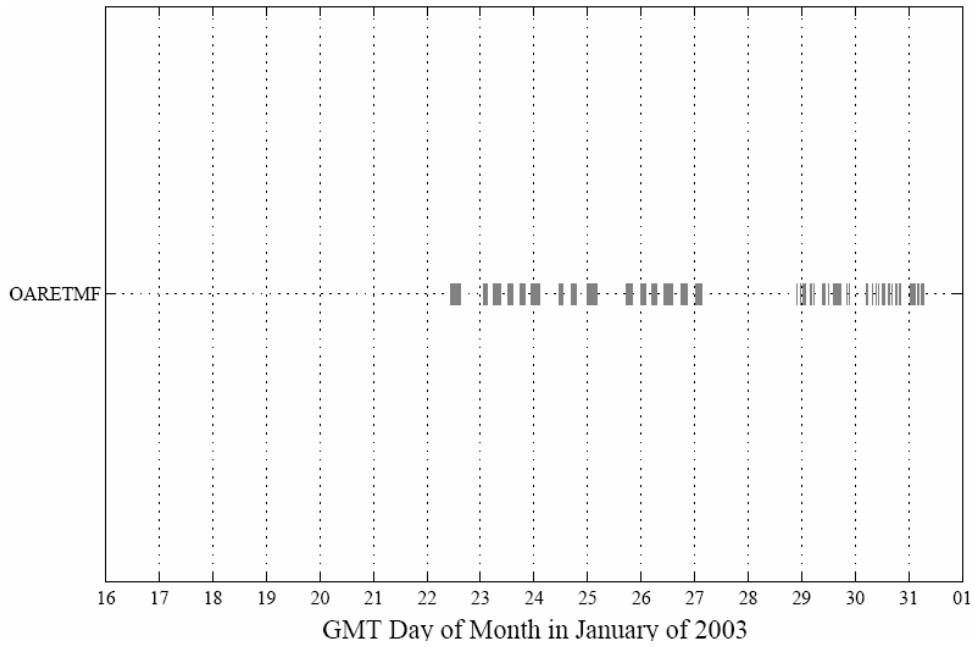


Figure 6.1 OARE Acceleration Data Collected during the STS-107 Mission

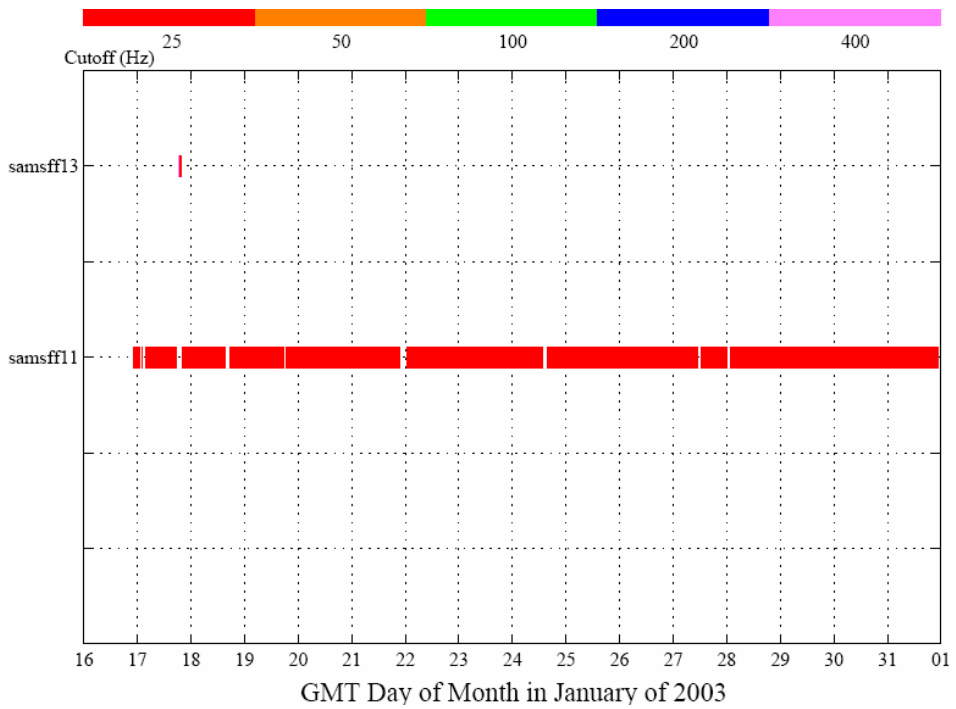


Figure 6.2 SAMS-FF, TSH_11, Acceleration Data Collected during the STS-107 Mission

PIMS STS-107 Mission Microgravity Environment Summary Report: January 16 to February 1, 2003

oare_mesabias, mesabias at STS-107, Cargo Bay:[1153.30 -1.30 317.80]

Increment: 0, Flight: STS-107

OARE C-Range Bias Measurements and Curve Fit

oare[-90.0 0.0 0.0]

Start GMT 22-January-2003, 022/10:45:23.000

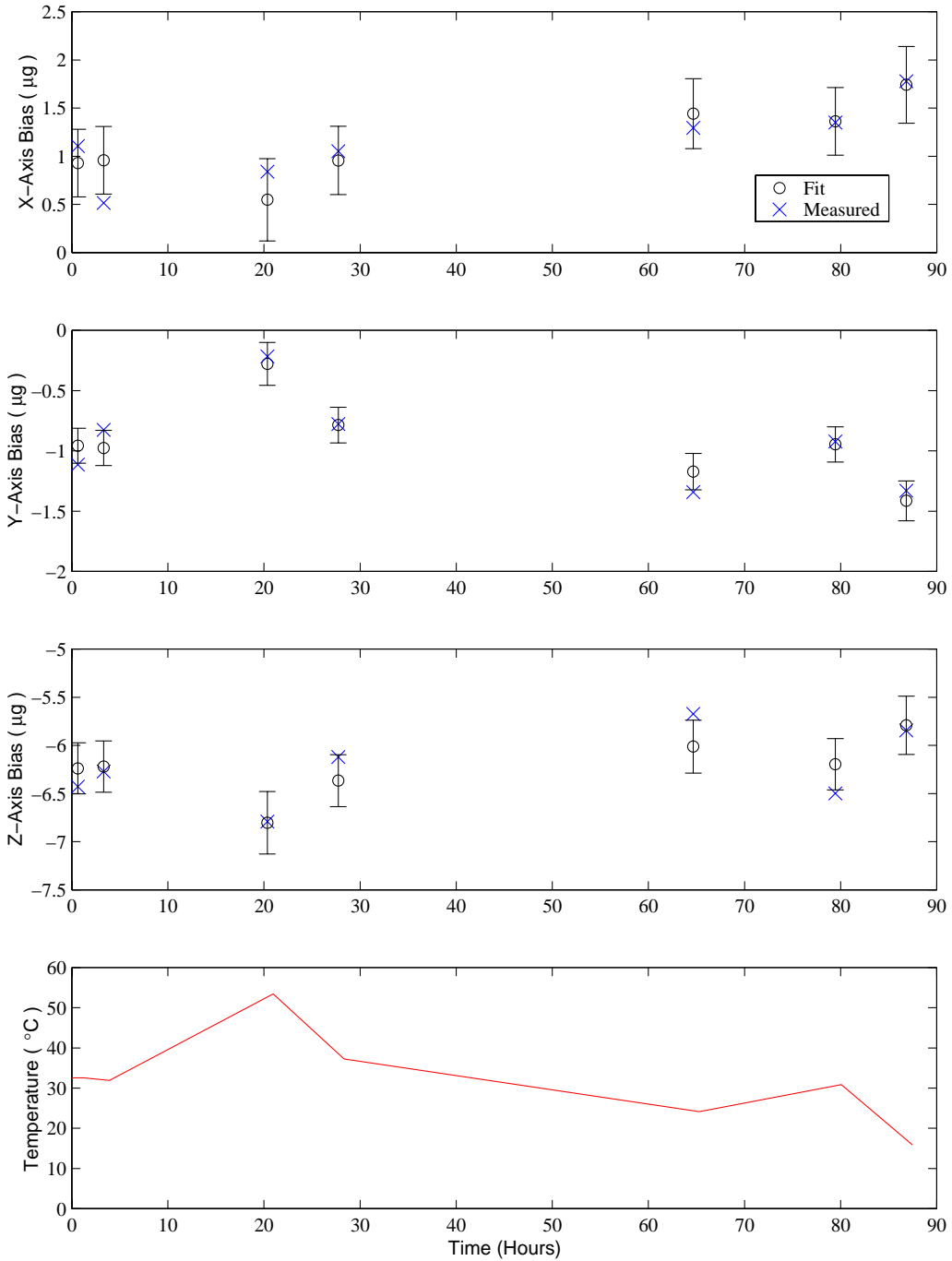


Figure 6.3 Valid C-Range Bias Measurements and Curve Fits

PIMS STS-107 Mission Microgravity Environment Summary Report: January 16 to February 1, 2003

oare_mesatmf, mesaraw at STS-107, Cargo Bay:[1153.30 -1.30 317.80]
0.0625 sa/sec (0.01 Hz)

Increment: 0, Flight: STS-107
oare[-90.0 0.0 0.0]

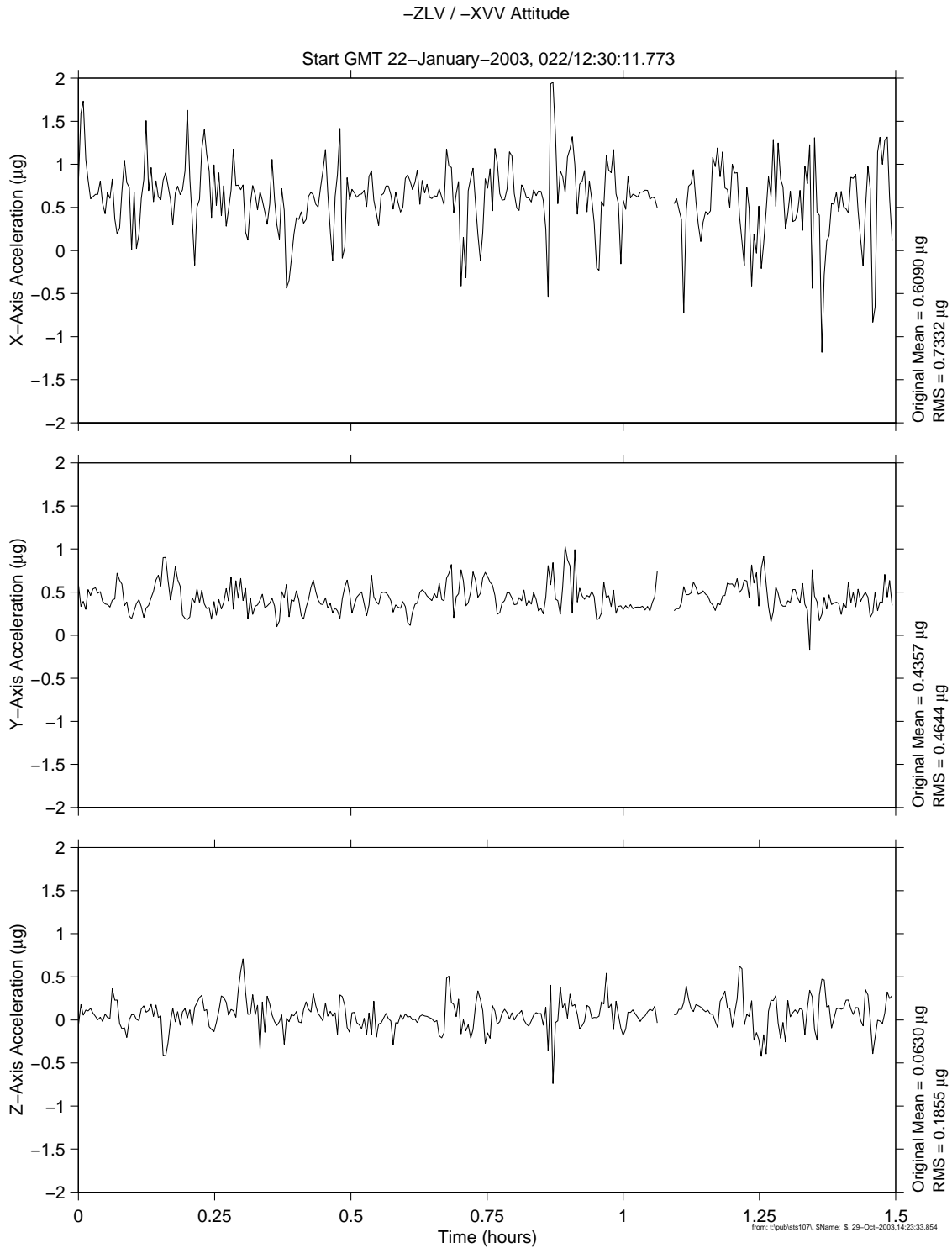


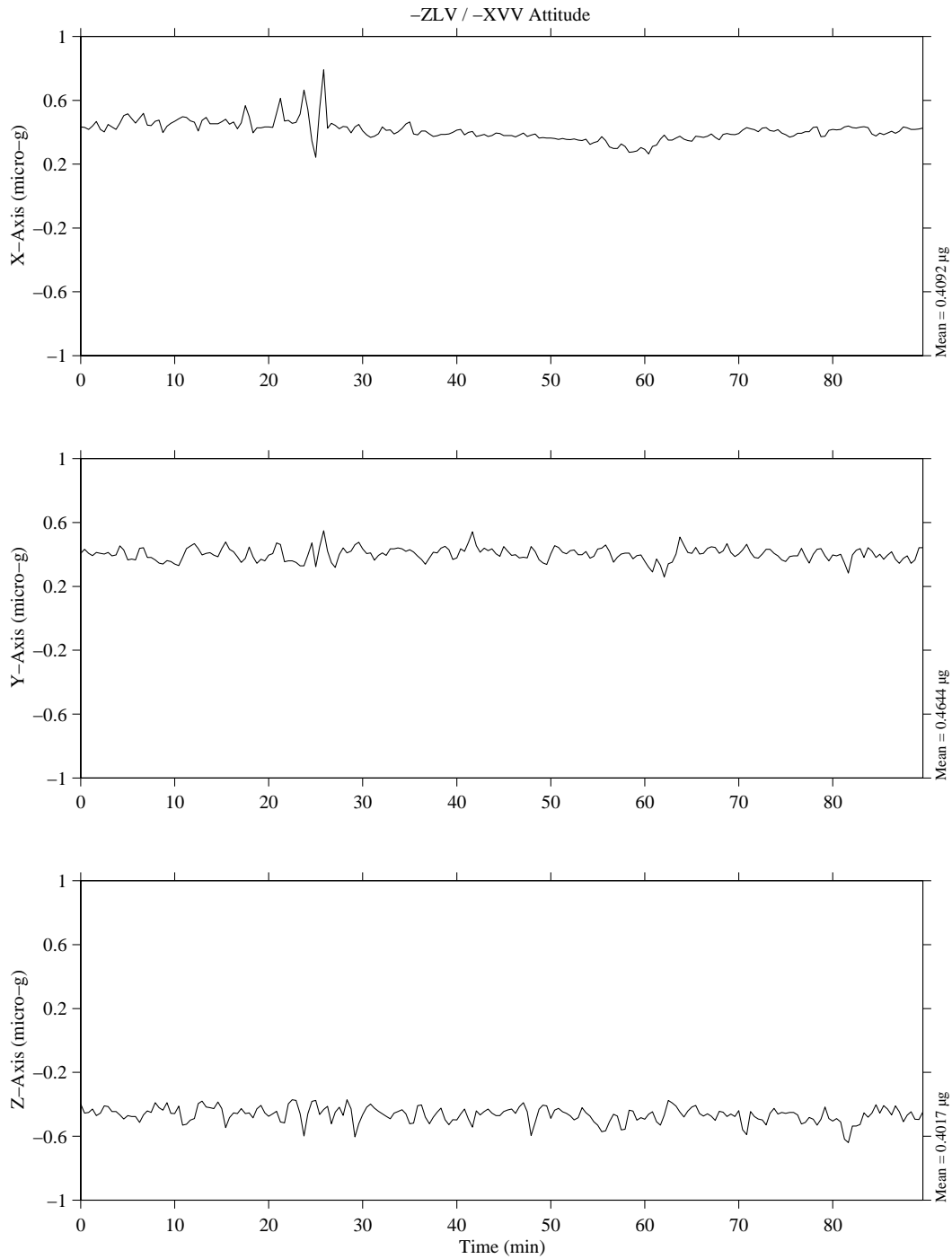
Figure 6.4 Time Series for -ZLV/-XVV Attitude during STS-107 Mission

PIMS STS-107 Mission Microgravity Environment Summary Report: January 16 to February 1, 2003

OARE, Trimmed Mean Filtered
OARE Location

MET Start at 001/18:00:15.840

Frame of Reference: Inertial
USMP-4
OARE Coordinates



MATLAB: 29-Oct-2003, 02:32 pm

Figure 6.5 Time Series for -ZLV/-XVV Attitude during USMP-4 Mission

PIMS STS-107 Mission Microgravity Environment Summary Report: January 16 to February 1, 2003

oare_mesatmf, mesaraw at STS-107, Cargo Bay:[1153.30 -1.30 317.80]
0.0625 sa/sec (0.01 Hz)

Increment: 0, Flight: STS-107
BODY[0.0 0.0 0.0]

Free Drift and Transition

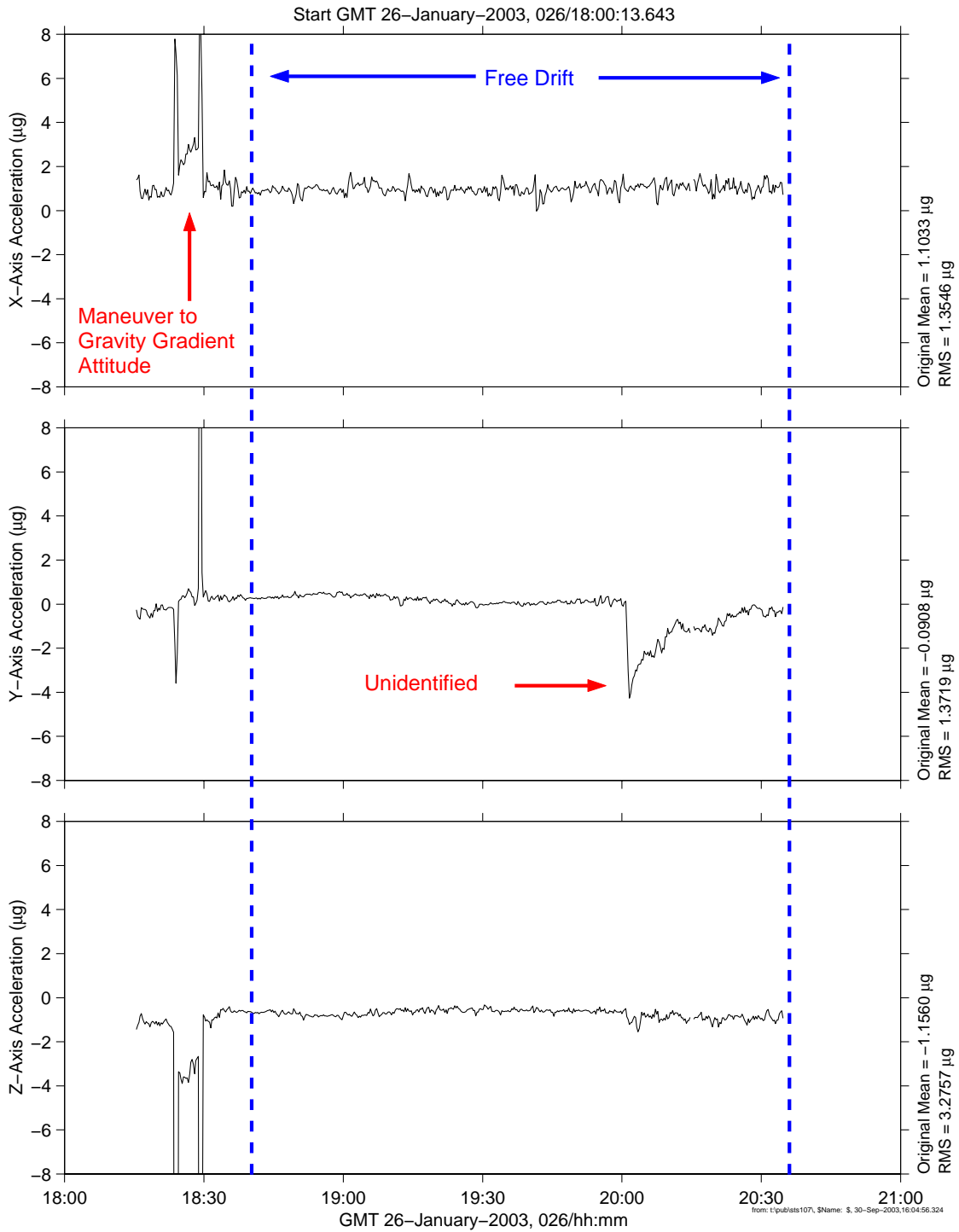


Figure 6.6 Time Series for Gravity Gradient Transition and Free Drift

**PIMS STS-107 Mission Microgravity Environment Summary Report:
January 16 to February 1, 2003**

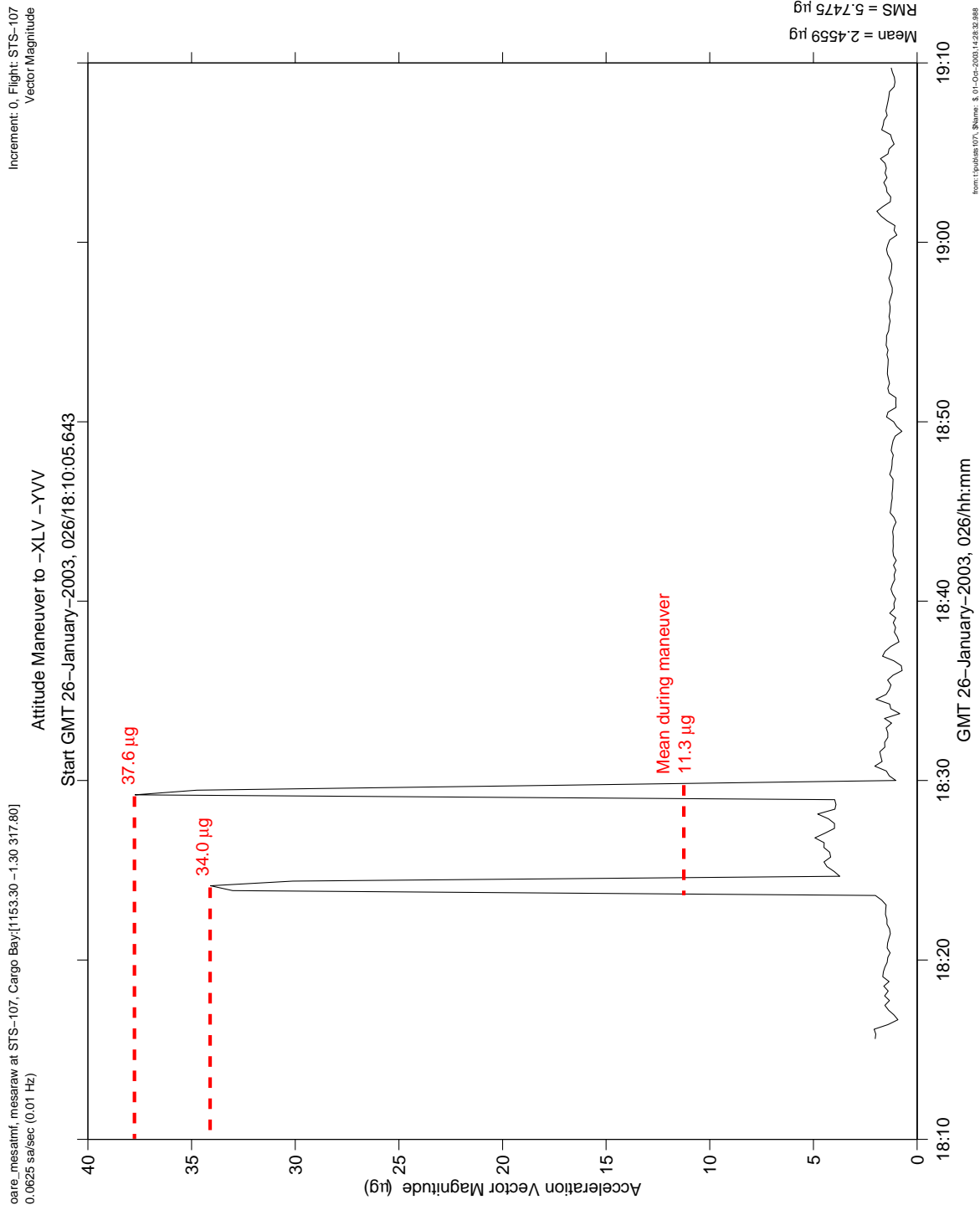


Figure 6-7 RSS for Maneuver to Gravity Gradient Attitude

PIMS STS-107 Mission Microgravity Environment Summary Report: January 16 to February 1, 2003

oare_mesatmf, mesatmf mapped to Center of CM-2 Chamber: [-919.80 -43.40 -395.90]
0.0625 sa/sec (0.01 Hz)

Increment: 0, Flight: STS-107
BODY[0.0 0.0 0.0]

SOFBALL Test Point 14A

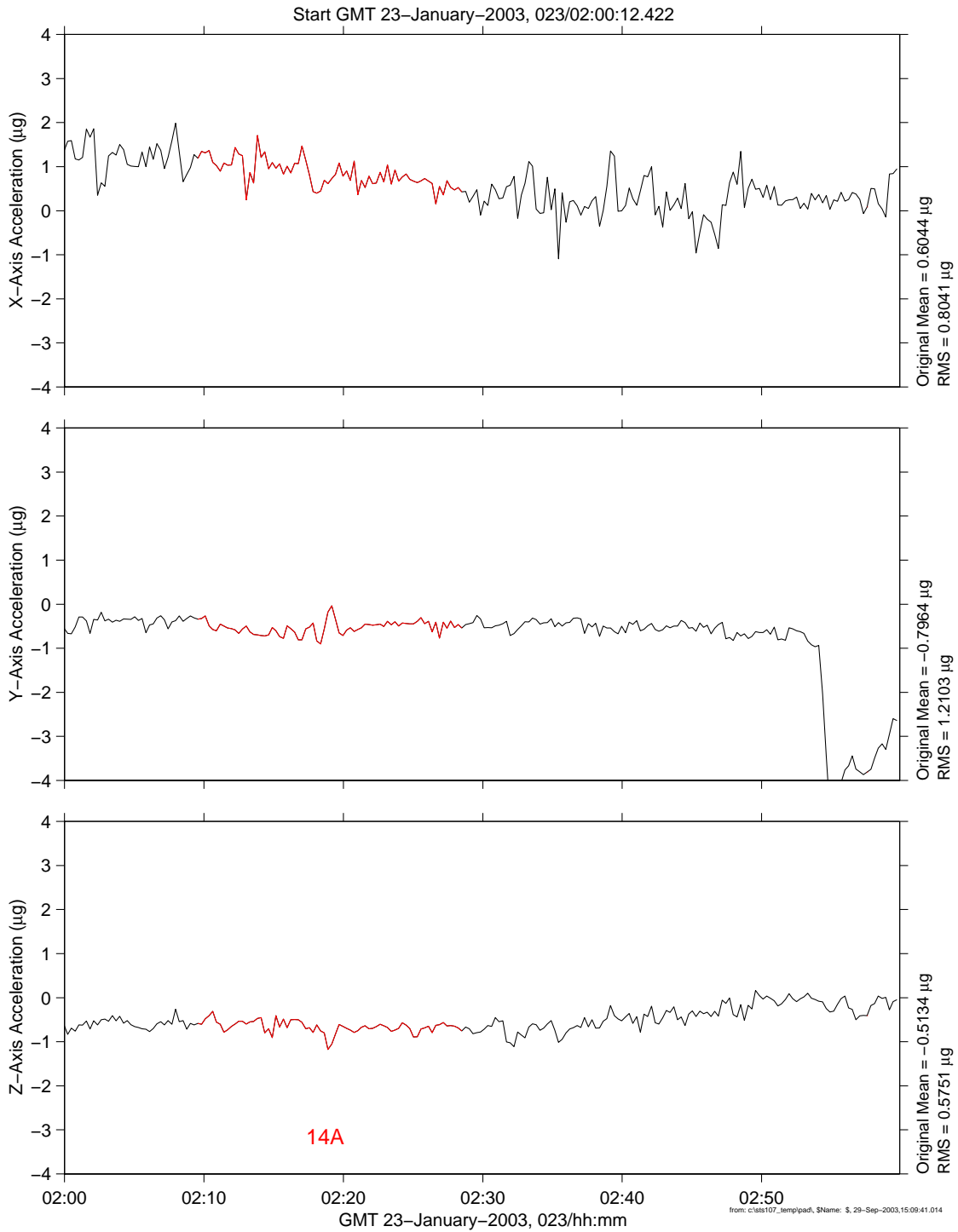


Figure 6.8 Time Series for SOFBALL Test Point 14A

PIMS STS-107 Mission Microgravity Environment Summary Report: January 16 to February 1, 2003

oare_mesatmf, mesatmf mapped to Center of CM-2 Chamber: [-919.80 -43.40 -395.90]
0.0625 sa/sec (0.01 Hz)

Increment: 0, Flight: STS-107
BODY[0.0 0.0 0.0]

SOFBALL Test Points 02A, 02B, 02C

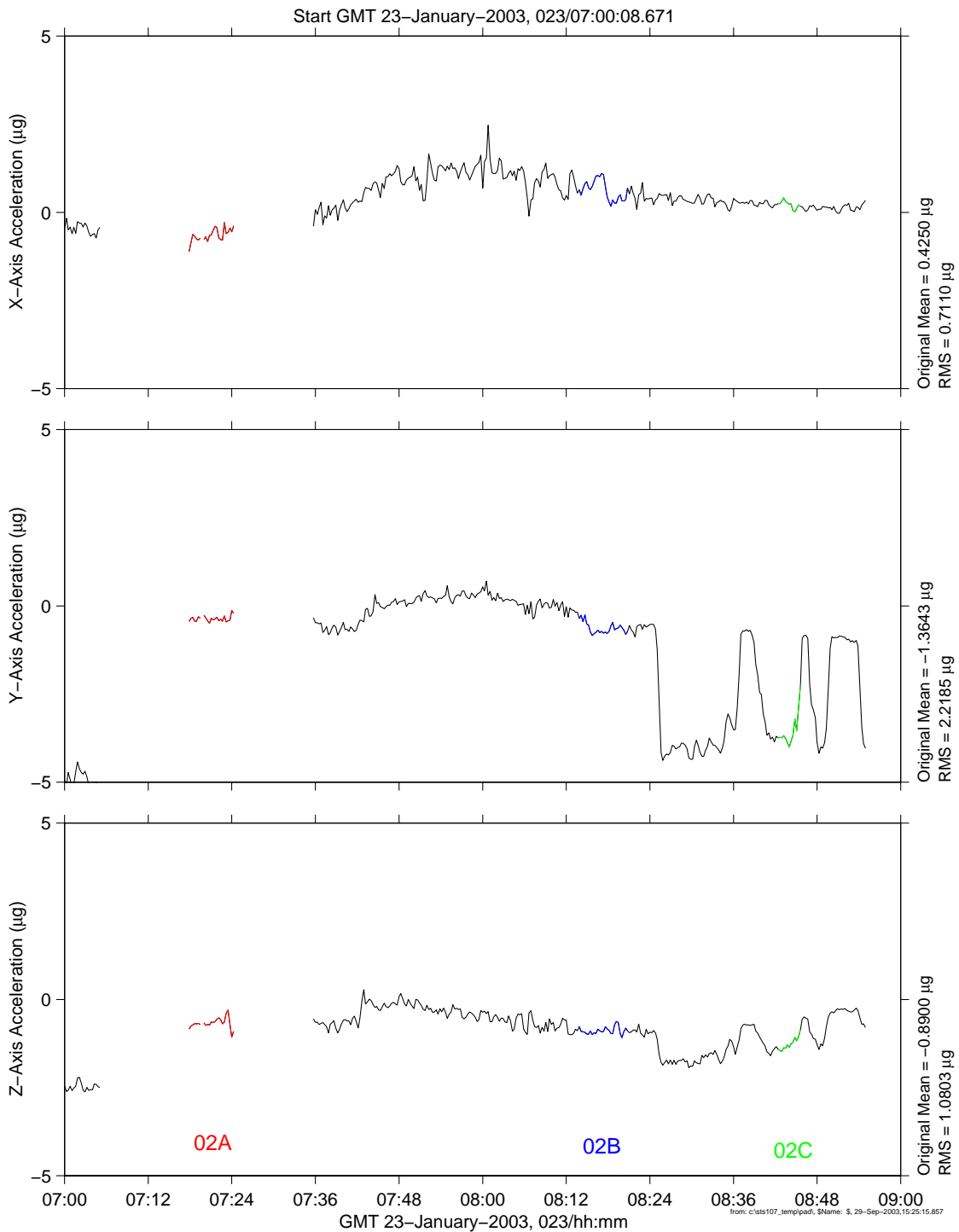


Figure 6.9 Time Series for SOFBALL Test Points 02A, 02B and 02C

PIMS STS-107 Mission Microgravity Environment Summary Report: January 16 to February 1, 2003

oare_mesatmf, mesatmf mapped to Center of CM-2 Chamber: [-919.80 -43.40 -395.90]
0.0625 sa/sec (0.01 Hz)

Increment: 0, Flight: STS-107
BODY[0.0 0.0 0.0]

SOFBALL Test Points 08A, 08B

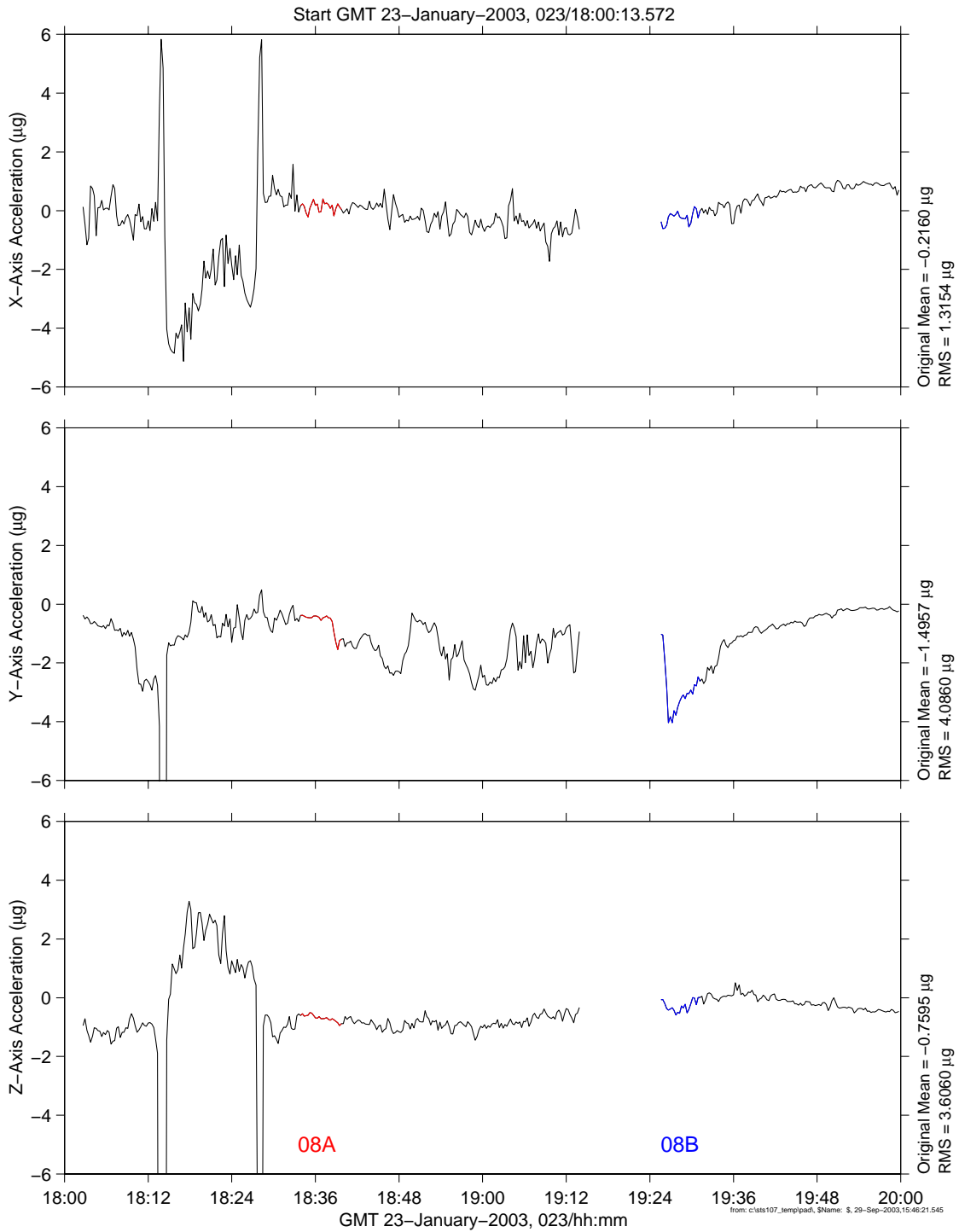


Figure 6.10 Time Series for SOFBALL Test Points 08A and 08B

PIMS STS-107 Mission Microgravity Environment Summary Report: January 16 to February 1, 2003

oare_mesatmf, mesatmf mapped to Center of CM-2 Chamber: [-919.80 -43.40 -395.90]
0.0625 sa/sec (0.01 Hz)

Increment: 0, Flight: STS-107
BODY[0.0 0.0 0.0]

SOFBALL Test Points 05A, 05B, 05M

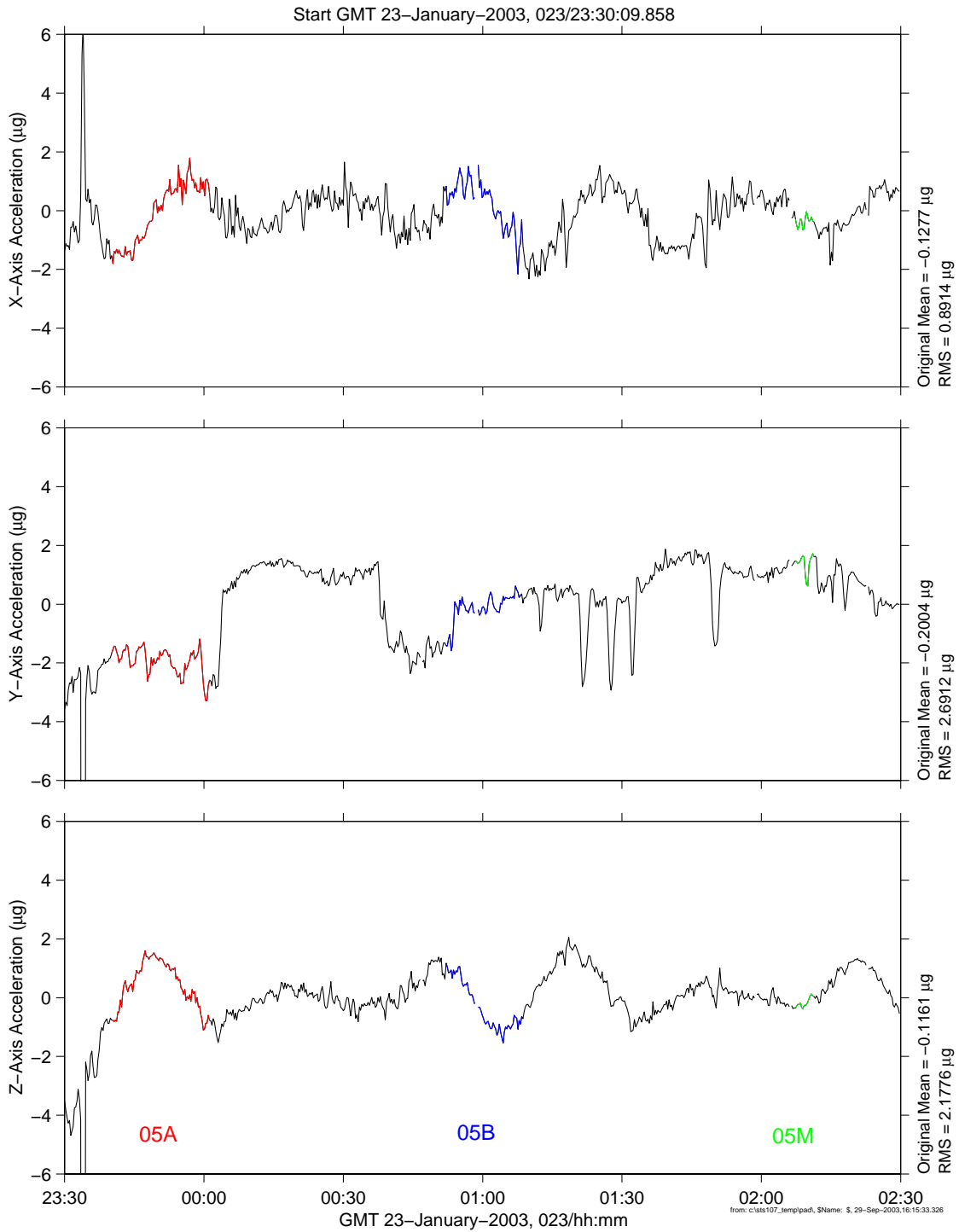


Figure 6.11 Time Series for SOFBALL Test Points 05A, 05B and 05M

PIMS STS-107 Mission Microgravity Environment Summary Report: January 16 to February 1, 2003

oare_mesatmf, mesatmf mapped to Center of CM-2 Chamber: [-919.80 -43.40 -395.90]
0.0625 sa/sec (0.01 Hz)

Increment: 0, Flight: STS-107
BODY[0.0 0.0 0.0]

SOFBALL Test Point 09A

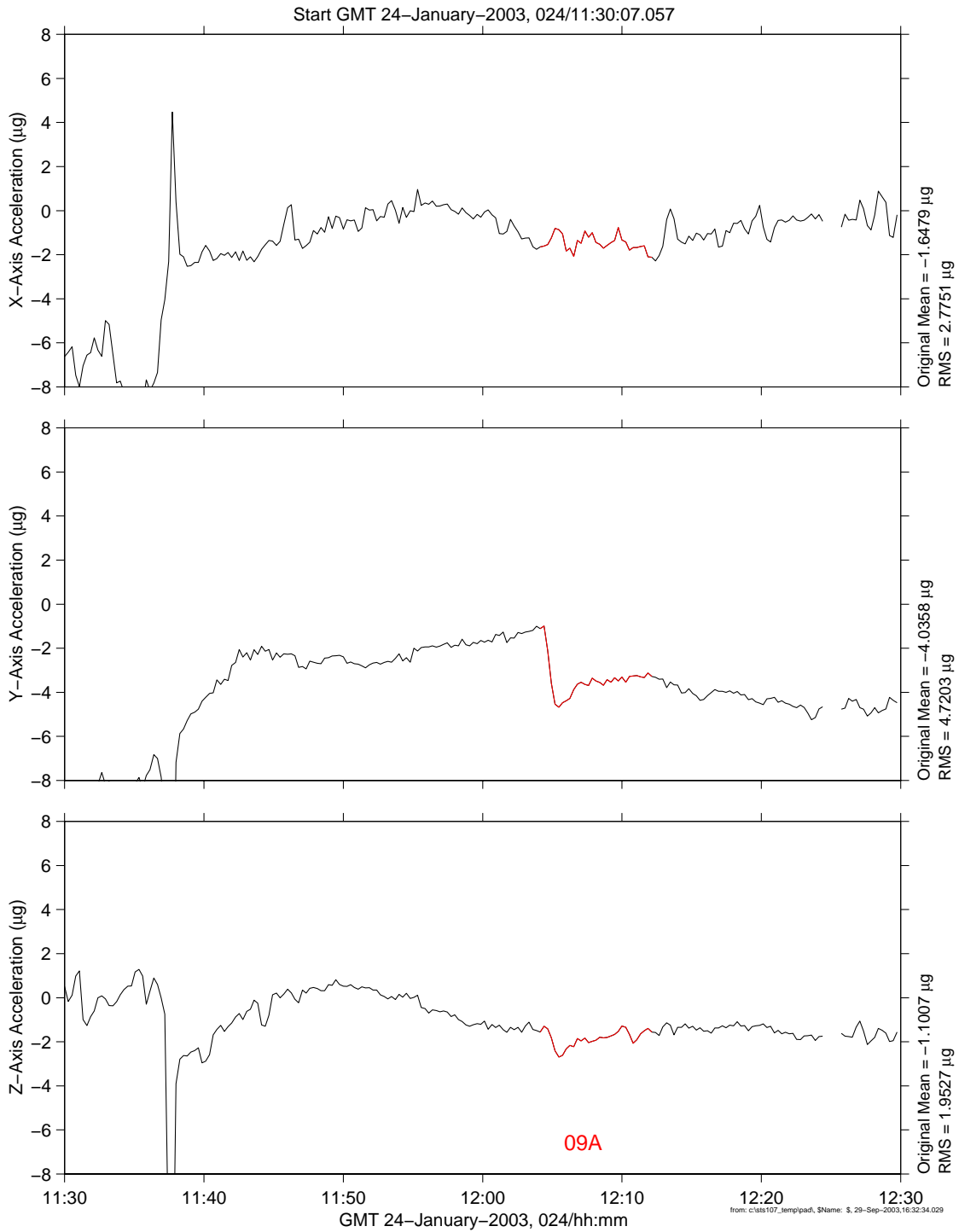


Figure 6.12 Time Series for SOFBALL Test Point 09A

PIMS STS-107 Mission Microgravity Environment Summary Report: January 16 to February 1, 2003

oare_mesatmf, mesatmf mapped to Center of CM-2 Chamber: [-919.80 -43.40 -395.90]
0.0625 sa/sec (0.01 Hz)

Increment: 0, Flight: STS-107
BODY[0.0 0.0 0.0]

SOFBALL Test Points 12A, 12B

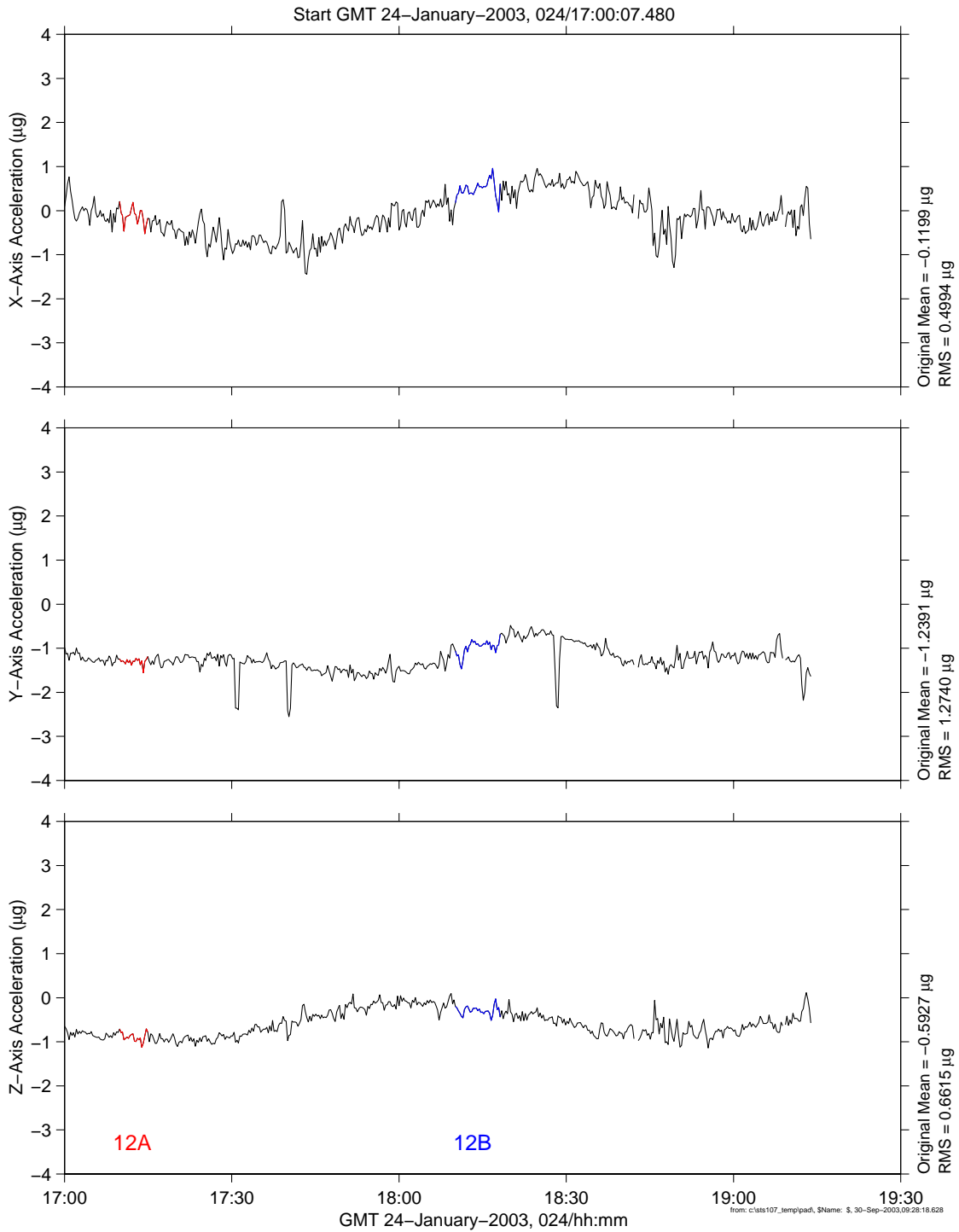


Figure 6.13 Time Series for SOFBALL Test Points 12A and 12B

PIMS STS-107 Mission Microgravity Environment Summary Report: January 16 to February 1, 2003

oare_mesatmf, mesatmf mapped to Center of CM-2 Chamber: [-919.80 -43.40 -395.90]
0.0625 sa/sec (0.01 Hz)

Increment: 0, Flight: STS-107
BODY[0.0 0.0 0.0]

SOFBALL Test Points 06A, 06B, 06C, 06D

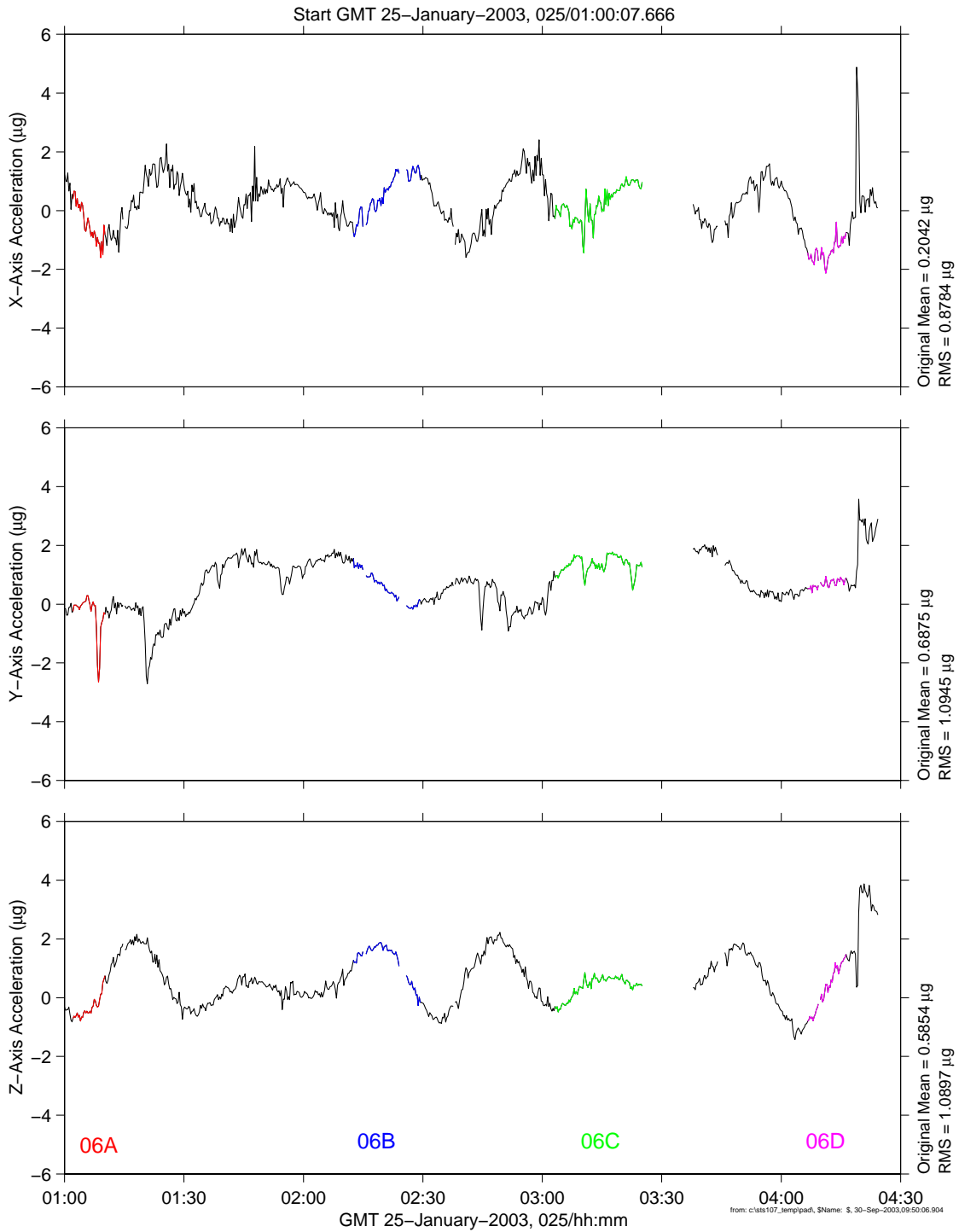


Figure 6.14 Time Series for SOFBALL Test Points 06A, 06B, 06C and 06D

PIMS STS-107 Mission Microgravity Environment Summary Report: January 16 to February 1, 2003

oare_mesatmf, mesatmf mapped to Center of CM-2 Chamber: [-919.80 -43.40 -395.90]
0.0625 sa/sec (0.01 Hz)

Increment: 0, Flight: STS-107
BODY[0.0 0.0 0.0]

SOFBALL Test Points 10B, 10C

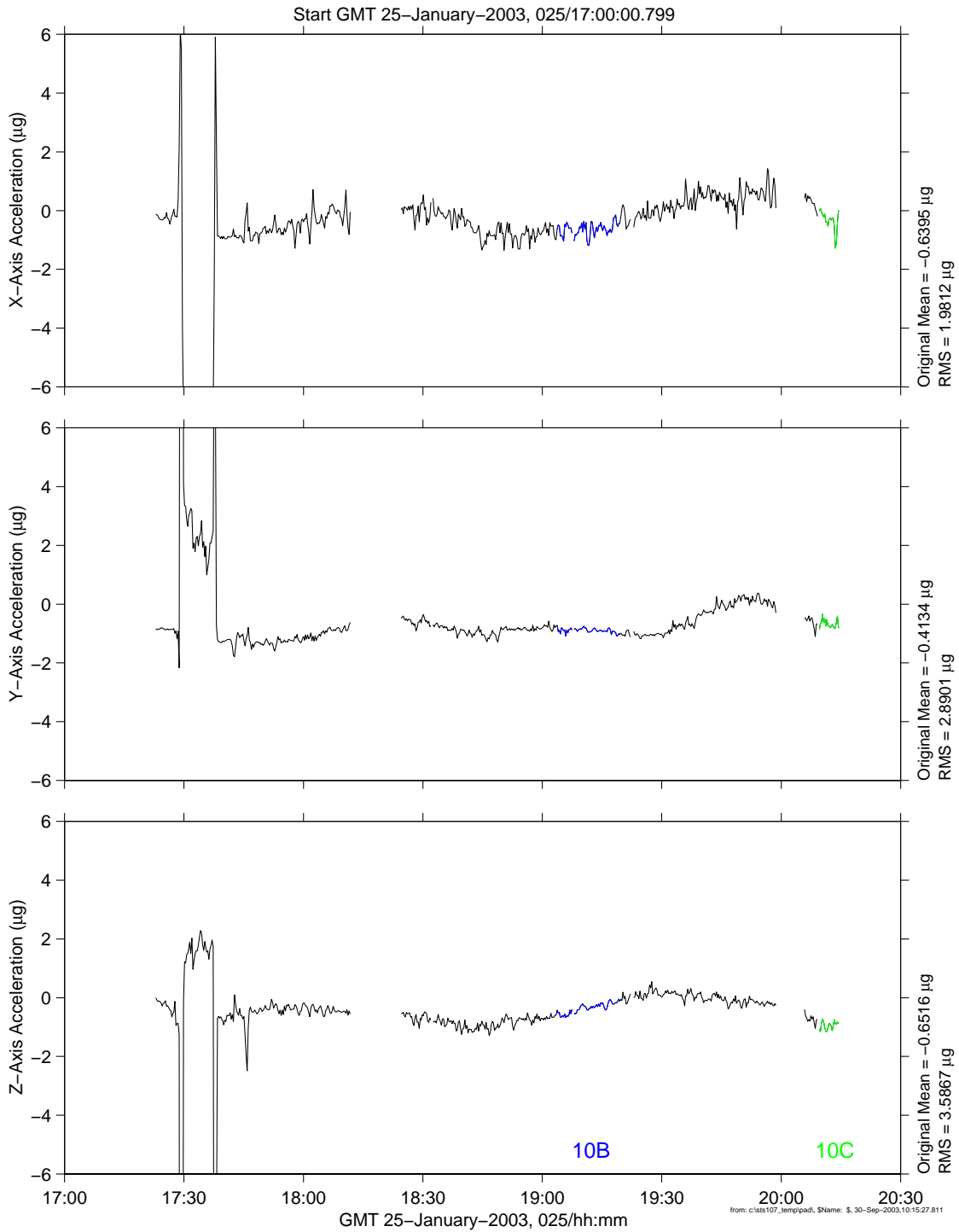


Figure 6.15 Time Series for SOFBALL Test Points 10B and 10C

PIMS STS-107 Mission Microgravity Environment Summary Report: January 16 to February 1, 2003

oare_mesatmf, mesatmf mapped to Center of CM-2 Chamber: [-919.80 -43.40 -395.90]
0.0625 sa/sec (0.01 Hz)

Increment: 0, Flight: STS-107
BODY[0.0 0.0 0.0]

SOFBALL Test Points 10M, 10N, 100

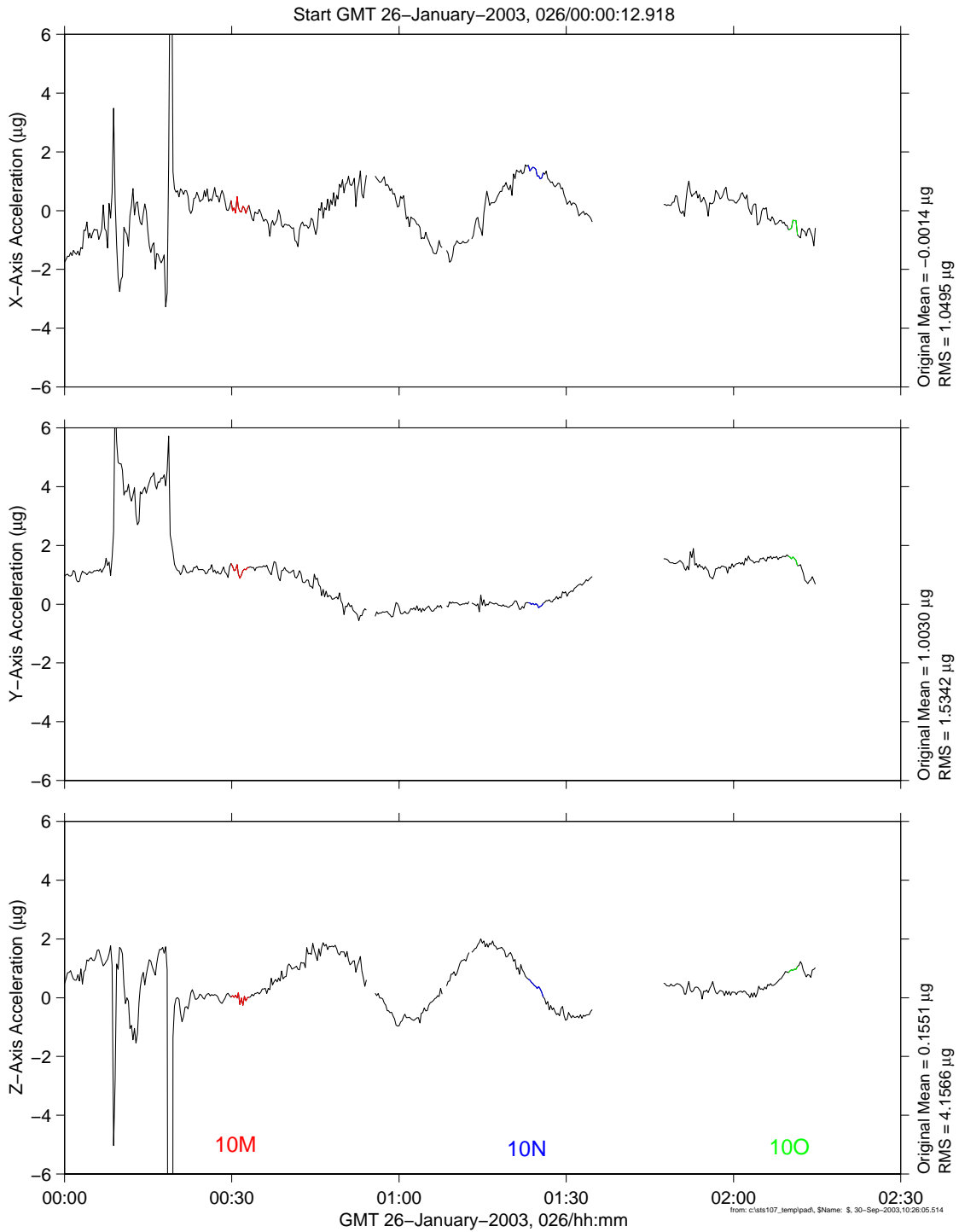


Figure 6.16 Time Series for SOFBALL Test Points 10M, 10N and 100

PIMS STS-107 Mission Microgravity Environment Summary Report: January 16 to February 1, 2003

oare_mesatmf, mesatmf mapped to Center of CM-2 Chamber: [-919.80 -43.40 -395.90]
0.0625 sa/sec (0.01 Hz)

Increment: 0, Flight: STS-107
BODY[0.0 0.0 0.0]

SOFBALL Test Points 04A, 04B, 04C

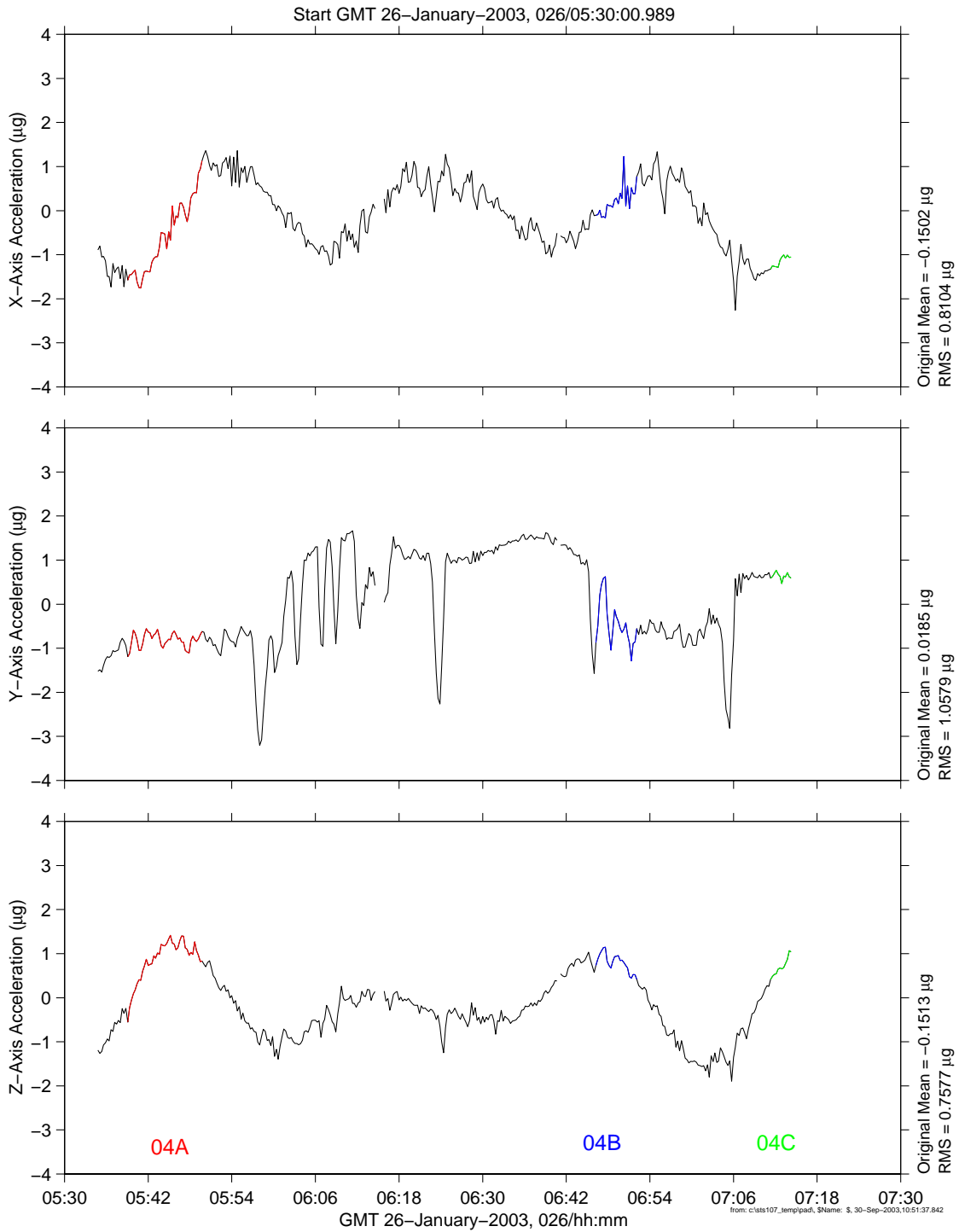


Figure 6.17 Time Series for SOFBALL Test Points 04A, 04B and 04C

PIMS STS-107 Mission Microgravity Environment Summary Report: January 16 to February 1, 2003

oare_mesatmf, mesatmf mapped to Center of CM-2 Chamber: [-919.80 -43.40 -395.90]
0.0625 sa/sec (0.01 Hz)

Increment: 0, Flight: STS-107
BODY[0.0 0.0 0.0]

SOFBALL Test Points 07A, 07B

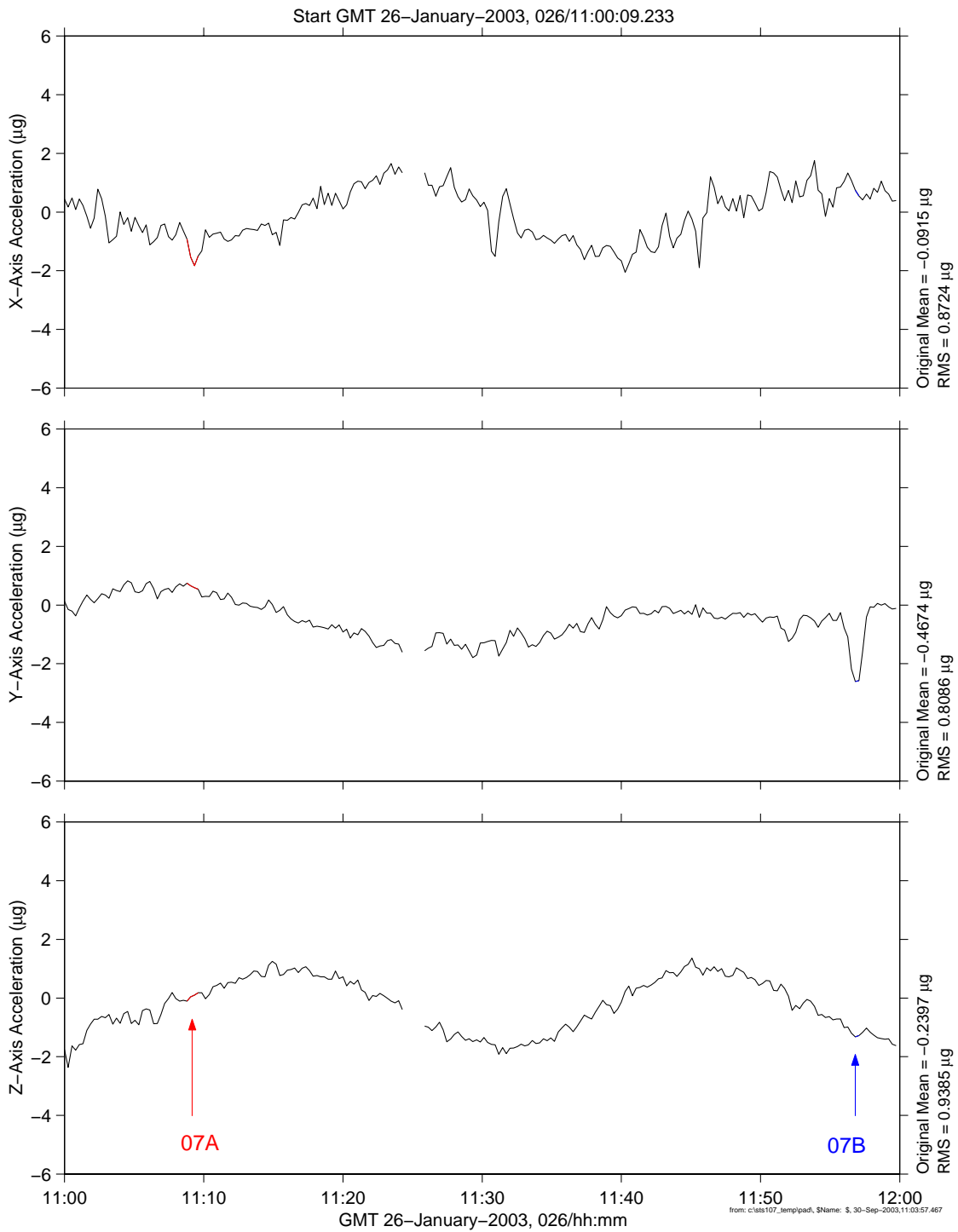


Figure 6.18 Time Series for SOFBALL Test Points 07A and 07B

PIMS STS-107 Mission Microgravity Environment Summary Report: January 16 to February 1, 2003

oare_mesatmf, mesatmf mapped to Center of CM-2 Chamber: [-919.80 -43.40 -395.90]
0.0625 sa/sec (0.01 Hz)

Increment: 0, Flight: STS-107
BODY[0.0 0.0 0.0]

SOFBALL Test Points 07C, 07D

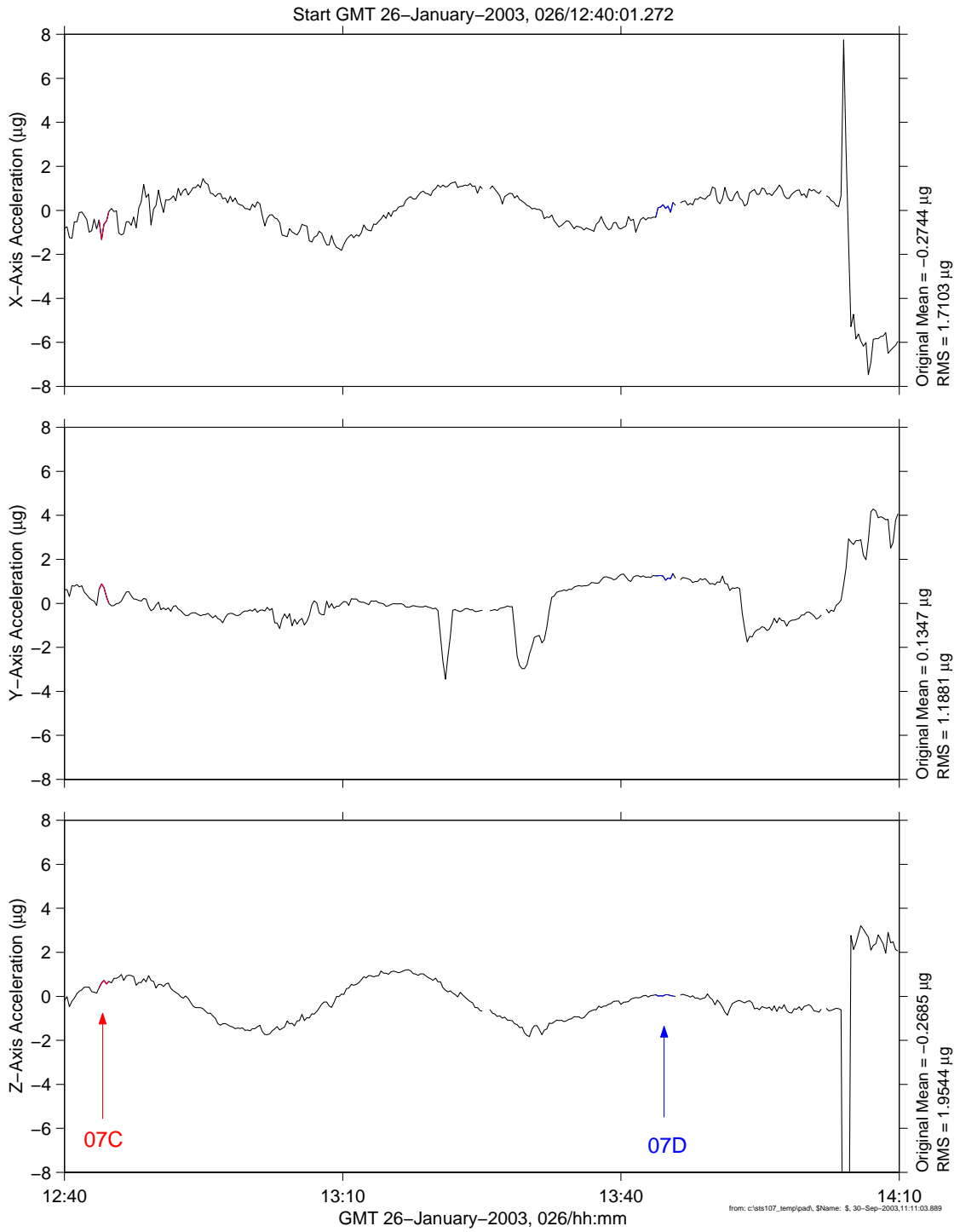


Figure 6.19 Time Series for SOFBALL Test Point 07C and 07D

PIMS STS-107 Mission Microgravity Environment Summary Report: January 16 to February 1, 2003

oare_mesatmf, mesatmf mapped to Center of CM-2 Chamber: [-919.80 -43.40 -395.90]
0.0625 sa/sec (0.01 Hz)

Increment: 0, Flight: STS-107
BODY[0.0 0.0 0.0]

SOFBALL Test Points 13A (1-4)

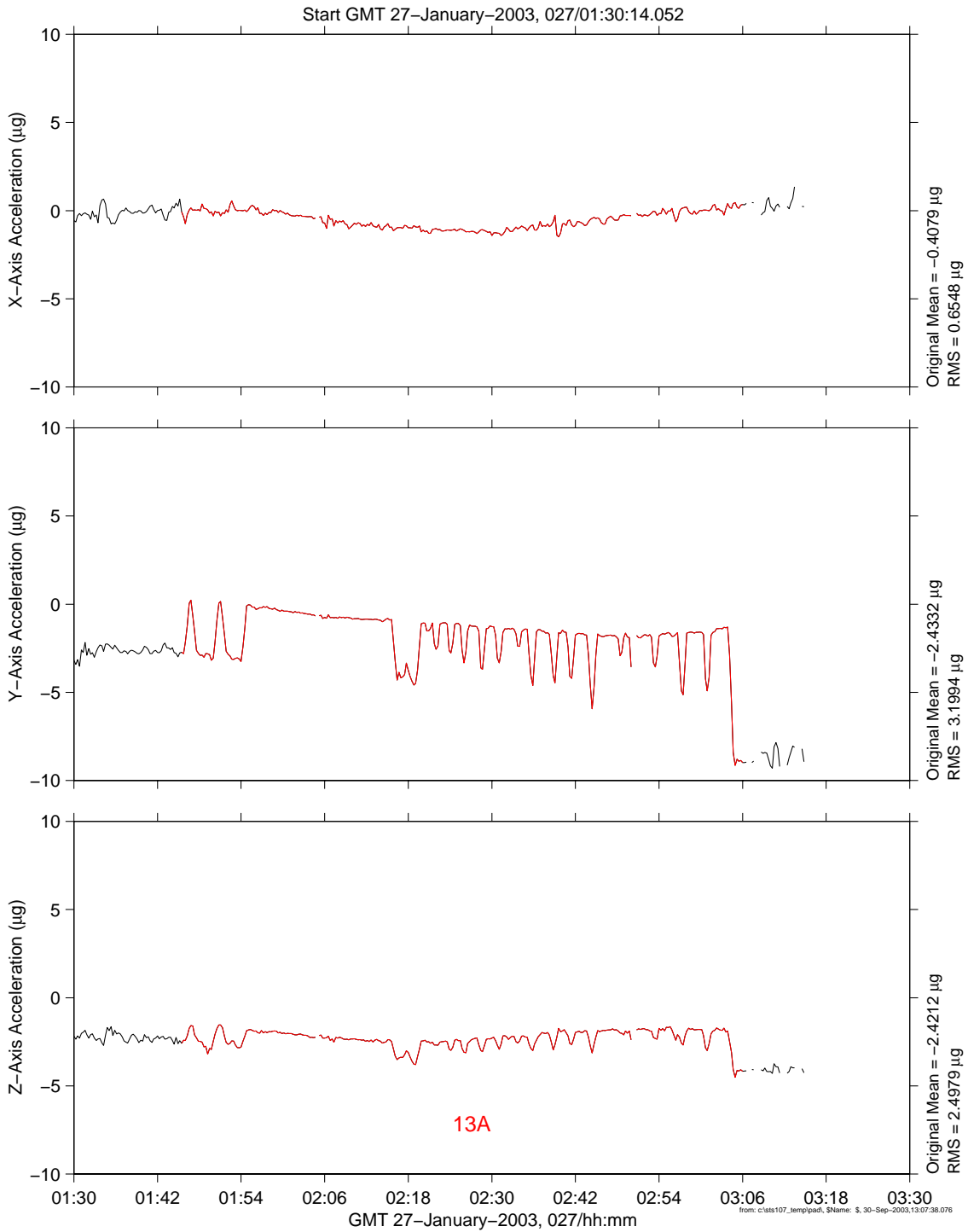


Figure 6.21 Time Series for SOFBALL Test Point 13A

**PIMS STS-107 Mission Microgravity Environment Summary Report:
January 16 to February 1, 2003**

6.2 Vibratory Microgravity Environment

The vibratory acceleration regime consists of the acceleration spectrum above about 0.01 Hertz (Hz), with magnitudes that can vary greatly depending on the nature of the disturbance source and on the transmissibility from the source to the location of interest. Higher frequency (vibratory) accelerations of this type are typically associated with experiment-related equipment, vehicle operations, vehicle systems, and crew activity.

This report examines vibratory accelerations as they relate to experiment operations in section 6.2.1. In section 6.2.2, we examine accelerations attributable to vehicle subsystems. The last major category of vibratory disturbances considered for this report is crew activity as discussed in section 6.2.3. The vibratory acceleration data analysis for this report was based on measurements made by the SAMS-FF TSH-11 sensor, which was located on the port side of the SPACEHAB module in the CM-2 rack about 2 feet behind the mid bulkhead (Figure 2.1C).

6.2.1 Experiment Operations

This section discusses the Enhanced Orbiter Refrigerator/Freezer (EORF) and experiment operations related to SOFBALL, Water Mist, LSP, Vapor Compression Distillation (VCD), Biobox, and MGM.

6.2.1.1 Enhanced Orbiter Refrigerator/Freezer (EORF)

The EORF provides a thermally conditioned environment for science experiments by means of a vapor compression refrigeration system. The EORF unit was housed on the aft bulkhead of the SPACEHAB module (position AC05 of Figure 2.1A). The vibratory measurements referred to throughout this report were collected near the CM-2 in SPACEHAB (see layout in Figure 2.1C to compare these locations).

To qualify the vibratory impact of the EORF, consider Figure 6.22. This 24-hour spectrogram shows a train of red horizontal streaks just above 21 Hz. This is the spectral signature of the EORF [11]. That is, these streaks indicate when the compressor was on. Examination of roadmap spectrograms generated for the entirety of the SAMS-FF vibratory data show that the duty cycle of this compressor varied throughout the mission with a trend toward being on for longer periods as the mission progressed.

To quantify the vibratory impact of the EORF, consider Figure 6.23. This 24-hour interval RMS plot also shows the on/off cycles and covers the frequency range from 20 to 22.6 Hz, which bounds the spectral deviations of the apparatus. Further analysis of these data reveals that when the EORF was on, the median RMS acceleration for this 24-hour period was about 235.0 μg_{RMS} and when it was off the median value was 27.8 μg_{RMS} .

Opportunity and convenience allowed characterization of an unknown disturbance during the same 24-hour period used to characterize the EORF above. This disturbance was pervasive

**PIMS STS-107 Mission Microgravity Environment Summary Report:
January 16 to February 1, 2003**

throughout much of the mission. This disturbance was narrowband at about 25.2 Hz with a median interval RMS value of 38.8 μg_{RMS} for the period shown in Figure 6.24.

6.2.1.2 Structure of Flame Balls at Low Lewis-Number

In the vibratory regime, the principal investigator for SOFBALL, Dr. Paul Ronney, expressed concern for short-duration, high-intensity events such as vehicle thruster firings during critical experiment operations. He conveyed this concern in the form of a leaky integrator algorithm as shown in the following e-mail excerpt:

```

We could have something like an integrator with discharge time, like a leaky capacitor. In that
way, the noise of SAMS won't lead to a false alarm, but will still be able to detect short-
duration, high-intensity events like VRCS firings. That is, we could have a routine like this:

Impulse = 0                                (total impulse = 0 at start of test)

Loop until test over:
Impulse = Impulse + g(t)*Delta_t           (add contribution at current timestep)
If Impulse > Max then Gosub Alert          (Raise flag if impulse budget exceeded)
Impulse = Impulse*(1 - Discharge*Delta_t)  (Here Discharge is a constant whose value is perhaps
                                           0.1/sec, so that noise is bled off over a period of 10
                                           sec)
End loop

```

To better understand the realization of this algorithm, let's call the variable "Impulse" just before the "if" statement uppercase V, and the one after the "if" statement lowercase v. Also, let the parenthetic term just before the "End loop" be called uppercase P; where $P = (1-D\Delta t) = (1-D/f_s) = 0.999$. This comes from the discharge parameter, $D = 0.1/\text{second}$ and $\Delta t = 1/f_s = 1/100 = 0.01$ second. We can write a few iterations of this algorithm in sequence to show this:

$$\begin{aligned}
 v_0 &= 0 \\
 v_1 &= (v_0 + a_1\Delta t)P = Pa_1\Delta t \\
 v_2 &= (v_1 + a_2\Delta t)P = Pv_1 + Pa_2\Delta t \\
 v_3 &= (v_2 + a_3\Delta t)P = Pv_2 + Pa_3\Delta t
 \end{aligned}$$

where $a_i = i^{\text{th}}$ acceleration magnitude and $v_i = i^{\text{th}}$ velocity magnitude, which we will compare to the velocity threshold of 50 $\mu\text{g} \cdot \text{sec}$. We compare lowercase v (and not uppercase V) to the desired threshold (note that since $P = 0.999$, lowercase v is nearly identical to uppercase V). Also, we can generalize the output sequence like so:

$$v_k = (v_{k-1} + a_k\Delta t)P = Pv_{k-1} + Pa_k\Delta t \tag{Eq. 1}$$

This is the difference equation for a first-order recursive digital filter. To derive the transfer function using the z-transform, proceed as in Example 3.10 of [12] to get:

$$H(z) = P\Delta t / (1 - Pz^{-1}) \tag{Eq. 2}$$

**PIMS STS-107 Mission Microgravity Environment Summary Report:
January 16 to February 1, 2003**

This has the form of a single-pole lowpass filter, which can be implemented in our processing software much more efficiently than the algorithmic loop suggested above. The actual implementation is discussed further below.

The velocity output of this algorithm is the weighted (leaky) integration of the acceleration input as shown here:

$$v_n = P^n a_0 \Delta t + P^{n-1} a_1 \Delta t + \dots + P^2 a_{n-2} \Delta t + P a_{n-1} \Delta t \quad \text{Eq. 3}$$

The “leakiness” in this integration stems from the fact that P is less than one, so raising this value of P to a large exponent results in a relatively small number. Therefore, older acceleration inputs are weighted less than recent ones. The older the acceleration value, the smaller it is weighted in this summation¹. Another way to look at this is the output is a weighted (or scaled) mean of the input. In this light, it is easy to see that the input should not be the acceleration magnitude (particularly for vibratory acceleration data when the threshold is 50 µg *sec). For example, when a lab refrigerator or other equipment is on, the average acceleration magnitude (with a cutoff of 25 Hz) can easily surpass 100 µg. It was agreed during a telecom with the SOFBALL team on 3/29/00 that we would implement this algorithm on the 3 orthogonal components of the acceleration. Then, the root-sum-of-squares of these results yields resultant velocity magnitude as a function of time. This is the quantity that was compared to the SOFBALL threshold of 50 µg *sec in the figures referenced in Table 6.6 below.

TABLE 6.6 LEAKY INTEGRATION OF SAMS-FF FOR SOFBALL TEST POINTS

Test Point Done	GMT Start	GMT End	Velocity Magnitude (µg · sec)		See
			Mean	Max	
14A	23-Jan-2003,02:09:36	23-Jan-2003,02:29:00	12.0	55.2	Figure 6.25
14B (14A reburn)	23-Jan-2003,02:57:41	23-Jan-2003,02:57:52	11.2	19.7	no plot
02A	23-Jan-2003,07:17:49	23-Jan-2003,07:30:38	9.8	72.2	Figure 6.26
02B (02A reburn)	23-Jan-2003,08:13:59	23-Jan-2003,08:21:06	9.6	42.8	Figure 6.27
02C (02B return)	23-Jan-2003,08:42:27	23-Jan-2003,08:45:57	5.6	29.6	Figure 6.28
03A	23-Jan-2003,14:33:07	23-Jan-2003,14:37:19	10.1	96.9	Figure 6.29
08A	23-Jan-2003,18:33:55	23-Jan-2003,18:40:09	7.8	32.7	Figure 6.30
08B	23-Jan-2003,19:24:19	23-Jan-2003,19:31:33	9.3	366.6	Figure 6.31
05A	23-Jan-2003,23:40:15	24-Jan-2003,00:01:29	12.9	101.1	Figure 6.32
05B	24-Jan-2003,00:52:14	24-Jan-2003,01:08:41	16.1	78.3	Figure 6.33
05M	24-Jan-2003,02:07:22	24-Jan-2003,02:11:33	10.5	51.6	Figure 6.34
09A	24-Jan-2003,12:04:10	24-Jan-2003,12:12:24	13.8	204.9	Figure 6.35
09B (09A reburn)	24-Jan-2003,13:07:12	24-Jan-2003,13:11:26	13.2	56.5	Figure 6.36

¹ If P = 1 (that is D = 1/Δt), then we would use memory of all and the output velocity would simply be an integration of the acceleration input.

**PIMS STS-107 Mission Microgravity Environment Summary Report:
January 16 to February 1, 2003**

TABLE 6.6 LEAKY INTEGRATION OF SAMS-FF FOR SOFBALL TEST POINTS

Test Point Done	GMT Start	GMT End	Velocity Magnitude ($\mu\text{g} \cdot \text{sec}$)		See
			Mean	Max	
12A	24-Jan-2003,17:09:50	24-Jan-2003,17:15:04	8.6	32.2	Figure 6.37
12B	24-Jan-2003,18:10:13	24-Jan-2003,18:18:26	7.4	36.0	Figure 6.38
12O	24-Jan-2003,19:18:58	24-Jan-2003,19:19:42	7.5	18.9	no plot
06A	25-Jan-2003,01:02:05	25-Jan-2003,01:10:26	14.5	84.1	Figure 6.39
06B	25-Jan-2003,02:12:32	25-Jan-2003,02:29:12	9.4	45.5	Figure 6.40
06C	25-Jan-2003,03:03:18	25-Jan-2003,03:28:17	8.5	53.6	Figure 6.41
06D	25-Jan-2003,04:06:42	25-Jan-2003,04:16:27	10.6	46.4	Figure 6.42
11B	25-Jan-2003,11:54:16	25-Jan-2003,12:06:01	15.1	67.9	Figure 6.43
11C	25-Jan-2003,12:59:12	25-Jan-2003,13:07:32	7.7	35.3	Figure 6.44
10A	25-Jan-2003,17:47:43	25-Jan-2003,17:47:47	5.9	15.0	no plot
10B	25-Jan-2003,19:03:38	25-Jan-2003,19:19:38	8.4	34.1	Figure 6.45
10C	25-Jan-2003,20:09:23	25-Jan-2003,20:16:13	11.5	54.7	Figure 6.46
10M	26-Jan-2003,00:29:55	26-Jan-2003,00:33:20	12.7	47.7	Figure 6.47
10N	26-Jan-2003,01:23:10	26-Jan-2003,01:26:10	9.1	59.7	Figure 6.48
10O	26-Jan-2003,02:09:57	26-Jan-2003,02:11:47	8.8	34.5	Figure 6.49
04A	26-Jan-2003,05:38:49	26-Jan-2003,05:49:49	9.3	43.0	Figure 6.50
04B	26-Jan-2003,06:46:03	26-Jan-2003,06:52:13	11.7	51.6	Figure 6.51
04C	26-Jan-2003,07:11:09	26-Jan-2003,07:17:54	9.0	32.7	Figure 6.52
07A	26-Jan-2003,11:08:55	26-Jan-2003,11:09:55	10.3	25.4	no plot
07B	26-Jan-2003,11:56:46	26-Jan-2003,11:57:26	13.6	45.7	no plot
07C	26-Jan-2003,12:43:30	26-Jan-2003,12:45:00	22.1	60.3	Figure 6.53
07D	26-Jan-2003,13:43:45	26-Jan-2003,13:45:45	8.3	29.1	Figure 6.54
07E	26-Jan-2003,14:03:50	26-Jan-2003,14:04:00	7.4	14.2	no plot
14M	26-Jan-2003,18:34:08	26-Jan-2003,18:47:23	8.2	41.8	Figure 6.55
14N	26-Jan-2003,19:32:00	26-Jan-2003,19:42:00	11.7	60.8	Figure 6.56
13A (1 of 4)	27-Jan-2003,01:45:27	27-Jan-2003,02:05:27	8.2	110.7	Figure 6.57
13A (2 of 4)	27-Jan-2003,02:05:27	27-Jan-2003,02:25:27	8.8	65.1	Figure 6.58
13A (3 of 4)	27-Jan-2003,02:25:27	27-Jan-2003,02:45:27	9.2	67.7	Figure 6.59
13A (4 of 4)	27-Jan-2003,02:45:27	27-Jan-2003,03:06:27	8.6	255.7	Figure 6.60

Note from Table 6.6 that short spans were analyzed, but not plotted. Also, rows for test points that had a maximum value above the SOFBALL threshold of $50 \mu\text{g} \cdot \text{sec}$ are shaded in the table. For contrast, compare the free drift portion of Figure 6.61 (the first 4 minutes 12 seconds indicated by the blue horizontal line) to the portion after that when the Vernier Reaction Control System (VCRS) thrusters were being used for attitude control. The (•) dots along the top of the figure correspond to firings of some combination of the six VCRS jets labeled R5D, R5R, L5L, L5D, F5R, and F5L [18]. These dot markers come from the Operational Data Retrieval Complex (ODRC) data that were gathered to indicate precisely when those thruster jets were fired. As

**PIMS STS-107 Mission Microgravity Environment Summary Report:
January 16 to February 1, 2003**

expected, numerous and closely-timed thruster firings would have resulted in undesirable conditions as shown by the threshold breach after the SOFBALL run had ended, when the velocity magnitude went well over 1,000 $\mu\text{g} \cdot \text{sec}$.

A crude yet telling method of spectrally quantifying a comparison for 3 cases of interest is shown in Figure 6.64. The red trace was computed from acceleration measurements collected before the free drift that accompanied SOFBALL test point 12B. The green and blue traces were computed from data collected during and after the free drift, respectively. The free drift (green) trace is expectedly lower owing primarily to the lack of thruster firing activity. On the other hand, coming out of free drift calls for a number of thruster firings to acquire and maintain a desired attitude. This is reflected in the heightened level of the blue trace, especially below 5 Hz. The large steps in all 3 curves at 17 Hz show the Ku-band antenna dithering disturbance (see section 6.2.2.1), while the huge step at about 21 Hz on the blue trace reflects EORF activity (see section 6.2.1.1 for more details).

6.2.1.3 Water Mist Fire-Suppression Experiment (*Mist*)

Analysis similar to that described above in section 6.2.1.2 was performed for the 32 Mist test points shown in Table 6.7.

TABLE 6.7 LEAKY INTEGRATION OF SAMS-FF FOR MIST TEST POINTS

Test Point	GMT Start	GMT End	Velocity Magnitude ($\mu\text{g} \cdot \text{sec}$)		Δt (sec)	See
			Mean	Max		
1 - 61M	28-Jan-2003,21:50:10	28-Jan-2003,22:04:10	21.9	196.3	12	Figure 6.65
2 - 22M	28-Jan-2003,23:34:19	28-Jan-2003,23:54:19	21.1	275.3	23.3	Figure 6.66
3 - 23M	29-Jan-2003,00:36:14	29-Jan-2003,01:01:14	12.8	278.9	11.6	Figure 6.67
4 - 24M	29-Jan-2003,01:35:16	29-Jan-2003,01:50:16	11.4	247.7	15.3	Figure 6.68
5 - 25M	29-Jan-2003,04:01:13	29-Jan-2003,04:47:13	12.4	250.9	15.4	no plot
6 - 27M	29-Jan-2003,05:31:16	29-Jan-2003,05:59:16	11.3	164.4	8.2	no plot
7 - 29M	29-Jan-2003,09:06:12	29-Jan-2003,09:36:12	20.1	129.3	8.6	no plot
8 - 01M	29-Jan-2003,10:21:08	29-Jan-2003,10:34:08	16.2	103.8	5.2	Figure 6.69
9 - 26M	29-Jan-2003,11:47:07	29-Jan-2003,12:27:07	25.5	434.4	22.6	no plot
10 - 68M	29-Jan-2003,14:02:12	29-Jan-2003,14:45:12	71.5	697.5	58.9	no plot
11 - 69M	29-Jan-2003,15:21:18	29-Jan-2003,15:41:18	20.2	342.8	18.4	Figure 6.70
12 - 34M	29-Jan-2003,16:11:38	29-Jan-2003,16:39:38	9.9	51	0 ²	no plot
13 - 30M	29-Jan-2003,16:58:16	29-Jan-2003,17:19:16	17.7	316.8	15.2	Figure 6.71
14 - 32M	29-Jan-2003,19:51:18	29-Jan-2003,20:31:18	15.4	256.1	15.7	no plot
15 - 36M	29-Jan-2003,21:06:16	29-Jan-2003,21:35:16	20.5	313.6	15.9	no plot
16 - 76M	29-Jan-2003,22:17:16	29-Jan-2003,22:31:16	15.9	90.3	4.3	Figure 6.72

² A duration of zero seconds for this test point indicates a single data point above the threshold. This “zero duration” breach happened twice for this test point, both at about GMT 29-Jan-2003, 029/16:28:28.

**PIMS STS-107 Mission Microgravity Environment Summary Report:
January 16 to February 1, 2003**

TABLE 6.7 LEAKY INTEGRATION OF SAMS-FF FOR MIST TEST POINTS

Test Point	GMT Start	GMT End	Velocity Magnitude ($\mu\text{g} \cdot \text{sec}$)		Δt (sec)	See
			Mean	Max		
17 - 41M	30-Jan-2003,05:09:29	30-Jan-2003,05:33:29	16.9	243.4	14.7	Figure 6.73
18 - 03M	30-Jan-2003,07:11:07	30-Jan-2003,07:54:07	43.3	339.7	28.5	no plot
19 - 02M	30-Jan-2003,08:49:12	30-Jan-2003,09:24:12	112.6	782.3	108.2	no plot
20 - 44M	30-Jan-2003,10:32:22	30-Jan-2003,10:45:22	25	339.1	18.7	Figure 6.74
21 - 07M	30-Jan-2003,12:06:19	30-Jan-2003,12:34:19	13.8	131.8	8.8	no plot
22 - 05M	30-Jan-2003,13:03:19	30-Jan-2003,13:25:19	14.6	108	1.7	Figure 6.75
23 - 49aM	30-Jan-2003,15:10:26	30-Jan-2003,15:25:26	20.3	243.9	14.7	Figure 6.76
24 - 95M	30-Jan-2003,16:29:41	30-Jan-2003,16:43:41	13.4	160.2	13.4	Figure 6.77
25 - 97M	30-Jan-2003,18:12:26	30-Jan-2003,18:36:26	16.8	210.3	13.6	Figure 6.78
26 - 99M	30-Jan-2003,20:02:10	30-Jan-2003,20:28:10	16.8	216.3	13.8	no plot
27 - 46M	31-Jan-2003,00:38:34	31-Jan-2003,01:14:34	19.1	322.2	15.3	no plot
28 - 80M	31-Jan-2003,01:41:17	31-Jan-2003,01:54:17	19.5	172.4	9.2	Figure 6.79
29 - 10M	31-Jan-2003,02:31:31	31-Jan-2003,02:46:31	14.3	200.9	11.6	Figure 6.80
30 - 50M	31-Jan-2003,03:59:15	31-Jan-2003,04:22:15	19.7	394.1	21.4	Figure 6.81
31 - 49bM	31-Jan-2003,05:32:07	31-Jan-2003,05:58:07	15.4	177.5	12.7	no plot
32 - 49cM	31-Jan-2003,06:25:14	31-Jan-2003,06:41:14	16.9	200.3	10.4	Figure 6.82

Test points that had long time spans were analyzed, but not plotted. This was a matter of how much data was practical to fit on the printed page. In addition to mean and maximum statistics, a maximum duration (Δt) is reported for each test point. This shows the largest contiguous span for which the velocity magnitude was above a threshold of $50 \mu\text{g} \cdot \text{sec}$ in the test point's time period. Two notable test point periods stand out in Table 6.7. Test point 12-34M was the most favorable in terms of velocity magnitude, while test point 19-02M was the least favorable. This can be explained with excerpts of the as-flown timeline produced after the mission. The excerpt in Figure 6.83 shows relatively few thruster firings compared to that of Figure 6.84 for the Mist test points under consideration.

6.2.1.4 Laminar Soot Processes (LSP)

Vibratory acceleration data information for the four LSP test points is shown in Table 6.8. The "Acceleration Peak" column shows the maximum acceleration vector magnitude measured during the indicated GMT span. The figures referenced in the last column show measured data.

**PIMS STS-107 Mission Microgravity Environment Summary Report:
January 16 to February 1, 2003**

TABLE 6.8 ACCELERATION DURING LSP TEST POINTS

Test Point	GMT Start	GMT End	Acceleration Peak (mg)	See
41e	19-Jan-2003,14:08:23	19-Jan-2003,14:13:38	1.63	Figure 6.85
04e	20-Jan-2003,00:13:06	20-Jan-2003,00:16:56	4.36	Figure 6.86
08p	20-Jan-2003,23:22:03	20-Jan-2003,23:27:19	5.64	Figure 6.87
53e	21-Jan-2003,18:47:15	21-Jan-2003,18:49:06	5.66	Figure 6.88

Analysis similar to that described above (in section 6.2.1.2) was also performed for the LSP test points as presented in Table 6.9.

TABLE 6.9 LEAKY INTEGRATION OF SAMS-FF FOR LSP TEST POINTS

Test Point	GMT Start	GMT End	Velocity Magnitude ($\mu\text{g} \cdot \text{sec}$)		Δt (sec)	Leaky Integration
			Mean	Max		
41e	19-Jan-2003,14:08:23	19-Jan-2003,14:13:38	28.9	284.1	18.2	Figure 6.89
04e	20-Jan-2003,00:13:06	20-Jan-2003,00:16:56	115.8	457.5	66	Figure 6.90
08p	20-Jan-2003,23:22:03	20-Jan-2003,23:27:19	10.7	59.3	0.1	Figure 6.91
53e	21-Jan-2003,18:47:15	21-Jan-2003,18:49:06	13.3	91.4	0.1	Figure 6.92

A query of the ODRC database at the JSC shows that the two significant breaches of the SOFBALL threshold ($50 \mu\text{g} \cdot \text{sec}$) seen in Figure 6.89 for test point 41e were closely-timed with VRCS firings. On the other hand, the large impulse just before GMT 21-Jan-03, 021/18:47:51 on all 3 axes of Figure 6.88 for test point 53e was not found in a query of the ODRC database for either VRCS or PRCS thruster firings. There is no explanation for this impulse yet. Finally, it's interesting to note that the four strong, regularly-spaced X-axis accelerations toward the end of both test point 04e and 08p seen in Figure 6.86 and Figure 6.87. No correlations were made with ODRC thruster firing data for these spikes; however, these are reminiscent of the mallet pounding that is part of setup for the combustion module (CM-2). This mallet pounding setup was previously done with the first combustion module (CM-1) during the Microgravity Science Laboratory (MSL-1) mission as detailed in [4]. A follow-up question to the science team on this matter indicates that these large transients were not the result of mallet pounding though.

6.2.1.5 Vapor Compression Distillation (VCD)

The VCD experiment is comprised of a fluids control pump assembly (FCPA), a distillation assembly (DA), and a motor Figure 6.93. Ground test data suggested that “the FCPA has a harmonic every 13 Hz, the DA with a small rotating centrifuge has harmonics every 3.4 Hz, and the motor has harmonics every 33 Hz.” [19] The electronic logbook that was maintained as part of PIMS real-time support at the JSC shows an entry at GMT 18-Jan-03, 018/19:10:51 that states “VCD spinning up at [19:09] from [Experiment Support Engineer] ESE-3.” The SAMS-FF data

**PIMS STS-107 Mission Microgravity Environment Summary Report:
January 16 to February 1, 2003**

plotted in the form of a spectrogram around that time is shown in Figure 6.94. It is important to note when looking at this figure that the cutoff frequency of the SAMS-FF sensor was 26.3 Hz, while the Nyquist frequency was 50 Hz. As a result, we can qualify disturbances up to 50 Hz, but cannot quantify disturbances above 26.3 Hz. The spectrogram shows two well-documented narrowband signatures: (1) the nearly ubiquitous Ku-band antenna dither at 17 Hz, and (2) the on/off cycling of the EORF at about 21.3 Hz with a second harmonic at 42.6 Hz. The narrowband signature attributed to VCD is easily discerned from the spectrogram as the 40.6 Hz narrowband disturbance that starts at the time suggested by the “spinning up” log entry cited above. Close examination of a long span of on-orbit vibratory data shows that this equipment’s signature wavers some from a low of about 40.2 Hz (near start) up to about 40.7 Hz, with a nominal value of 40.6 Hz. “Spinning up” suggests operation of the DA centrifuge, which apparently has a significant 12th harmonic vibratory component. Recall that ground data showed fundamental frequency of 3.4 Hz, so 12th harmonic is at $12 \times 3.4 = 40.8$ Hz, only slightly greater than the nominal 40.6 Hz measured by the SAMS-FF sensor. The Nyquist spectrogram of Figure 6.95, which shows a longer span, indicates that this VCD equipment turned off at about GMT 18-Jan-03, 018/22:11:00 (just over 3 hours of operation). An e-mail correspondence with VCD team provided information for the MET columns of Table 6.10 per their operations timeline. The GMT columns were calculated based on known GMT of Columbia’s launch.

TABLE 6.10 ESTIMATE OF VCD OPERATIONS TIMELINE

MET Start	MET End	GMT Start	GMT End	See
002/03:28	002/06:26	18-Jan-2003,19:07	18-Jan-2003,22:05	Figure 6.95
003/00:05	003/06:07	19-Jan-2003,15:44	19-Jan-2003,21:46	Figure 6.96 & Figure 6.97
003/23:36	004/07:36 ³	20-Jan-2003,15:15	20-Jan-2003,23:15	Figure 6.98 & Figure 6.99
006/02:44	006/06:23	22-Jan-2003,18:23	22-Jan-2003,22:02	Figure 6.100
006/23:44	007/04:35	23-Jan-2003,15:23	23-Jan-2003,20:14	Figure 6.101 & Figure 6.102
008/04:35	008/06:47	24-Jan-2003,20:14	24-Jan-2003,22:26	Figure 6.103

The SAMS-FF vibratory acceleration data offered another means of tracking the VCD operations timeline. Based on the narrowband signature from 12th harmonic of the DA centrifuge (at 40.6 Hz), the VCD timeline shown in Table 6.11 was inferred from vibratory measurements.

³ Notes from VCD team stated this “Probably stopped sooner.”

**PIMS STS-107 Mission Microgravity Environment Summary Report:
January 16 to February 1, 2003**

TABLE 6.11 VCD OPERATIONS TIMELINE INFERRED FROM VIBRATORY MEASUREMENTS

GMT Start	GMT End
18-Jan-2003,19:09	18-Jan-2003,22:11
19-Jan-2003,15:42	19-Jan-2003,21:44
20-Jan-2003,15:13	20-Jan-2003,21:11 ⁴
22-Jan-2003,18:21	22-Jan-2003,22:01
23-Jan-2003,15:20	23-Jan-2003,20:14
24-Jan-2003,20:14	24-Jan-2003,21:40

While comparisons can be made between various acceleration environment conditions, that is, some combination of when VCD equipment was on/off and during/without crew exercise, this should not be presented using the vibratory measurements collected on this mission. These comparisons results would be rendered meaningless or obscured by the following factors:

- The SAMS-FF sensor had a cutoff frequency of 26.3 Hz, while the primary impact of VCD equipment operations on the vibratory environment was seen to be at 40.6 Hz (the 12th harmonic of the DA centrifuge).
- Close examination of Figure 6.104 reveals that a weak signature for the fundamental frequency of the DA centrifuge was detected at just over 3 Hz. This signal was observed to vanish coincident with 12th harmonic as marked just to the left of the white horizontal line in this figure. The strength of this signal, however, is not such that appreciable differences can be presented, particularly in the presence of stronger neighboring spectral content like structural modes or crew exercise.

6.2.1.6 Biobox

The time span of interest for Biobox operations was GMT 16-Jan-2003, 016/15:39 and 22-Jan-2003, 022/16:49. The Biobox had a centrifuge that spun at 108 RPM (1.8 Hz), however the PCSA plot of Figure 6.105 shows no clear sign of this disturbance.

6.2.1.7 Mechanics of Granular Materials (MGM)

Table 6.12 lists the experiments conducted during the MGM investigation.

⁴ Gap in acceleration data at this time, so VCD equipment may have stopped later (and likely after time from footnote above).

**PIMS STS-107 Mission Microgravity Environment Summary Report:
January 16 to February 1, 2003**

TABLE 6.12 MGM EXPERIMENT TIMES

Experiment		GMT	
Order	Name	Start	End
1	A1	no data collected	no data collected
2	A2	18-Jan-2003,18:19:21	18-Jan-2003,21:38:27
3	D1	19-Jan-2003,20:17:57	20-Jan-2003,02:11:03
4	D2	20-Jan-2003,16:35:45	20-Jan-2003,20:27:29
5	D3	21-Jan-2003,05:14:23	21-Jan-2003,08:34:45
6	D4	21-Jan-2003,18:42:27	21-Jan-2003,22:44:36
7	C1	25-Jan-2003,01:41:18	25-Jan-2003,05:40:41
8	C2	25-Jan-2003,14:35:59	25-Jan-2003,18:53:51
9	D5	26-Jan-2003,00:53:10	26-Jan-2003,04:55:12
10	D6	27-Jan-2003,19:07:38	27-Jan-2003,23:45:09

The figures referenced in the rightmost column of Table 6.13 show the 10-second interval min/max acceleration values for the periods shown in the shaded rows of Table 6.12.

TABLE 6.13 MGM INTERVAL MIN/MAX RESULTS

Experiment Order-Name	Acceleration (mg)						See
	X-axis		Y-axis		Z-axis		
	min	max	min	max	min	max	
04-D2	-9.22	8.98	-13.67	15.30	-8.36	6.32	Figure 6.106
05-D3	-254.59	20.09	-16.60	77.59	-365.61	59.32	Figure 6.107
06-D4	-5.03	7.18	-6.06	9.09	-5.23	4.00	Figure 6.108
09-D5	-4.32	6.27	-8.77	6.18	-3.32	6.48	Figure 6.109
10-D6	-4.71	4.82	-3.11	3.75	-2.76	3.24	Figure 6.110

Note that among the five data sets analyzed for these min/max results, the experiment named “05-D3” was subjected to the largest accelerations, whereas the one named “D6” was in the most benign environment from this min/max perspective.

6.2.2 Vehicle Operations

This section includes vibratory acceleration disturbances related to Ku-band antenna dithering and thruster firings.

6.2.2.1 Ku-Band Antenna Dither

The plot of Figure 6.111 shows 24 hours of interval RMS acceleration values for the narrow frequency range from 16.93 to 17.13 Hz (centered on the Ku-band antenna dither frequency). The median RMS value here was 85.7 μg_{RMS} , and since this value was within the expected

**PIMS STS-107 Mission Microgravity Environment Summary Report:
January 16 to February 1, 2003**

range and this disturbance has been extensively characterized in numerous PIMS Shuttle microgravity environment reports [11],[13], we do not cover this topic in detail here.

6.2.2.2 Thruster Firings

In addition to the thruster firing impact shown in Figure 6.62 and discussed in section 6.2.1.2, we examine some the impact of thruster firing for the Mist test point 10-68M relative to the *SOFBALL* threshold in Figure 6.63. The series of thruster firings starting near GMT 29-Jan-03, 029/14:41:29 drive the environment well above the threshold. Figure 6.63 shows this same time span but from an acceleration magnitude perspective.

6.2.3 Crew Exercise

Crew ergometer exercise aboard the Shuttle has been characterized and documented in other PIMS microgravity environment reports [14-17]. As with most Shuttle missions, the crew seeks to mitigate the deleterious effects of near weightlessness on the body by exercising. This has an impact on the vibratory environment, particularly below about 6 Hz or so. The signature of crew ergometer exercise is shown in the 24-hour spectrogram of Figure 6.112. This figure shows a number of crew exercise periods with start times indicated by the time-axis ticks. Note the spectral peaks at the shoulder sway and pedaling frequencies (about 1.25 and 2.5 Hz, respectively) for each exercise session. This form of exercise also tended to excite structural modes between about 3 to 6 Hz. The 8-hour spectrogram of Figure 6.113 shows finer detail for crew exercise signature. Note that the well-documented signature of ergometer exercise, which started at GMT 23-Jan-03, 023/09:44 seems to have come part way into a similar signature at a slightly lower frequency. At the time this report was written, this is believed to be the second exercise device (inside the SPACEHAB Double Module, which was associated with an experiment.)

To quantify the impact of these exercise sessions, the interval RMS plot of Figure 6.114 shows the same 24-hour period as Figure 6.112. The red trace shows exercise periods, while the black trace shows non-exercise periods. The median RMS acceleration below 6 Hz during exercise was nearly 4 times higher than without exercise for this period. For a more detailed quantification of the exercise periods over this 24-hour period, consider the legend in Table 6.14 that applies to Figure 6.115.

**PIMS STS-107 Mission Microgravity Environment Summary Report:
January 16 to February 1, 2003**

TABLE 6.14 CREW EXERCISE LEGEND FOR FIGURE 6.115

Data Set #	GMT Start hh:mm:ss	Exercise Device
1	00:27:59	ergometer
2	03:43:20	ergometer
3	09:31:07	other
4	09:52:33	both
5	10:16:58	ergometer
6	15:19:30	ergometer
7	16:19:03	other
8	20:29:47	other
9	21:29:20	ergometer
10	22:03:17	ergometer

The figure shows expected range of RMS levels below 10 Hz. As discussed previously [11], the high degree of variability among exercise periods is attributable mainly to the vigorousness of the individual exercising for that period. A common consequence of exercise occurs when the pedaling rate is such that it excites an Orbiter structural mode around 4.7 to 4.8 Hz. This is seen as the large step at that frequency for most traces in Figure 6.115. Note that the exercise device listed as “other” in Table 6.14 refers to the second signature discussed earlier.

Roadmap spectrograms like the one shown in Figure 6.113 are available for all of the SAMS-FF data recorded during this mission. Interested readers who did not receive those as part of the report distribution can contact the authors for access to those. These roadmap spectrograms explicitly show exercise signatures from day to day throughout the mission.

6.2.4 Principal Component Spectral Analysis (PCSA)

The Principal Component Spectral Analysis (PCSA) histogram is computed from a large number of constituent PSDs. The resultant three-dimensional plot serves to summarize magnitude and frequency variations of significant or persistent spectral contributors and envelops all of the computed spectra over the time frame of interest. The two-dimensional histogram is comprised of frequency-magnitude bins in units of Hz and $\log_{10}(g^2/Hz)$. The third dimension, represented by a color scale, is the percentage of time that a spectral value was counted within a given frequency-magnitude bin.

The PCSA plot of Figure 6.116 was calculated and displayed to summarize the vibratory acceleration spectrum for this mission. This figure represents more than 276 hours of acceleration data measurements and is comprised of 48,535 constituent PSDs spanning from GMT 16-Jan-03 through 31-Jan-03. Note the dominance of 3 identified disturbance sources: (1) structural modes below 10 Hz, (2) the Ku-band antenna dither at 17 Hz, and (3) the EORF signature around 21 Hz.

**PIMS STS-107 Mission Microgravity Environment Summary Report:
January 16 to February 1, 2003**

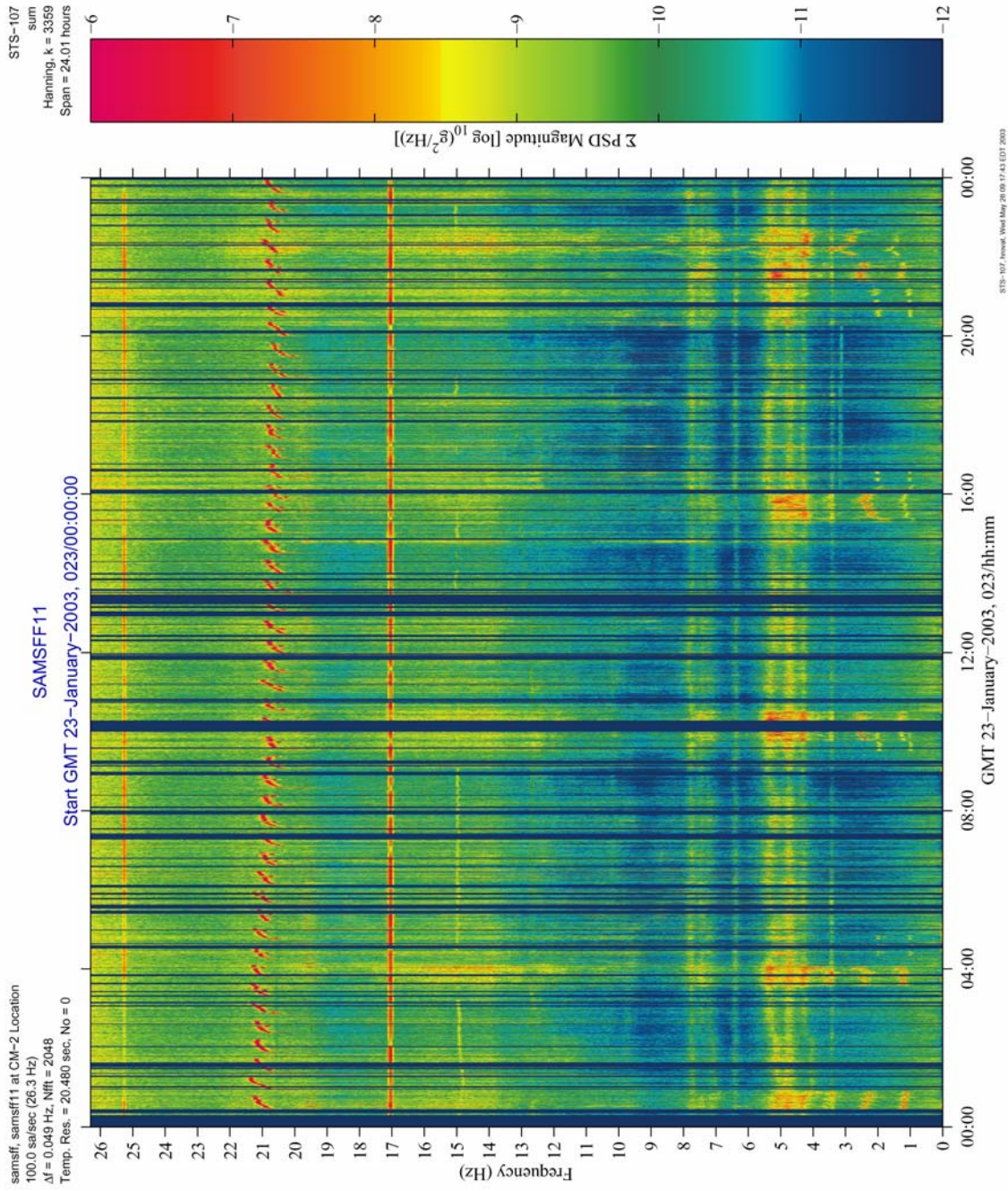


Figure 6.22 Spectrogram Of EORF

**PIMS STS-107 Mission Microgravity Environment Summary Report:
January 16 to February 1, 2003**

STS-107
sum
Hanning, k = 3359
Span = 24.01 hours

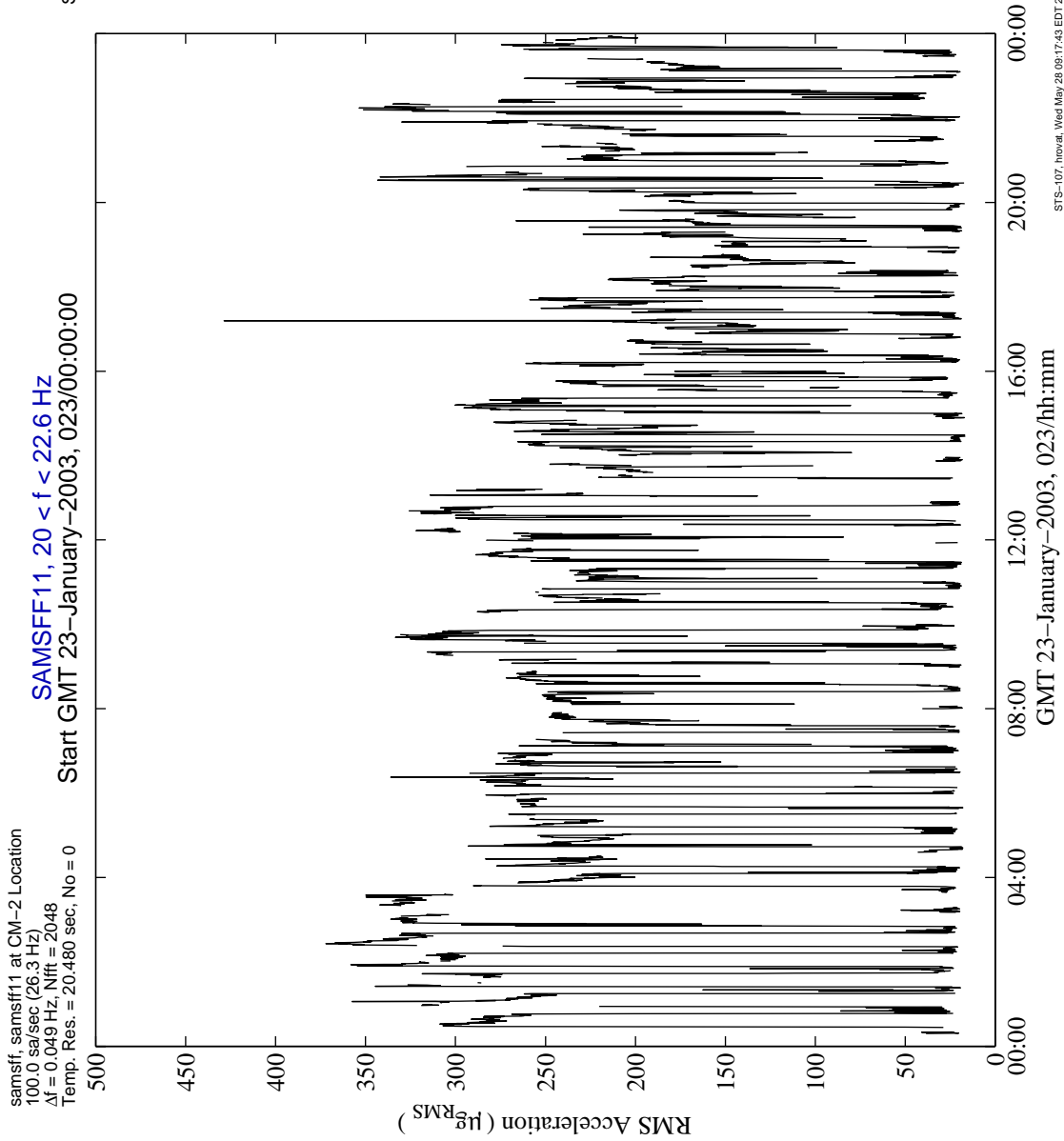


Figure 6.23 Interval RMS Of EORF

**PIMS STS-107 Mission Microgravity Environment Summary Report:
January 16 to February 1, 2003**

STS-107
sum
Hanning, k = 3359
Span = 24.01 hours

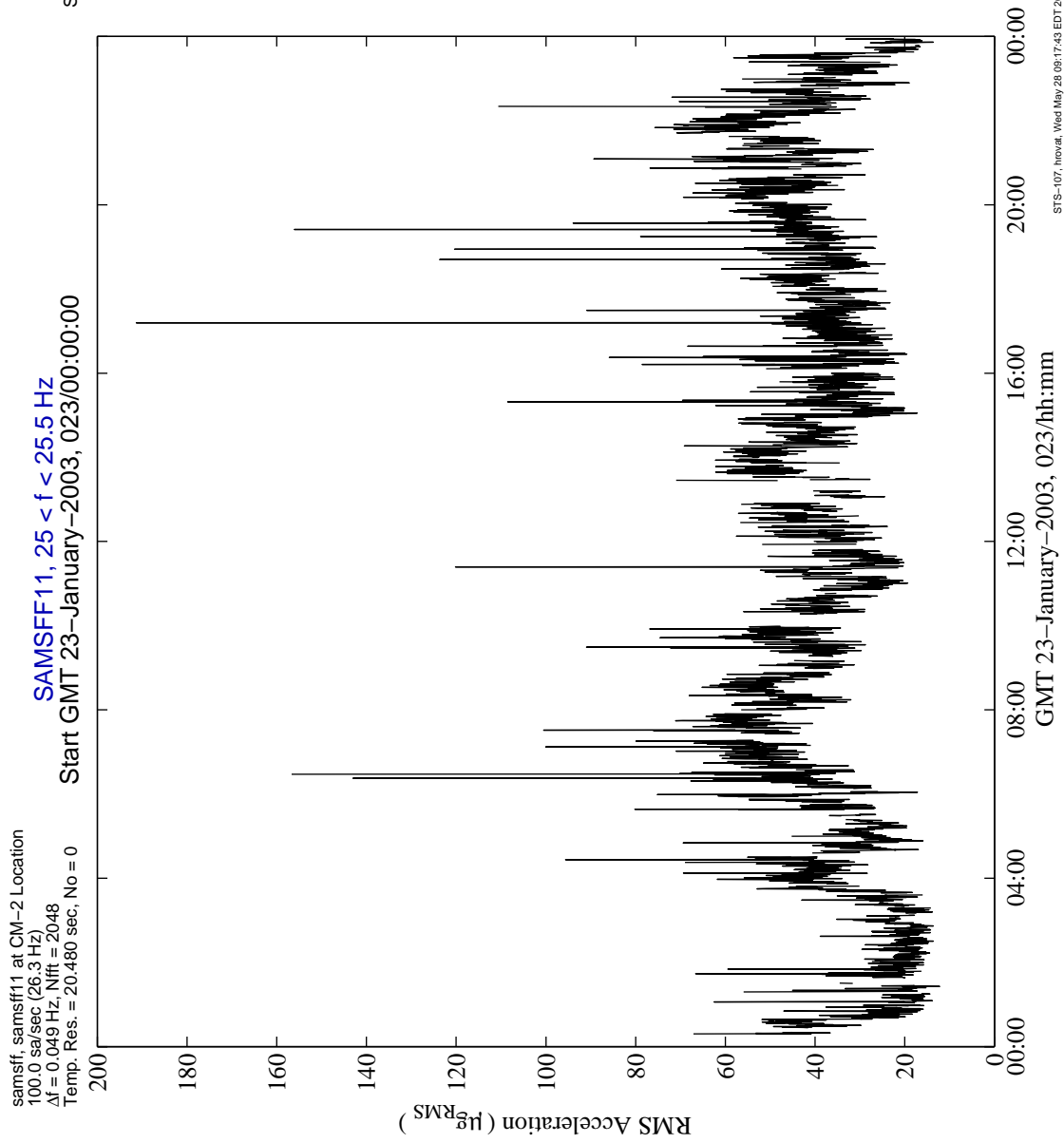


Figure 6.24 Interval RMS Of Unknown Narrowband Above 25 Hz

PIMS STS-107 Mission Microgravity Environment Summary Report:
January 16 to February 1, 2003

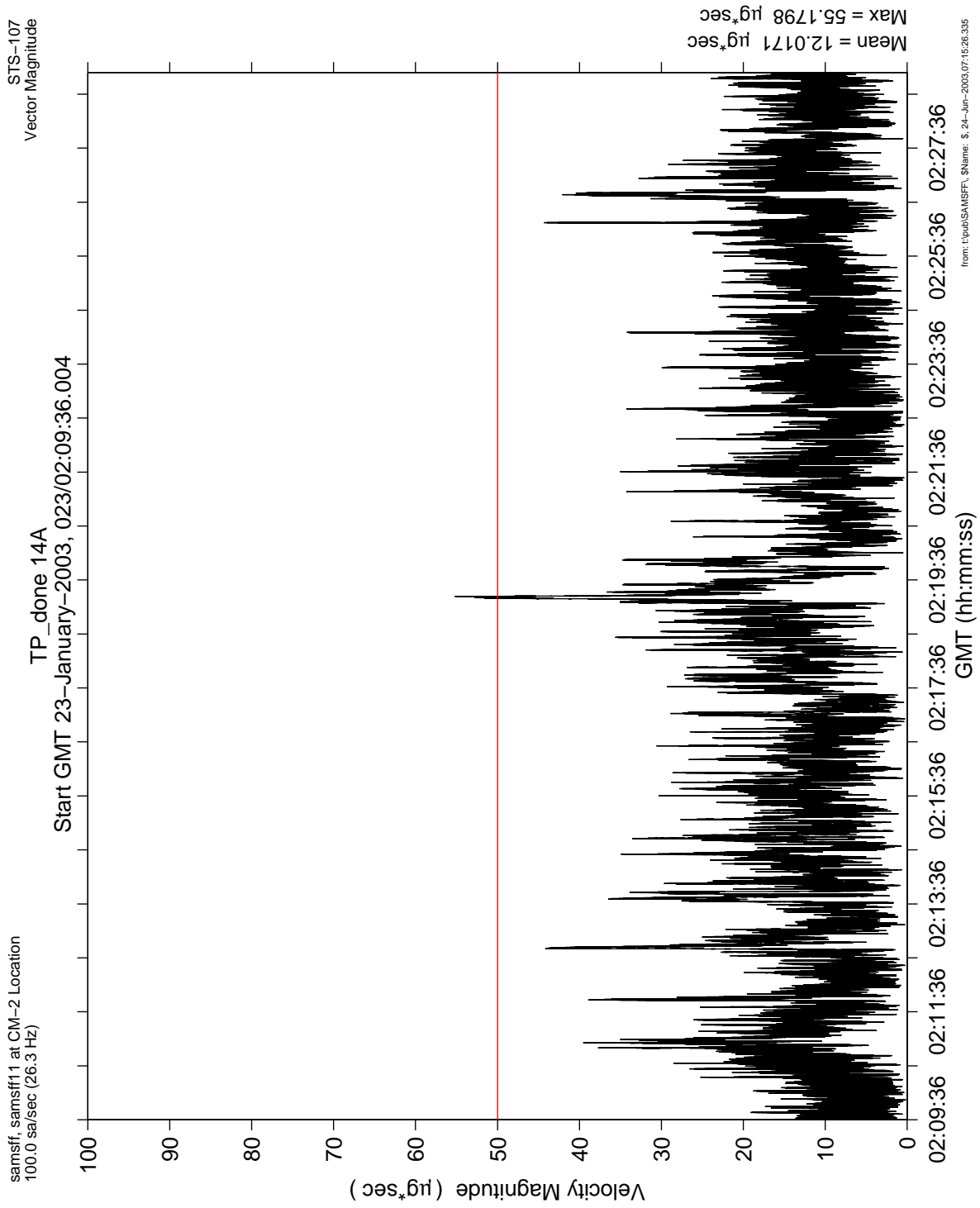


Figure 6.25 Leaky Integration For SOFBALL Test Point 14A

**PIMS STS-107 Mission Microgravity Environment Summary Report:
January 16 to February 1, 2003**

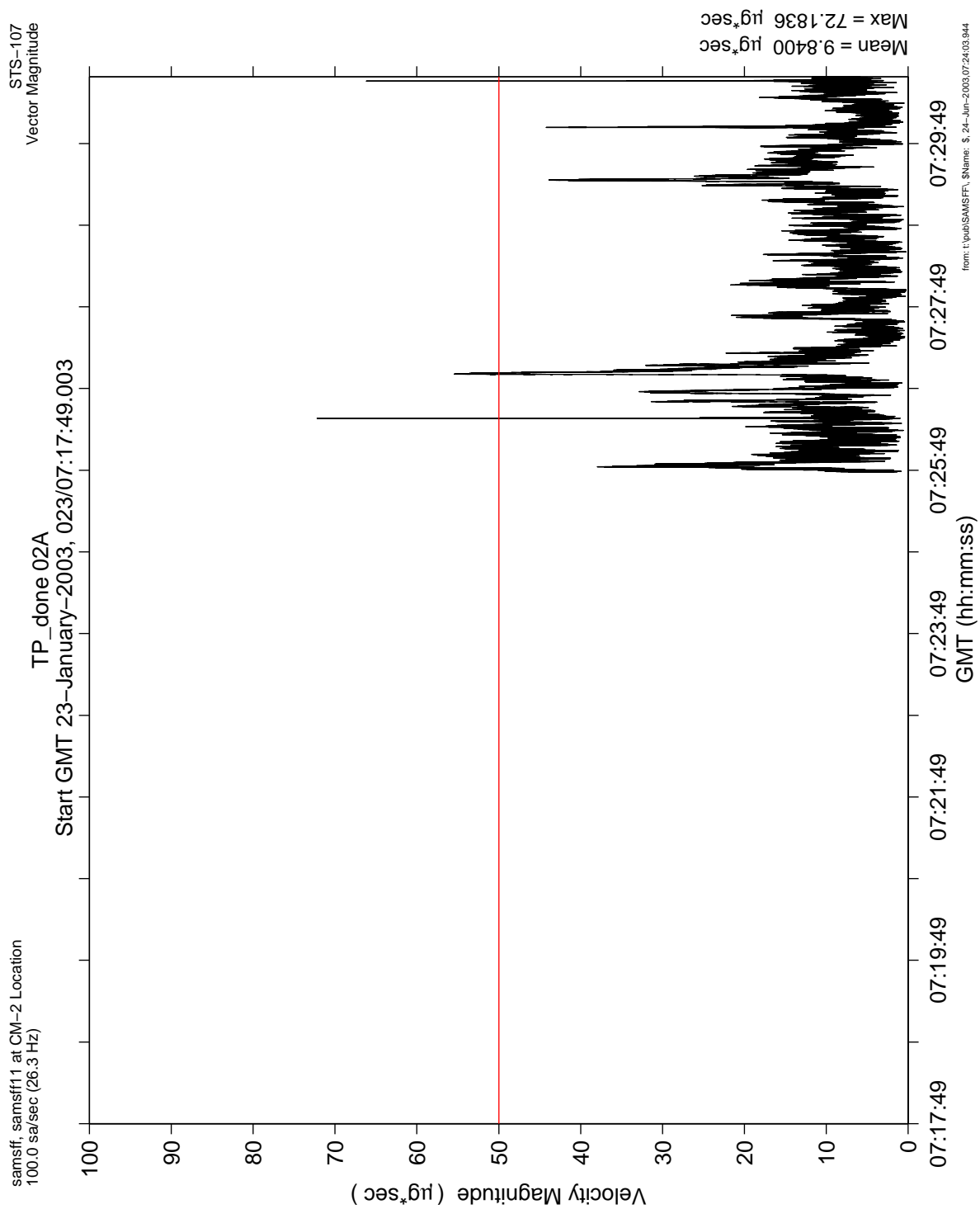


Figure 6.26 Leaky Integration For SOFBALL Test Point 02A

PIMS STS-107 Mission Microgravity Environment Summary Report:
January 16 to February 1, 2003

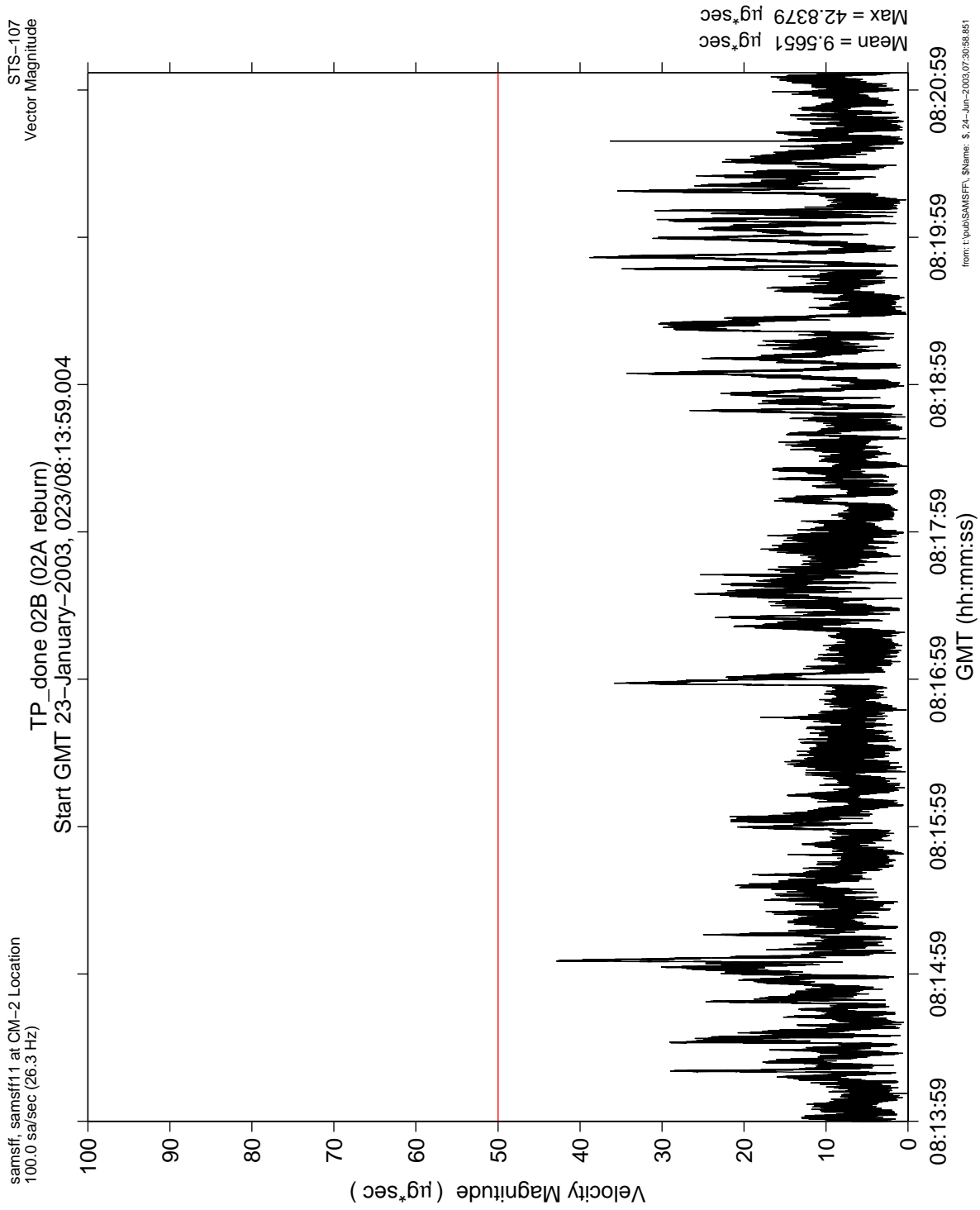


Figure 6.27 Leaky Integration For SOFBALL Test Point 02B (02A Reburn)

**PIMS STS-107 Mission Microgravity Environment Summary Report:
January 16 to February 1, 2003**

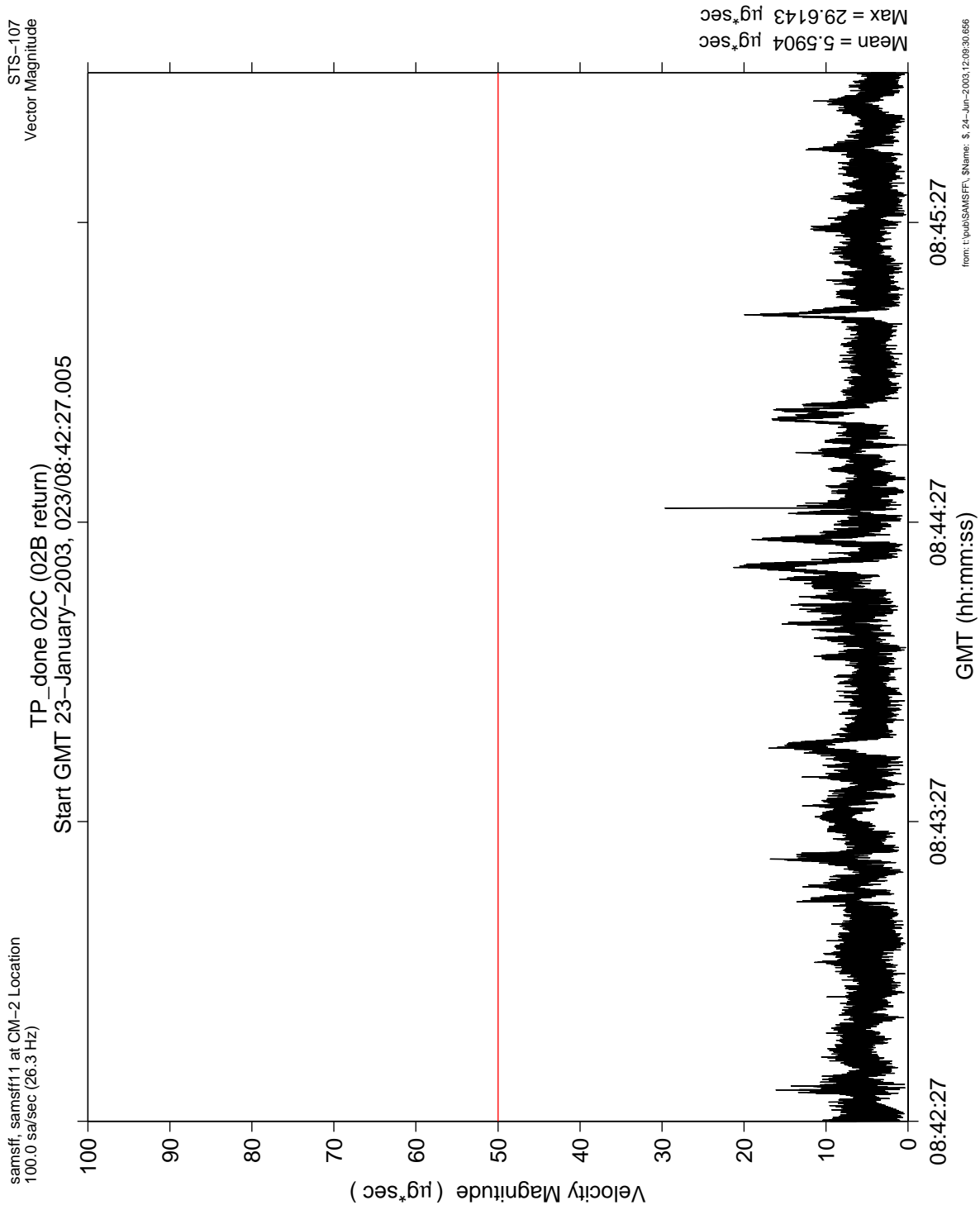


Figure 6.28 Leaky Integration For SOFBALL Test Point 02C (02B Reburn)

PIMS STS-107 Mission Microgravity Environment Summary Report:
January 16 to February 1, 2003

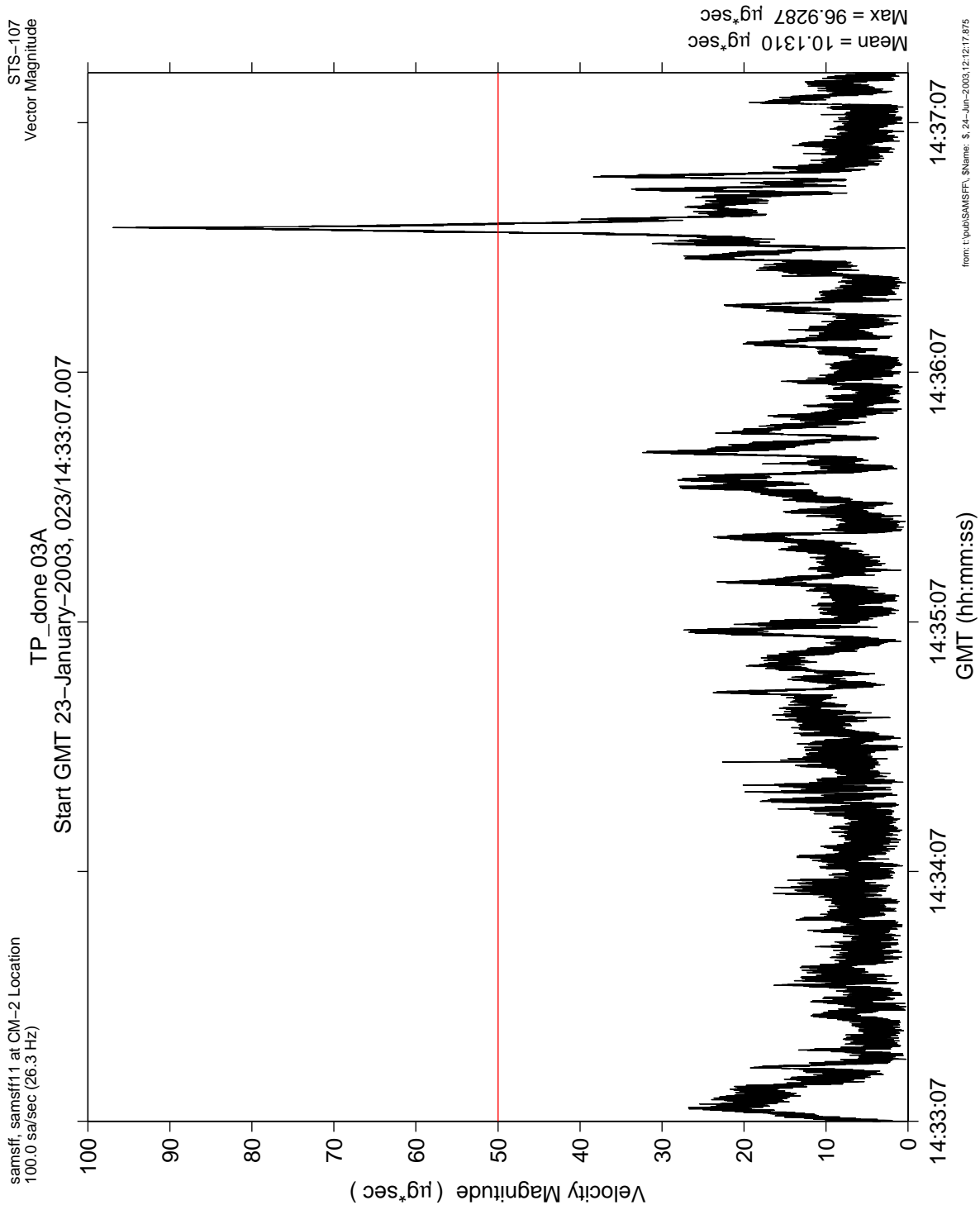


Figure 6.29 Leaky Integration For SOFBALL Test Point 03A

PIMS STS-107 Mission Microgravity Environment Summary Report:
January 16 to February 1, 2003

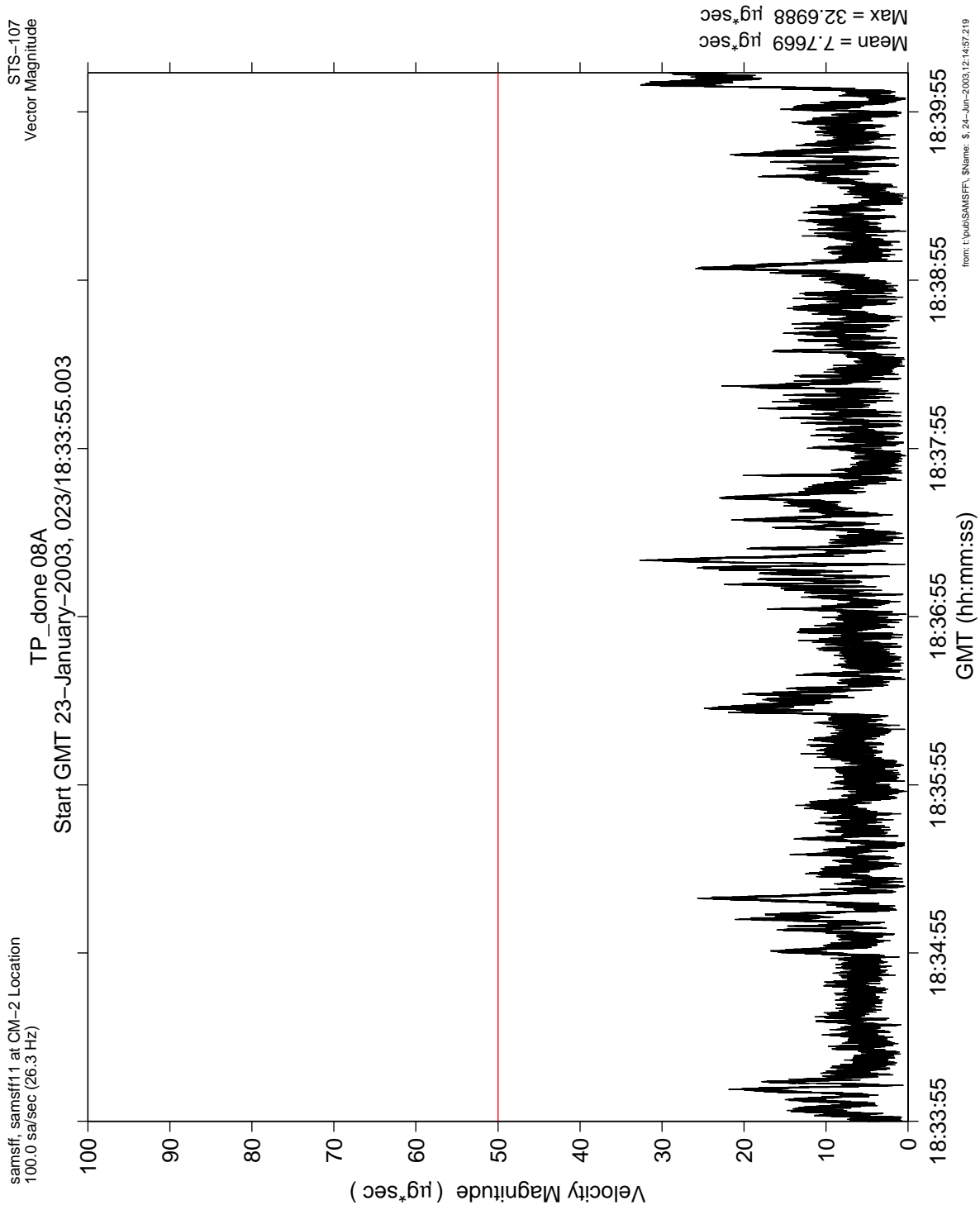


Figure 6.30 Leaky Integration For SOFBALL Test Point 08A

**PIMS STS-107 Mission Microgravity Environment Summary Report:
January 16 to February 1, 2003**

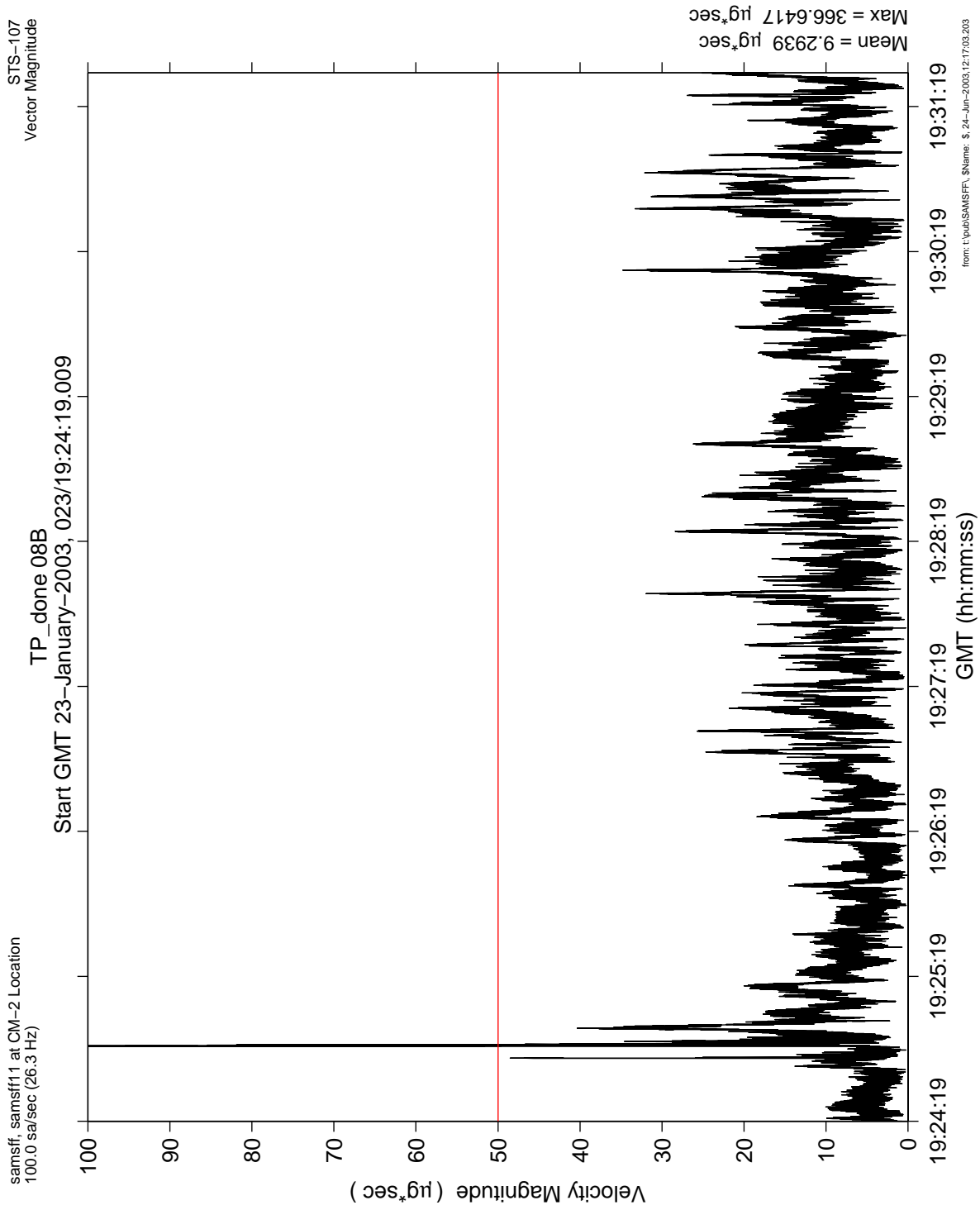


Figure 6.31 Leaky Integration For SOFBALL Test Point 08B

**PIMS STS-107 Mission Microgravity Environment Summary Report:
January 16 to February 1, 2003**

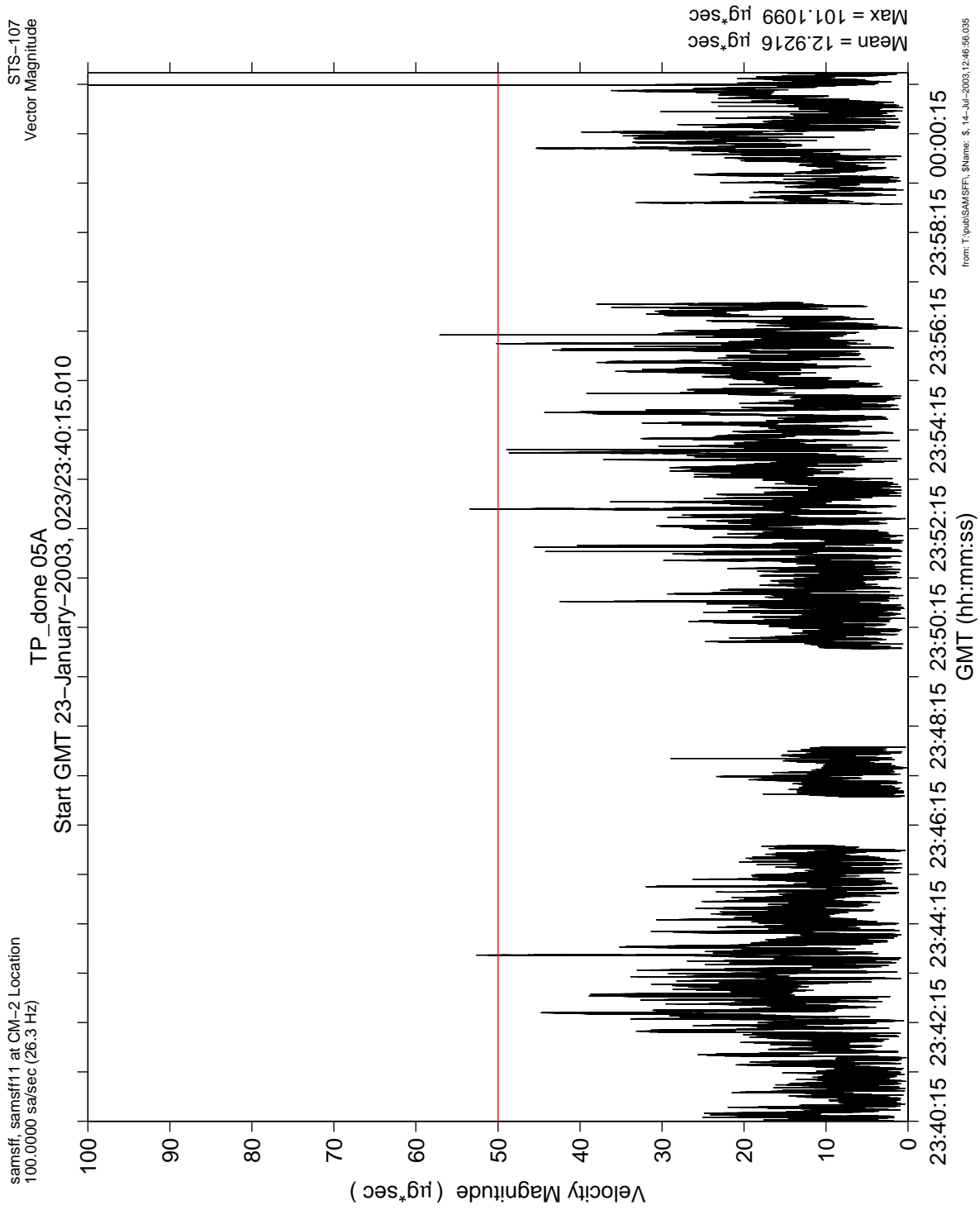


Figure 6.32 Leaky Integration For SOFBALL Test Point 05A

PIMS STS-107 Mission Microgravity Environment Summary Report:
January 16 to February 1, 2003

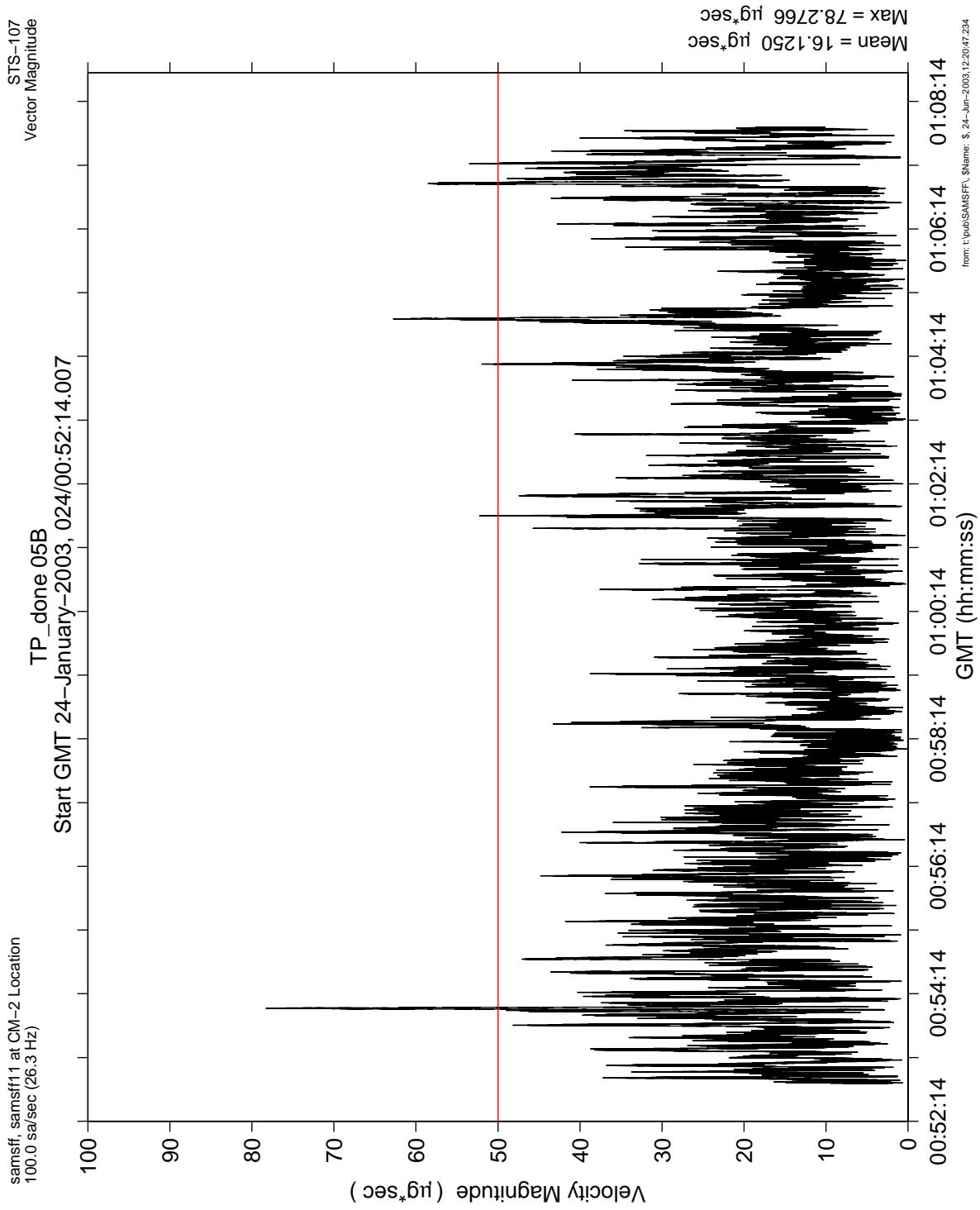


Figure 6.33 Leaky Integration For SOFBALL Test Point 05B

**PIMS STS-107 Mission Microgravity Environment Summary Report:
January 16 to February 1, 2003**

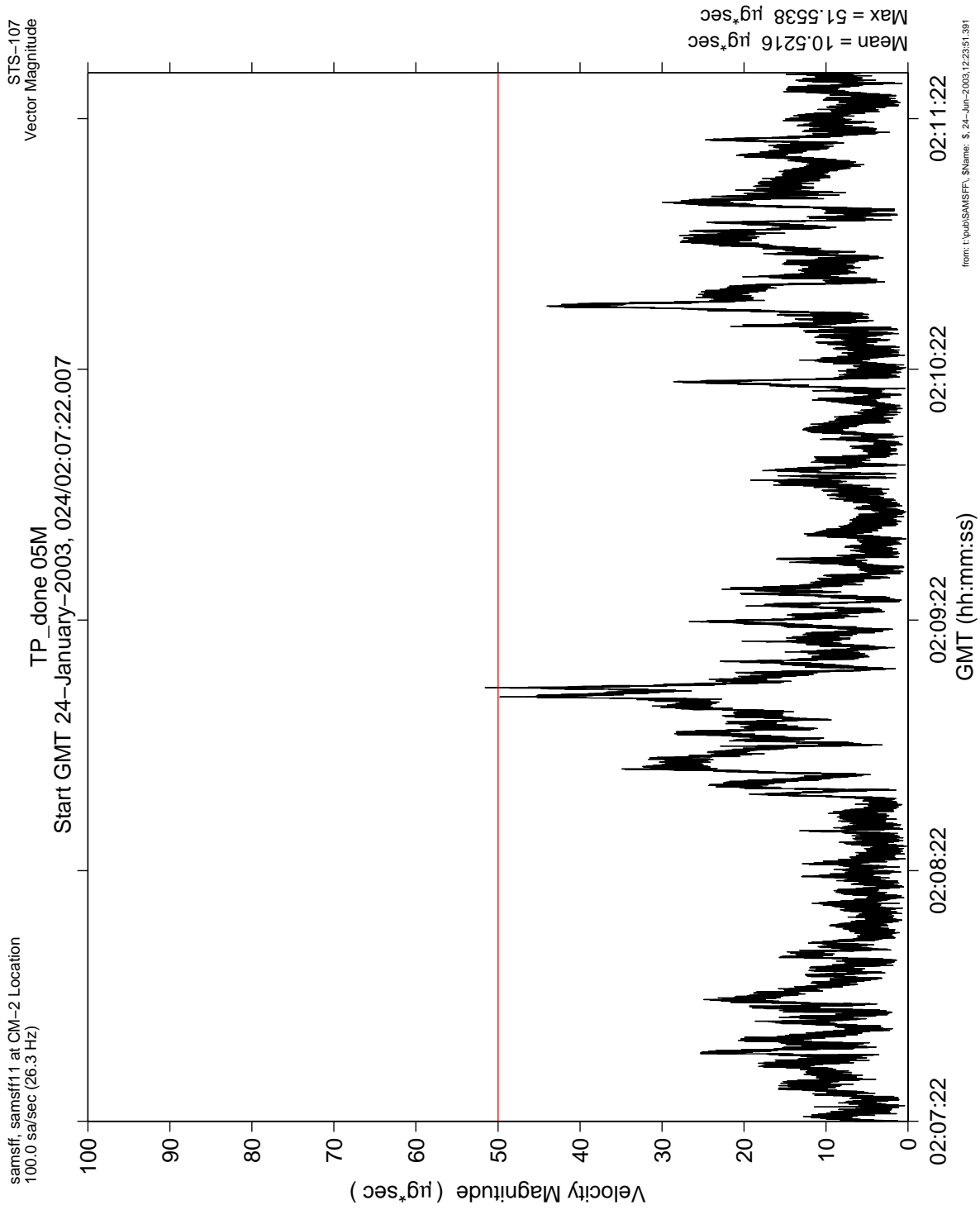


Figure 6.34 Leaky Integration For SOFBALL Test Point 05M

PIMS STS-107 Mission Microgravity Environment Summary Report:
January 16 to February 1, 2003

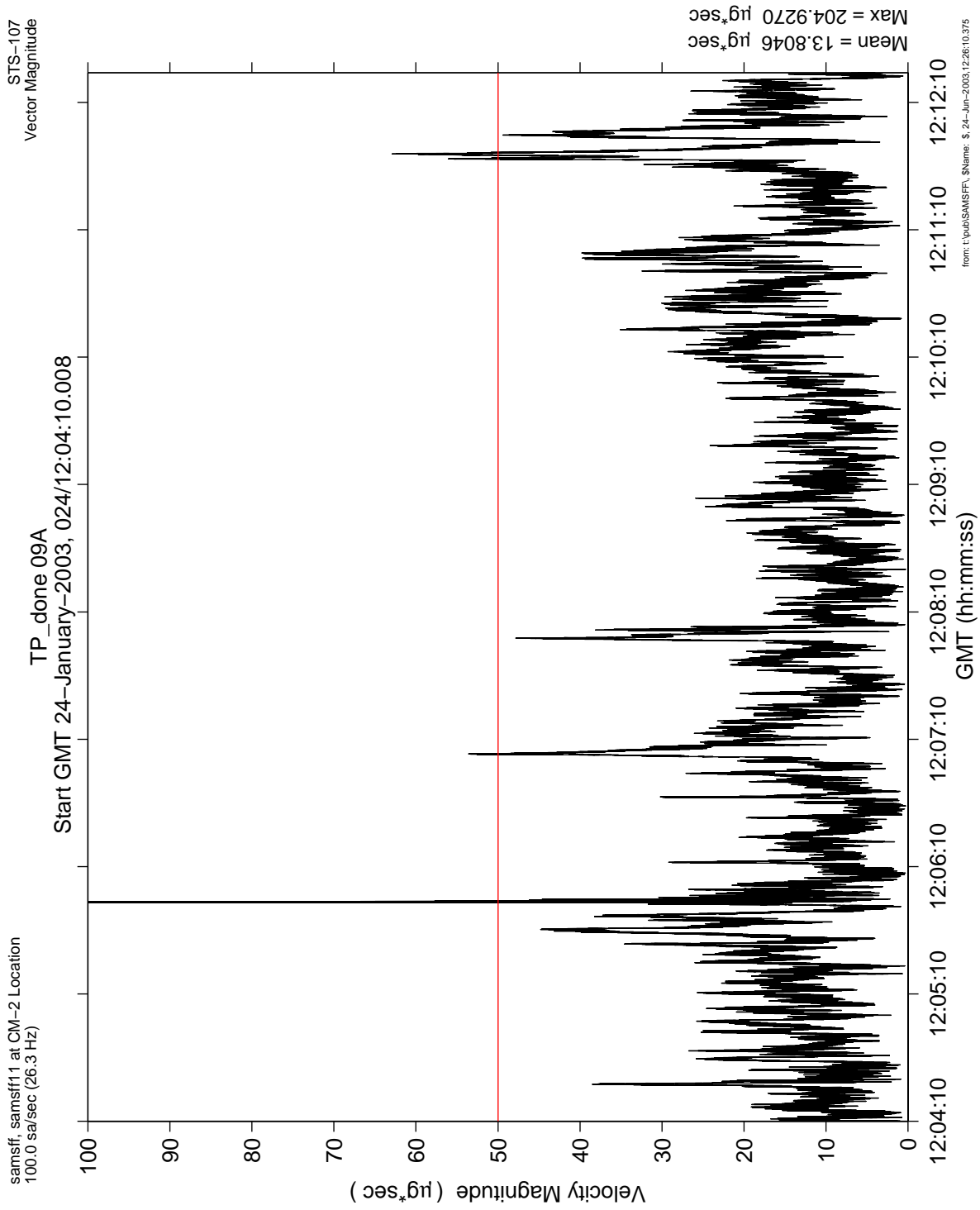


Figure 6.35 Leaky Integration For SOFBALL Test Point 09A

**PIMS STS-107 Mission Microgravity Environment Summary Report:
January 16 to February 1, 2003**

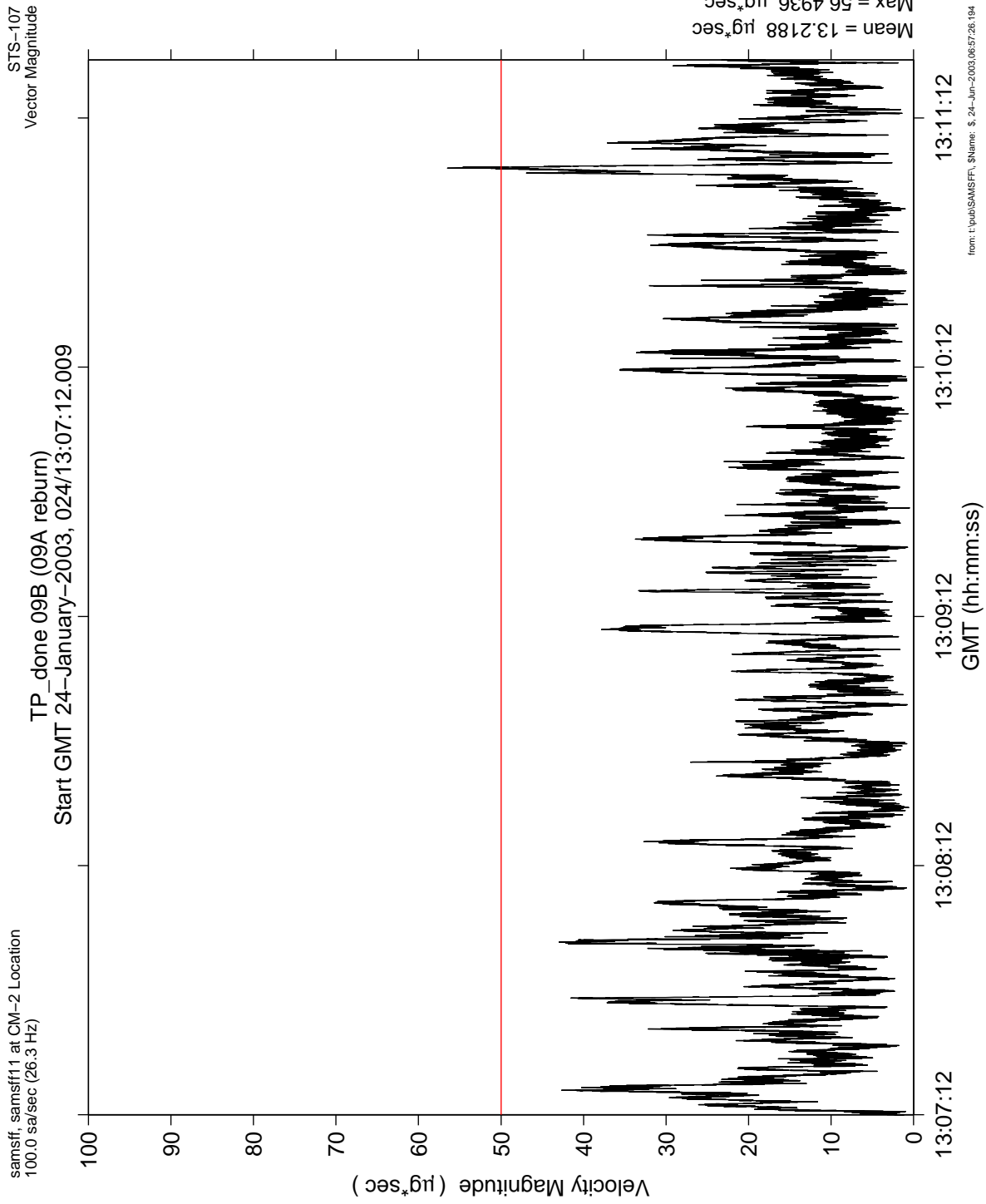


Figure 6.36 Leaky Integration For SOFBALL Test Point 09B (09A Reburn)

PIMS STS-107 Mission Microgravity Environment Summary Report:
January 16 to February 1, 2003

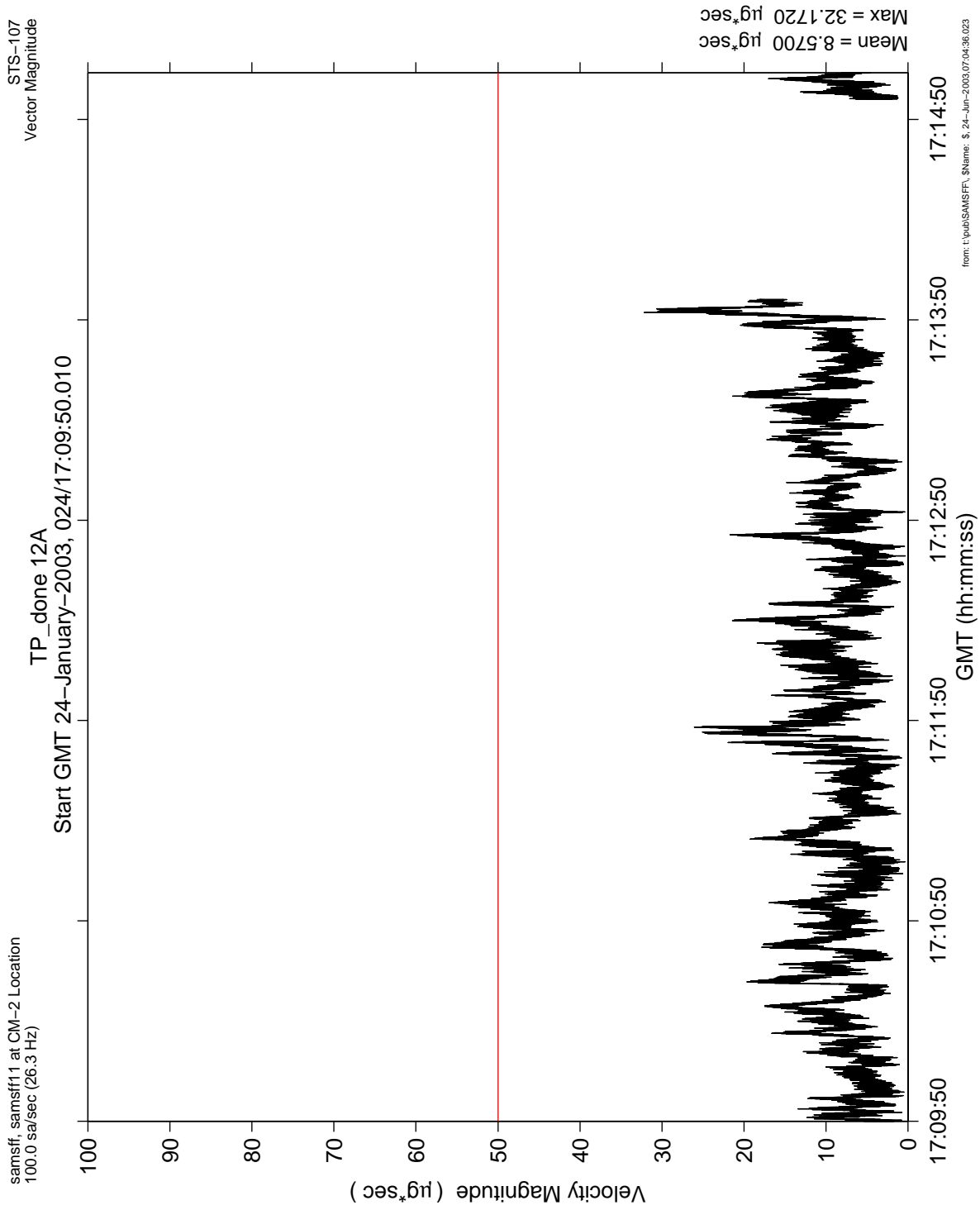


Figure 6.37 Leaky Integration For SOFBALL Test Point 12A

PIMS STS-107 Mission Microgravity Environment Summary Report:
January 16 to February 1, 2003

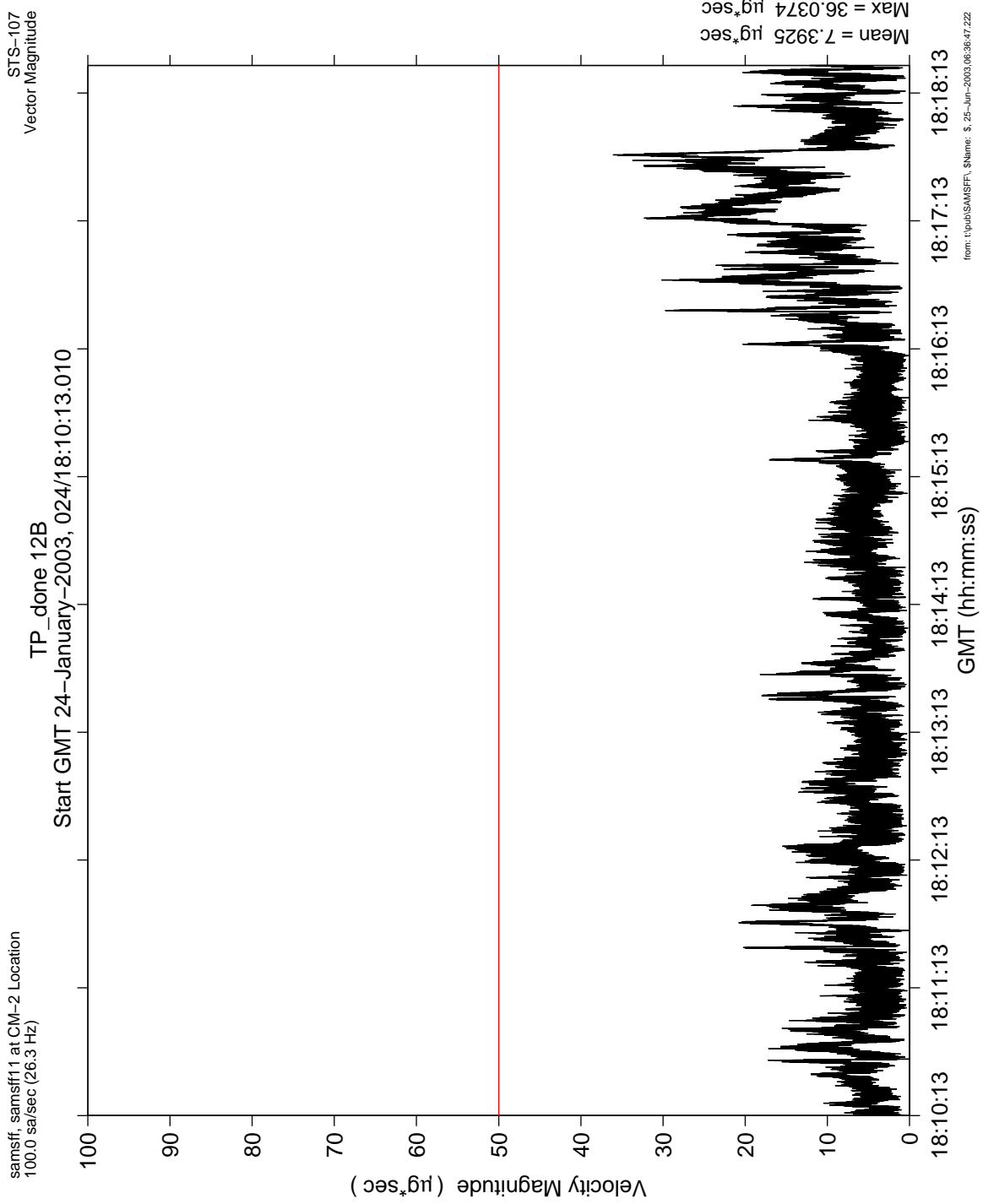


Figure 6.38 Leaky Integration For SOFBALL Test Point 12B

PIMS STS-107 Mission Microgravity Environment Summary Report:
January 16 to February 1, 2003

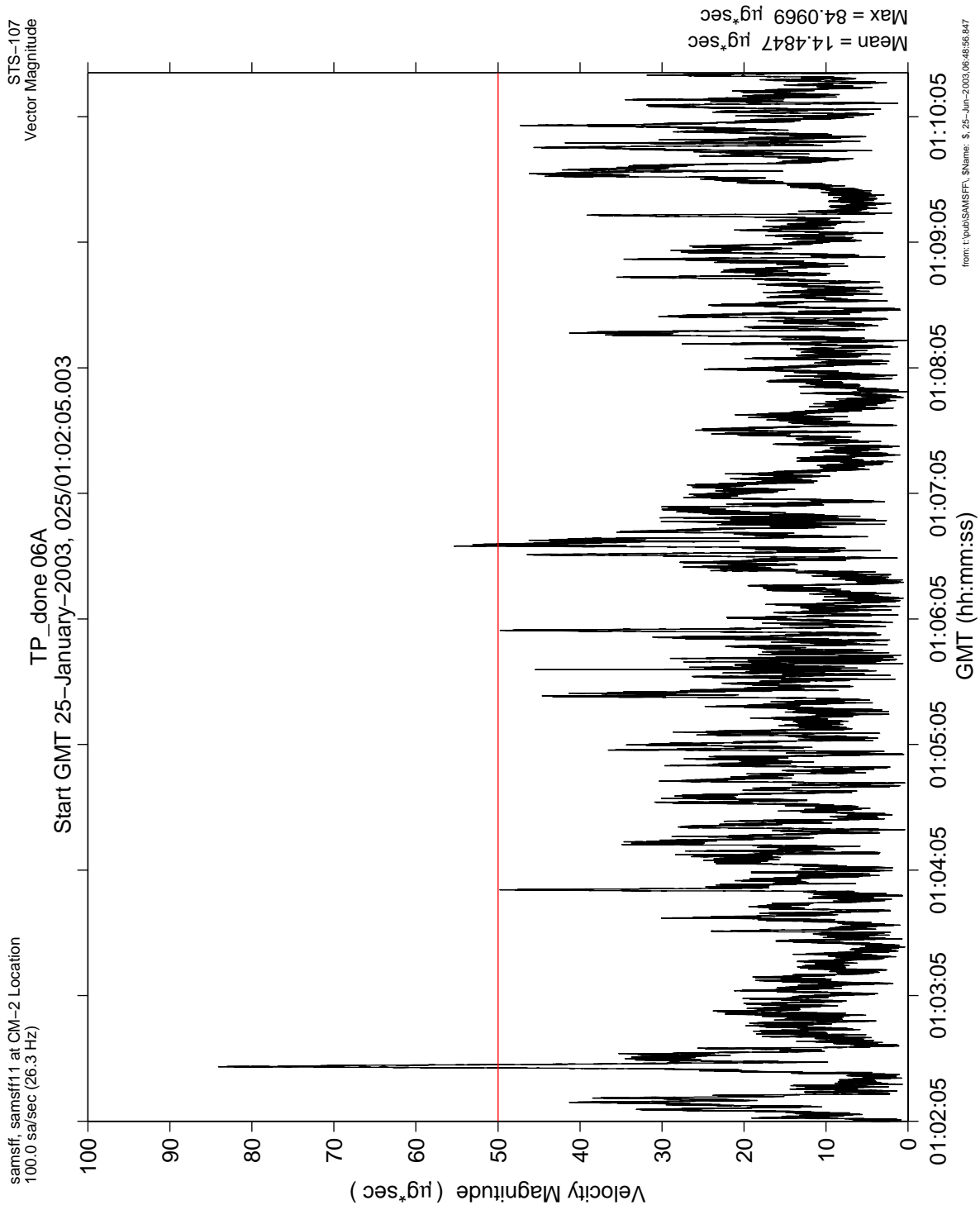


Figure 6.39 Leaky Integration For SOFBALL Test Point 06A

**PIMS STS-107 Mission Microgravity Environment Summary Report:
January 16 to February 1, 2003**

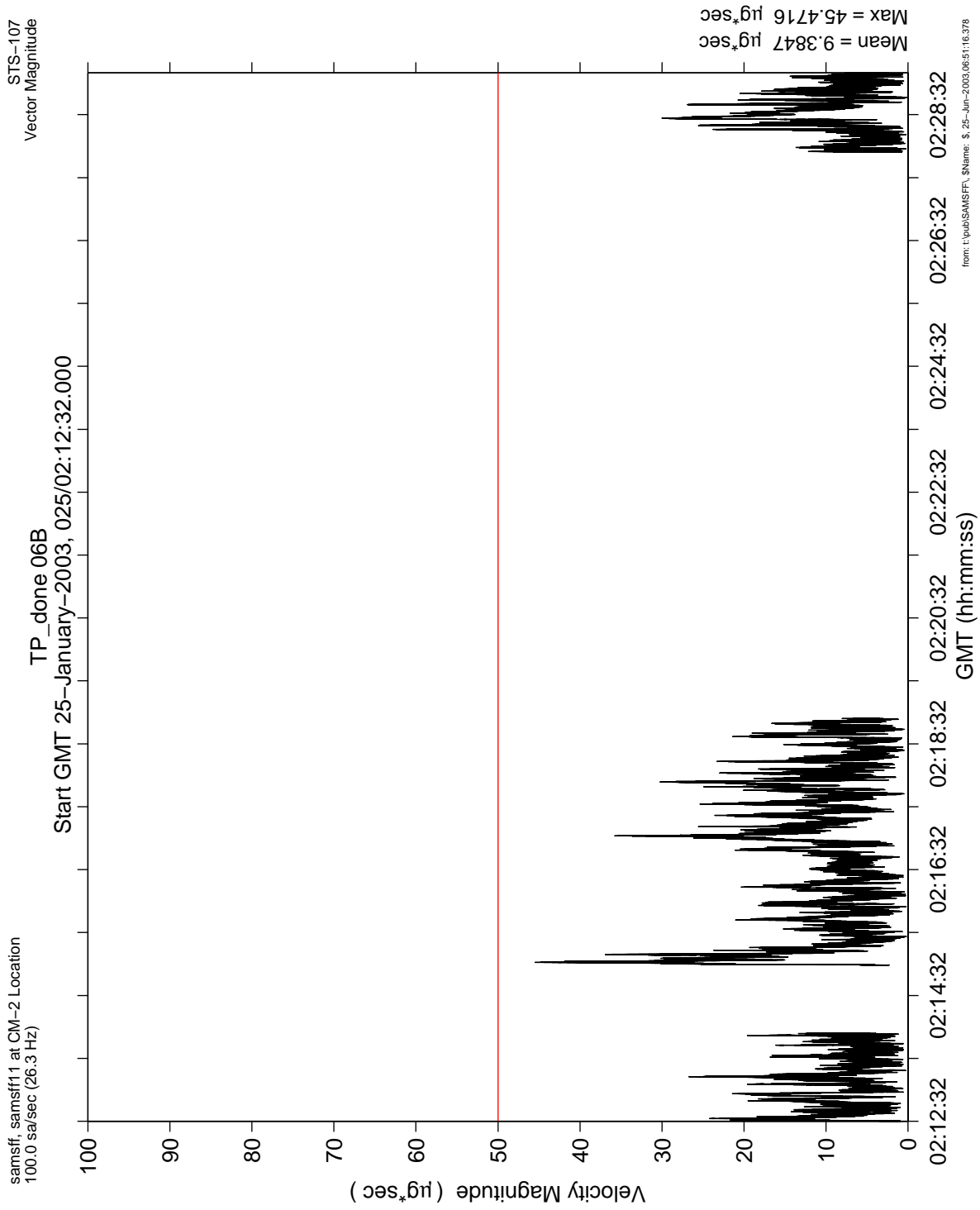


Figure 6.40 Leaky Integration For SOFBALL Test Point 06B

PIMS STS-107 Mission Microgravity Environment Summary Report:
January 16 to February 1, 2003

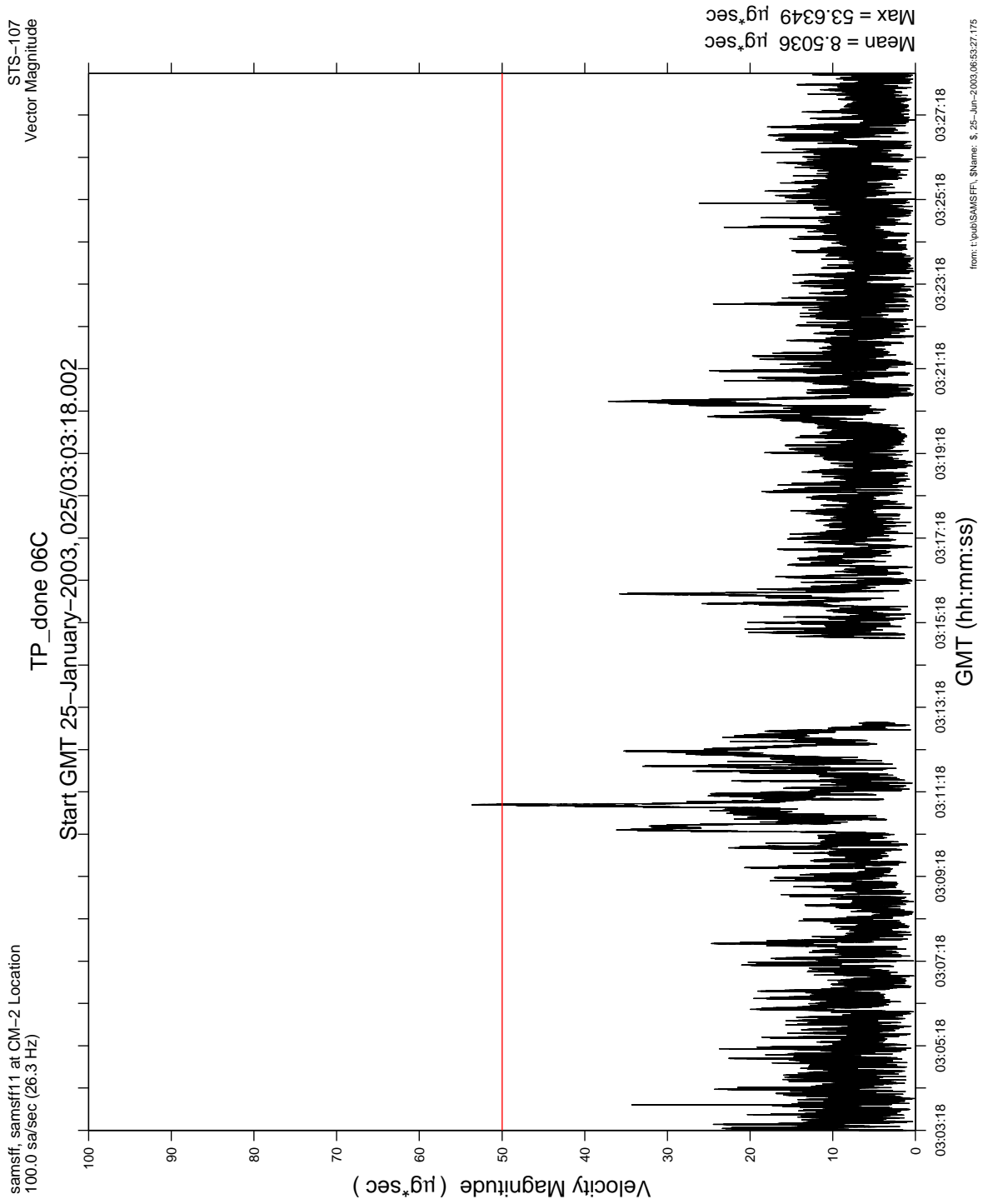


Figure 6.41 Integration For SOFBALL Test Point 06C

PIMS STS-107 Mission Microgravity Environment Summary Report:
January 16 to February 1, 2003

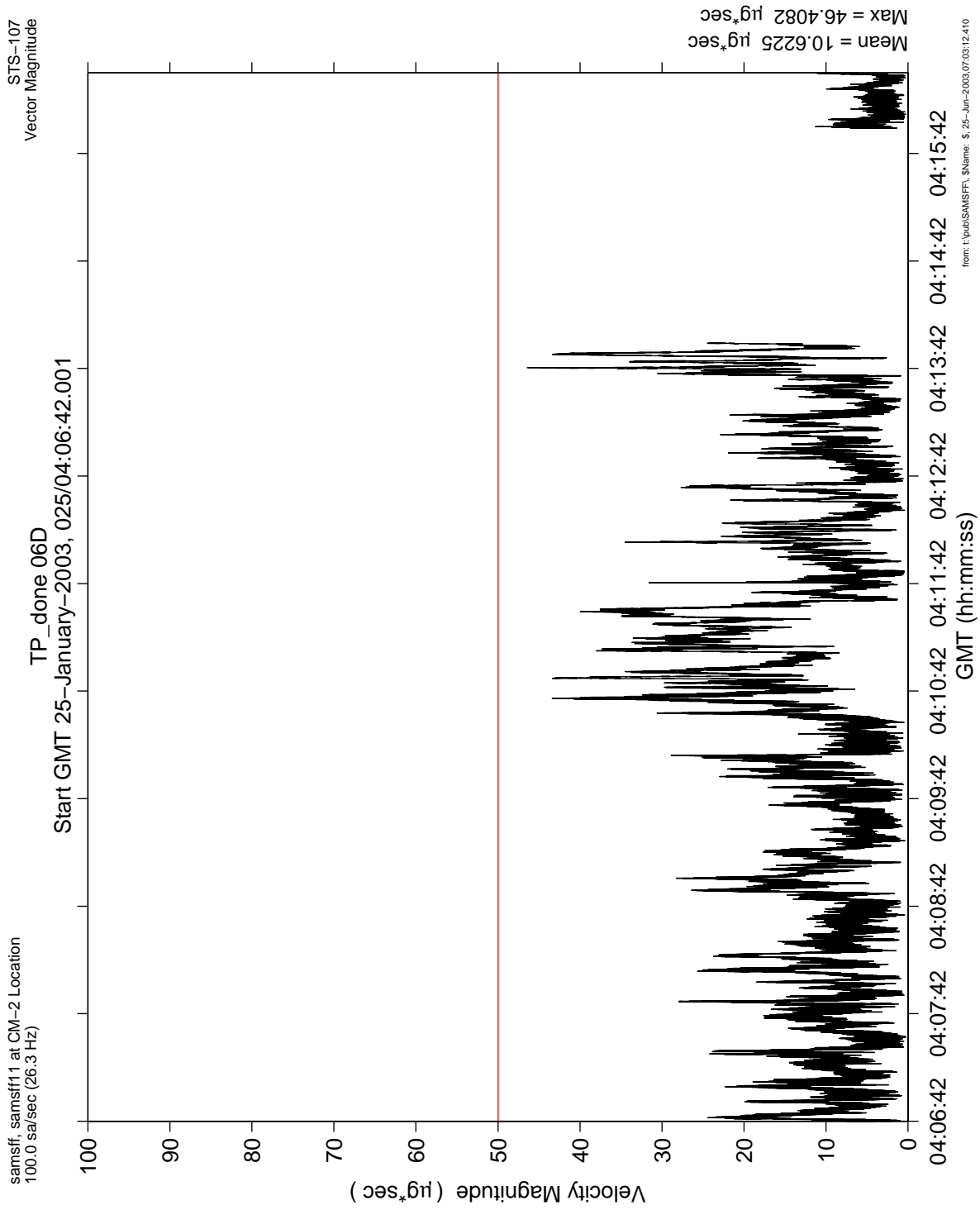


Figure 6.42 Leaky Integration For SOFBALL Test Point 06D

PIMS STS-107 Mission Microgravity Environment Summary Report:
January 16 to February 1, 2003

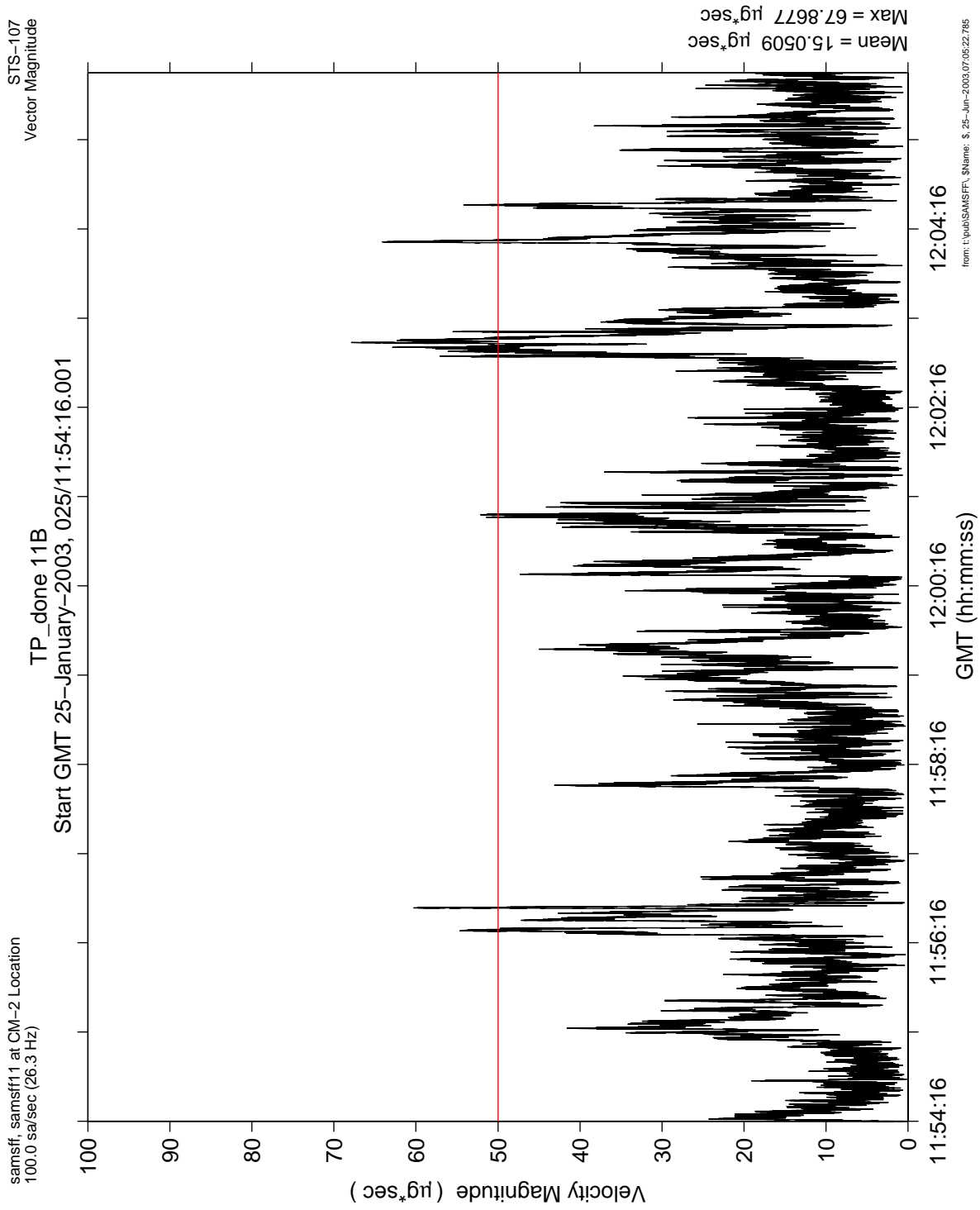


Figure 6.43 Leaky Integration For SOFBALL Test Point 11B

**PIMS STS-107 Mission Microgravity Environment Summary Report:
January 16 to February 1, 2003**

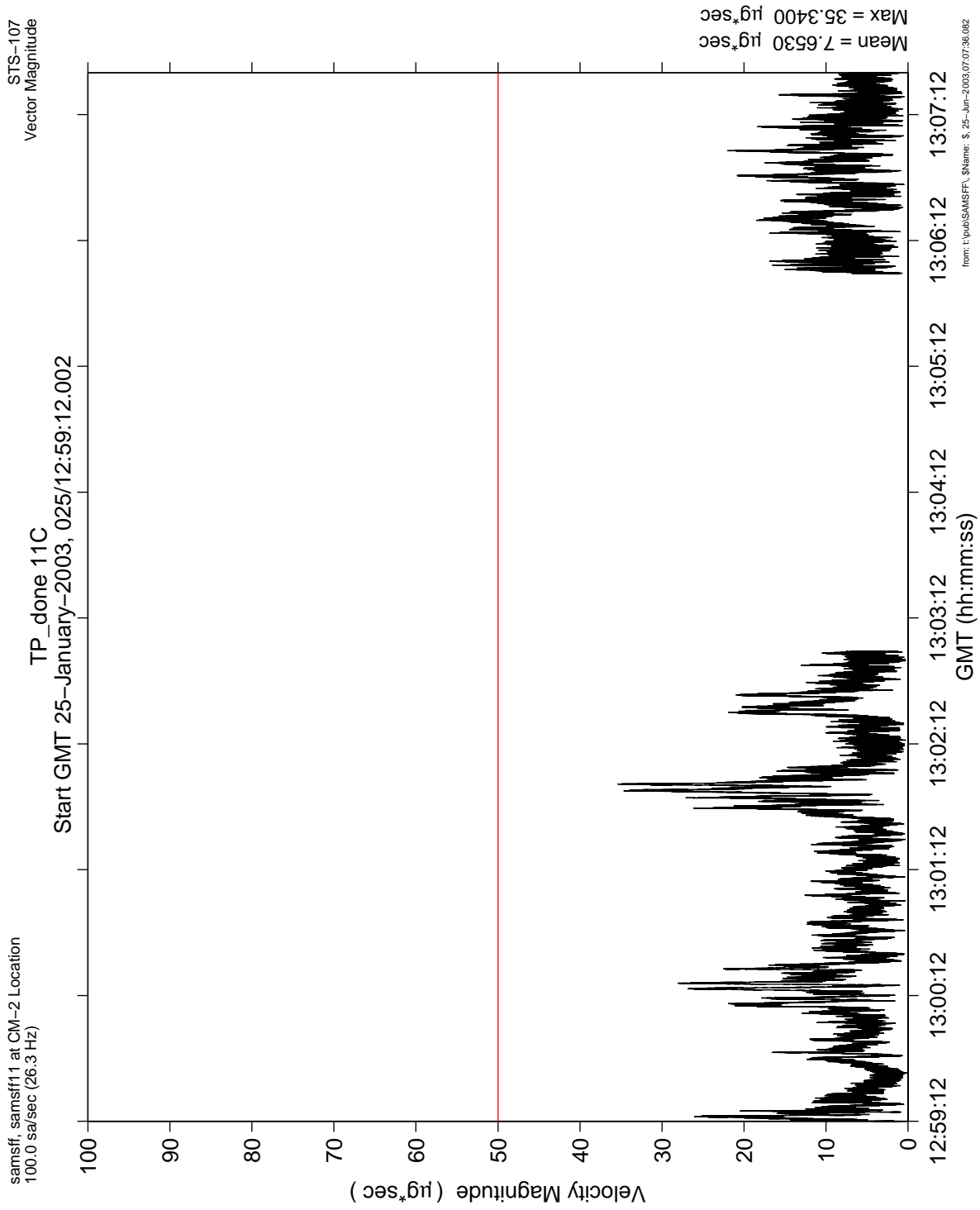


Figure 6.44 Leaky Integration For SOFBALL Test Point 11C

PIMS STS-107 Mission Microgravity Environment Summary Report:
January 16 to February 1, 2003

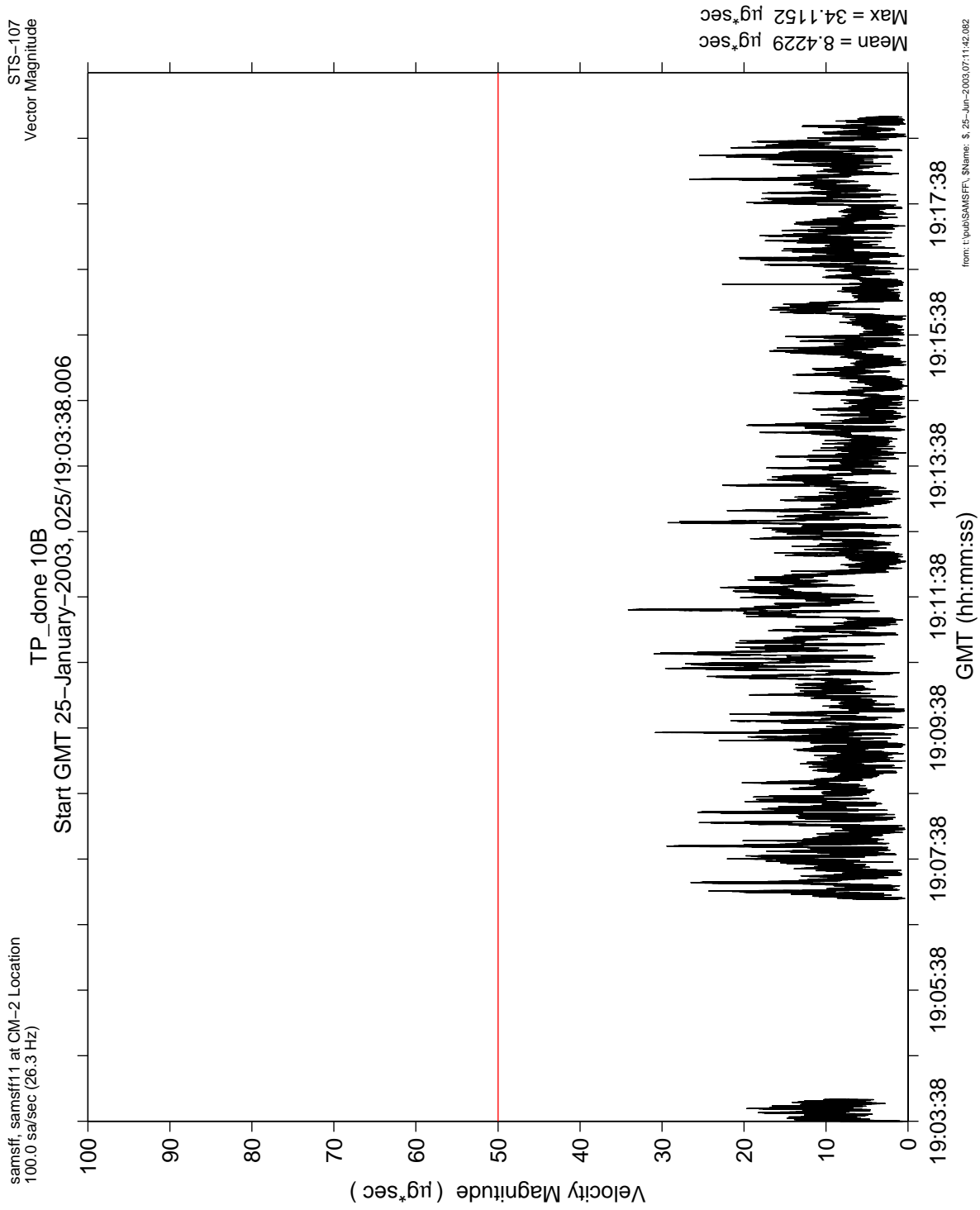


Figure 6.45 Leaky Integration For SOFBALL Test Point 10B

**PIMS STS-107 Mission Microgravity Environment Summary Report:
January 16 to February 1, 2003**

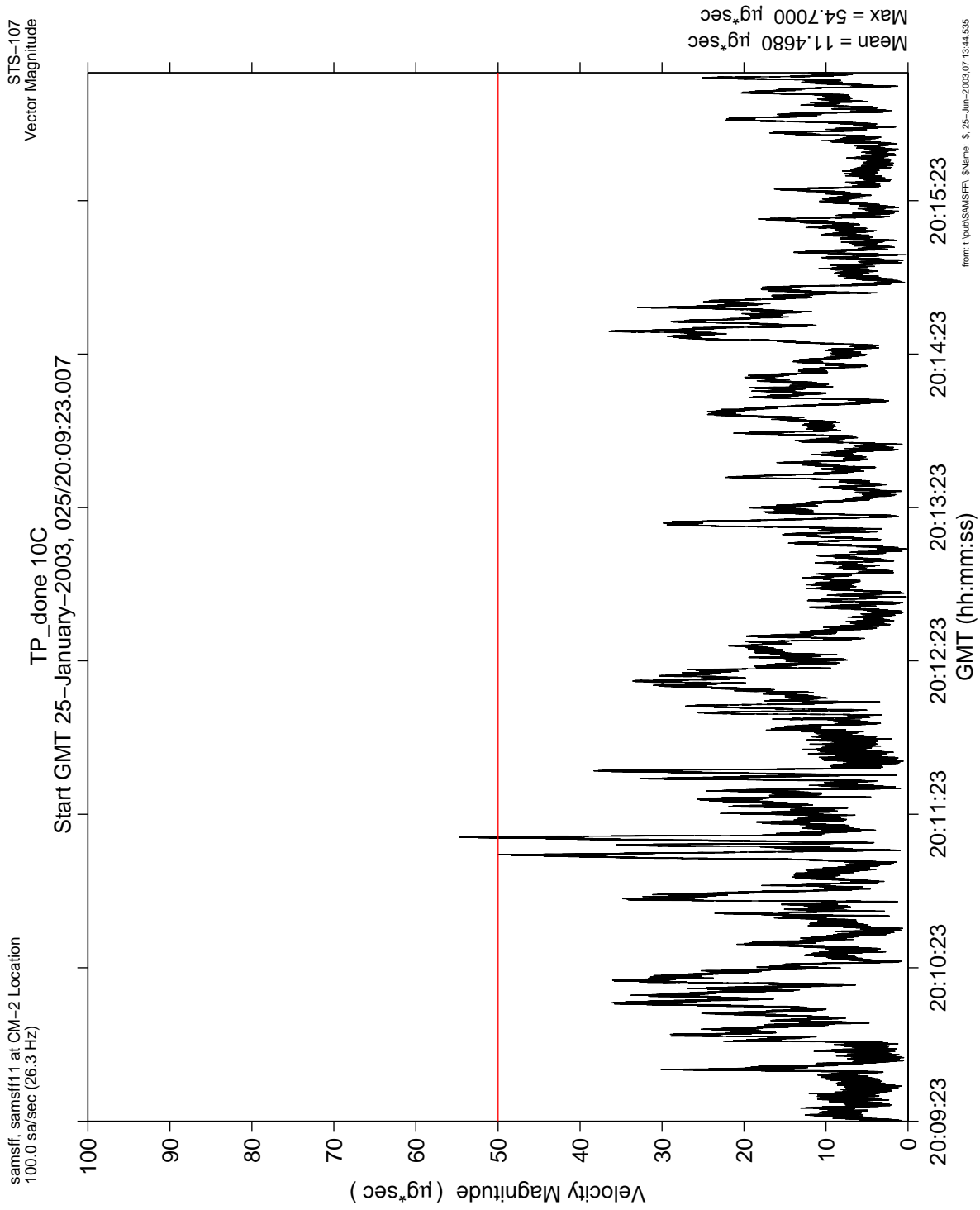


Figure 6.46 Leaky Integration For SOFBALL Test Point 10C

**PIMS STS-107 Mission Microgravity Environment Summary Report:
January 16 to February 1, 2003**

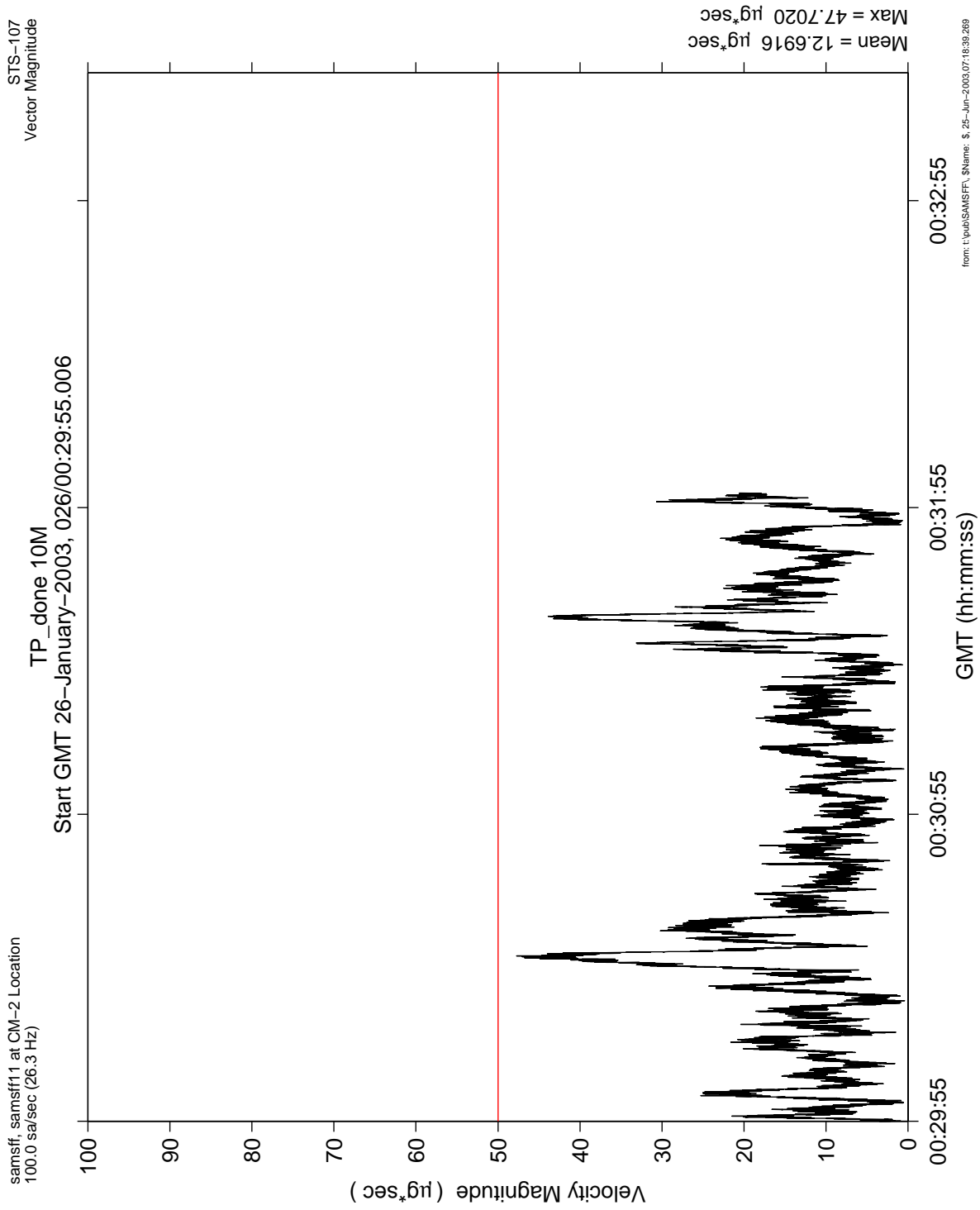


Figure 6.47 Leaky Integration For SOFBALL Test Point 10M

PIMS STS-107 Mission Microgravity Environment Summary Report:
January 16 to February 1, 2003

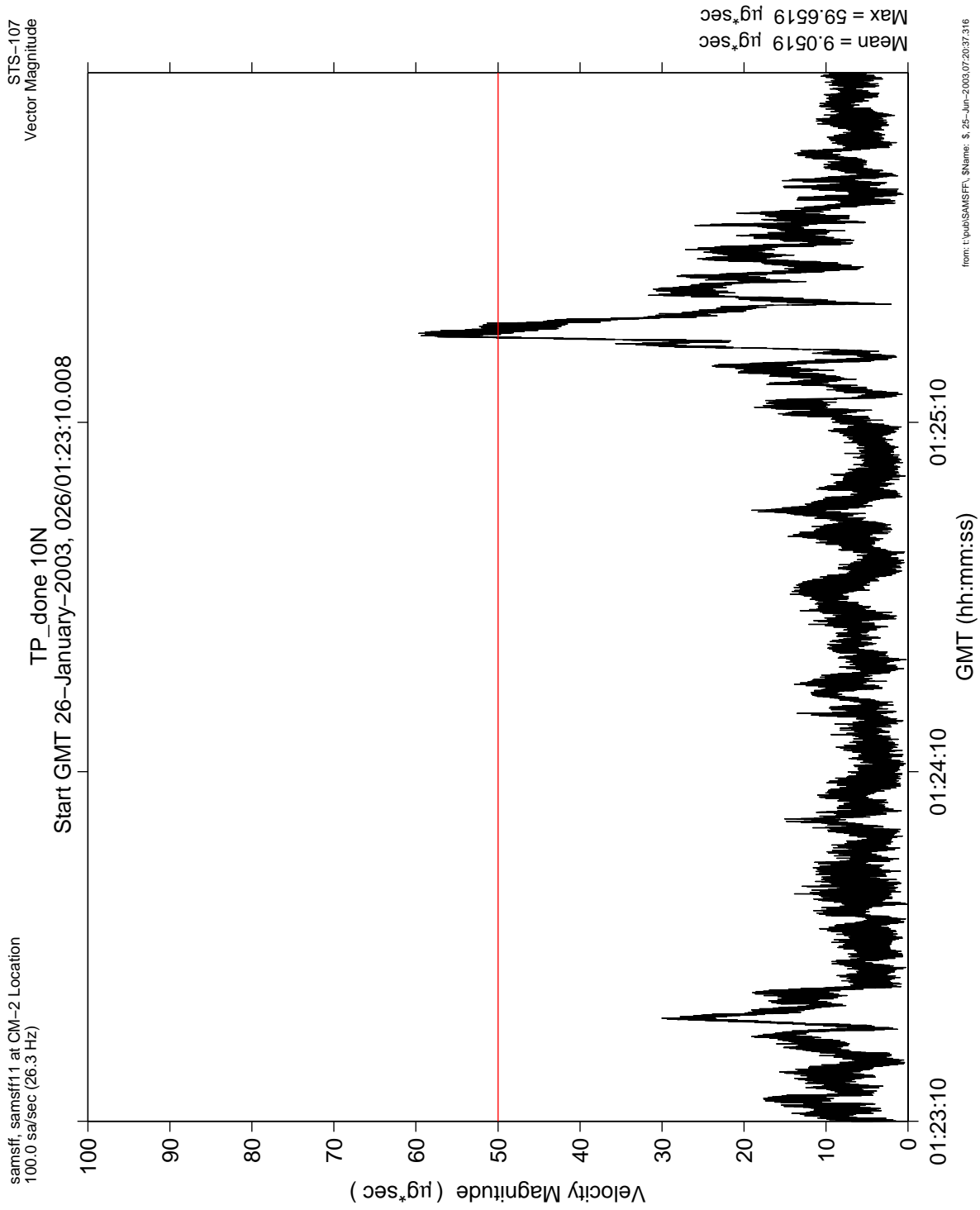


Figure 6.48 Leaky Integration For SOFBALL Test Point 10N

PIMS STS-107 Mission Microgravity Environment Summary Report:
January 16 to February 1, 2003

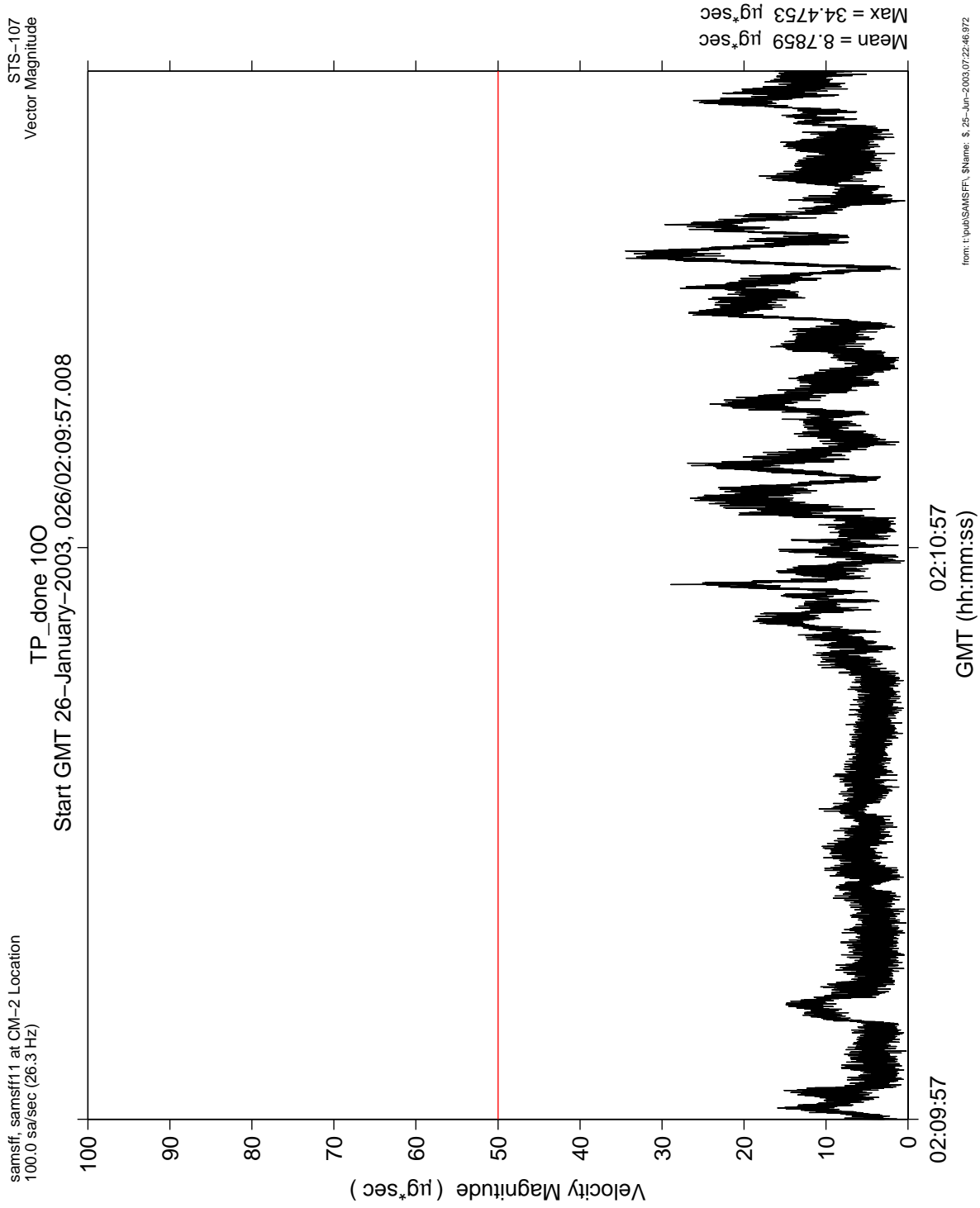


Figure 6.49 Leaky Integration For SOFBALL Test Point 100

PIMS STS-107 Mission Microgravity Environment Summary Report:
January 16 to February 1, 2003

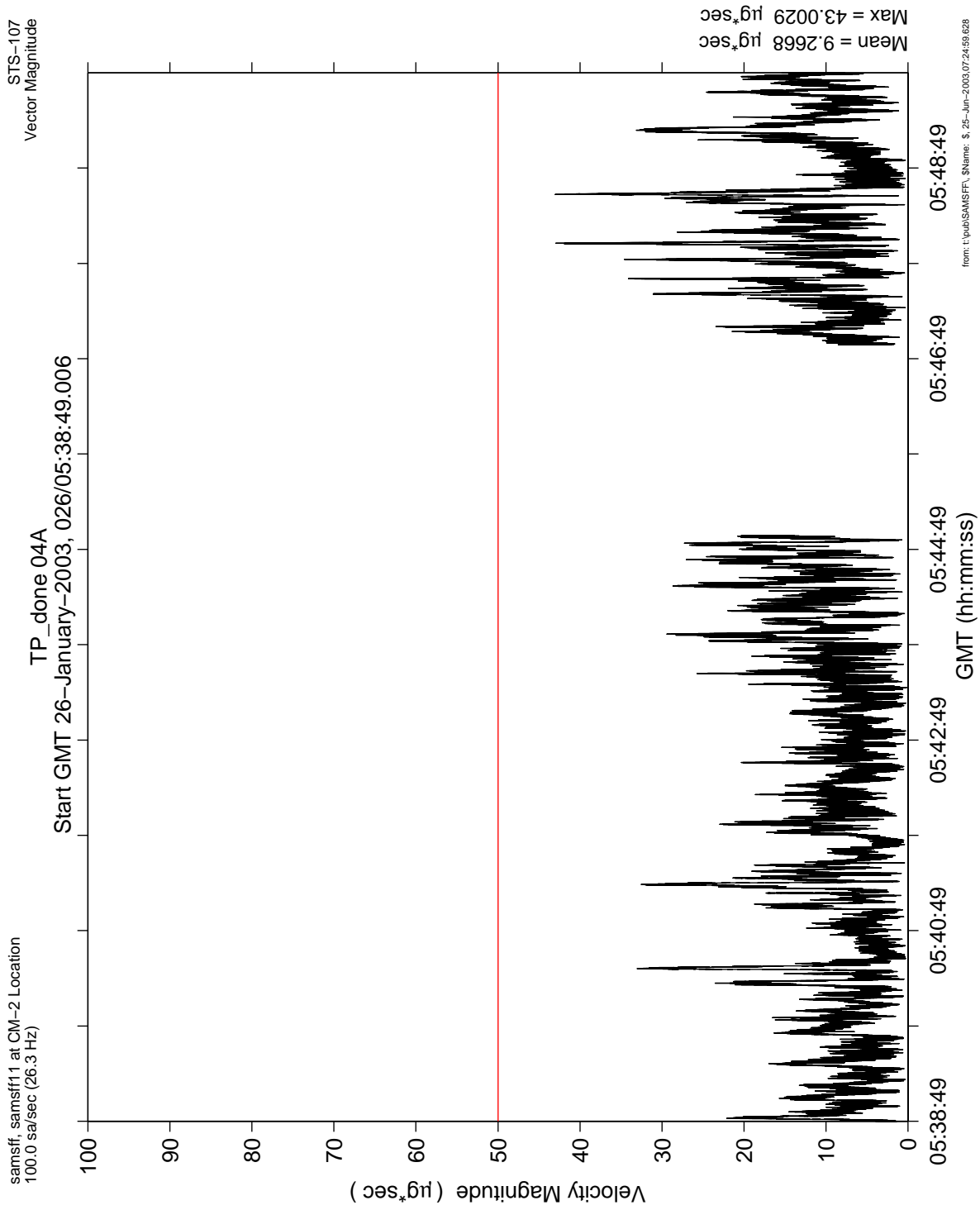


Figure 6.50 Leaky Integration For SOFBALL Test Point 04A

PIMS STS-107 Mission Microgravity Environment Summary Report:
January 16 to February 1, 2003

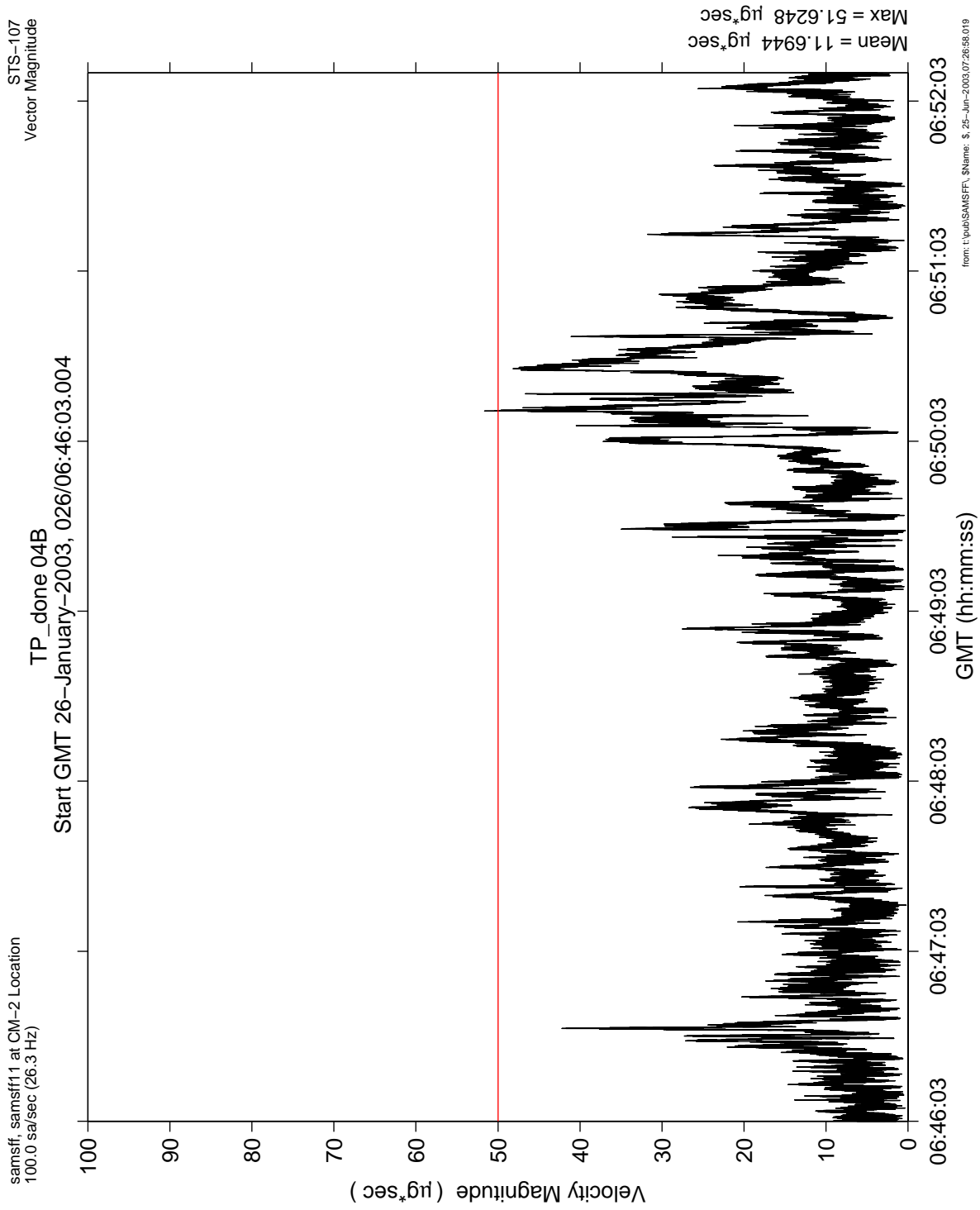


Figure 6.51 Leaky Integration For SOFBALL Test Point 04B

**PIMS STS-107 Mission Microgravity Environment Summary Report:
January 16 to February 1, 2003**

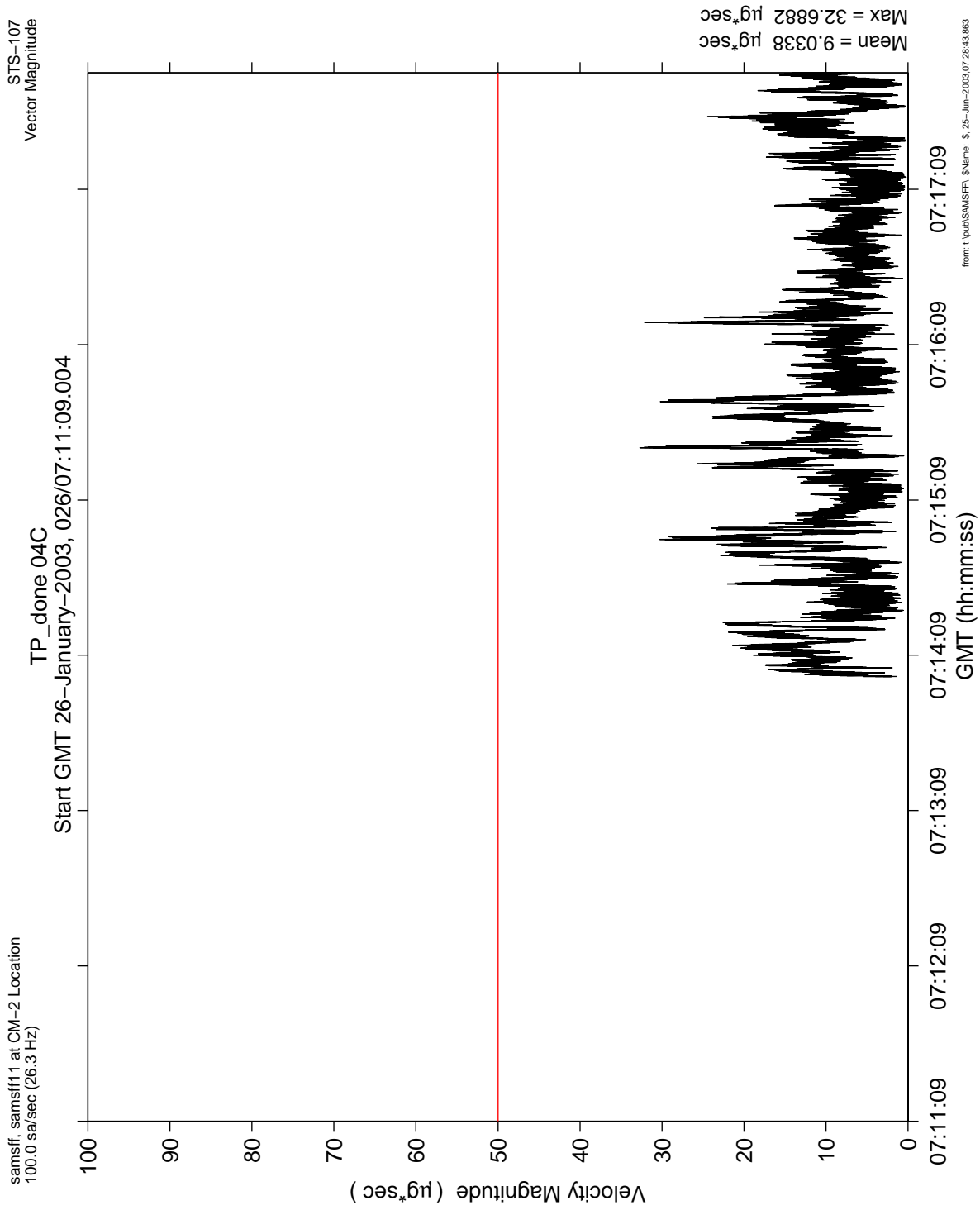


Figure 6.52 Leaky Integration For SOFBALL Test Point 04C

**PIMS STS-107 Mission Microgravity Environment Summary Report:
January 16 to February 1, 2003**

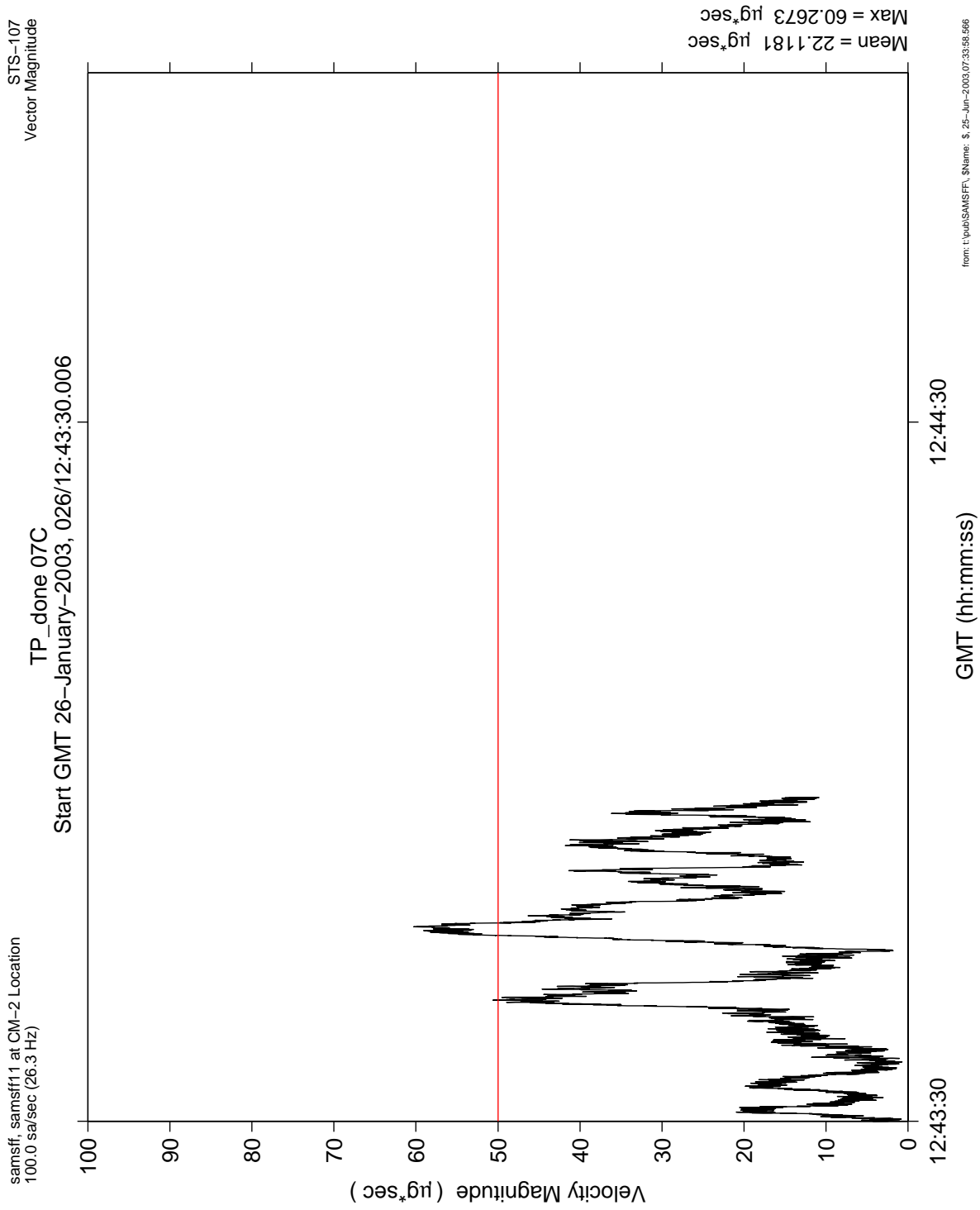


Figure 6.53 Leaky Integration For SOFBALL Test Point 07C

**PIMS STS-107 Mission Microgravity Environment Summary Report:
January 16 to February 1, 2003**

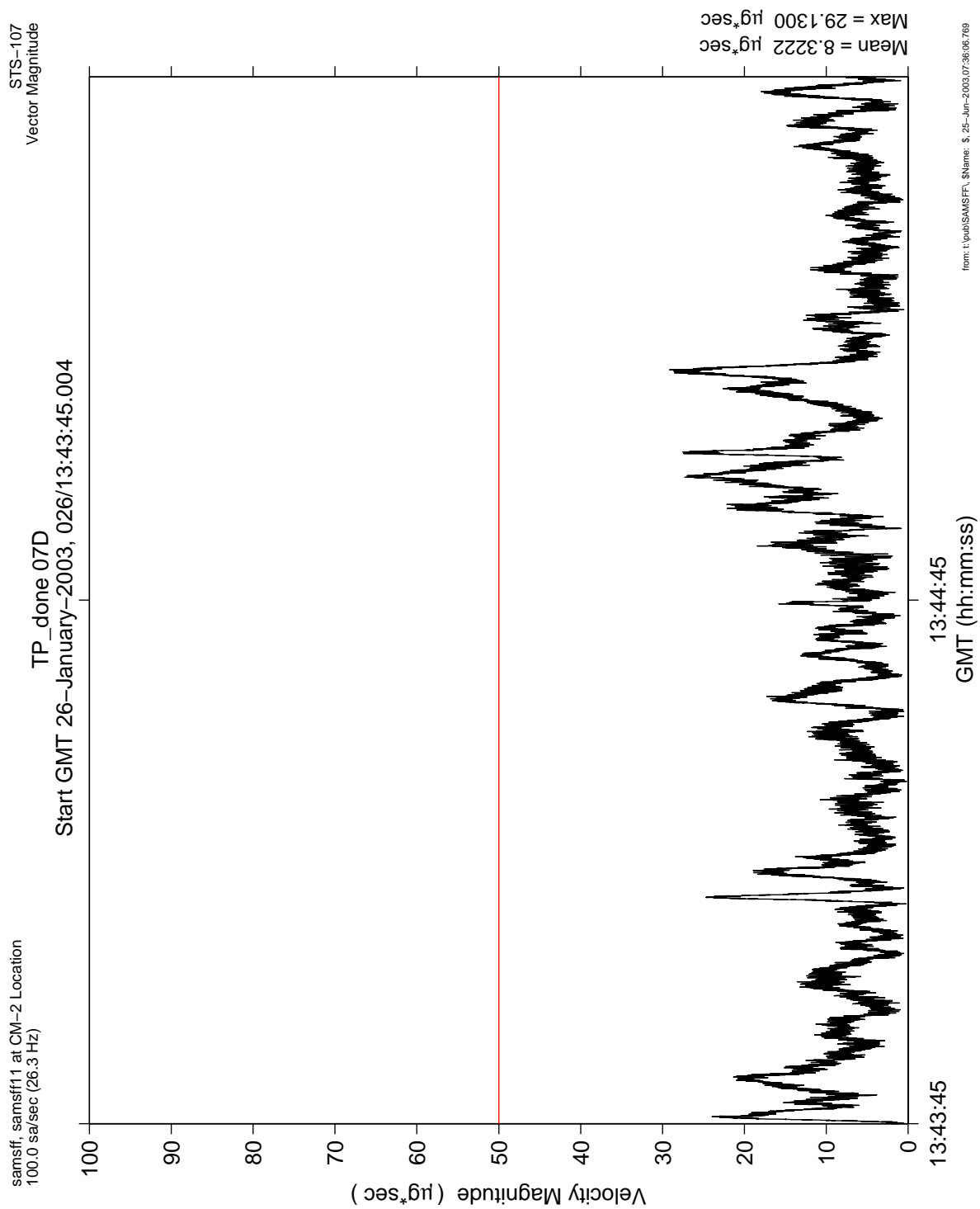


Figure 6.54 Leaky Integration For SOFBALL Test Point 07D

**PIMS STS-107 Mission Microgravity Environment Summary Report:
January 16 to February 1, 2003**

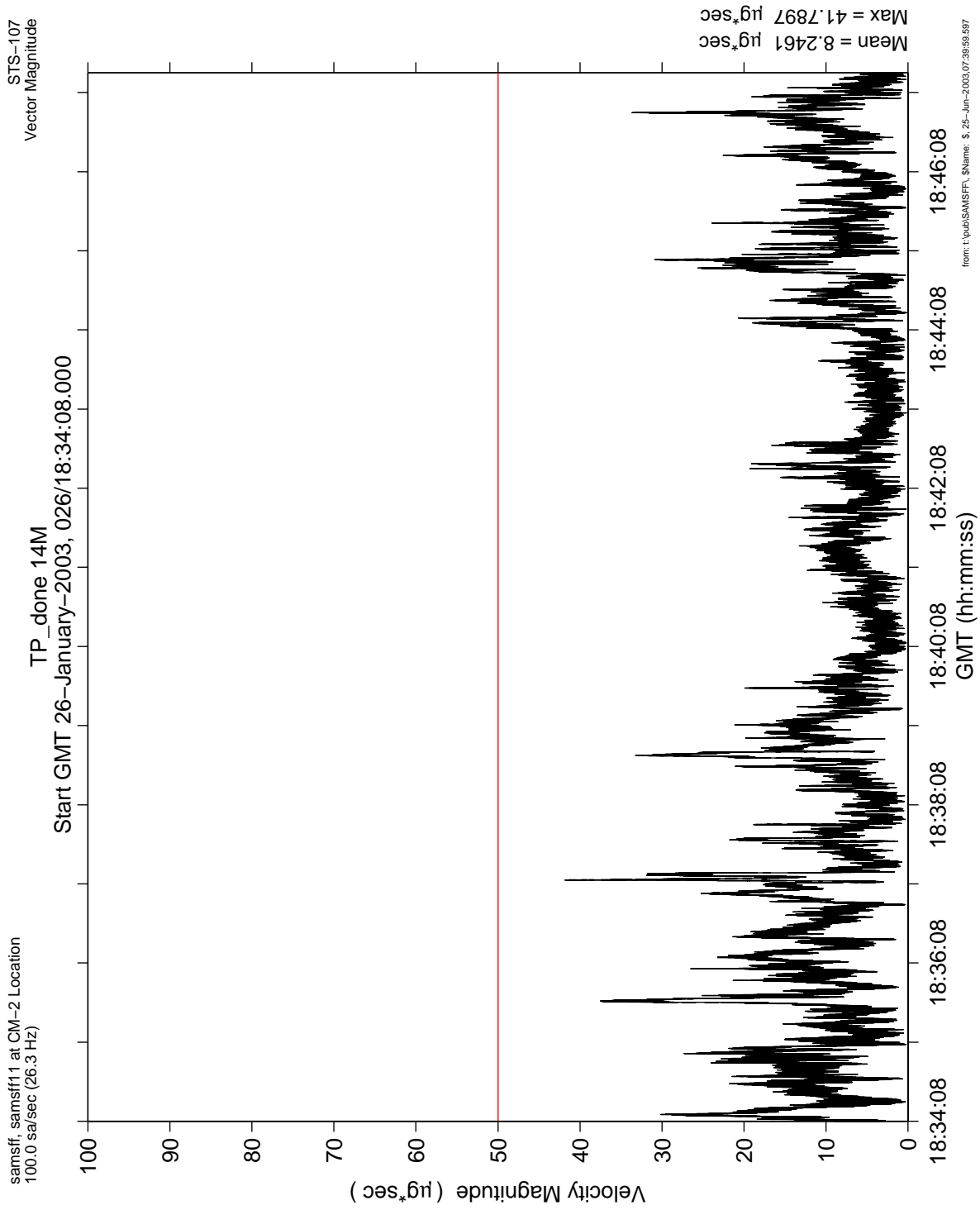


Figure 6.55 Leaky Integration For SOFBALL Test Point 14M

PIMS STS-107 Mission Microgravity Environment Summary Report:
January 16 to February 1, 2003

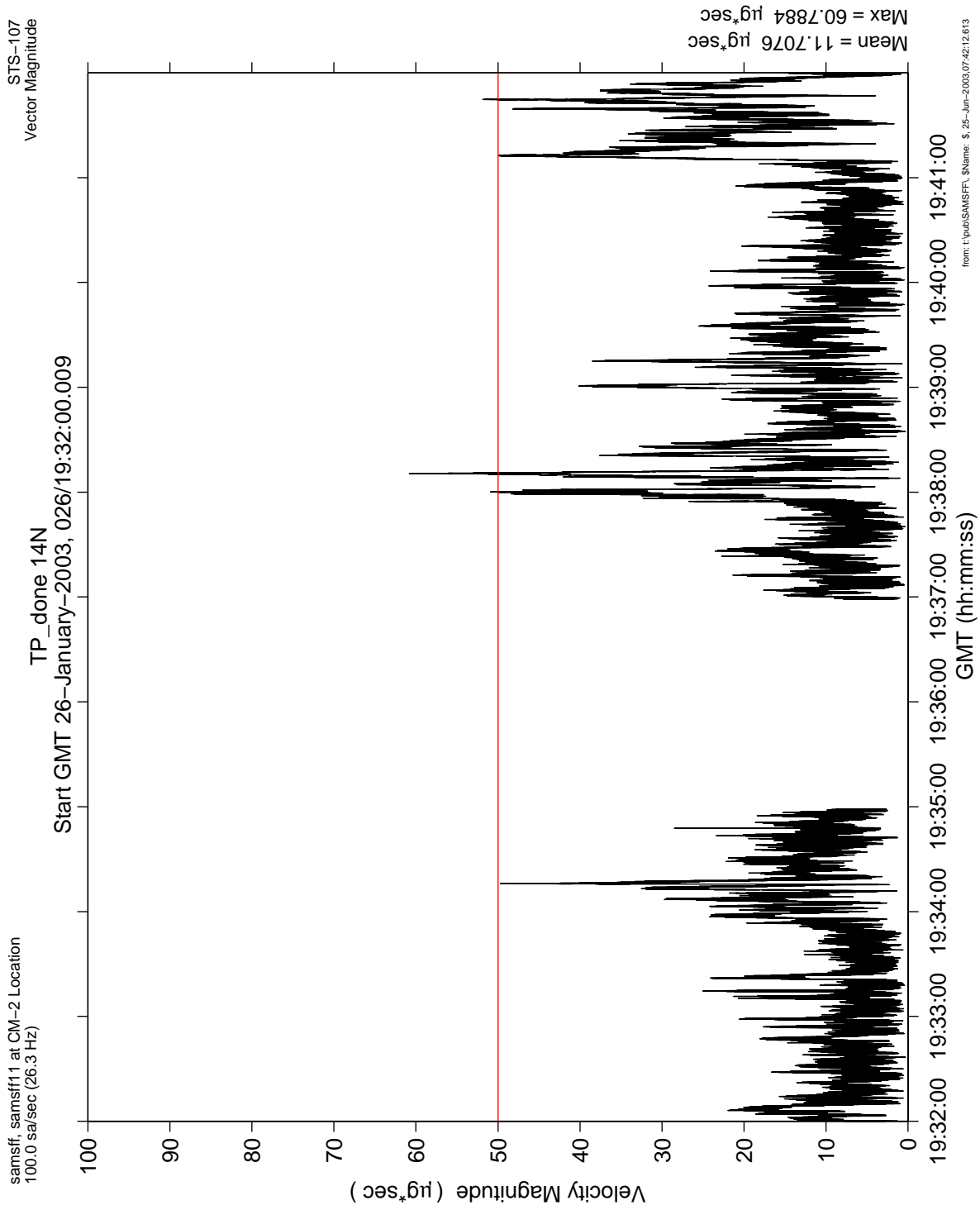


Figure 6.56 Leaky Integration For SOFBALL Test Point 14N

**PIMS STS-107 Mission Microgravity Environment Summary Report:
January 16 to February 1, 2003**

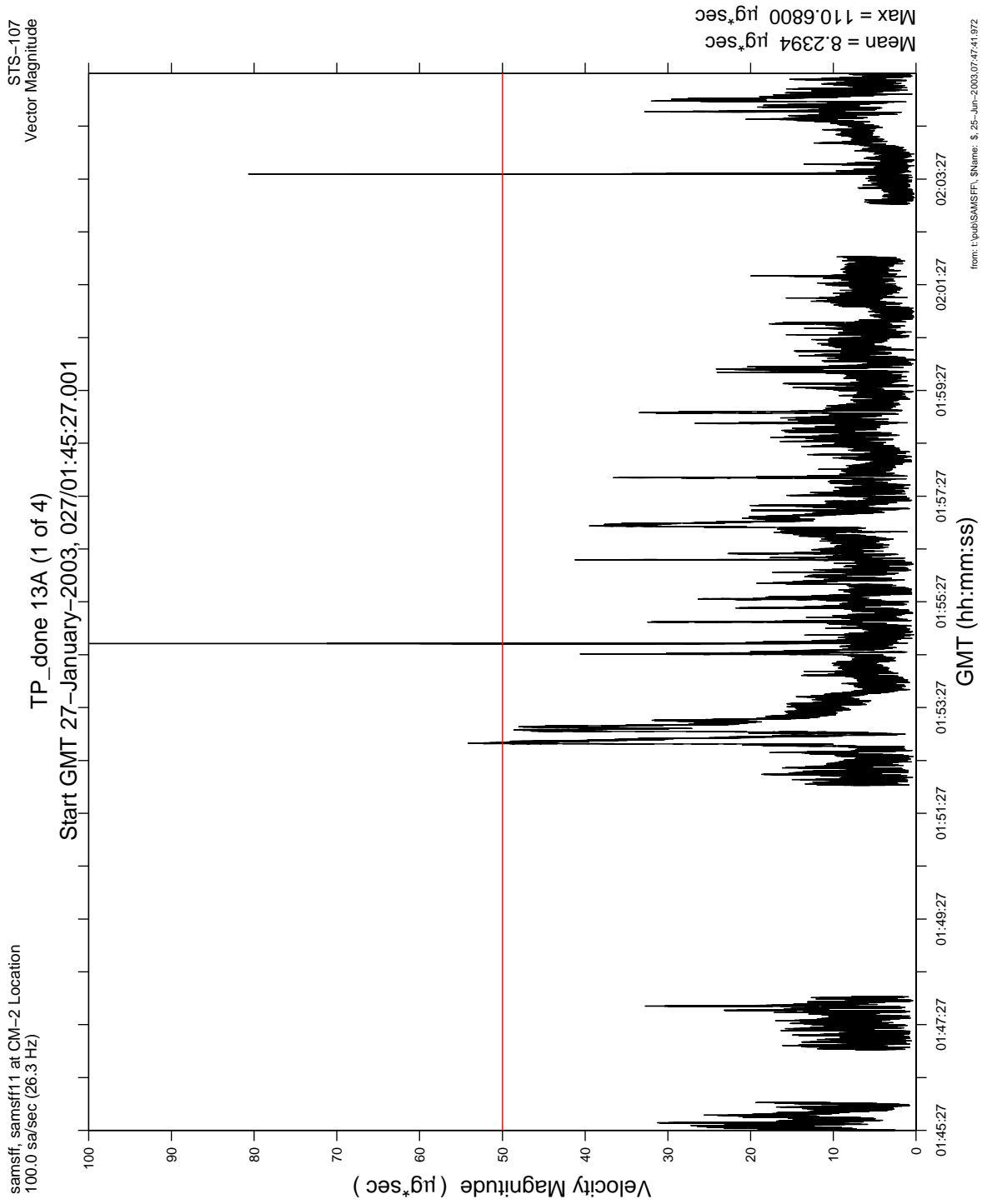


Figure 6.57 Leaky Integration For SOFBALL Test Point 13A (1 of 4)

PIMS STS-107 Mission Microgravity Environment Summary Report:
January 16 to February 1, 2003

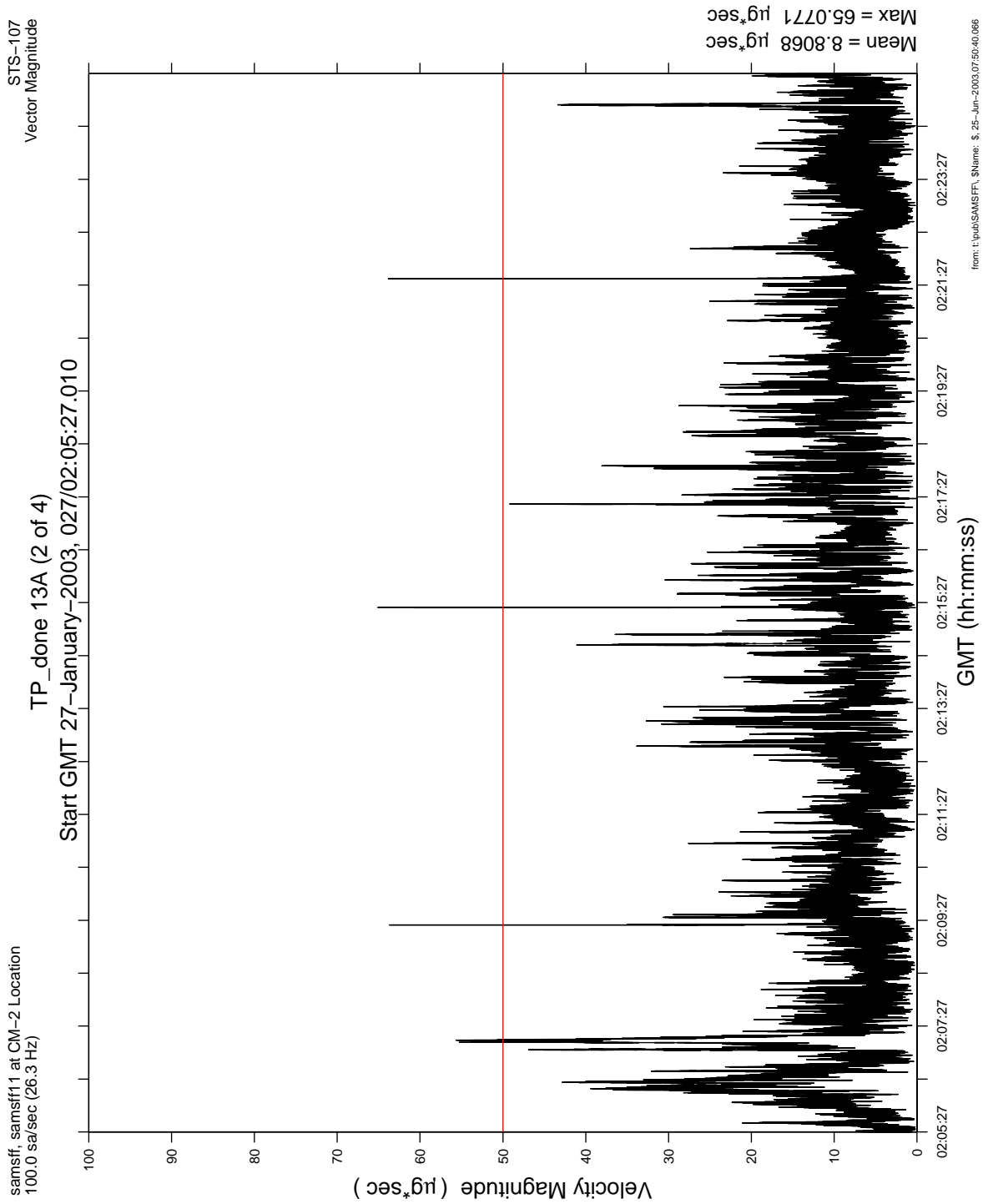


Figure 6.58 Leaky Integration For SOFBALL Test Point 13A (2 of 4)

**PIMS STS-107 Mission Microgravity Environment Summary Report:
January 16 to February 1, 2003**

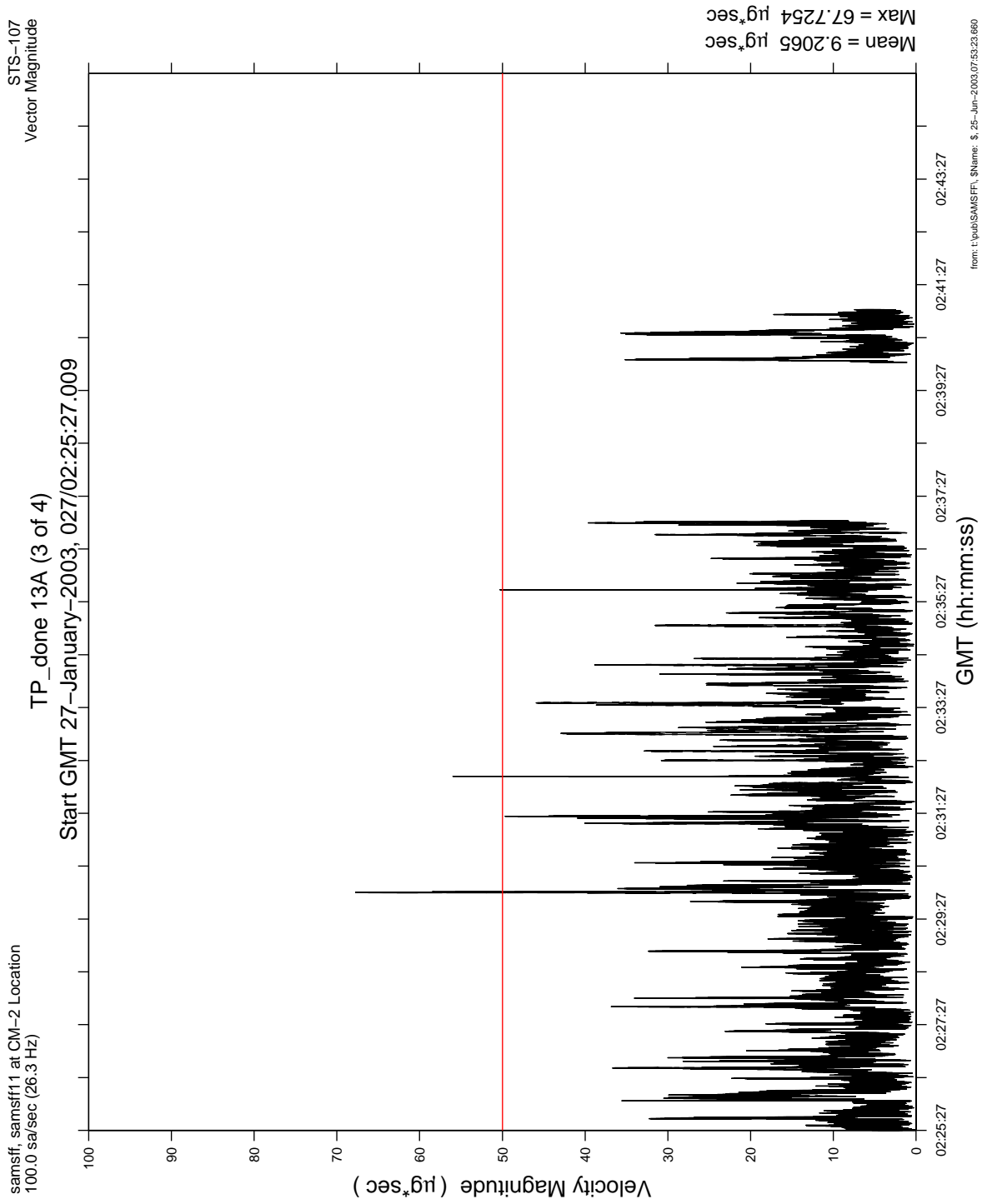


Figure 6.59 Leaky Integration For SOFBALL Test Point 13A (3 of 4)

**PIMS STS-107 Mission Microgravity Environment Summary Report:
January 16 to February 1, 2003**

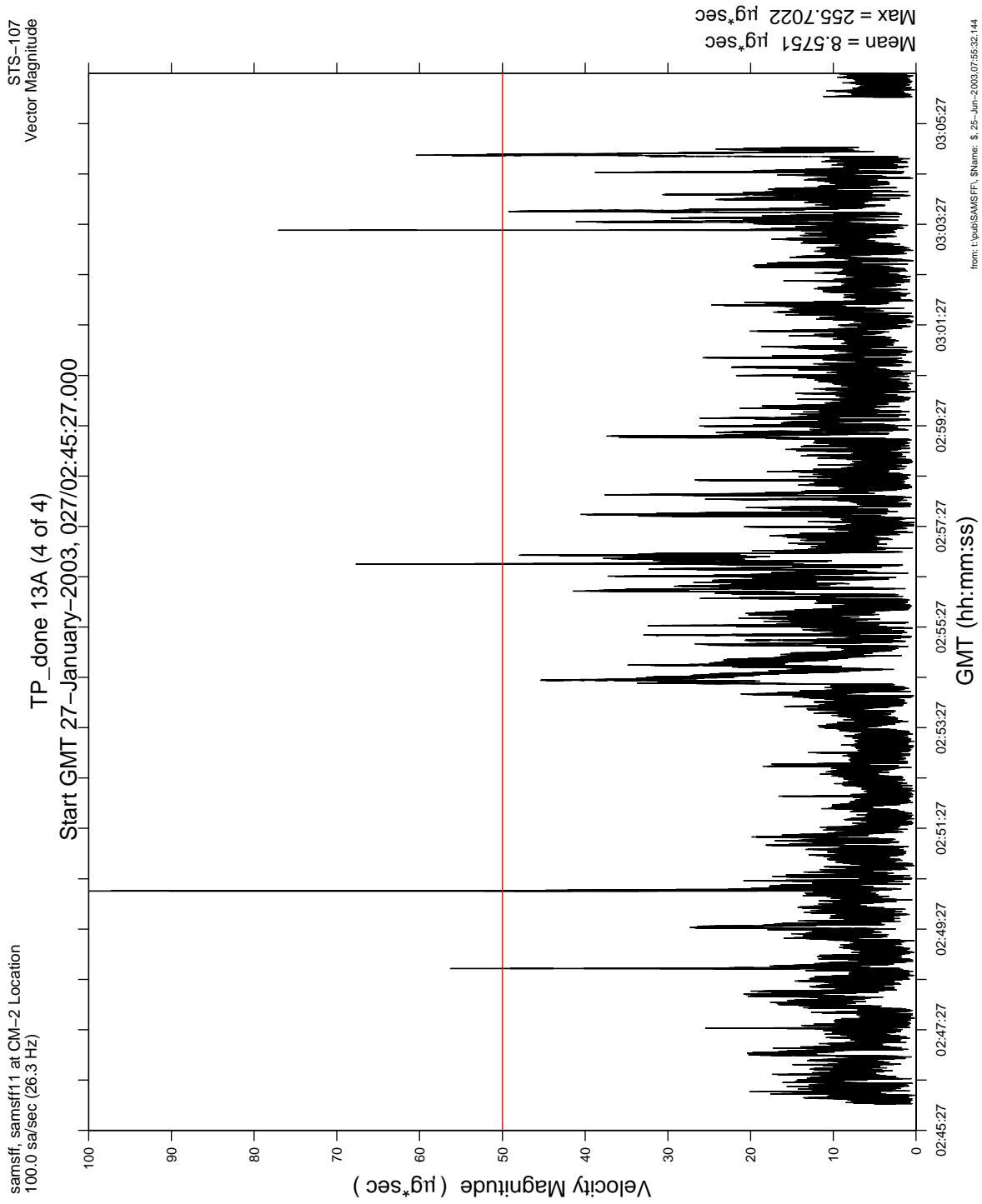


Figure 6.60 Leaky Integration For SOFBALL Test Point 13A (4 of 4)

**PIMS STS-107 Mission Microgravity Environment Summary Report:
January 16 to February 1, 2003**

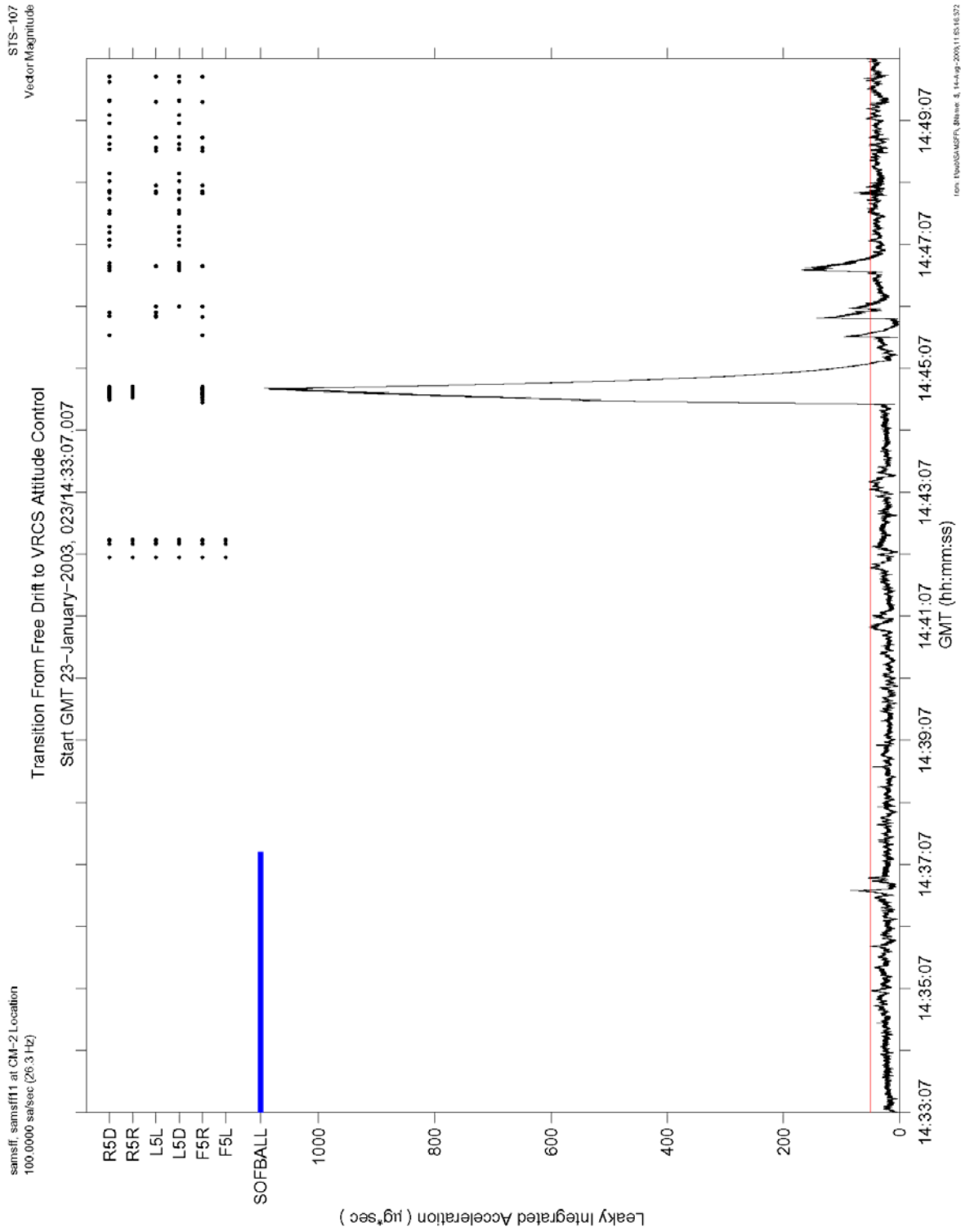


Figure 6.61 Leaky Integration For Transition Out Of Free Drift

**PIMS STS-107 Mission Microgravity Environment Summary Report:
January 16 to February 1, 2003**

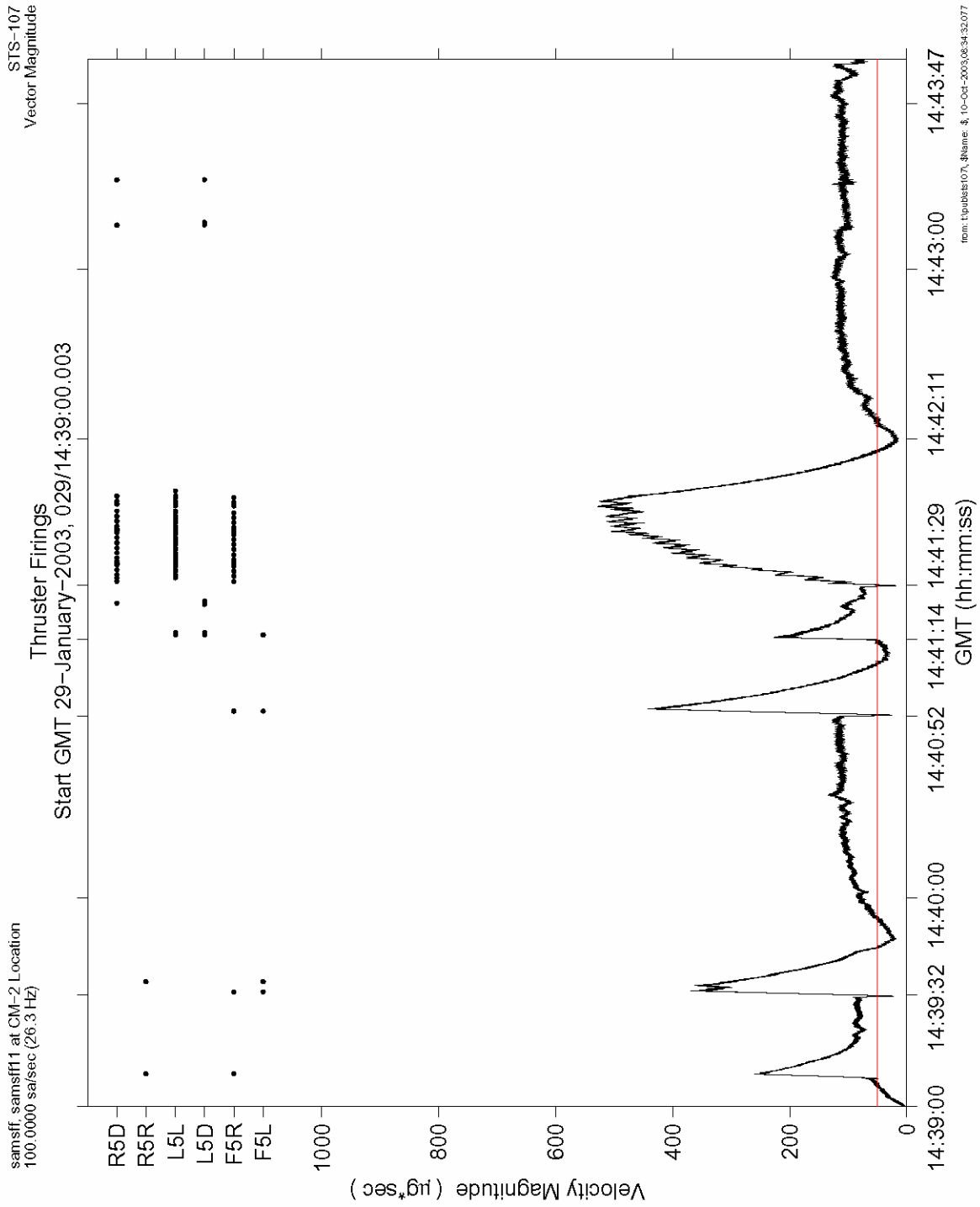


Figure 6.62 Leaky Integration Of Thruster Firings For Mist Test Point 10 - 68M

**PIMS STS-107 Mission Microgravity Environment Summary Report:
January 16 to February 1, 2003**

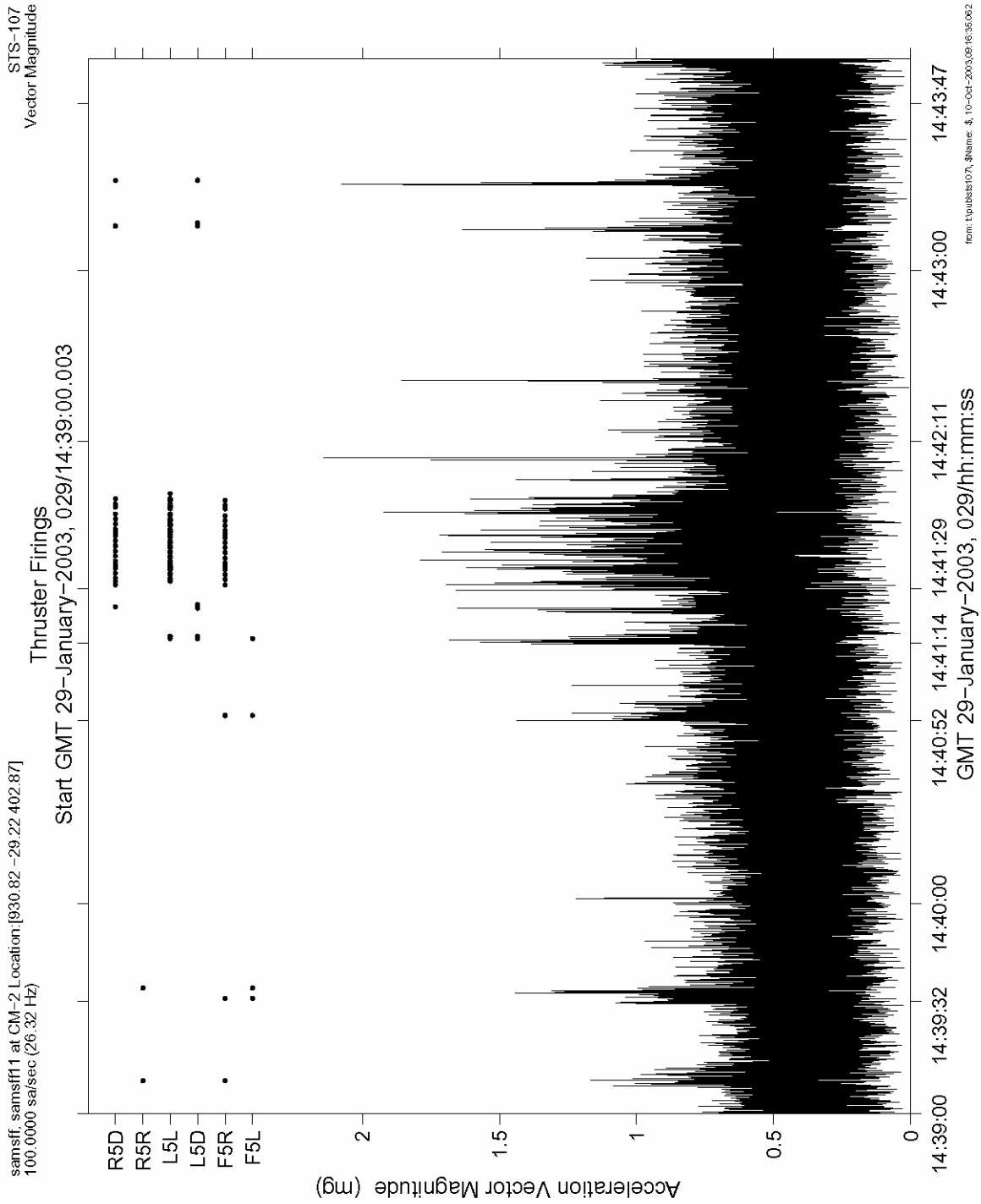


Figure 6.63 Acceleration Magnitude Of Thruster Firings For Mist Test Point 10 - 68M

PIMS STS-107 Mission Microgravity Environment Summary Report: January 16 to February 1, 2003

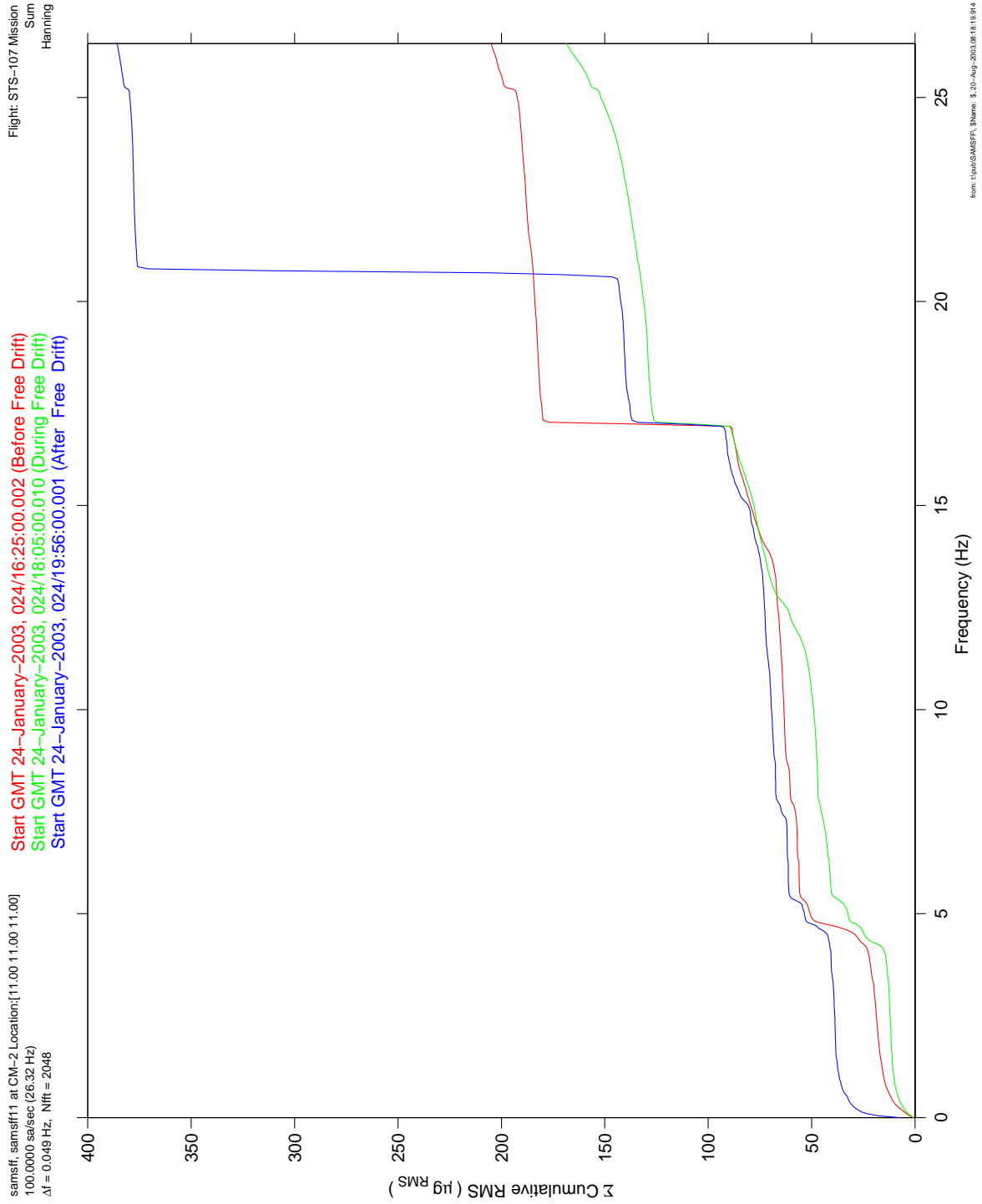


Figure 6.64 Cumulative RMS vs. Frequency Free Drift Comparison

**PIMS STS-107 Mission Microgravity Environment Summary Report:
January 16 to February 1, 2003**

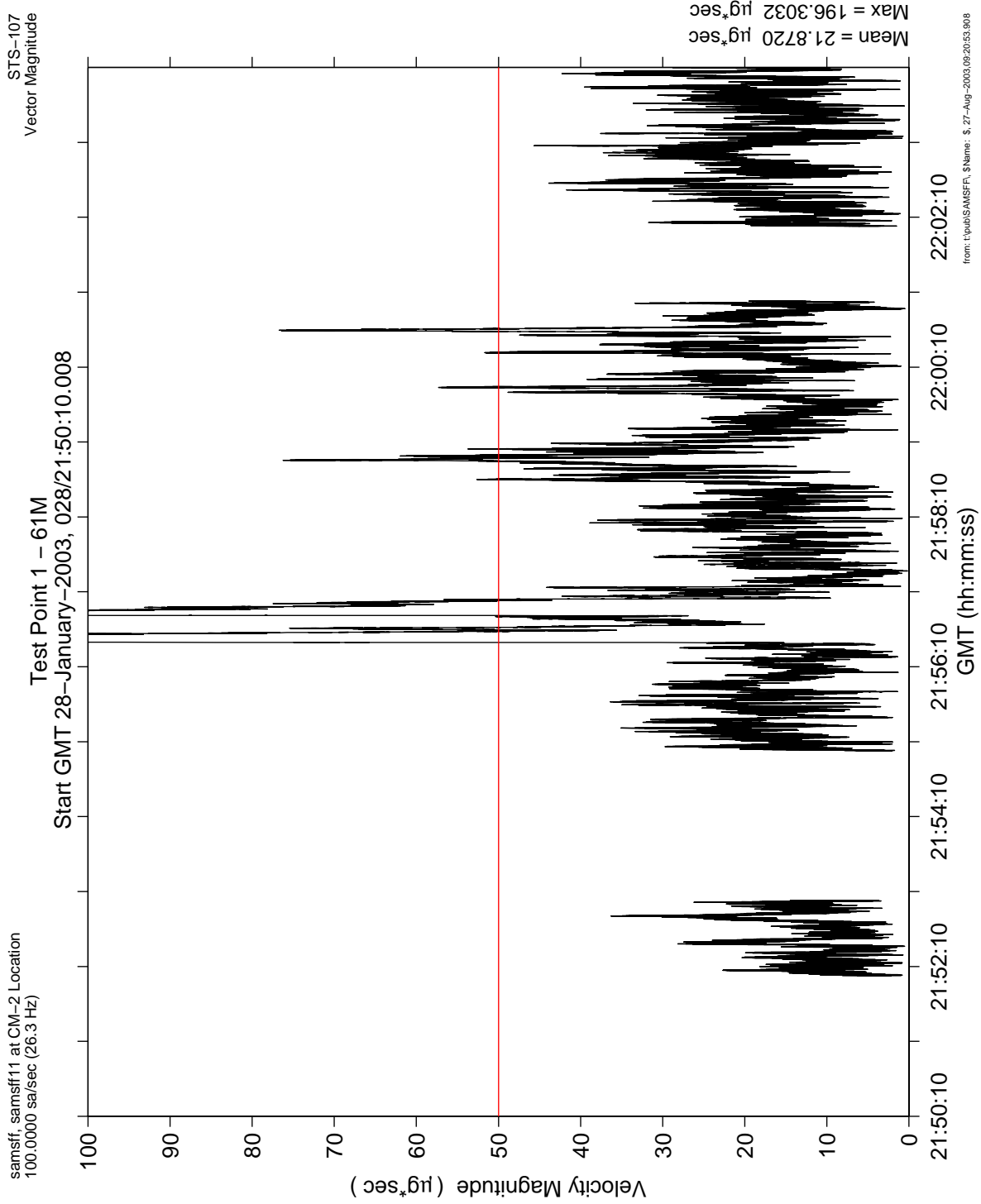


Figure 6.65 Leaky Integration For Mist Test Point 1-61M

PIMS STS-107 Mission Microgravity Environment Summary Report:
January 16 to February 1, 2003

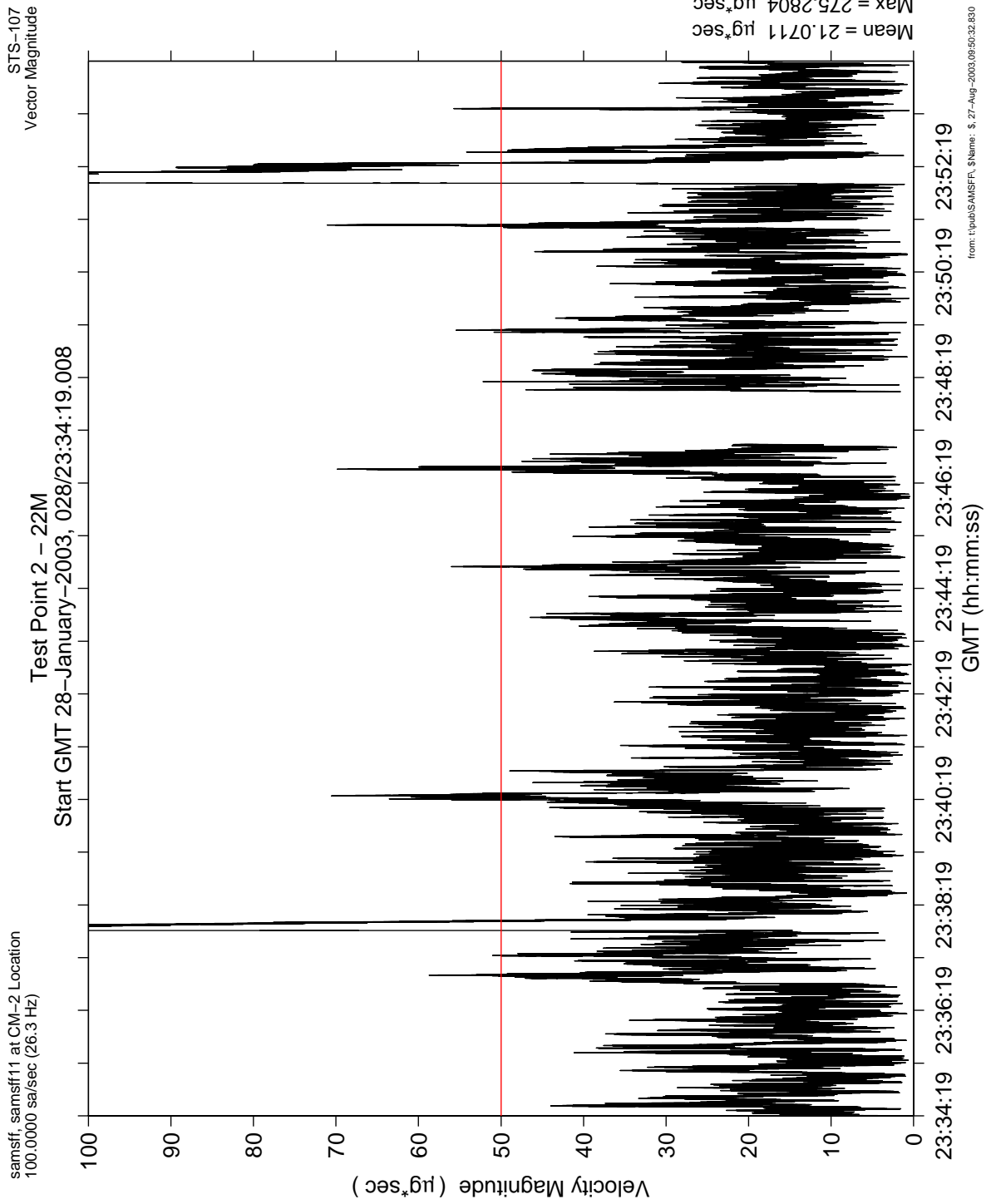


Figure 6.66 Leaky Integration For Mist Test Point 2-22M

PIMS STS-107 Mission Microgravity Environment Summary Report:
January 16 to February 1, 2003

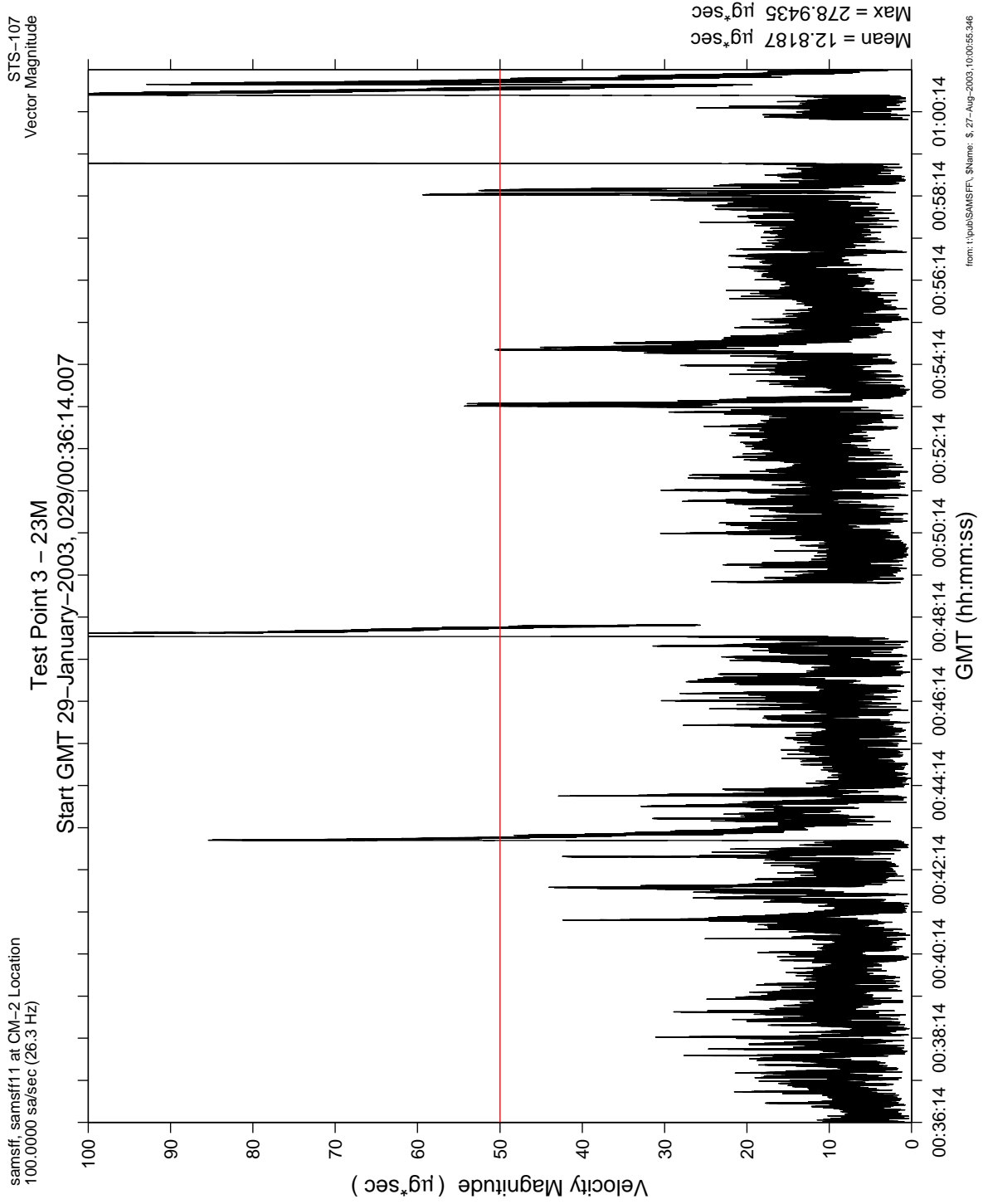


Figure 6.67 Leaky Integration For Mist Test Point 3-23M

**PIMS STS-107 Mission Microgravity Environment Summary Report:
January 16 to February 1, 2003**

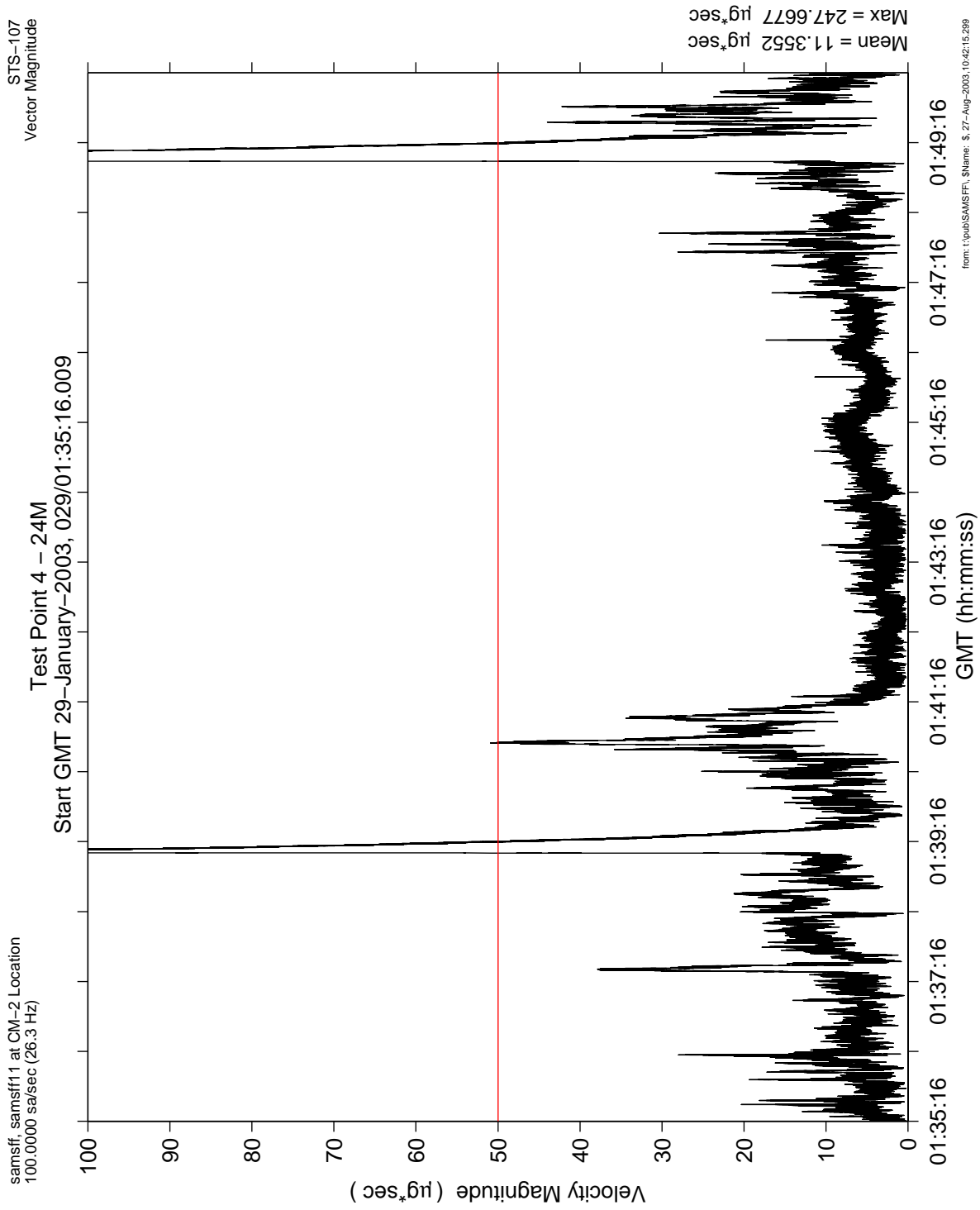


Figure 6.68 Leaky Integration For Mist Test Point 4-24M

PIMS STS-107 Mission Microgravity Environment Summary Report:
January 16 to February 1, 2003

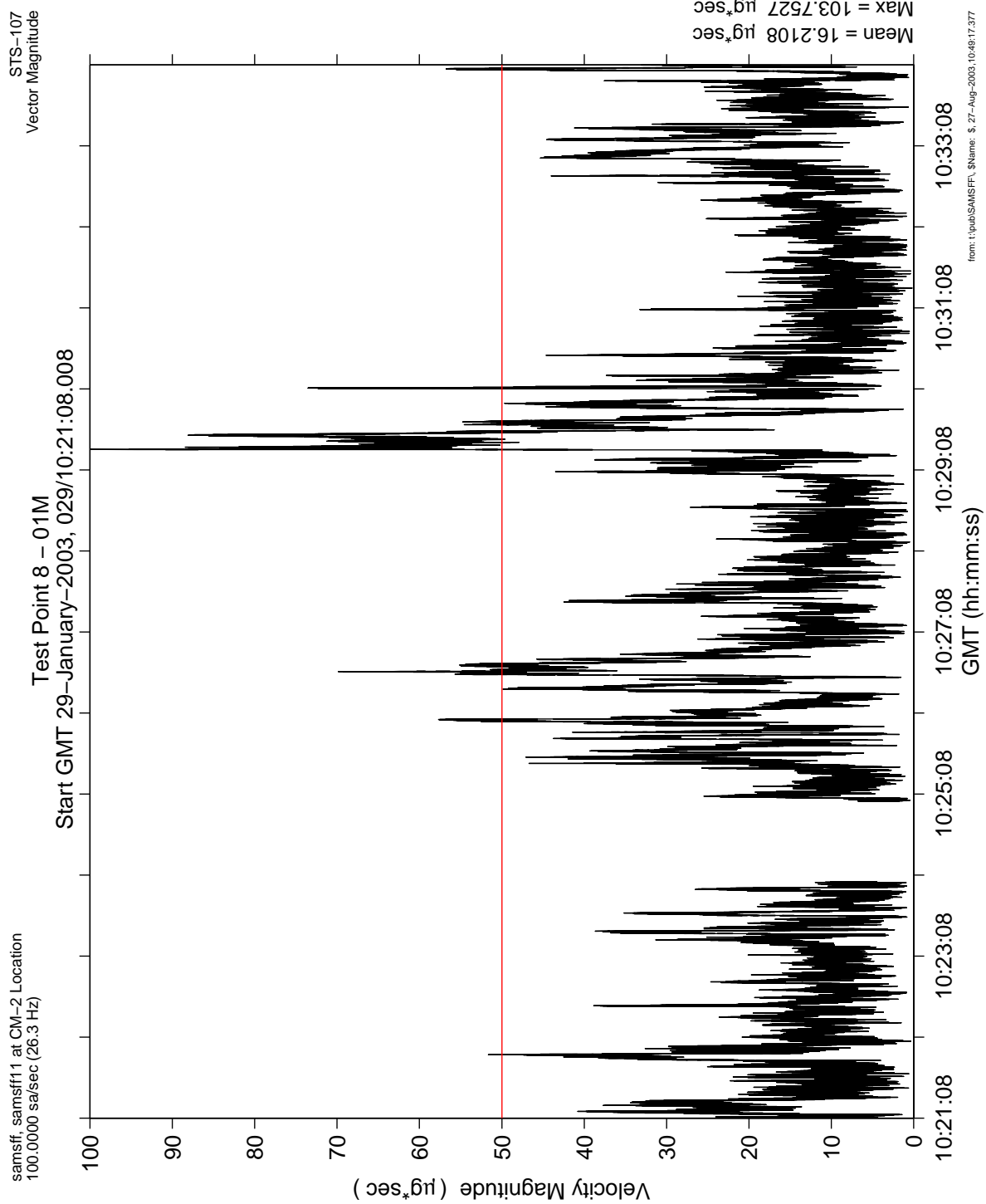


Figure 6.69 Leaky Integration For Mist Test Point 8-01M

**PIMS STS-107 Mission Microgravity Environment Summary Report:
January 16 to February 1, 2003**

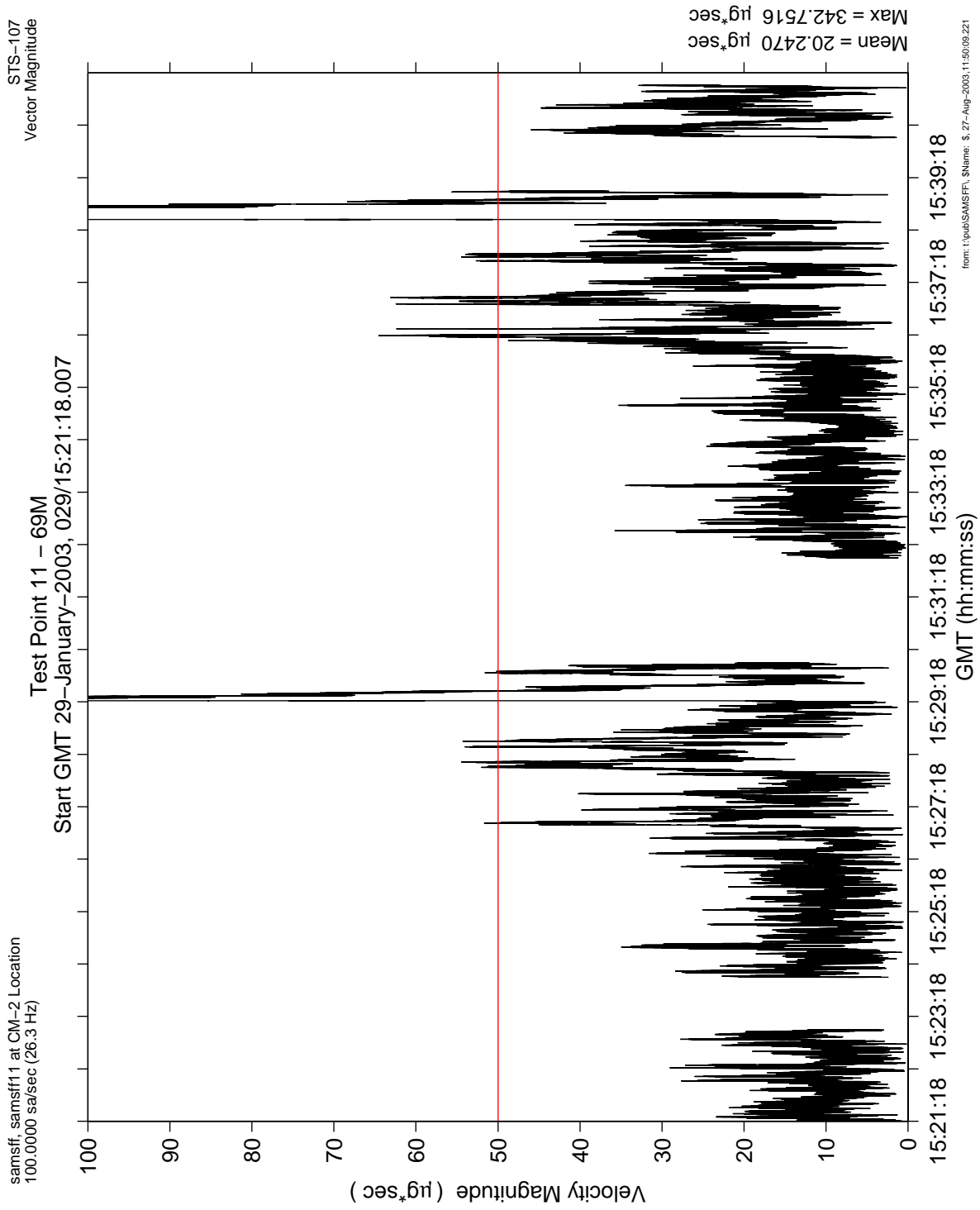


Figure 6.70 Leaky Integration For Mist Test Point 11-69M

PIMS STS-107 Mission Microgravity Environment Summary Report:
January 16 to February 1, 2003

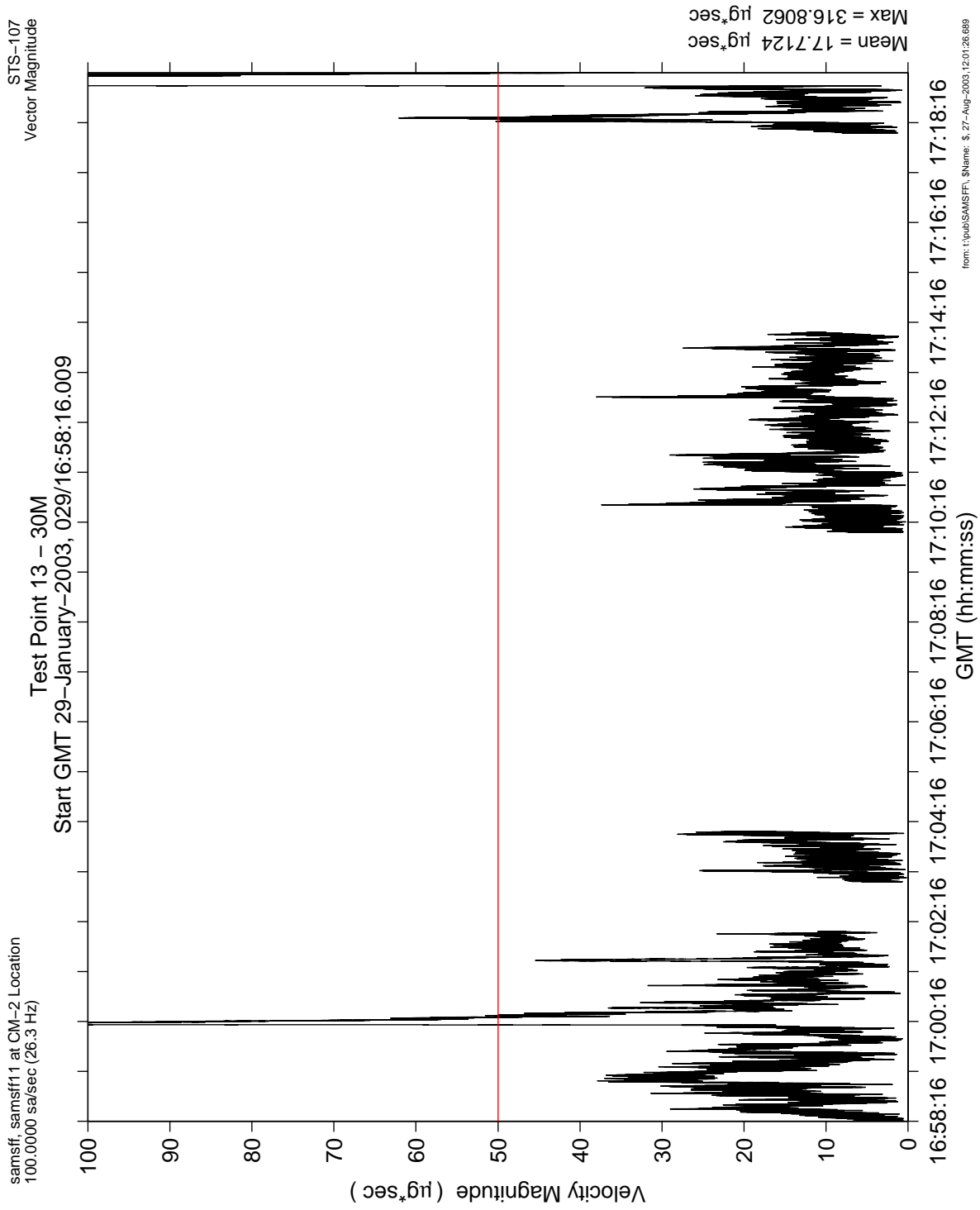


Figure 6.71 Leaky Integration For Mist Test Point 13-30M

PIMS STS-107 Mission Microgravity Environment Summary Report:
January 16 to February 1, 2003

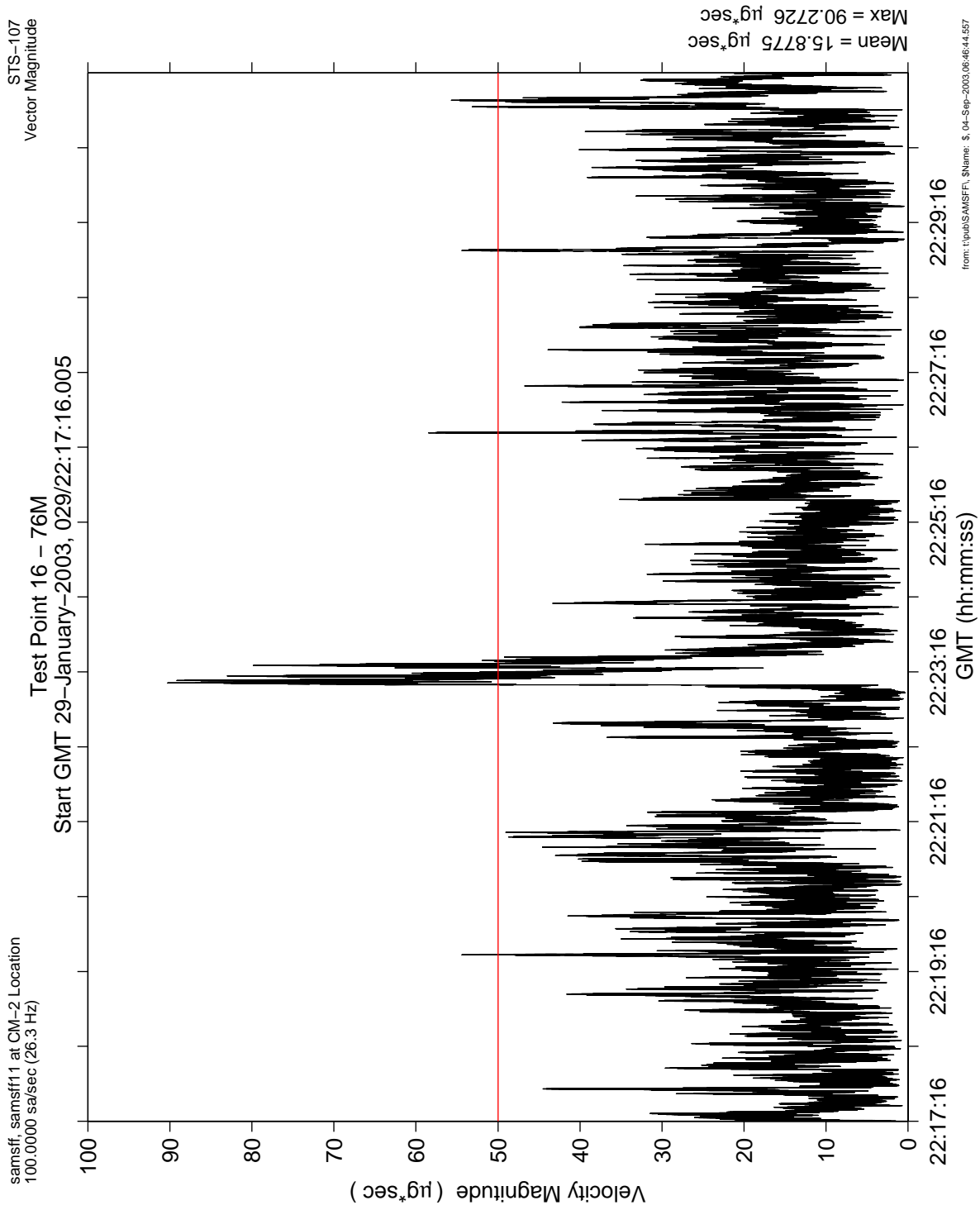


Figure 6.72 Leaky Integration For Mist Test Point 16-76M

PIMS STS-107 Mission Microgravity Environment Summary Report:
January 16 to February 1, 2003

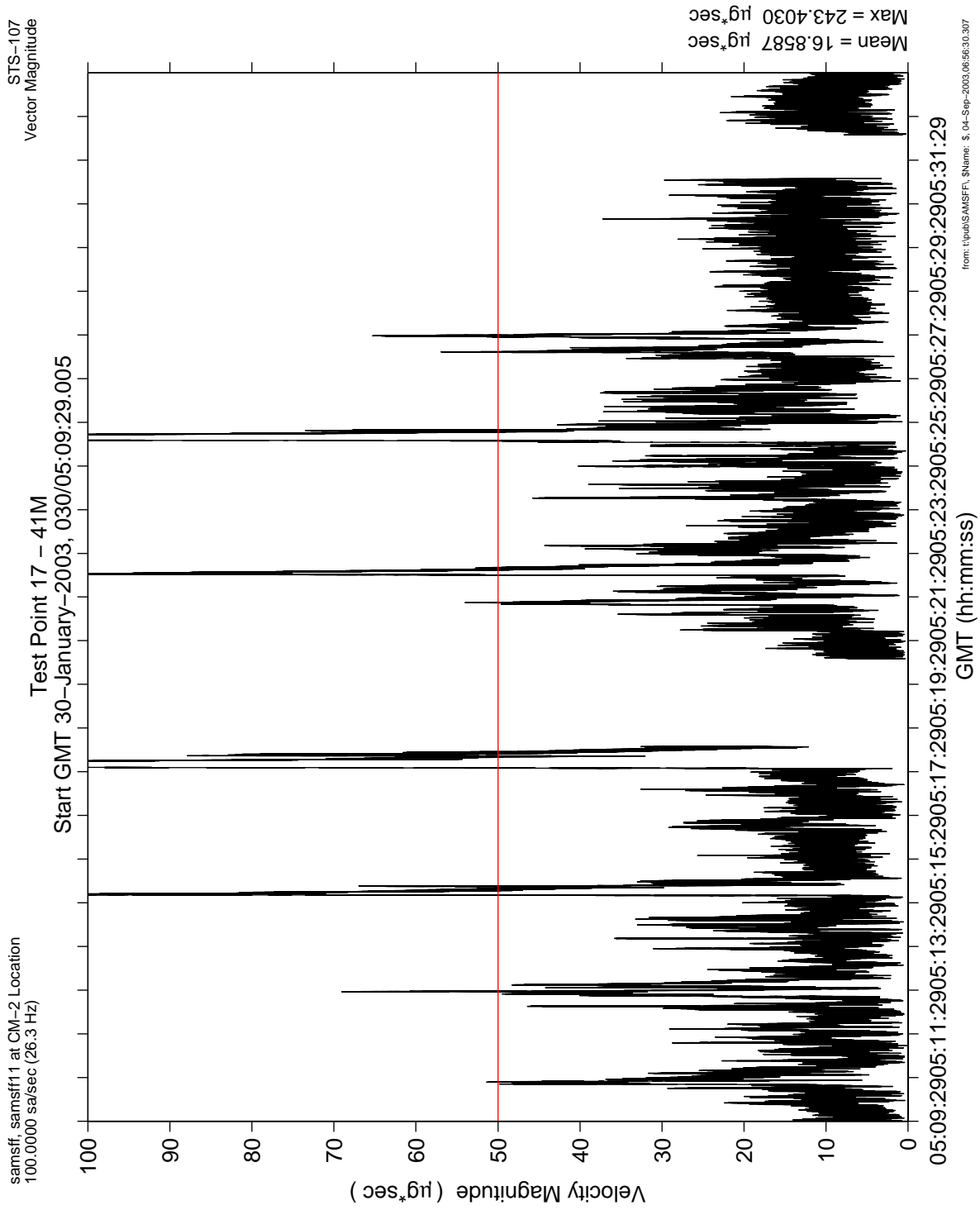


Figure 6.73 Leaky Integration For Mist Test Point 17-41M

PIMS STS-107 Mission Microgravity Environment Summary Report:
January 16 to February 1, 2003

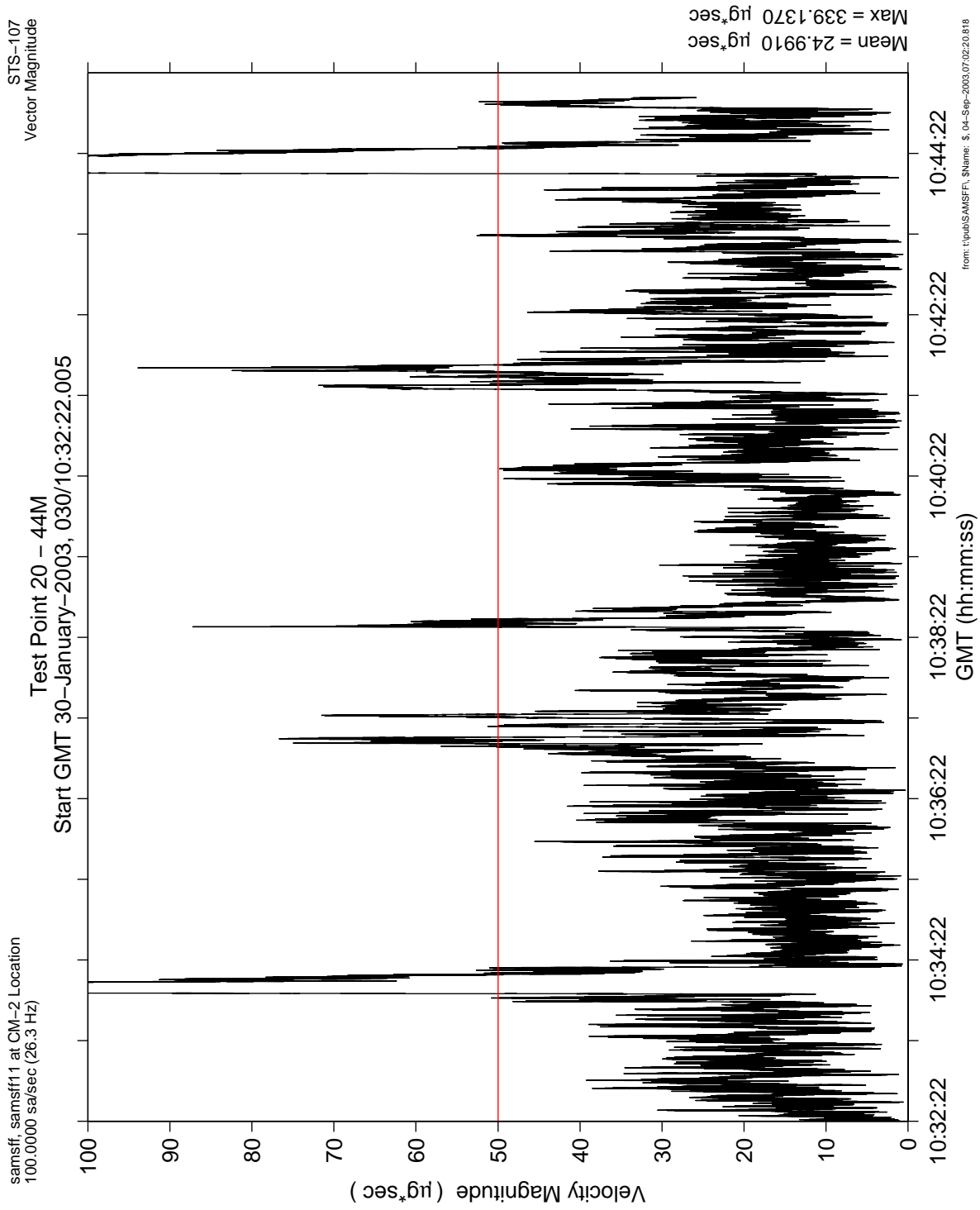


Figure 6.74 Leaky Integration For Mist Test Point 20-44M

PIMS STS-107 Mission Microgravity Environment Summary Report:
January 16 to February 1, 2003

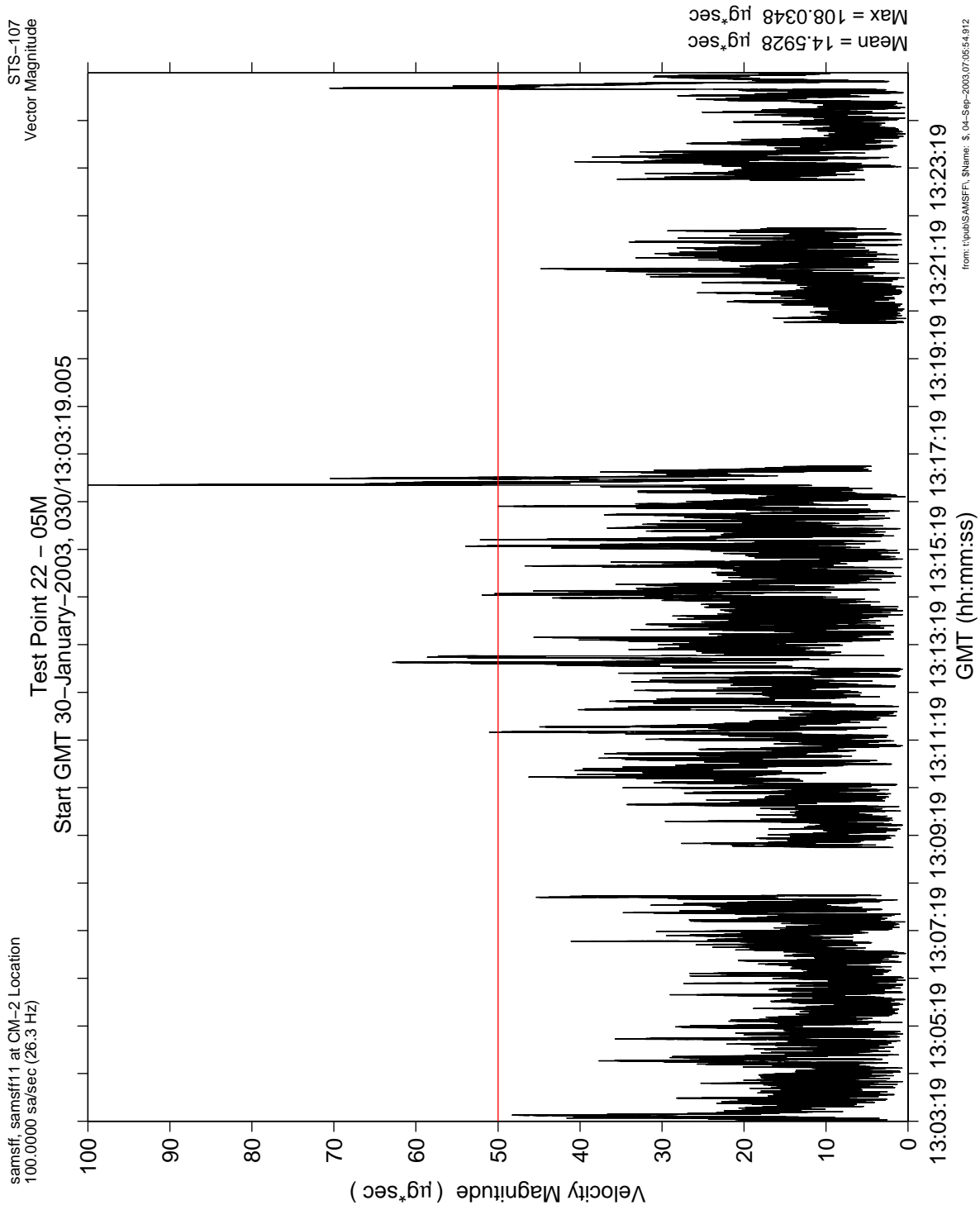


Figure 6.75 Leaky Integration For Mist Test Point 22-05M

PIMS STS-107 Mission Microgravity Environment Summary Report:
January 16 to February 1, 2003

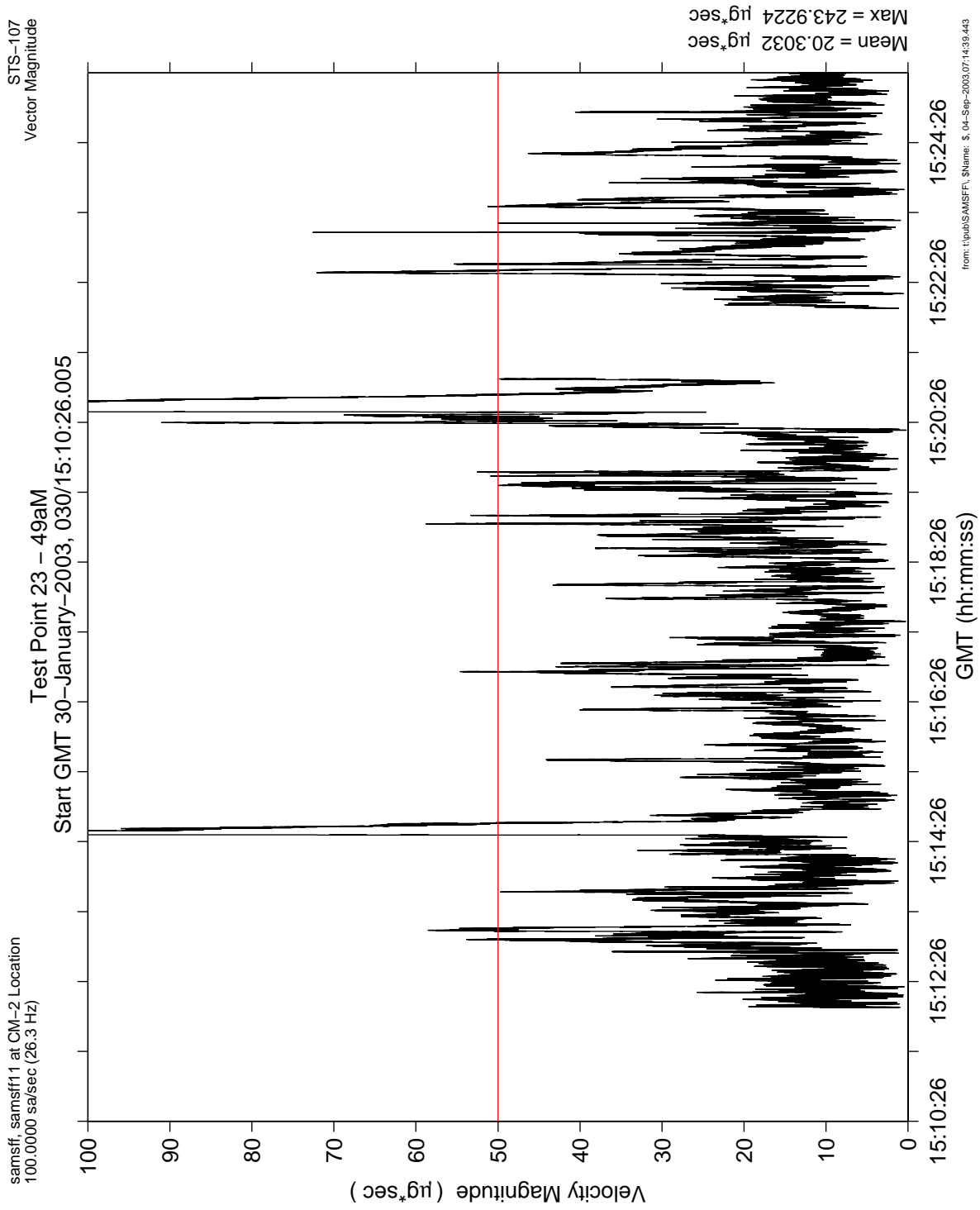


Figure 6.76 Leaky Integration For Mist Test Point 23-49aM

**PIMS STS-107 Mission Microgravity Environment Summary Report:
January 16 to February 1, 2003**

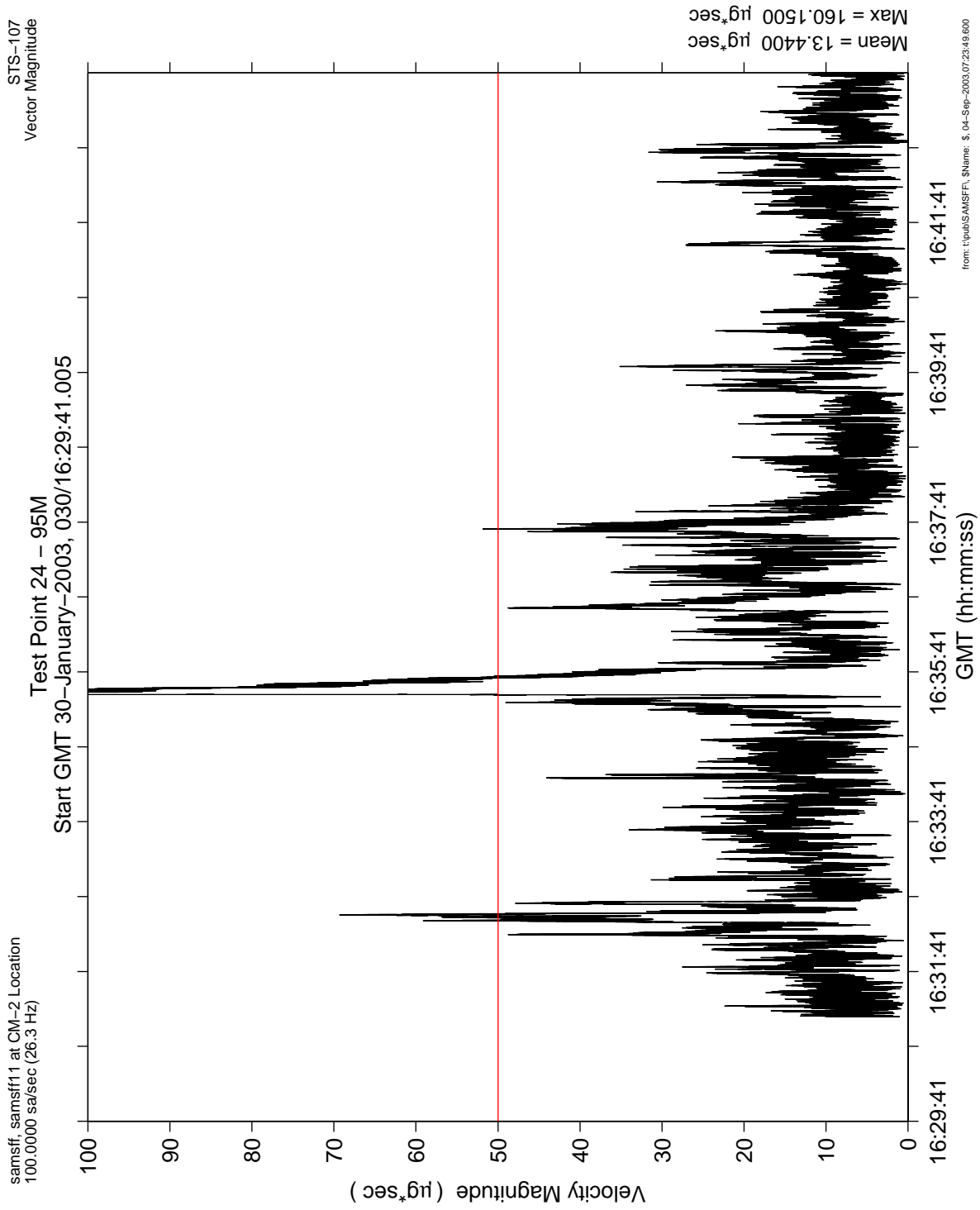


Figure 6.77 Leaky Integration For Mist Test Point 24-95M

PIMS STS-107 Mission Microgravity Environment Summary Report:
January 16 to February 1, 2003

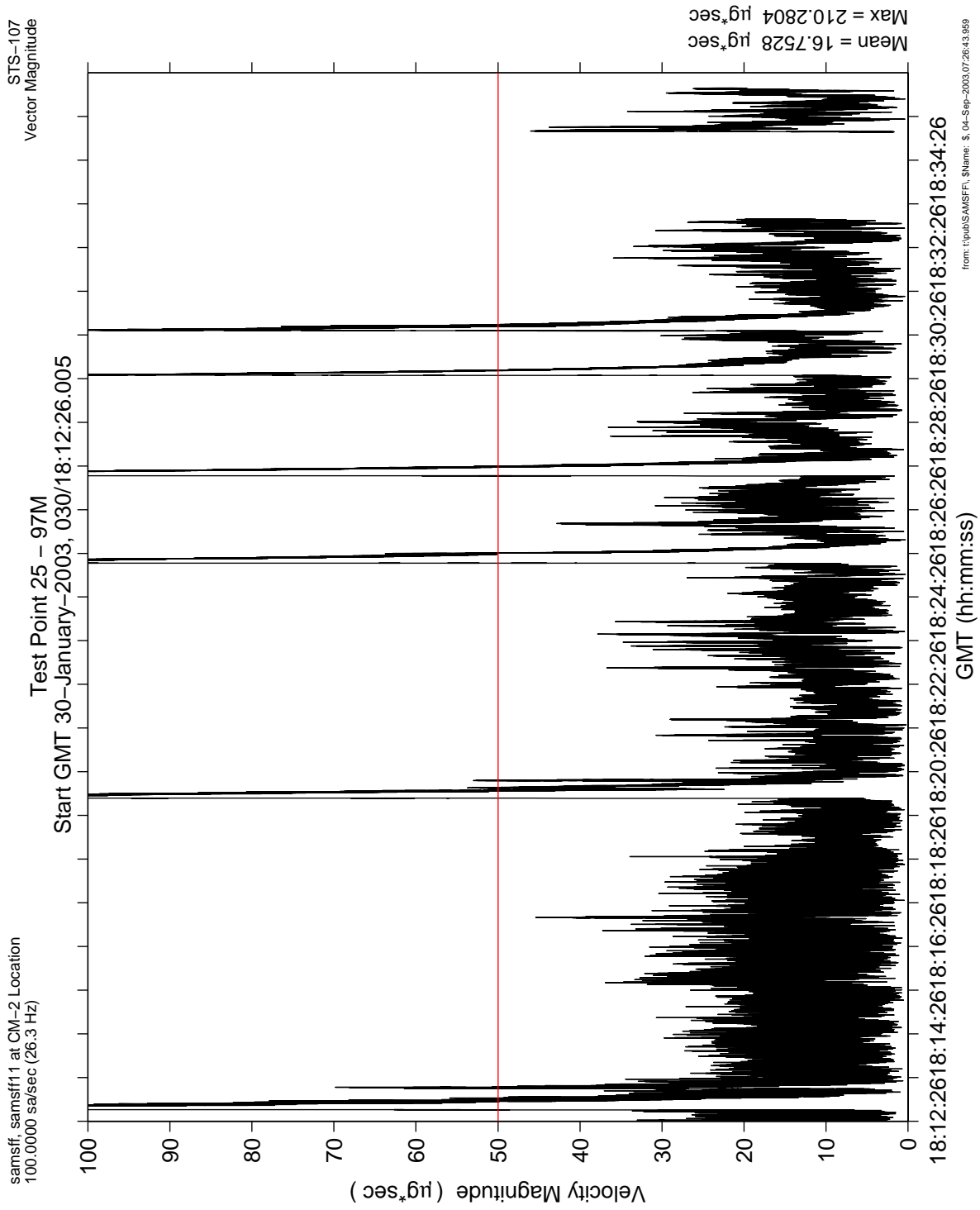


Figure 6.78 Leaky Integration For Mist Test Point 25-97M

**PIMS STS-107 Mission Microgravity Environment Summary Report:
January 16 to February 1, 2003**

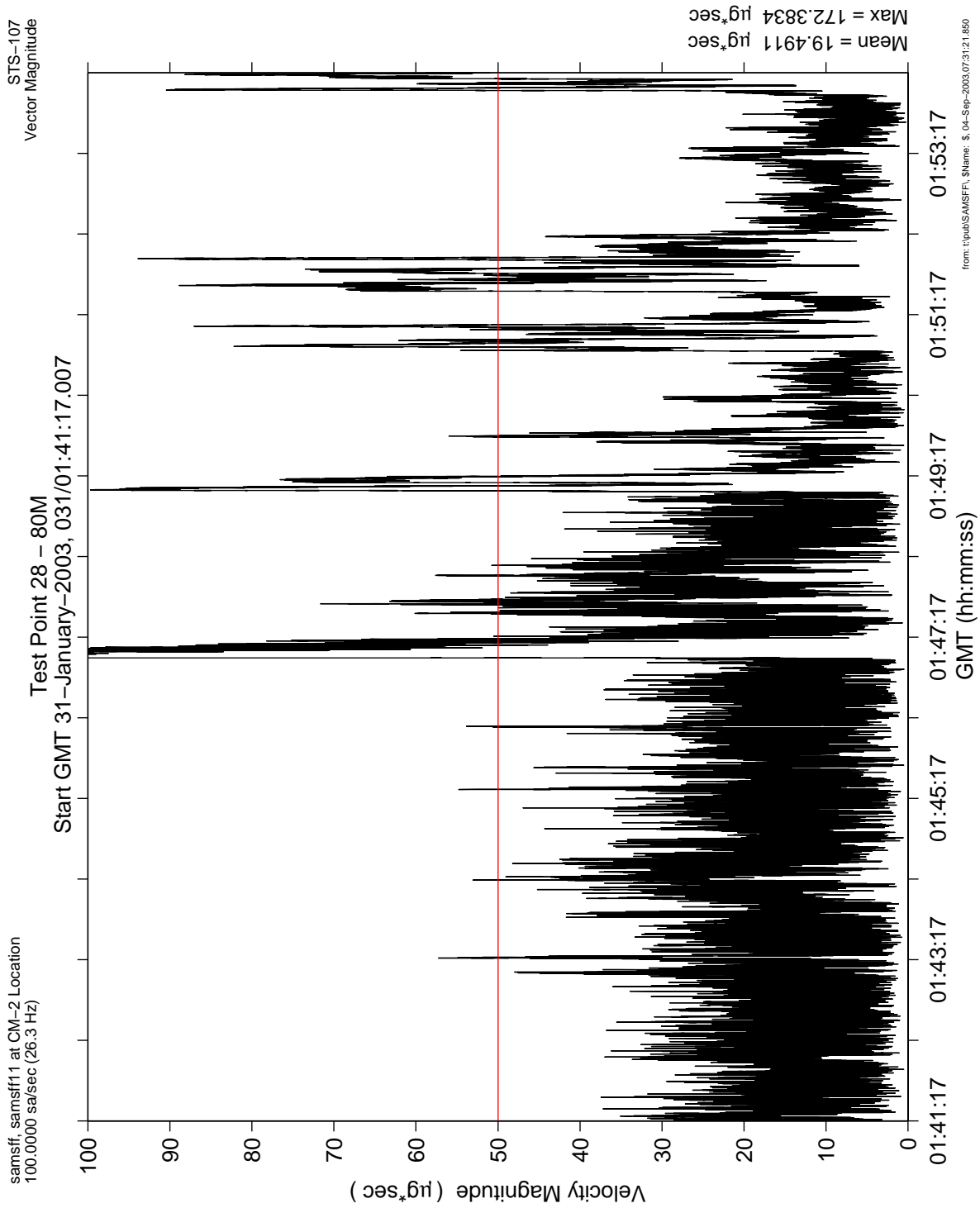


Figure 6.79 Leaky Integration For Mist Test Point 28-80M

**PIMS STS-107 Mission Microgravity Environment Summary Report:
January 16 to February 1, 2003**

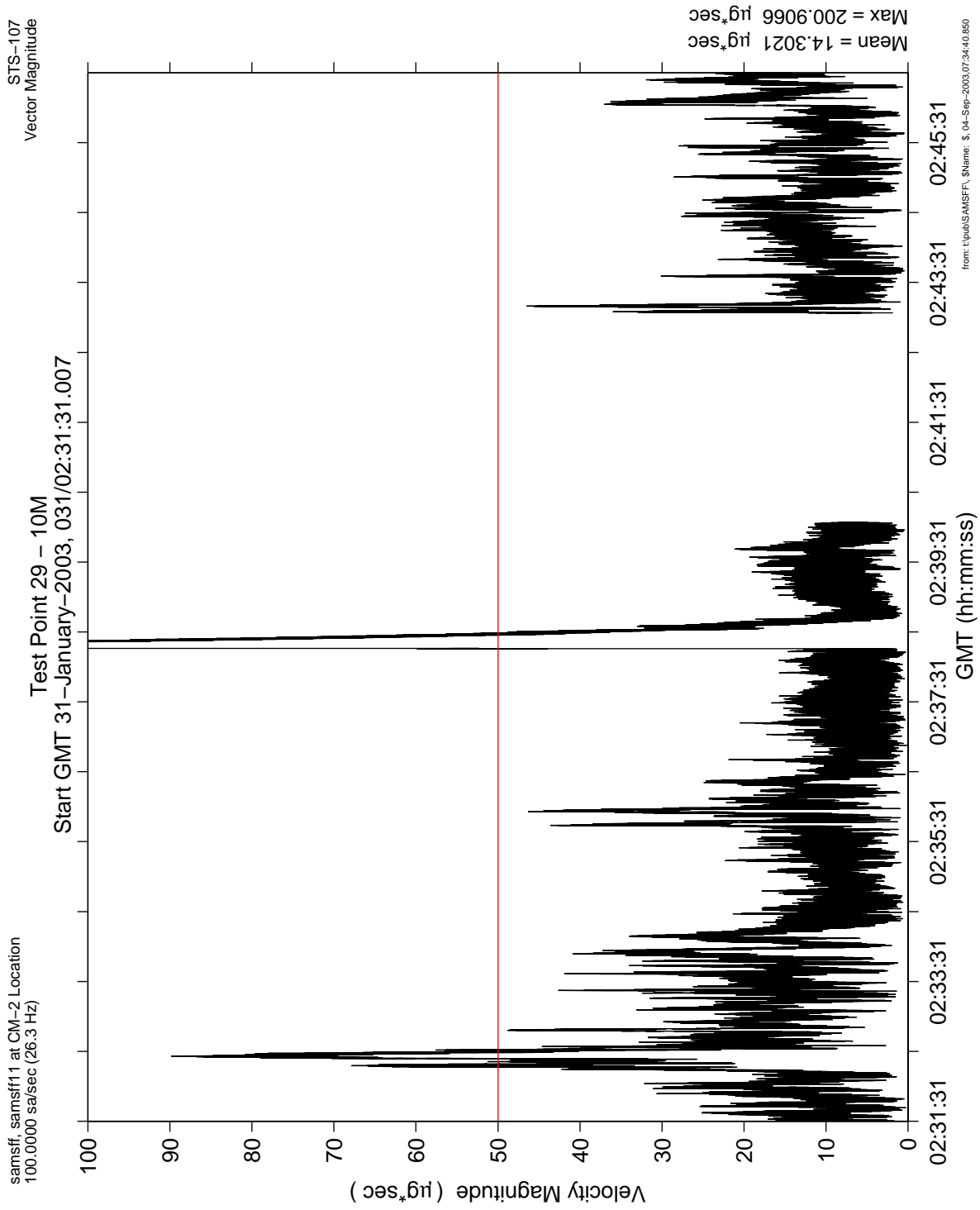


Figure 6.80 Leaky Integration For Mist Test Point 29-10M

**PIMS STS-107 Mission Microgravity Environment Summary Report:
January 16 to February 1, 2003**

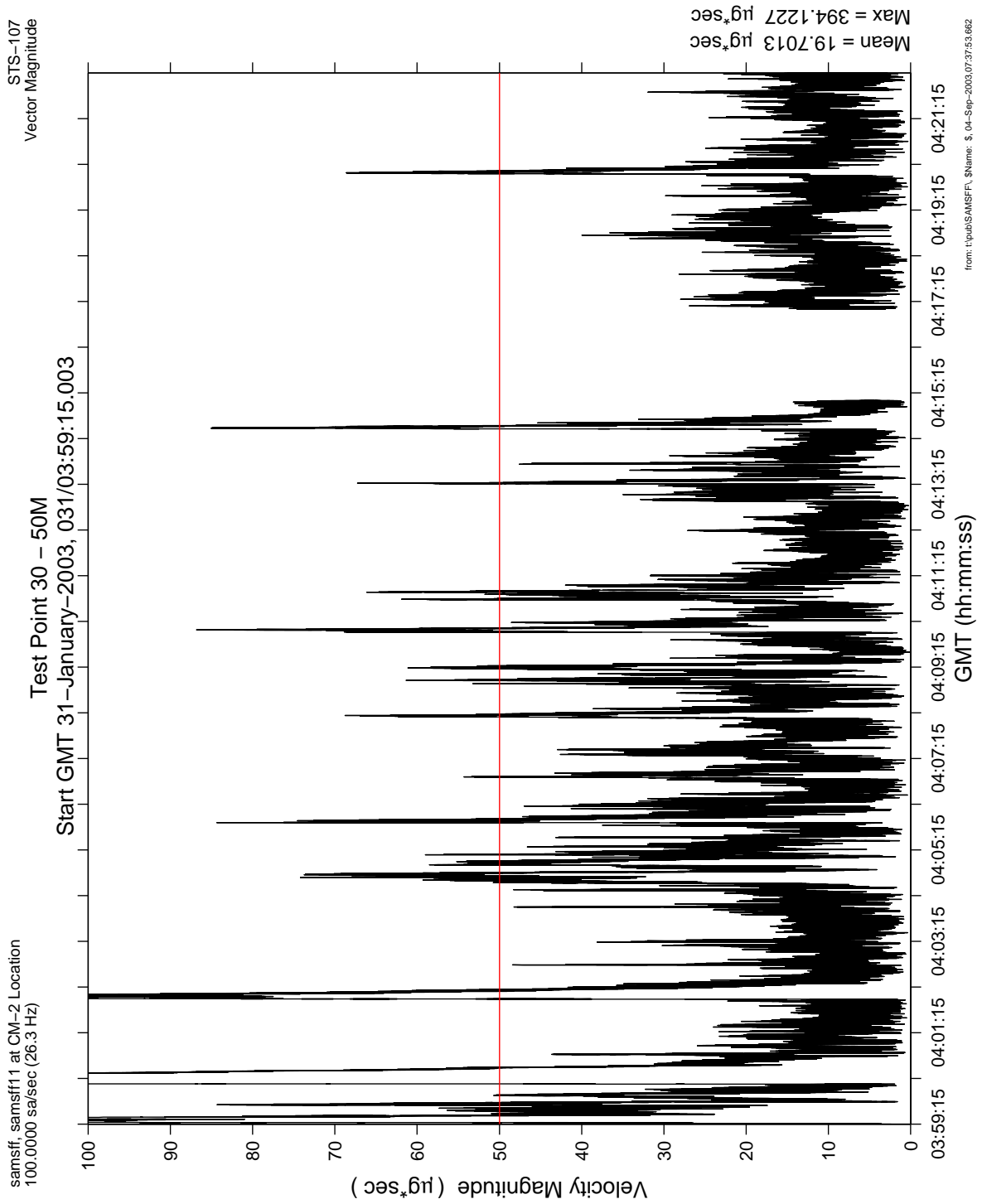


Figure 6.81 Leaky Integration For Mist Test Point 30-50M

**PIMS STS-107 Mission Microgravity Environment Summary Report:
January 16 to February 1, 2003**

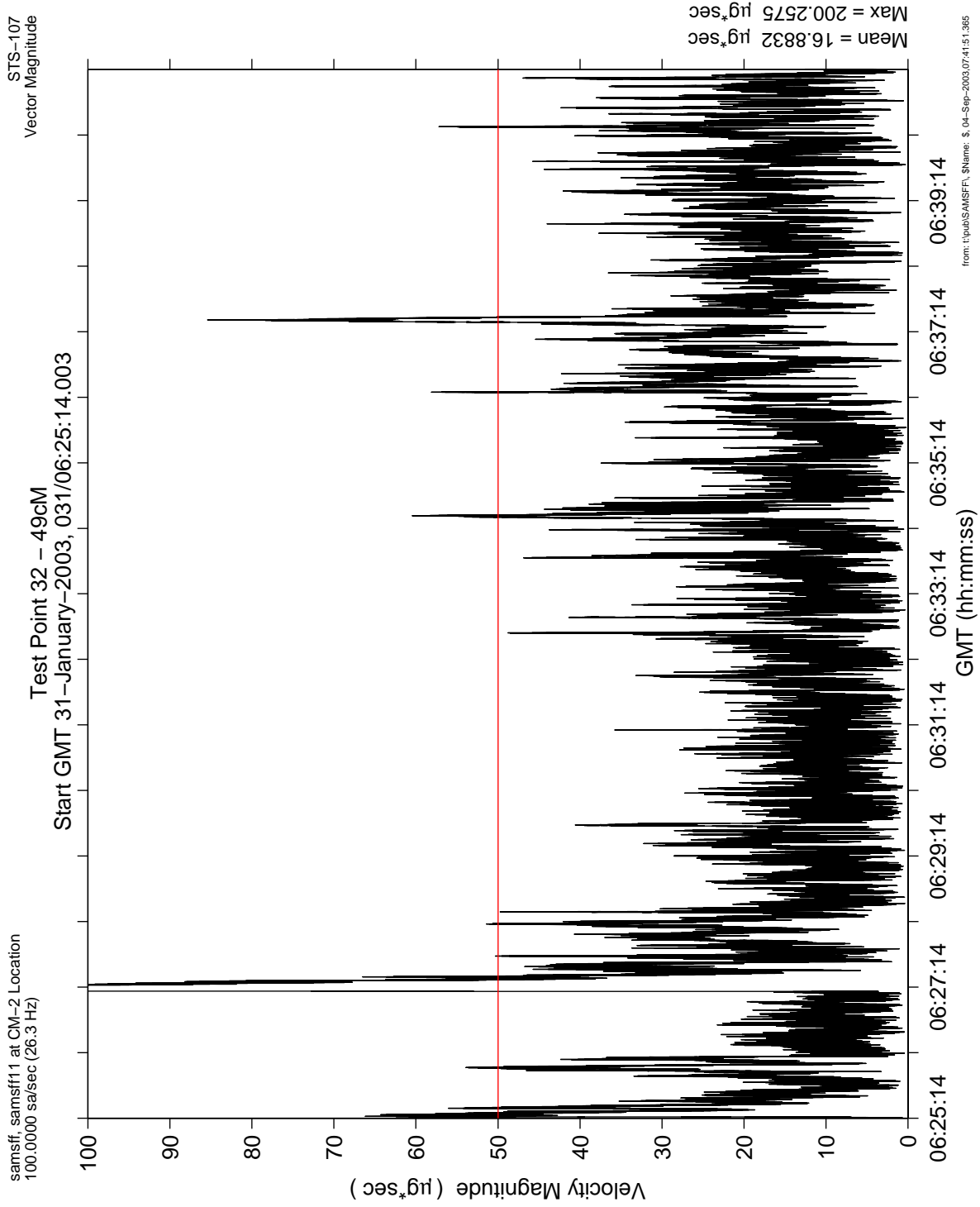


Figure 6.82 Leaky Integration For Mist Test Point 32-49cM

**PIMS STS-107 Mission Microgravity Environment Summary Report:
January 16 to February 1, 2003**

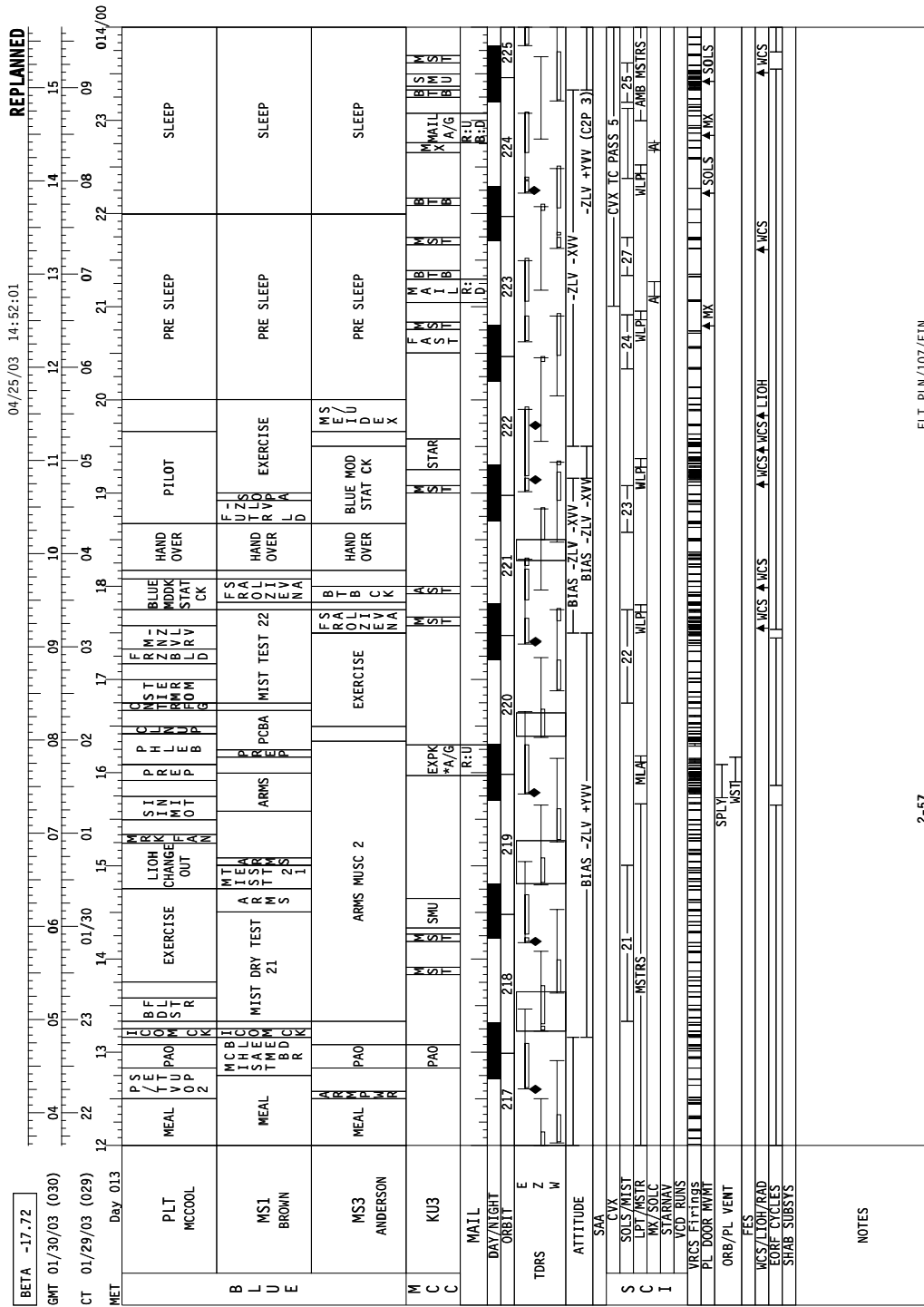


Figure 6.84 Excerpt of As-Flown Timeline for Mist Test Point 19-02M

PIMS STS-107 Mission Microgravity Environment Summary Report: January 16 to February 1, 2003

samsff, samsff11 at CM-2 Location:[11.00 11.00 11.00]
100.0000 sa/sec (26.32 Hz)

LSP Test Point 41e

Increment: 0, Flight: STS-107 Mission
STRUCTURAL[0.0 180.0 0.0]

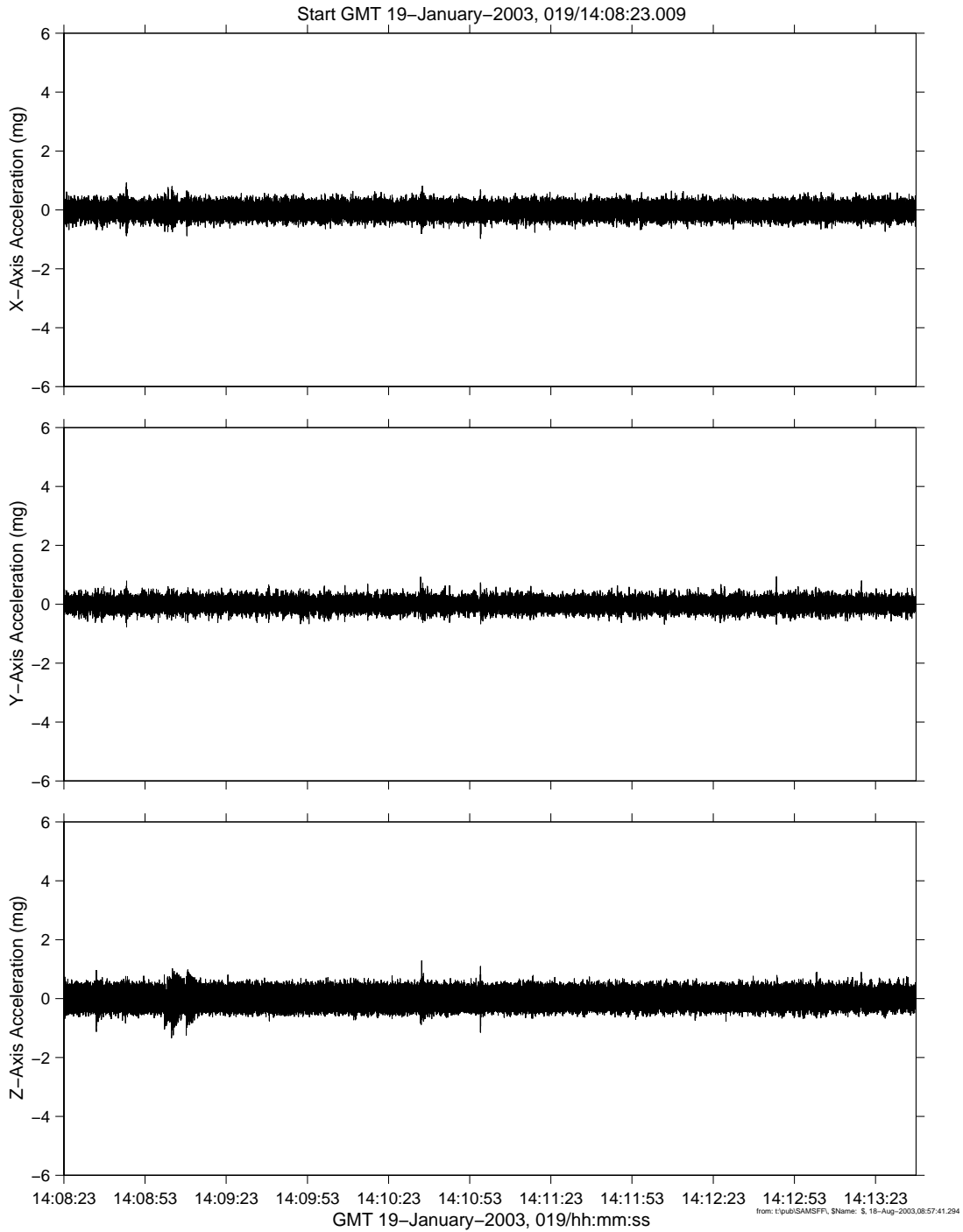


Figure 6.85 Time Series For LSP Test Point 41e

PIMS STS-107 Mission Microgravity Environment Summary Report: January 16 to February 1, 2003

samsff, samsff11 at CM-2 Location:[11.00 11.00 11.00]
100.0000 sa/sec (26.32 Hz)

Increment: 0, Flight: STS-107 Mission
STRUCTURAL[0.0 180.0 0.0]

LSP Test Point 04e

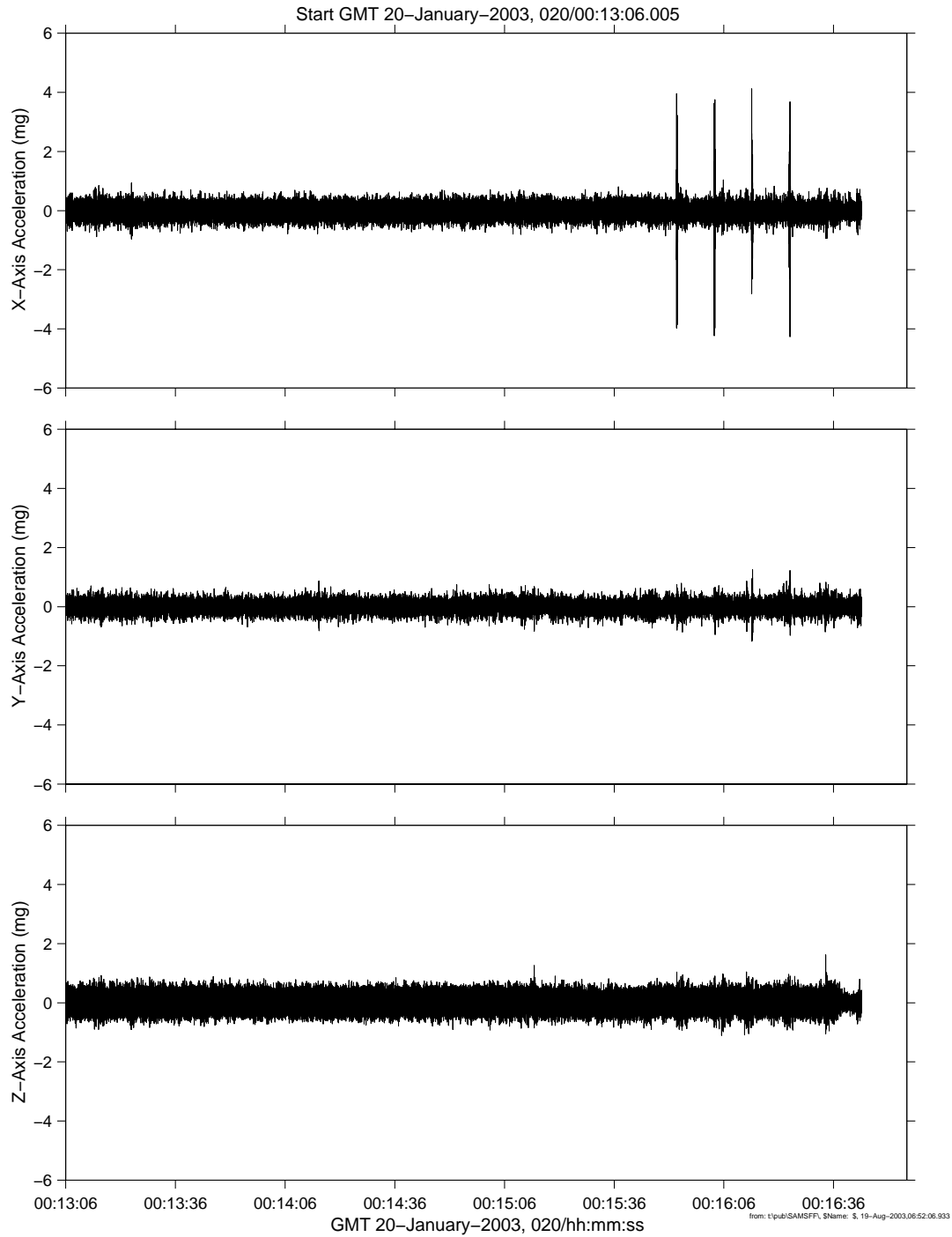


Figure 6.86 Time Series For LSP Test Point 04e

PIMS STS-107 Mission Microgravity Environment Summary Report: January 16 to February 1, 2003

samsff, samsff11 at CM-2 Location:[11.00 11.00 11.00]
100.0000 sa/sec (26.32 Hz)

LSP Test Point 08p

Increment: 0, Flight: STS-107 Mission
STRUCTURAL[0.0 180.0 0.0]

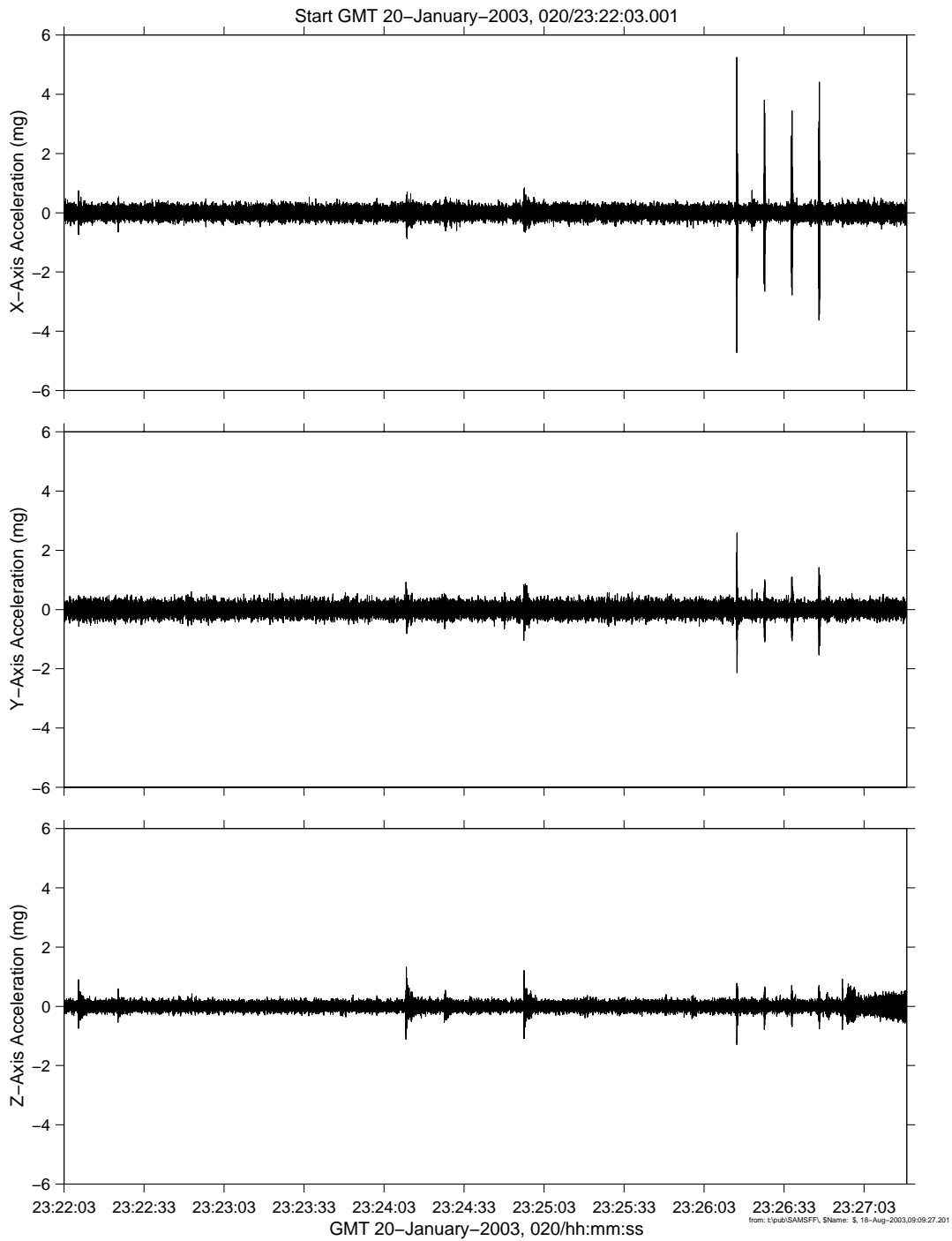


Figure 6.87 Time Series For LSP Test Point 08p

PIMS STS-107 Mission Microgravity Environment Summary Report: January 16 to February 1, 2003

samsff, samsff11 at CM-2 Location:[11.00 11.00 11.00]
100.0000 sa/sec (26.32 Hz)

Increment: 0, Flight: STS-107 Mission
STRUCTURAL[0.0 180.0 0.0]

LSP Test Point 53e

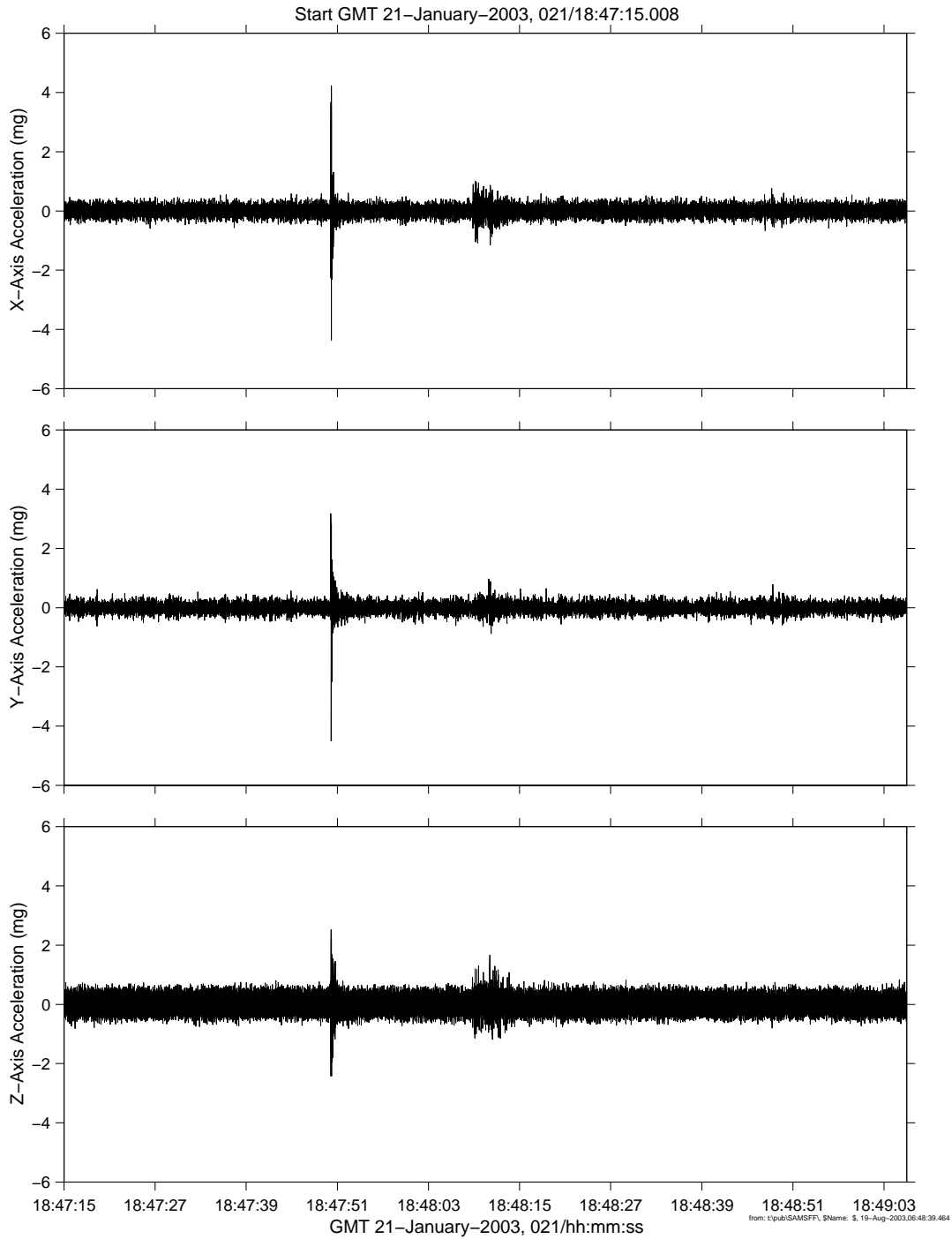


Figure 6.88 Time Series For LSP Test Point 53e

PIMS STS-107 Mission Microgravity Environment Summary Report:
January 16 to February 1, 2003

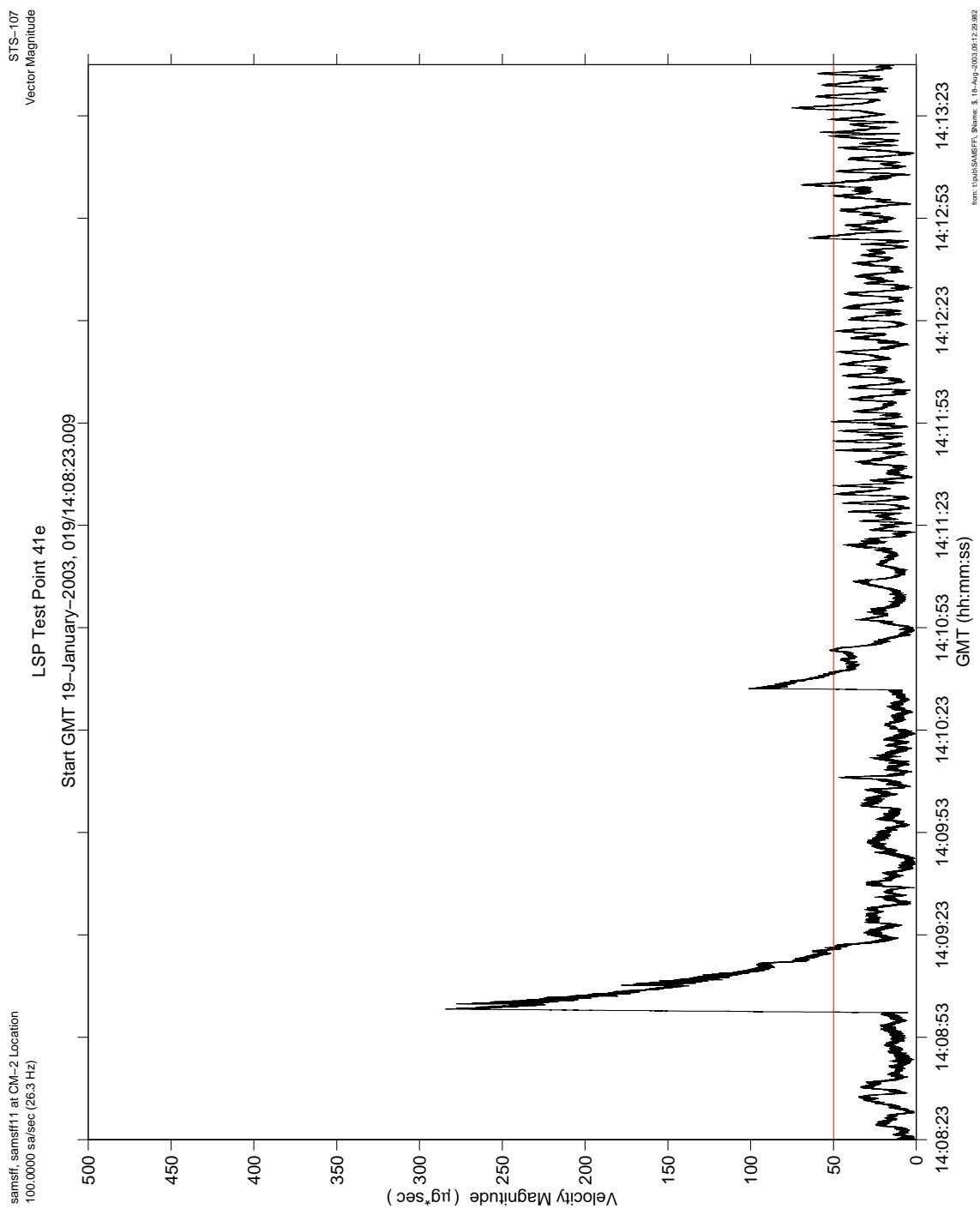


Figure 6.89 Leaky Integration For LSP Test Point 41e

PIMS STS-107 Mission Microgravity Environment Summary Report:
January 16 to February 1, 2003

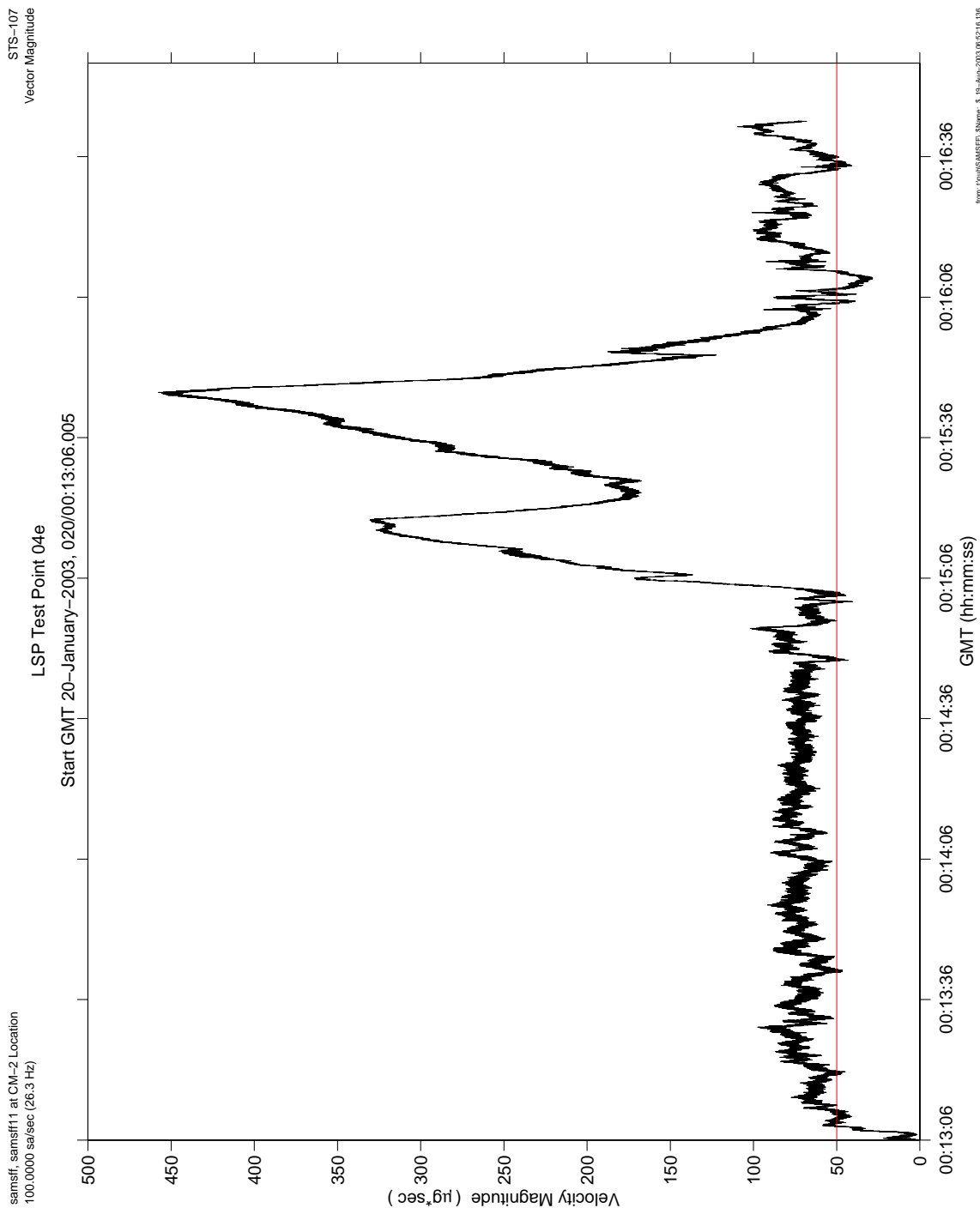


Figure 6.90 Leaky Integration For LSP Test Point 04e

PIMS STS-107 Mission Microgravity Environment Summary Report:
January 16 to February 1, 2003

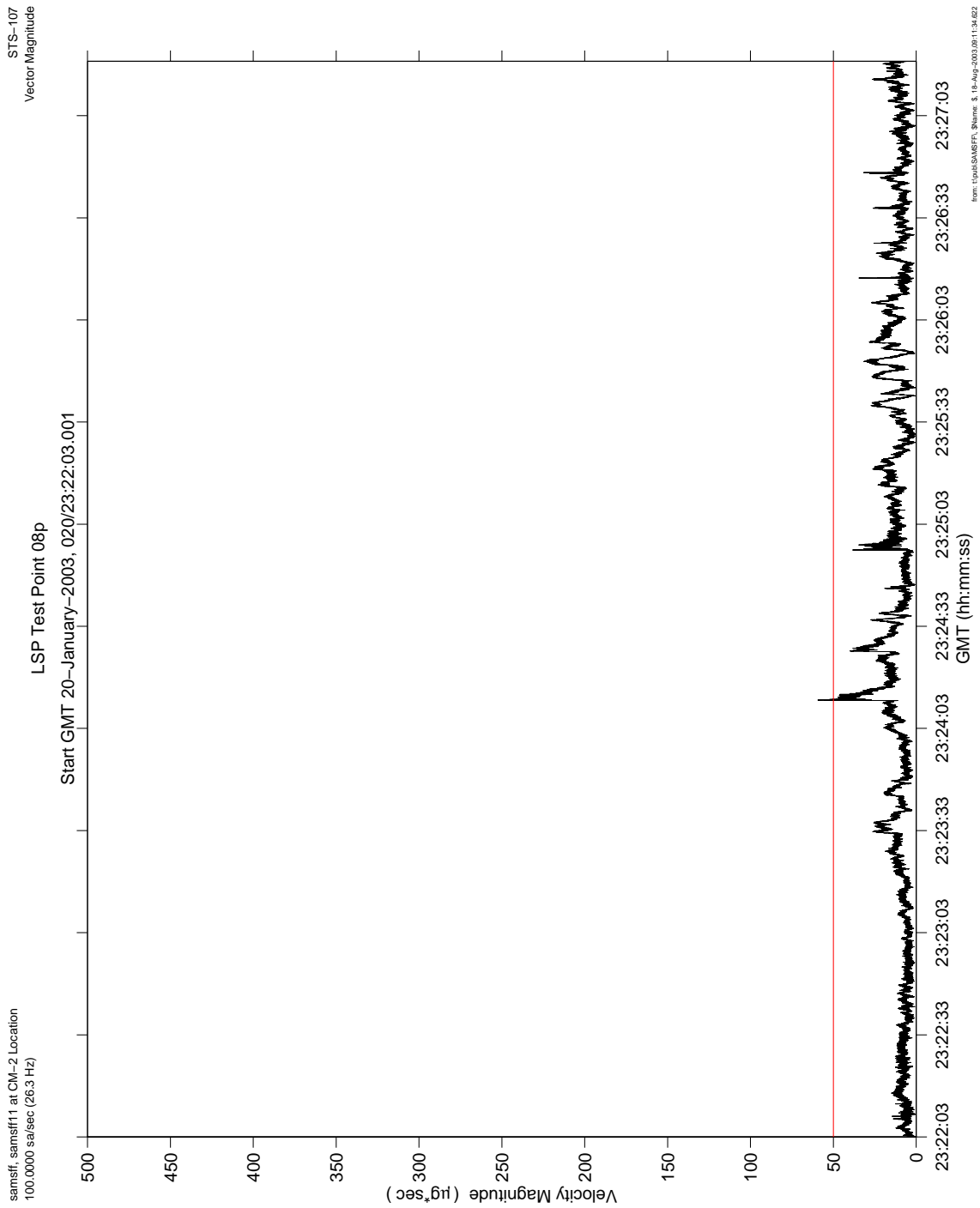


Figure 6.91 Leaky Integration For LSP Test Point 08p

PIMS STS-107 Mission Microgravity Environment Summary Report:
January 16 to February 1, 2003

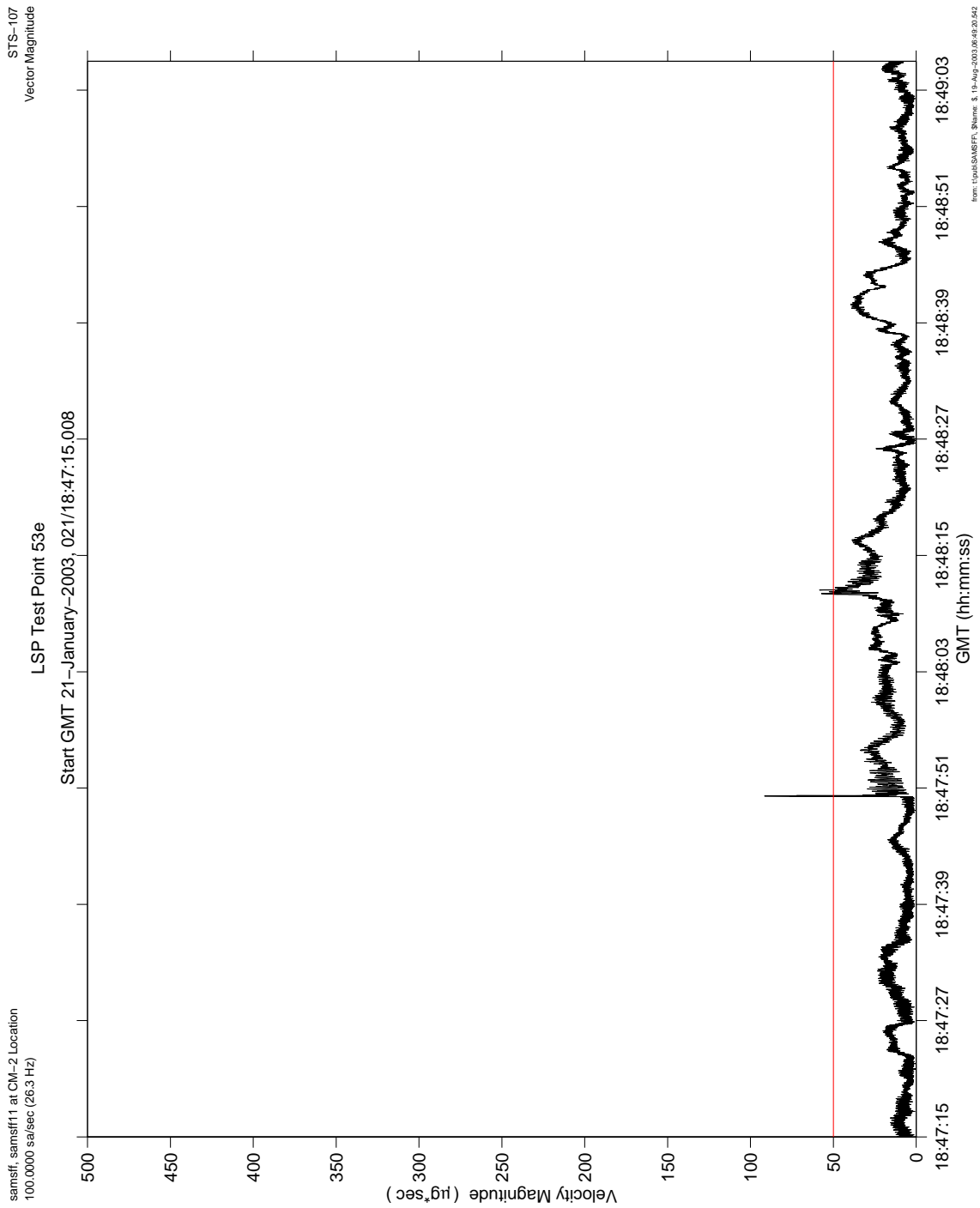


Figure 6.92 Leaky Integration For LSP Test Point 53e

PIMS STS-107 Mission Microgravity Environment Summary Report:
January 16 to February 1, 2003

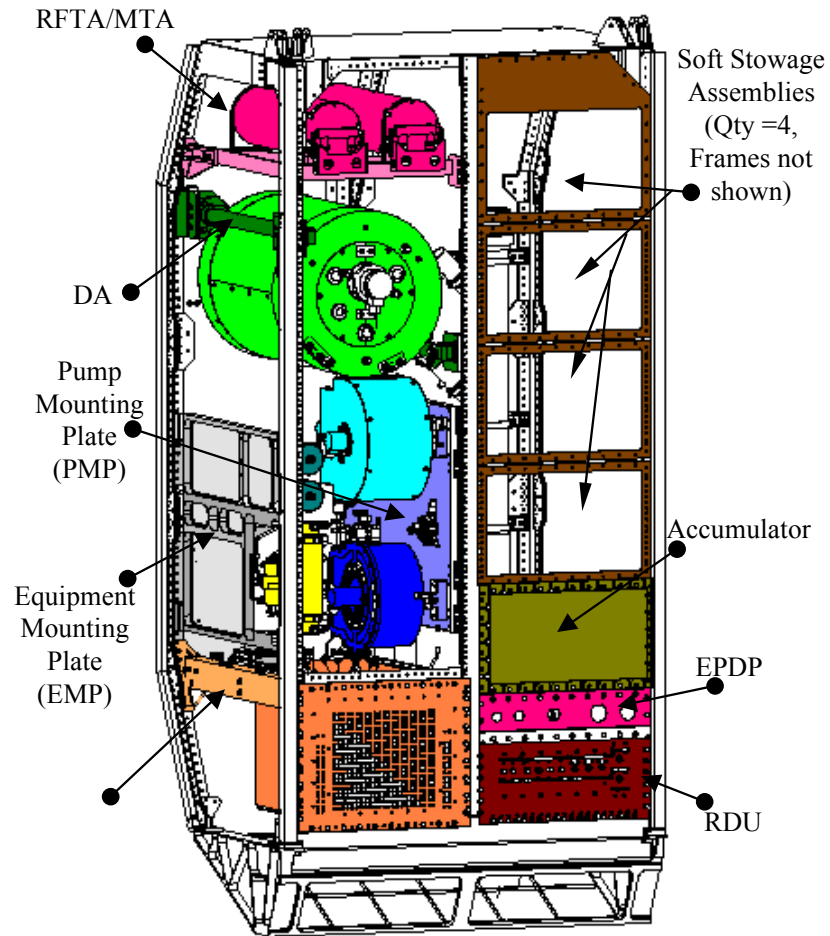


Figure 6.93 Vapor Compression Distillation Flight Experiment (VCD FE) Facility

**PIMS STS-107 Mission Microgravity Environment Summary Report:
January 16 to February 1, 2003**

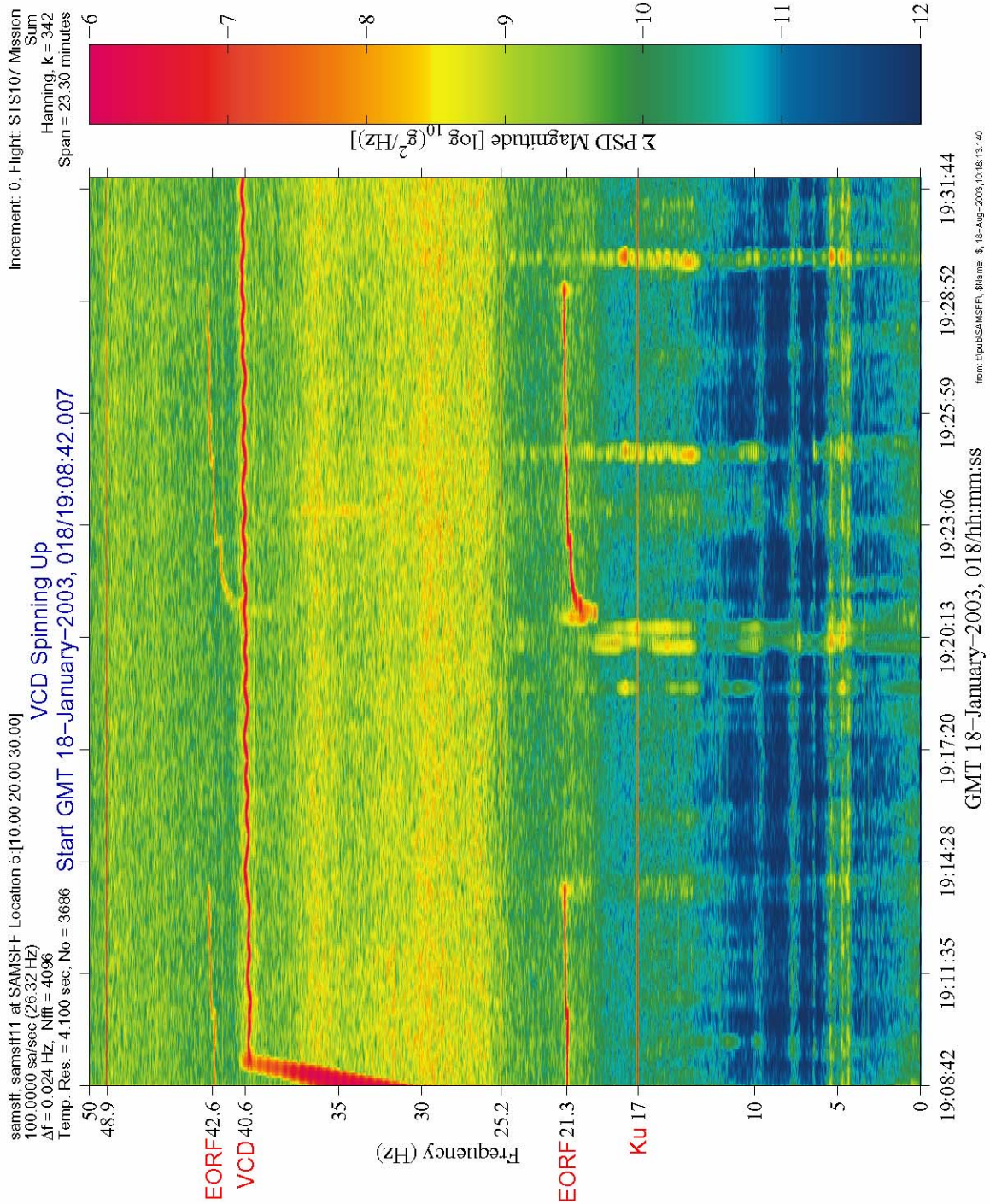


Figure 6.94 Spectrogram of VCD Spinning Up

**PIMS STS-107 Mission Microgravity Environment Summary Report:
January 16 to February 1, 2003**

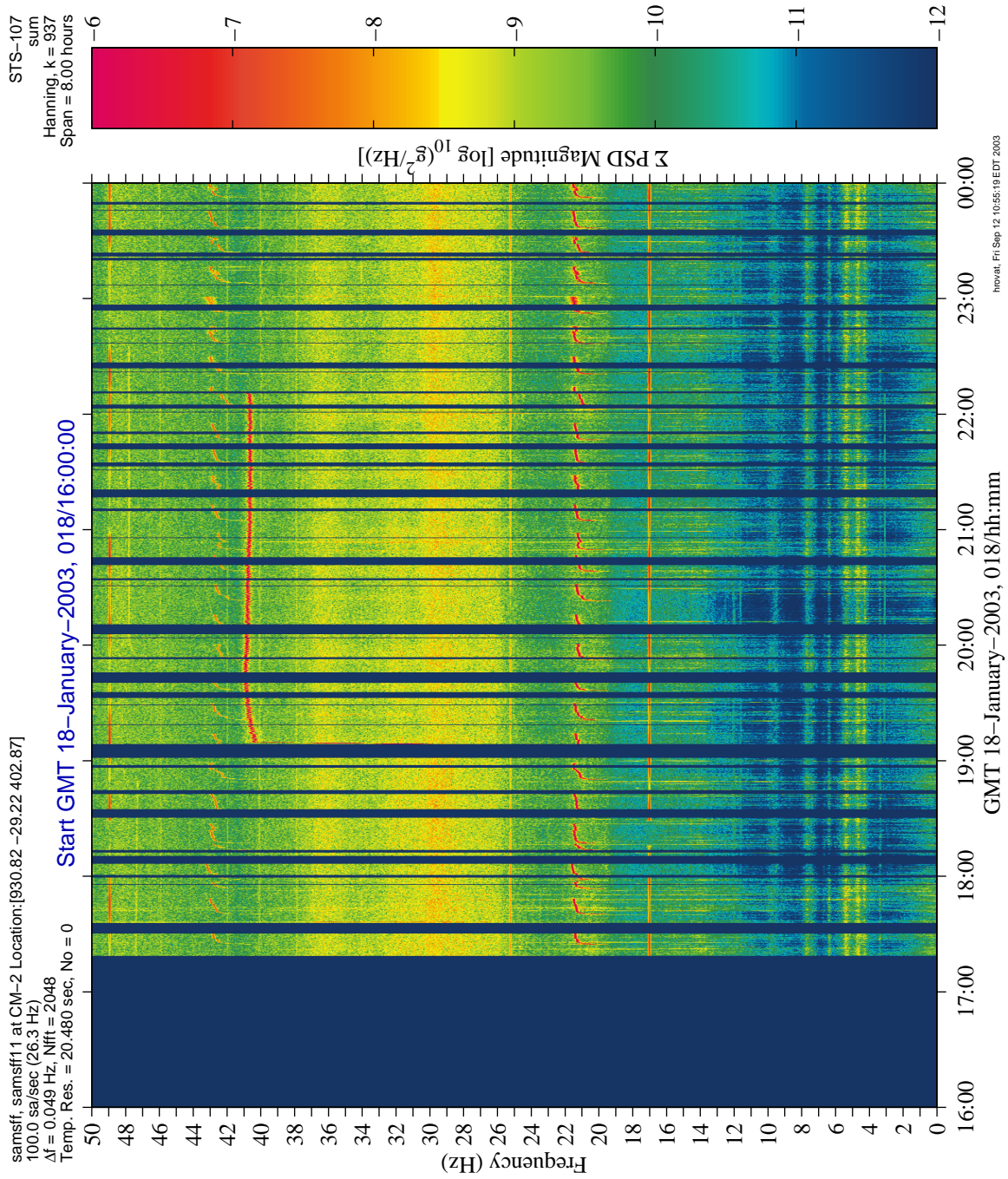


Figure 6.95 Spectrogram of VCD Equipment On/Off

**PIMS STS-107 Mission Microgravity Environment Summary Report:
January 16 to February 1, 2003**

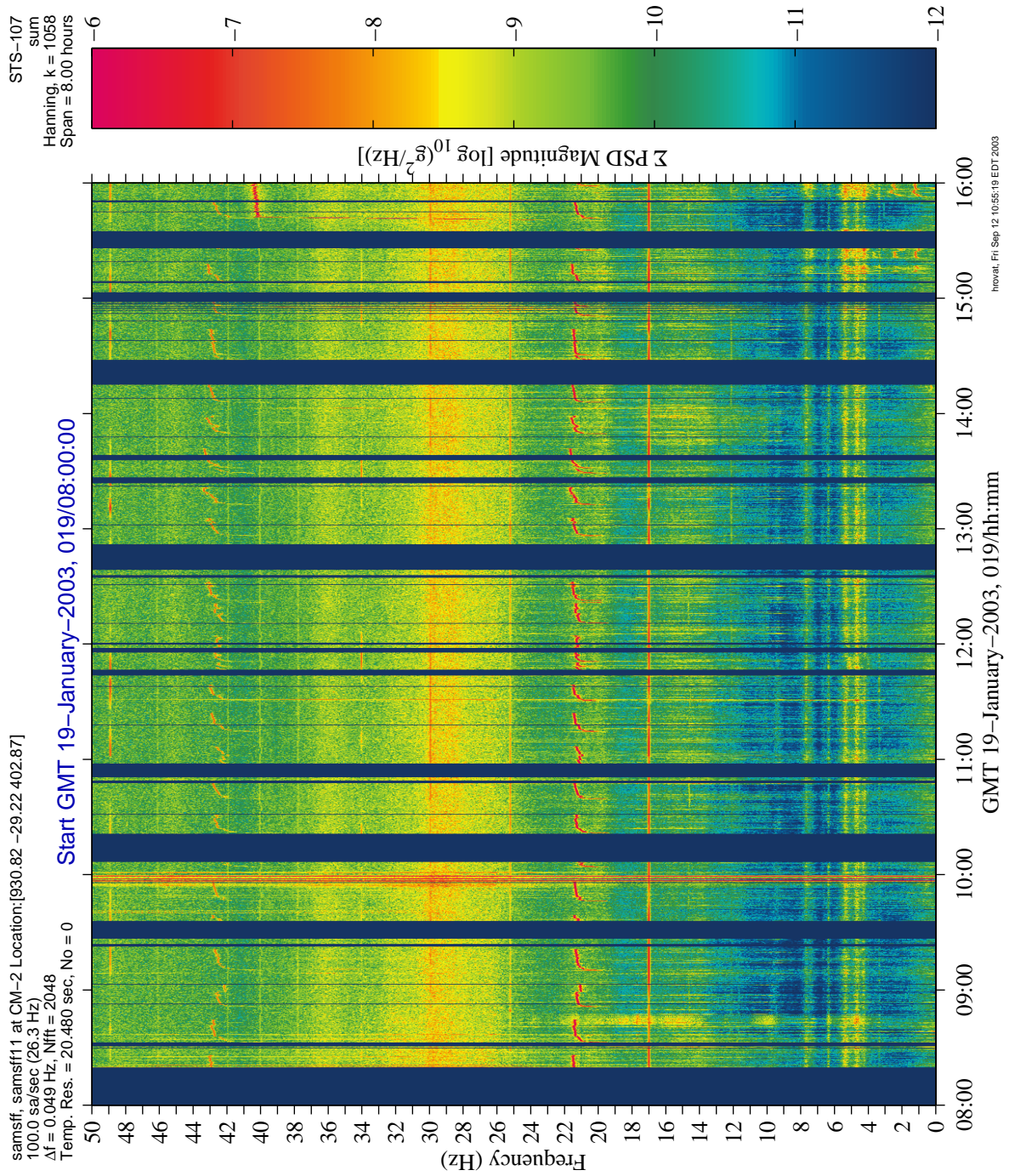


Figure 6.96 Spectrogram of VCD Equipment Operation Turn On

**PIMS STS-107 Mission Microgravity Environment Summary Report:
January 16 to February 1, 2003**

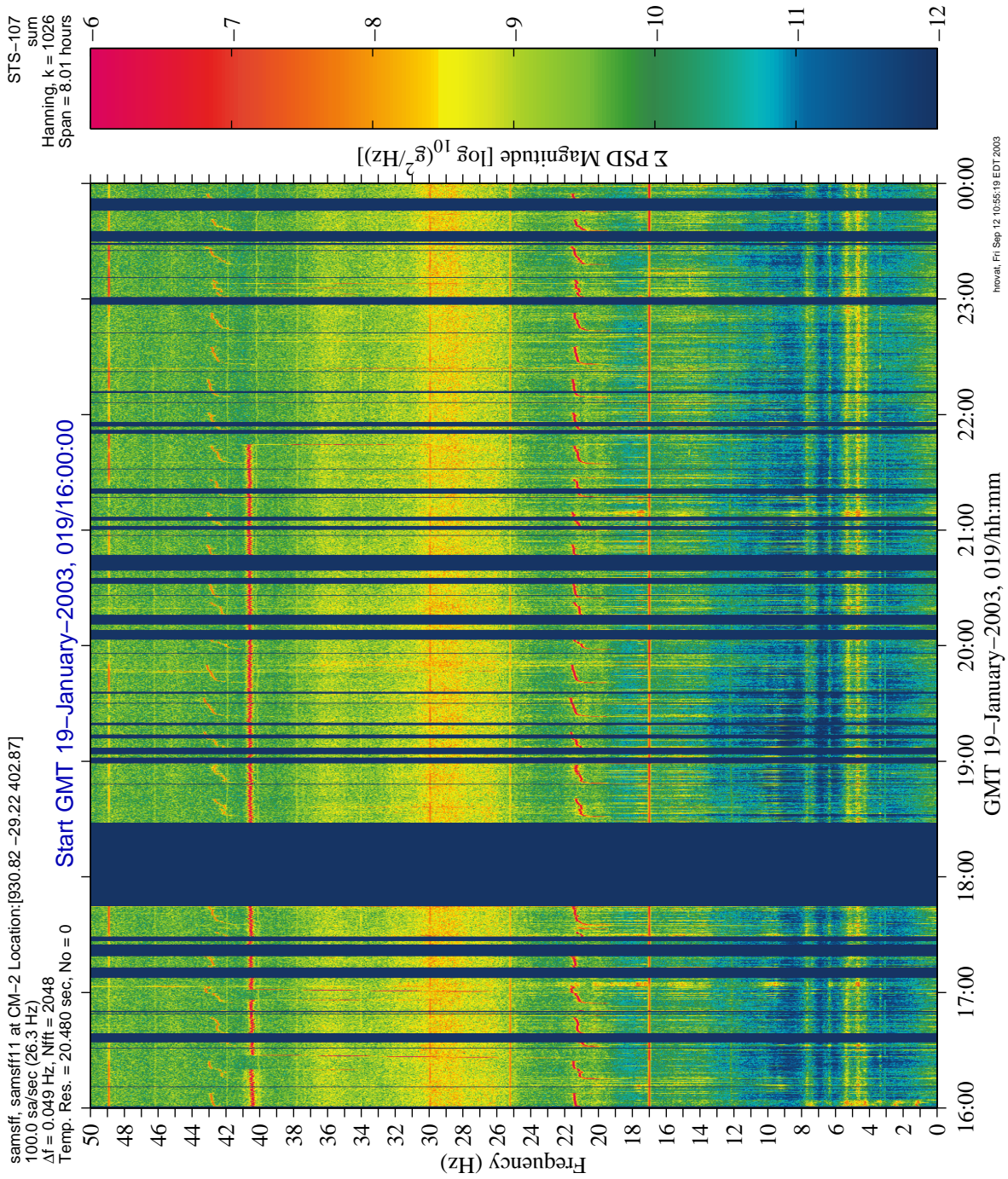


Figure 6.97 Spectrogram of VCD Equipment Operation Turn Off

**PIMS STS-107 Mission Microgravity Environment Summary Report:
January 16 to February 1, 2003**

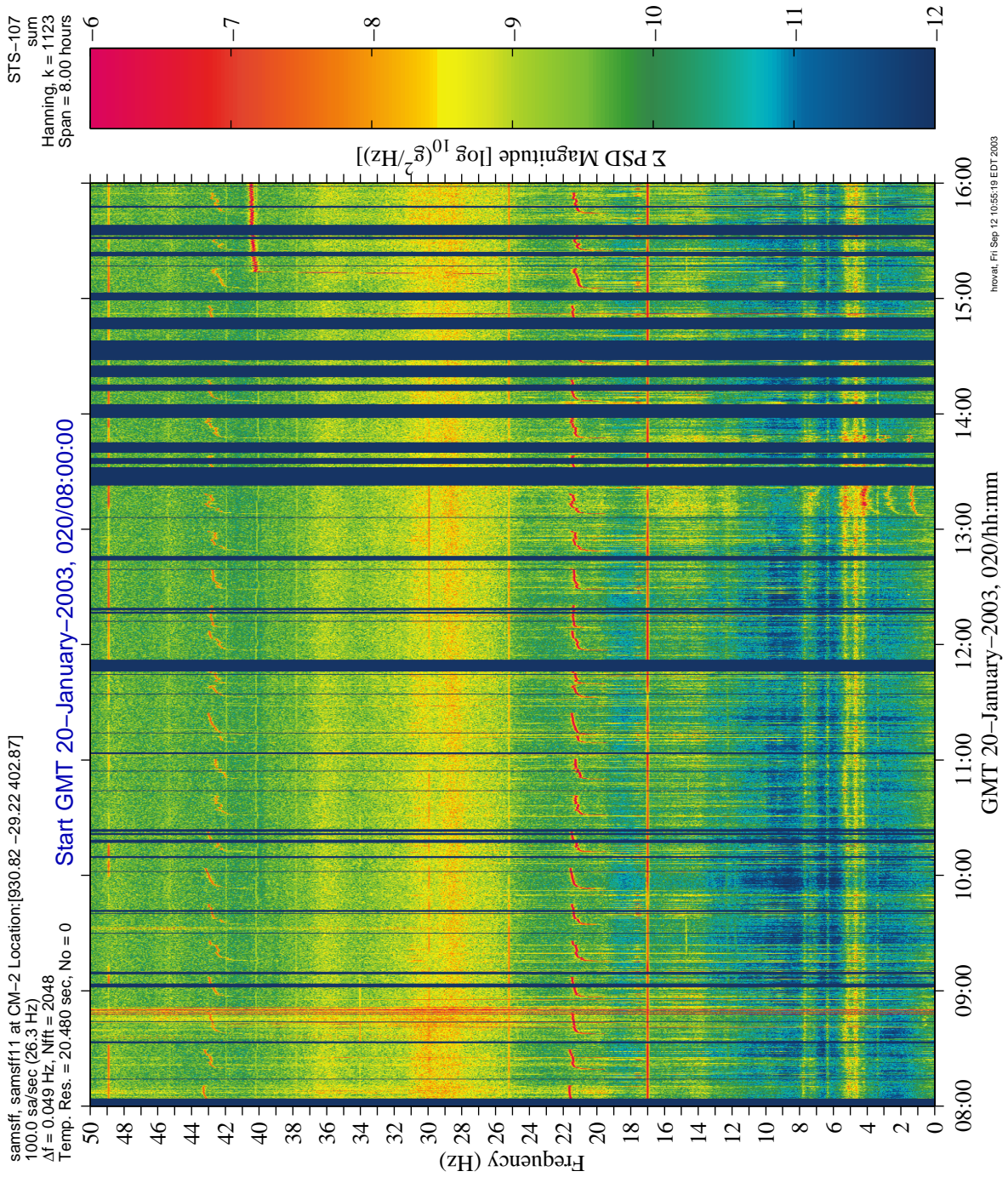


Figure 6.98 Spectrogram of VCD Equipment Operation Turn On

**PIMS STS-107 Mission Microgravity Environment Summary Report:
January 16 to February 1, 2003**

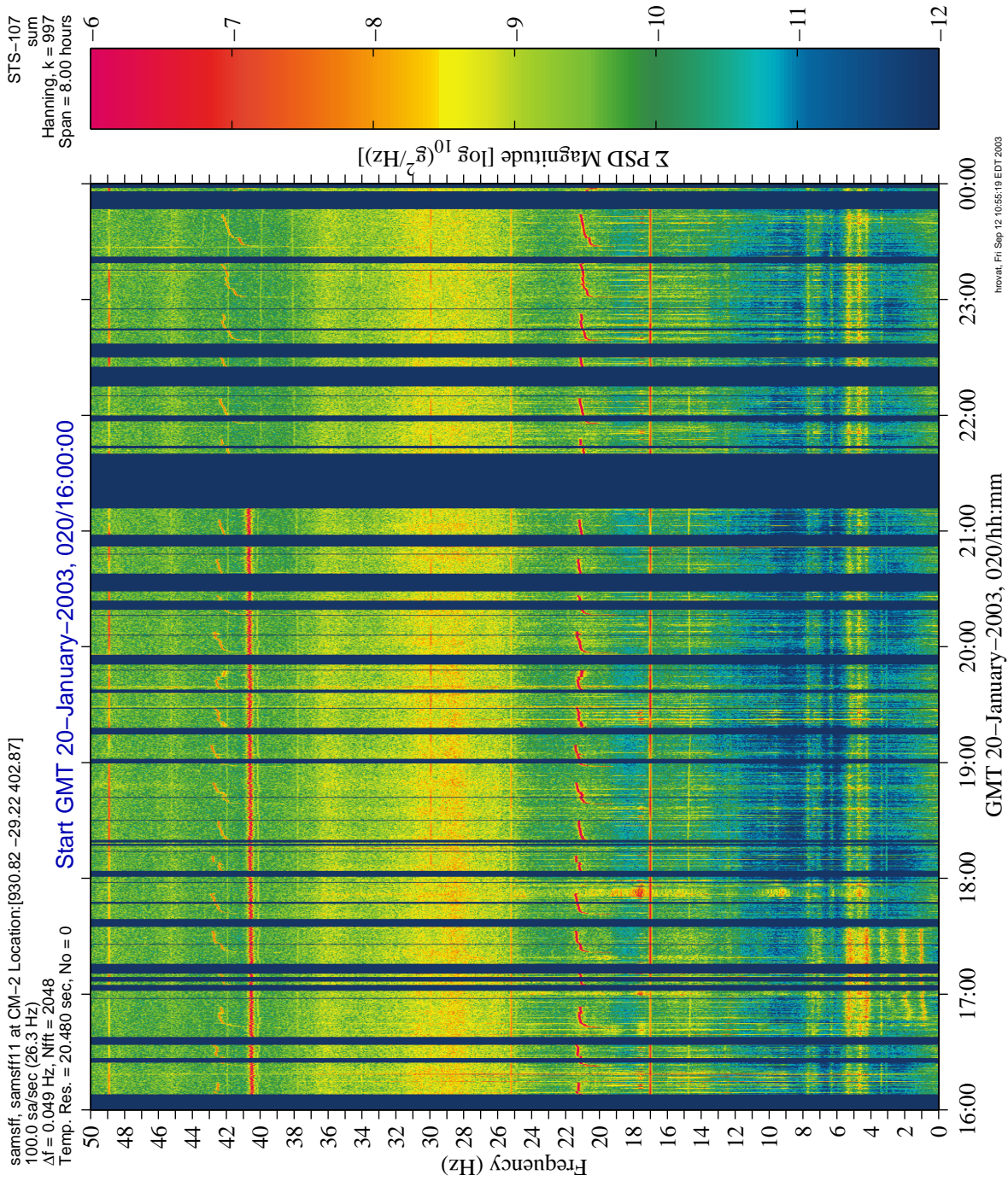


Figure 6.99 Spectrogram of VCD Equipment Operation Turn Off

**PIMS STS-107 Mission Microgravity Environment Summary Report:
January 16 to February 1, 2003**

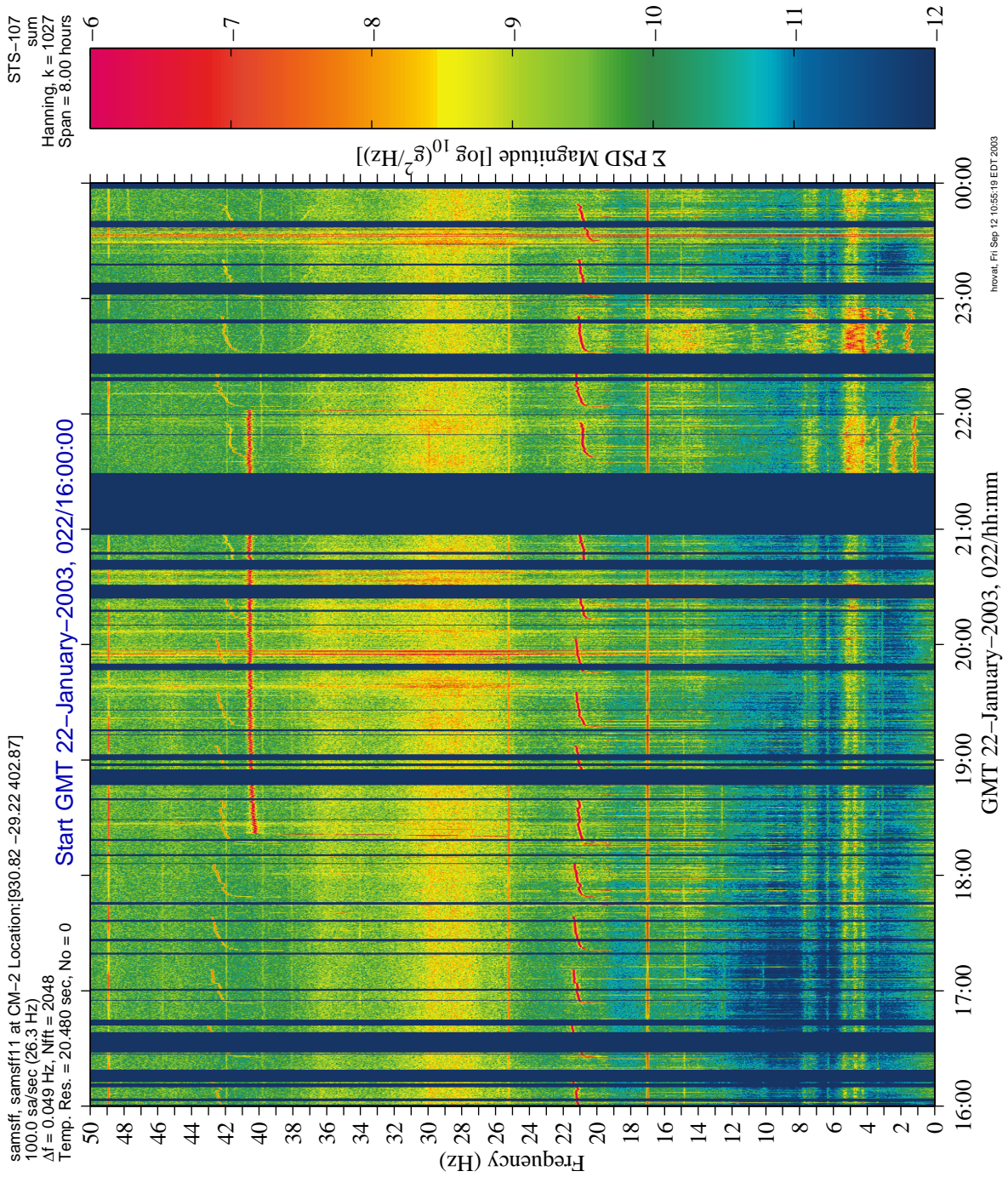


Figure 6.100 Spectrogram of VCD Equipment Operation On/Off

**PIMS STS-107 Mission Microgravity Environment Summary Report:
January 16 to February 1, 2003**

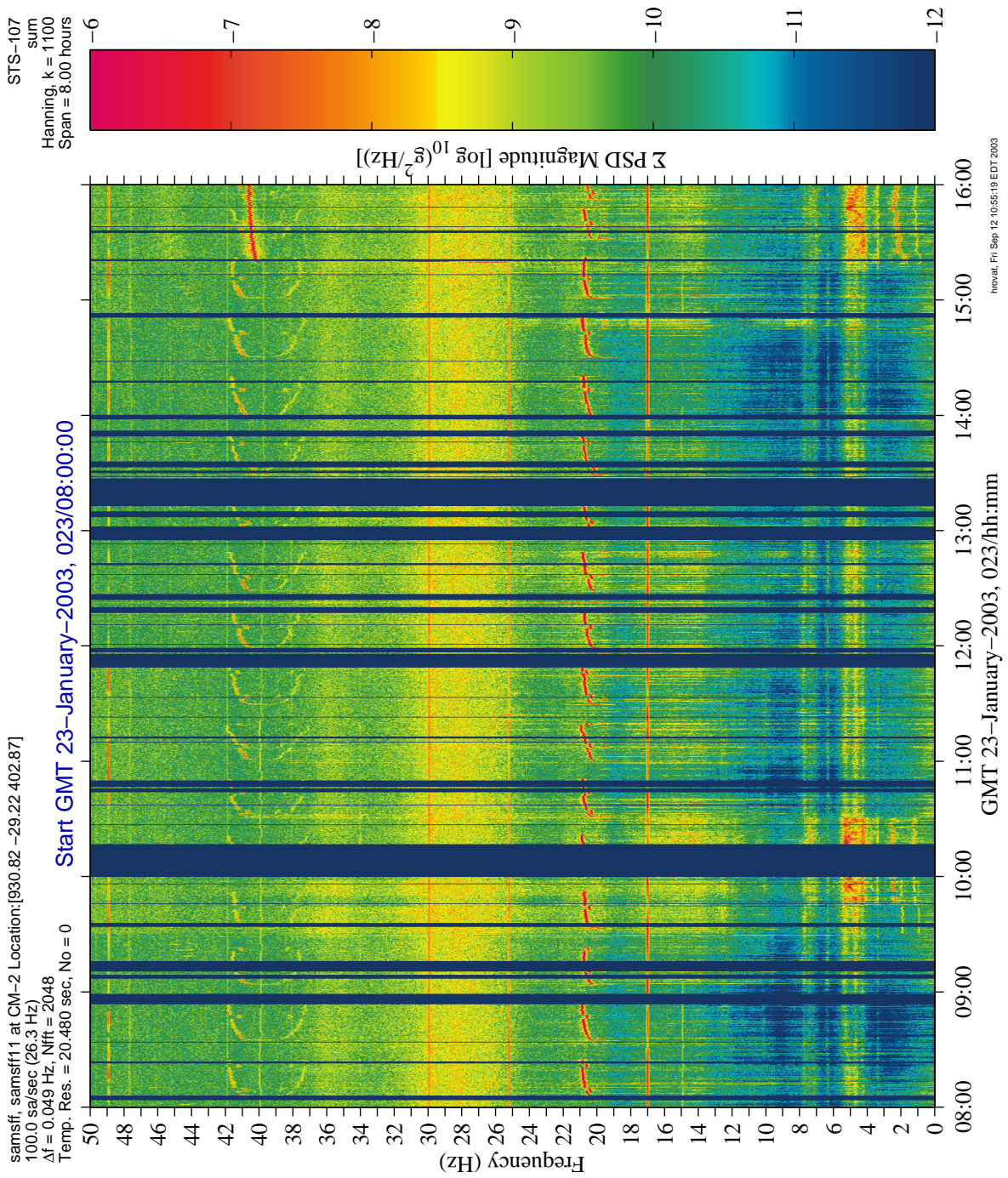


Figure 6.101 Spectrogram of VCD Equipment Operation Turn On

**PIMS STS-107 Mission Microgravity Environment Summary Report:
January 16 to February 1, 2003**

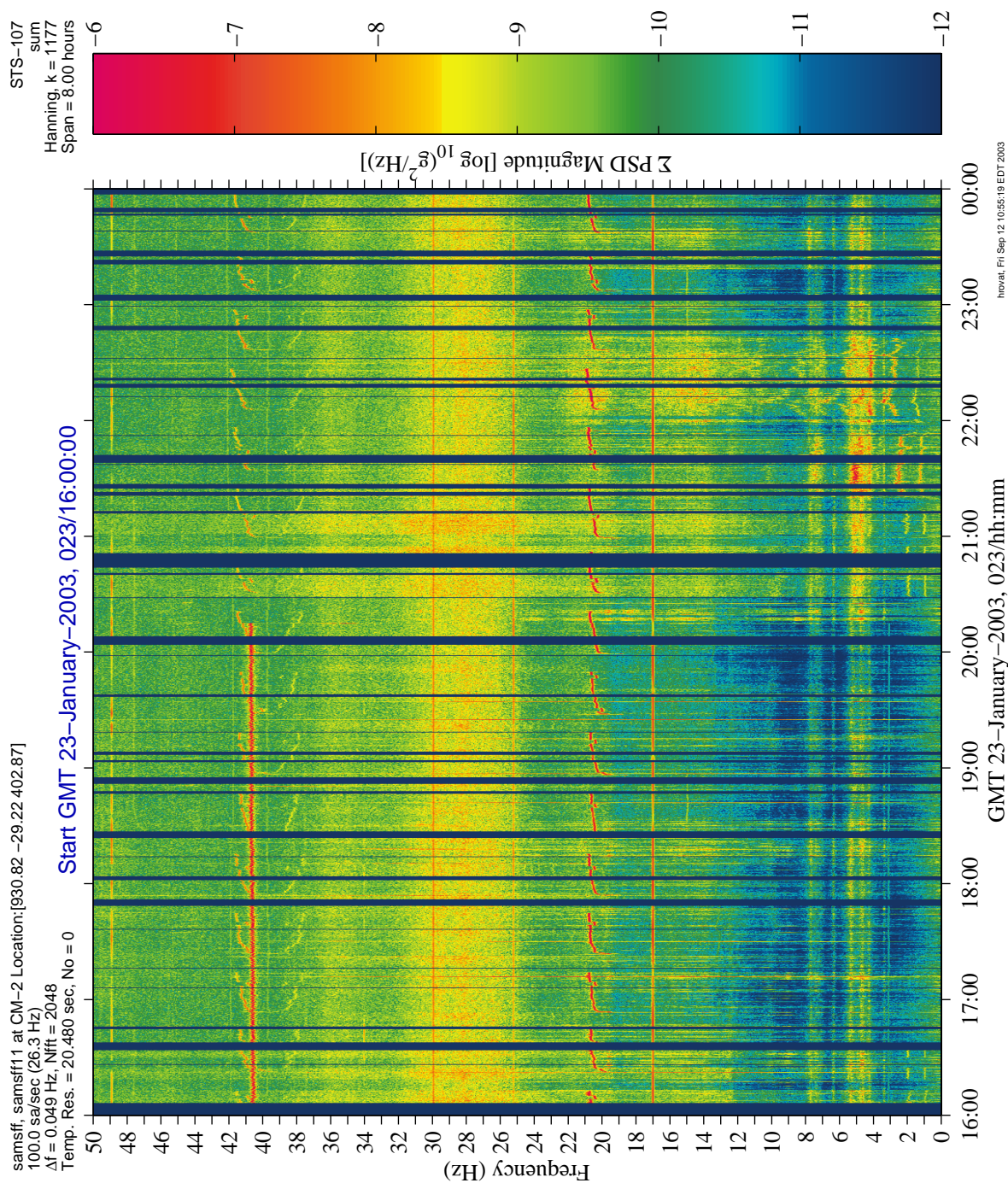


Figure 6.102 Spectrogram of VCD Equipment Operation Turn Off

**PIMS STS-107 Mission Microgravity Environment Summary Report:
January 16 to February 1, 2003**

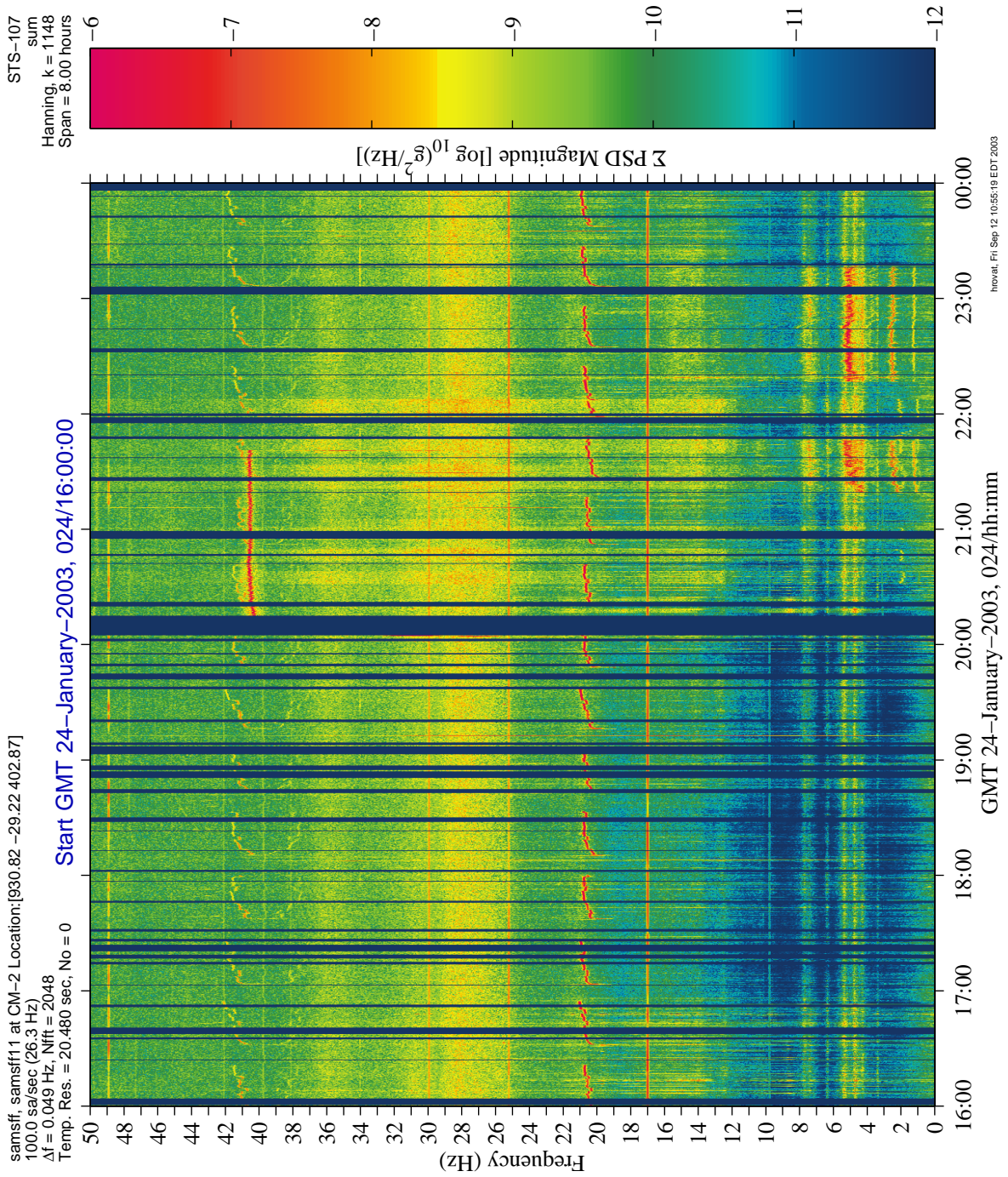


Figure 6.103 Spectrogram of VCD Equipment Operation On/Off

**PIMS STS-107 Mission Microgravity Environment Summary Report:
January 16 to February 1, 2003**

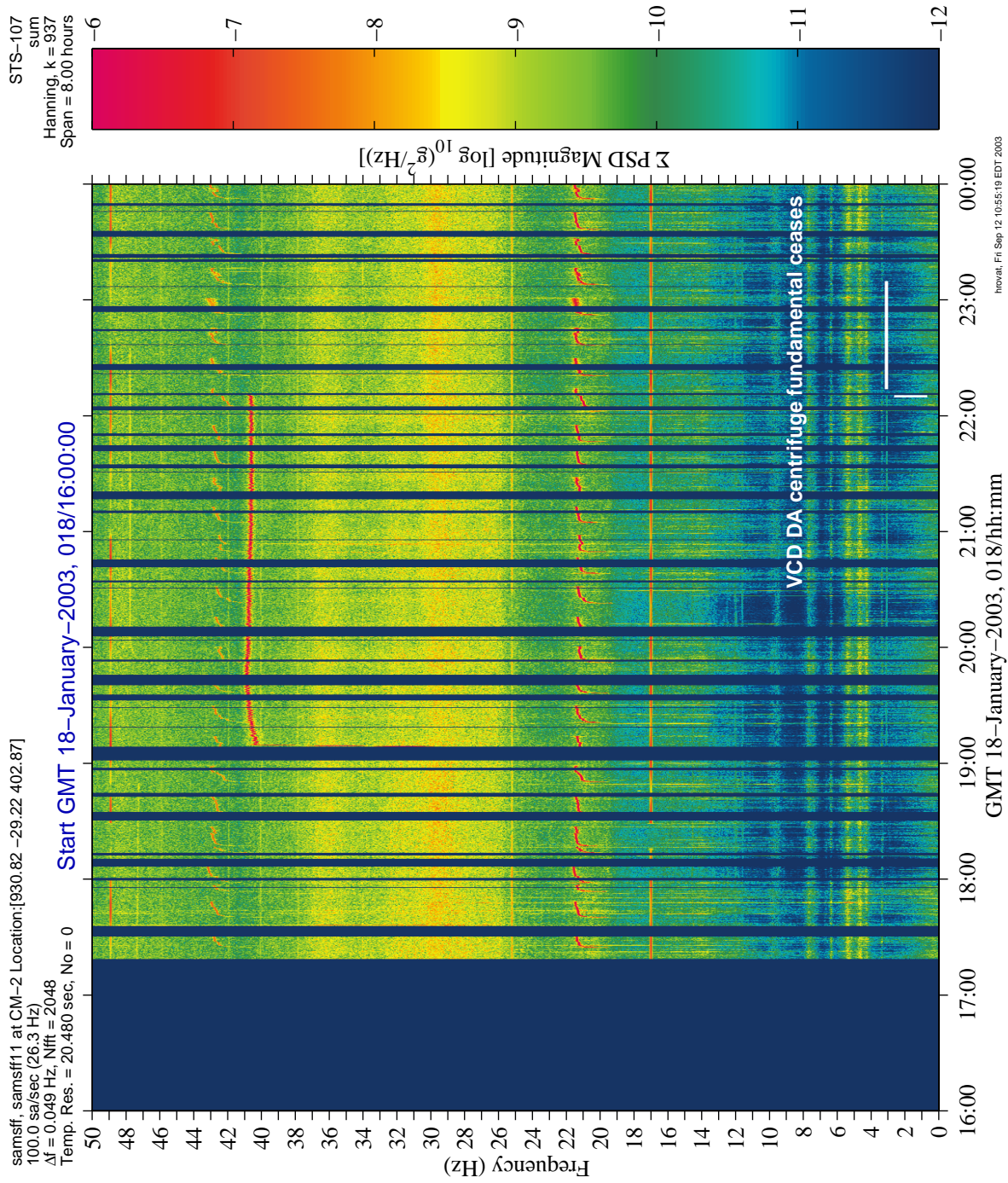


Figure 6.104 Spectrogram of Weak VCD Equipment Fundamental On/Off

**PIMS STS-107 Mission Microgravity Environment Summary Report:
January 16 to February 1, 2003**

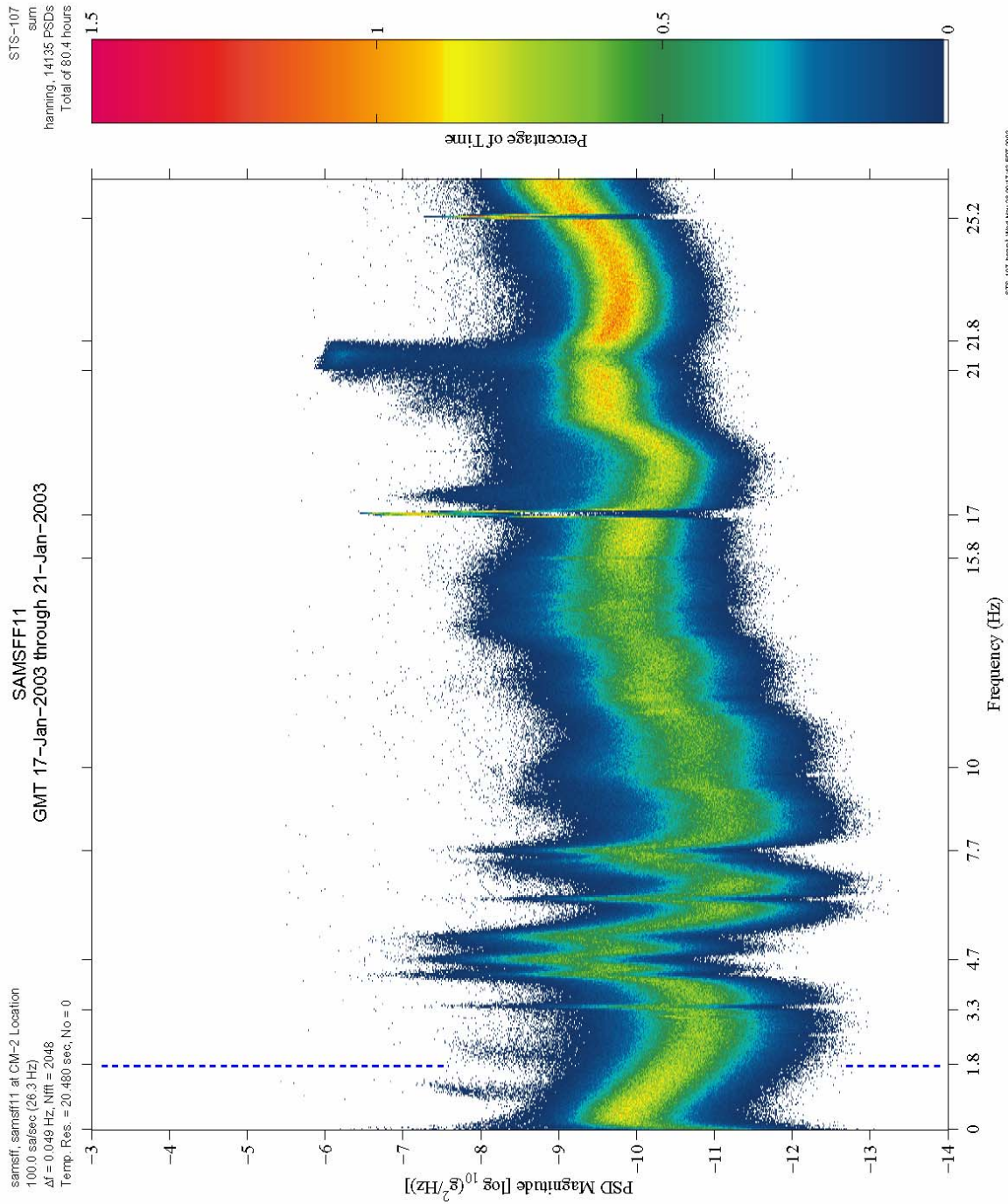


Figure 6.105 Principal Component Spectral Analysis for Biobox

PIMS STS-107 Mission Microgravity Environment Summary Report: January 16 to February 1, 2003

samsff, samsff11 at CM-2 Location:[930.82 -29.22 402.87]
0.1000 sa/sec (26.32 Hz)

MGM Experiment 04-D2

STS-107
STRUCTURAL[0.0 180.0 0.0]
Interval Minmax
Size: 10.00, Step: 10.00 sec.

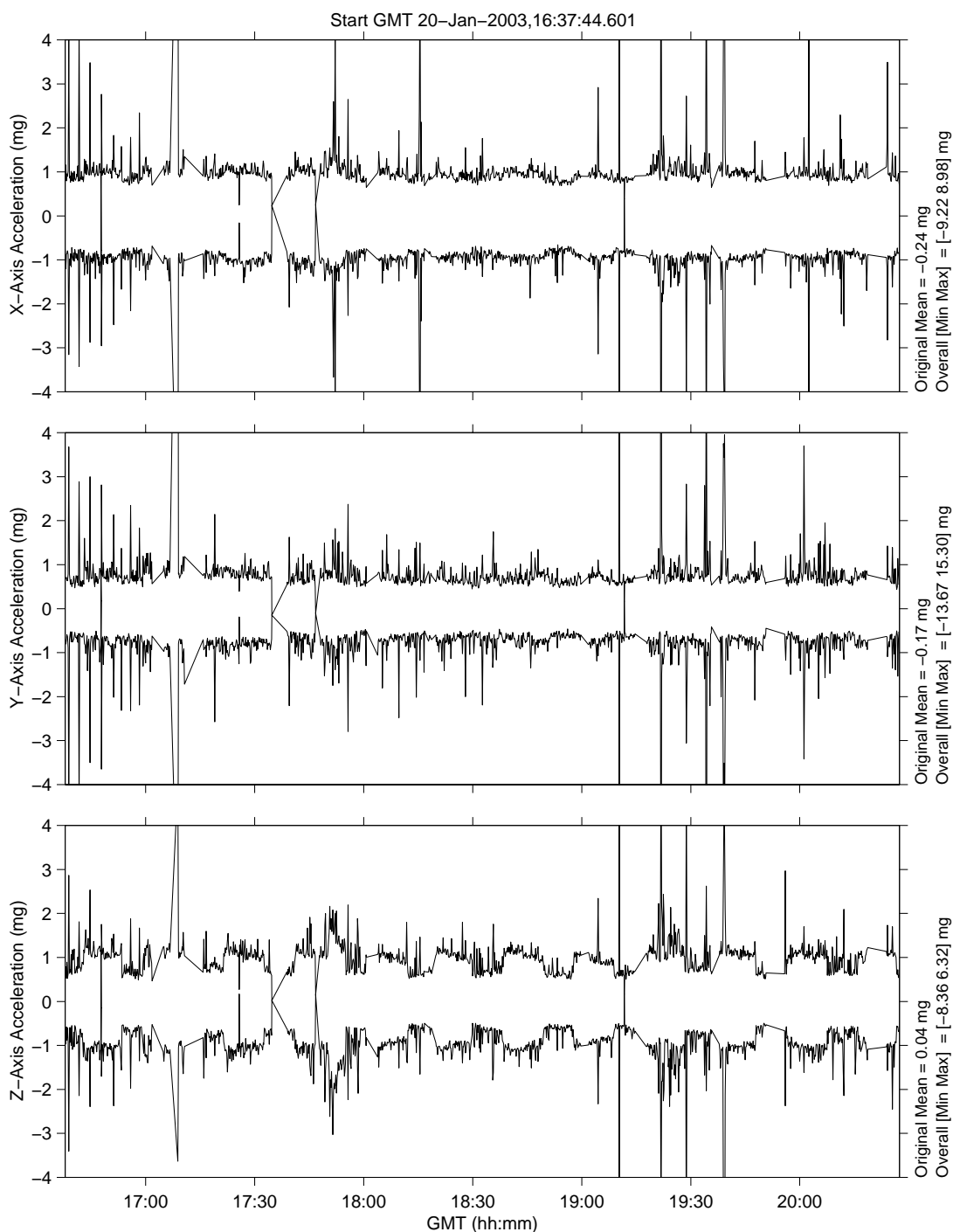


Figure 6.106 Interval Min/Max for MGM Experiment 04-D2

PIMS STS-107 Mission Microgravity Environment Summary Report: January 16 to February 1, 2003

samsff, samsff11 at CM-2 Location:[930.82 -29.22 402.87]
0.1000 sa/sec (26.32 Hz)

MGM Experiment 05-D3

STS-107
STRUCTURAL[0.0 180.0 0.0]
Interval Minmax
Size: 10.00, Step: 10.00 sec.

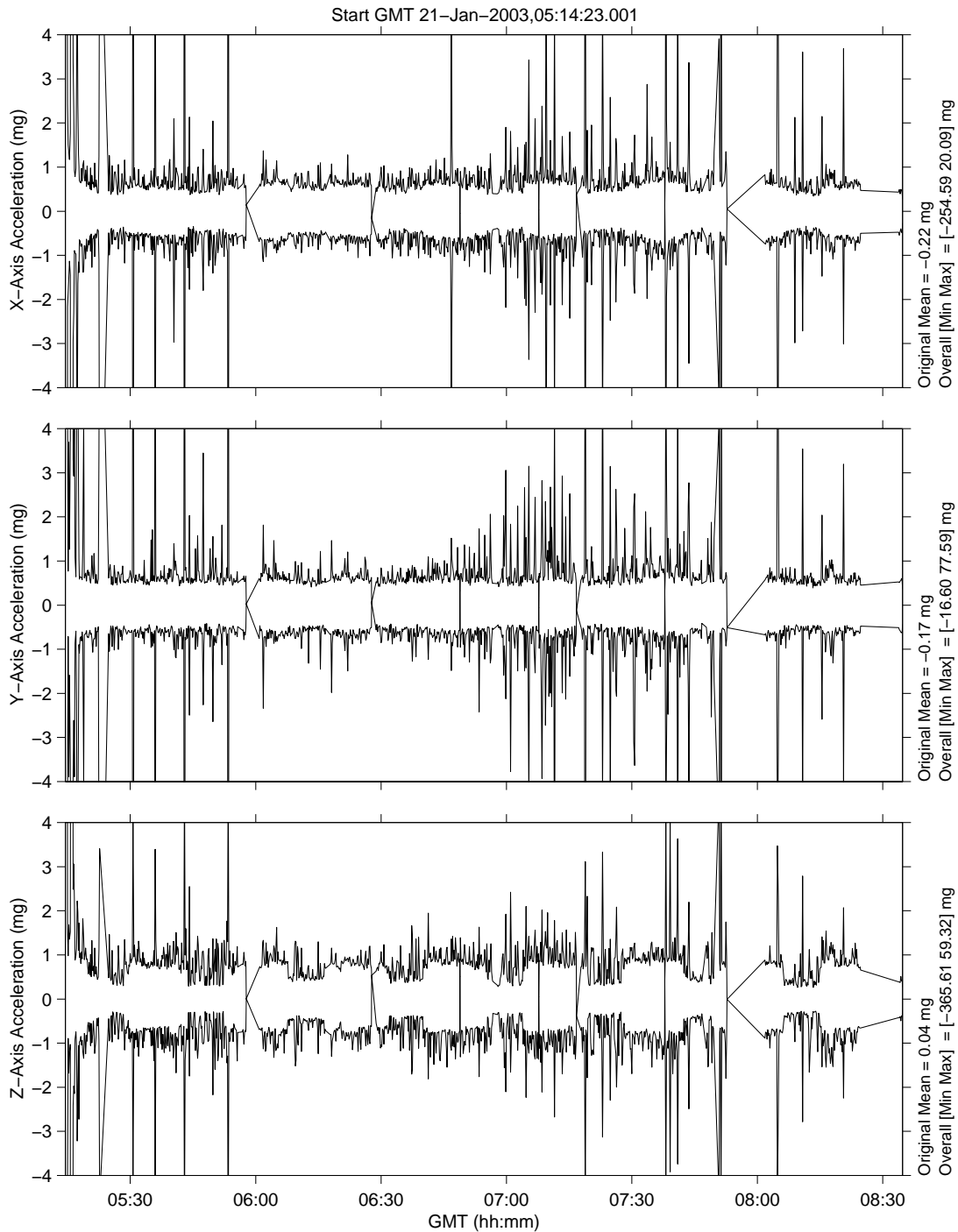


Figure 6.107 Interval Min/Max for MGM Experiment 05-D3

PIMS STS-107 Mission Microgravity Environment Summary Report: January 16 to February 1, 2003

samsff, samsff11 at CM-2 Location:[930.82 -29.22 402.87]
0.1000 sa/sec (26.32 Hz)

MGM Experiment 06-D4

STS-107
STRUCTURAL[0.0 180.0 0.0]
Interval Minmax
Size: 10.00, Step: 10.00 sec.

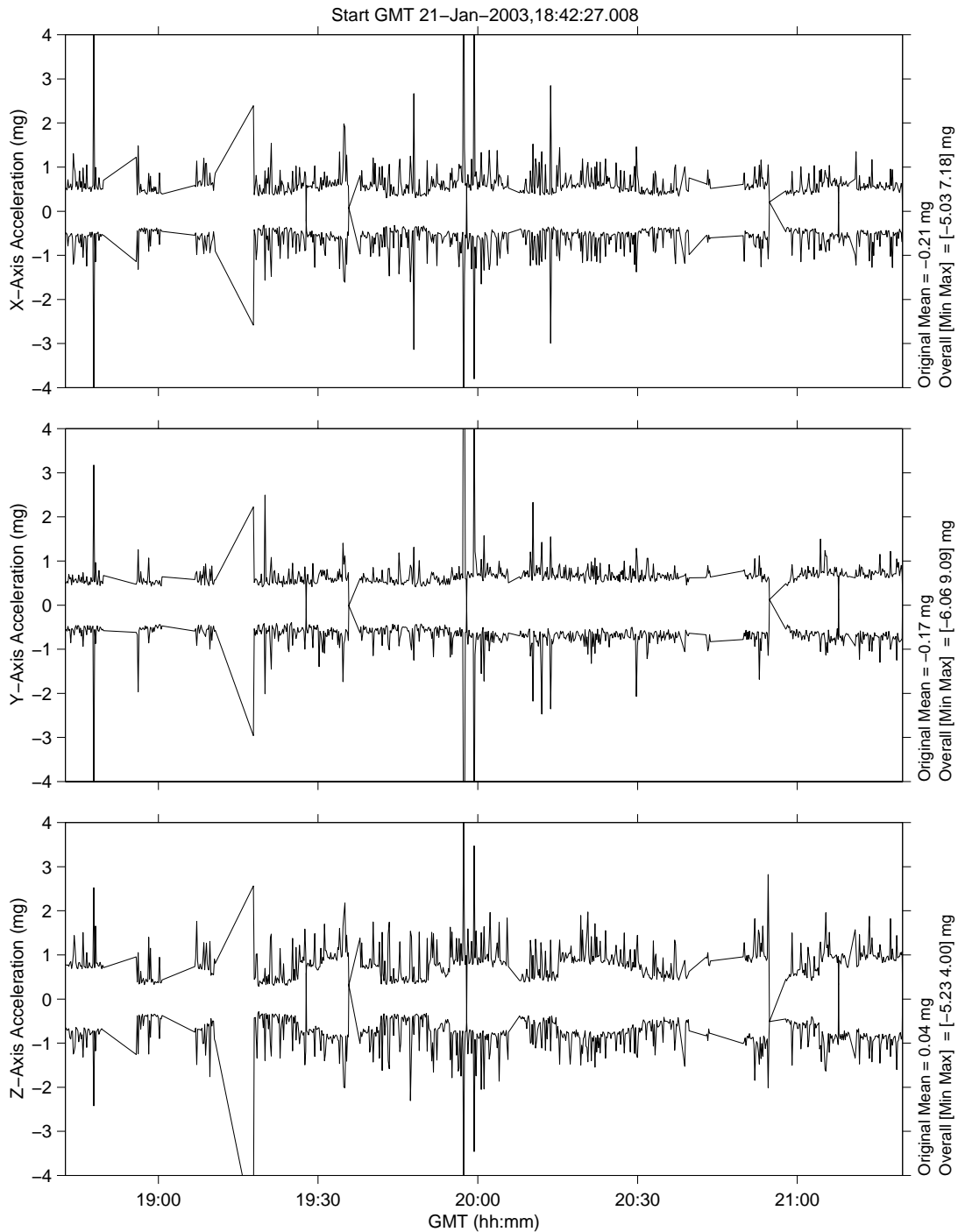


Figure 6.108 Interval Min/Max for MGM Experiment 06-D4

PIMS STS-107 Mission Microgravity Environment Summary Report: January 16 to February 1, 2003

samsff, samsff11 at CM-2 Location:[930.82 -29.22 402.87]
0.1000 sa/sec (26.32 Hz)

MGM Experiment 09-D5

STS-107
STRUCTURAL[0.0 180.0 0.0]
Interval Minmax
Size: 10.00, Step: 10.00 sec.

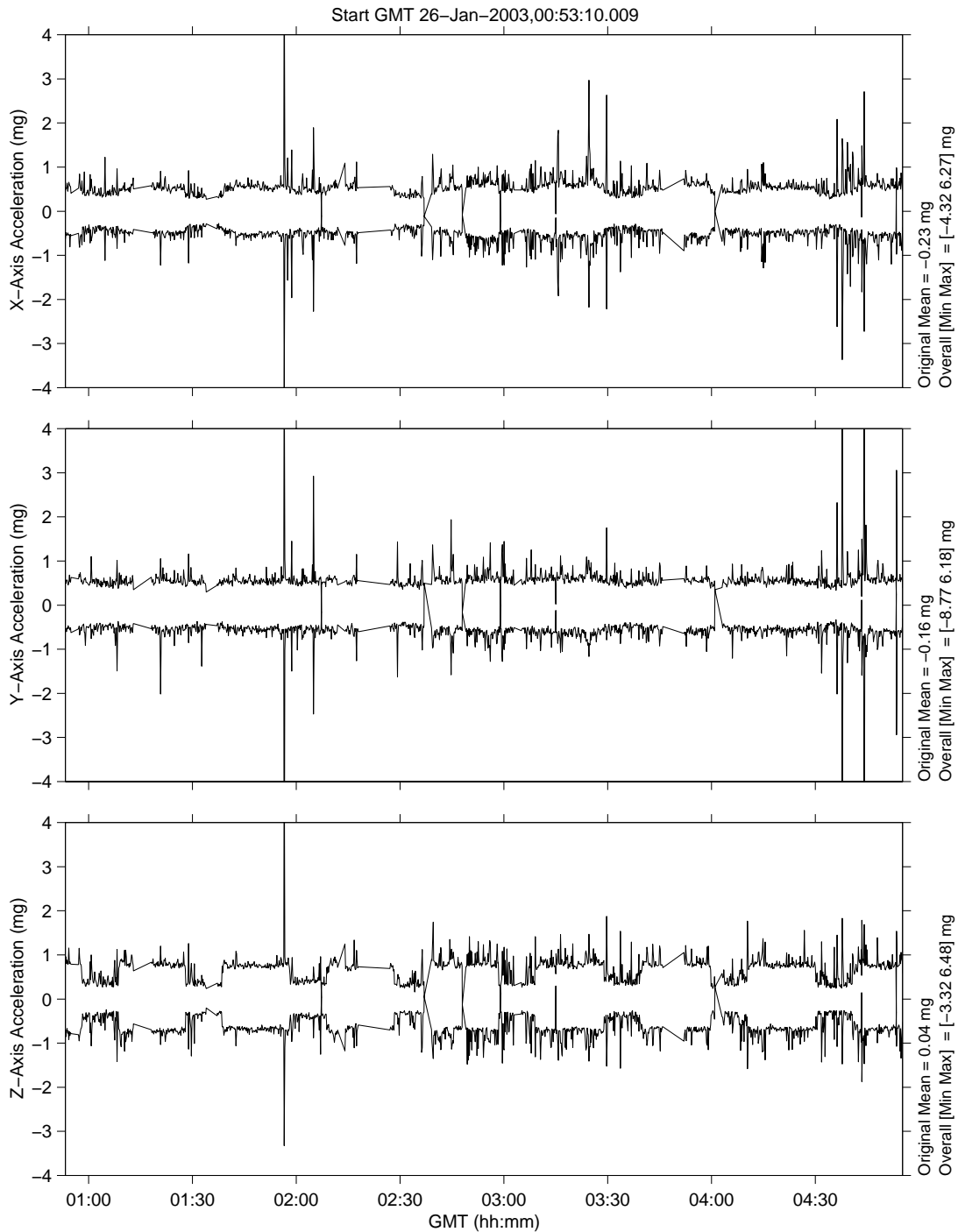


Figure 6.109 Interval Min/Max for MGM Experiment 09-D5

PIMS STS-107 Mission Microgravity Environment Summary Report: January 16 to February 1, 2003

samsff, samsff11 at CM-2 Location:[930.82 -29.22 402.87]
0.1000 sa/sec (26.32 Hz)

MGM Experiment 10-D6

STS-107
STRUCTURAL[0.0 180.0 0.0]
Interval Minmax
Size: 10.00, Step: 10.00 sec.

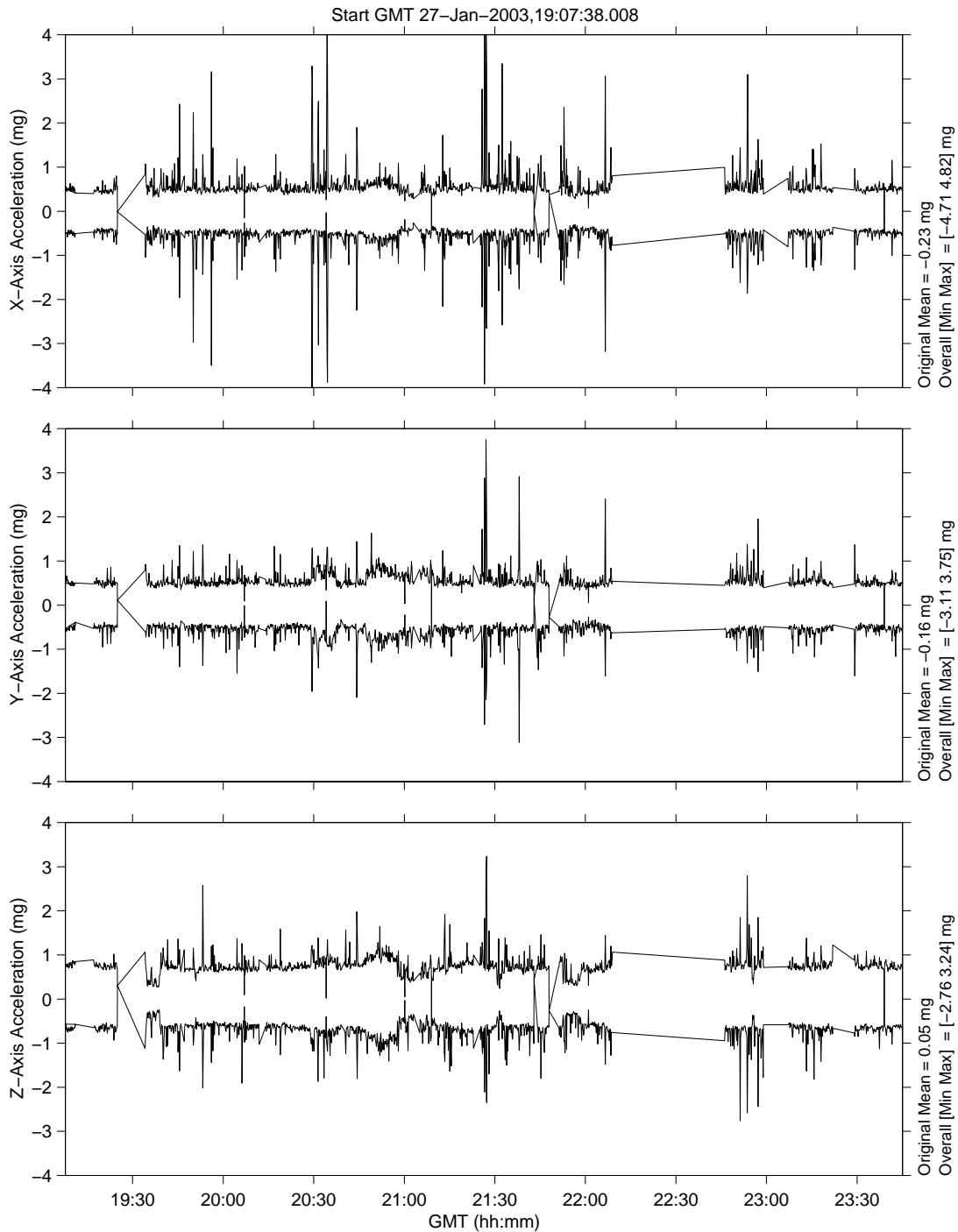


Figure 6.110 Interval Min/Max for MGM Experiment 10-D6

PIMS STS-107 Mission Microgravity Environment Summary Report:
January 16 to February 1, 2003

STS-107
sum
Hanning, k = 3359
Span = 24.01 hours

SAMSFF11, 16.93 < f < 17.13 Hz
Start GMT 23-January-2003, 023/00:00:00

samsff, samsff11 at CM-2 Location
100.0 sav/sec (26.3 Hz)
 $\Delta f = 0.049$ Hz; Nfft = 2048
Temp. Res. = 20.480 sec, No = 0

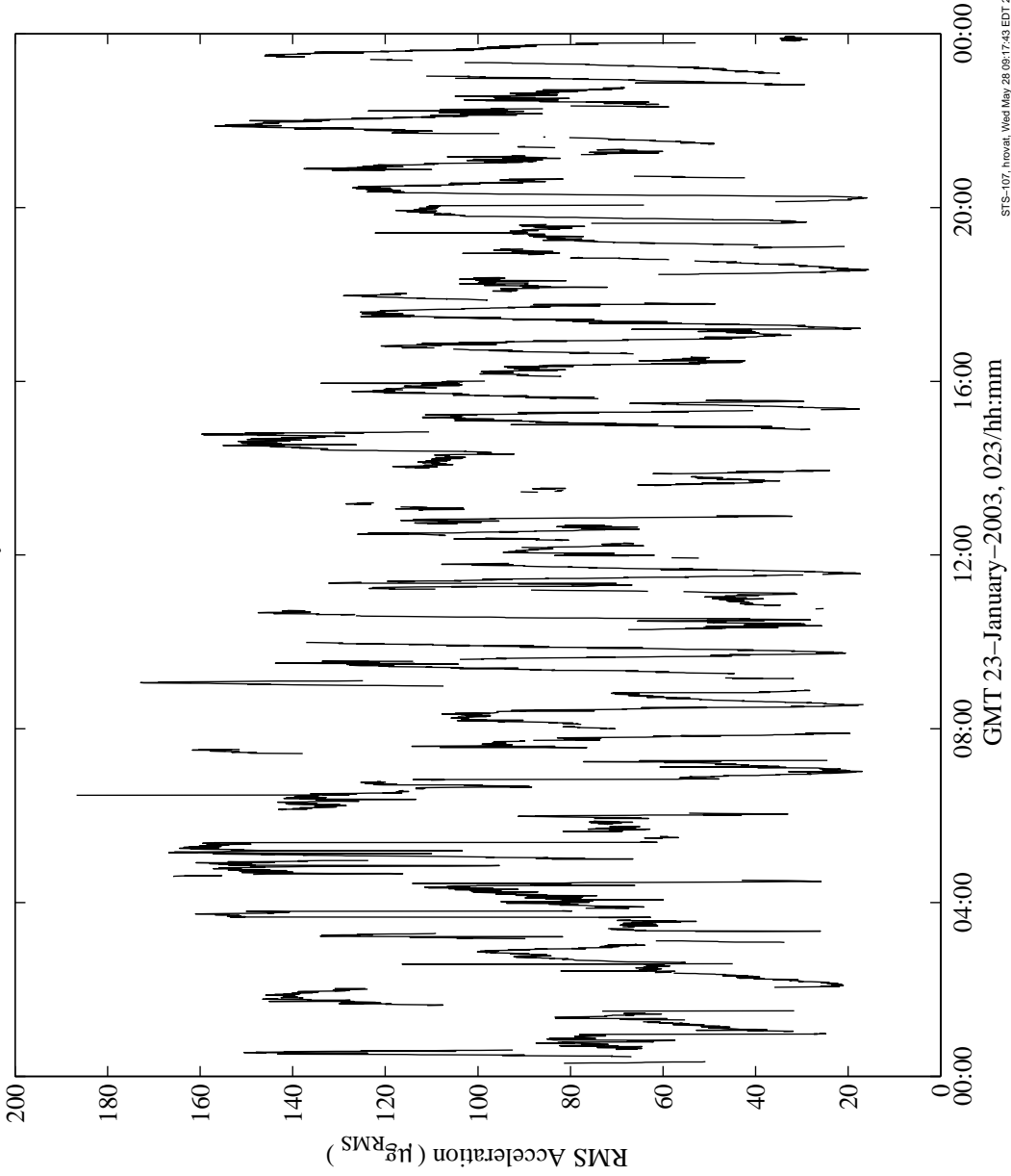


Figure 6.111 Interval RMS of Ku-Band Antenna Dither

**PIMS STS-107 Mission Microgravity Environment Summary Report:
January 16 to February 1, 2003**

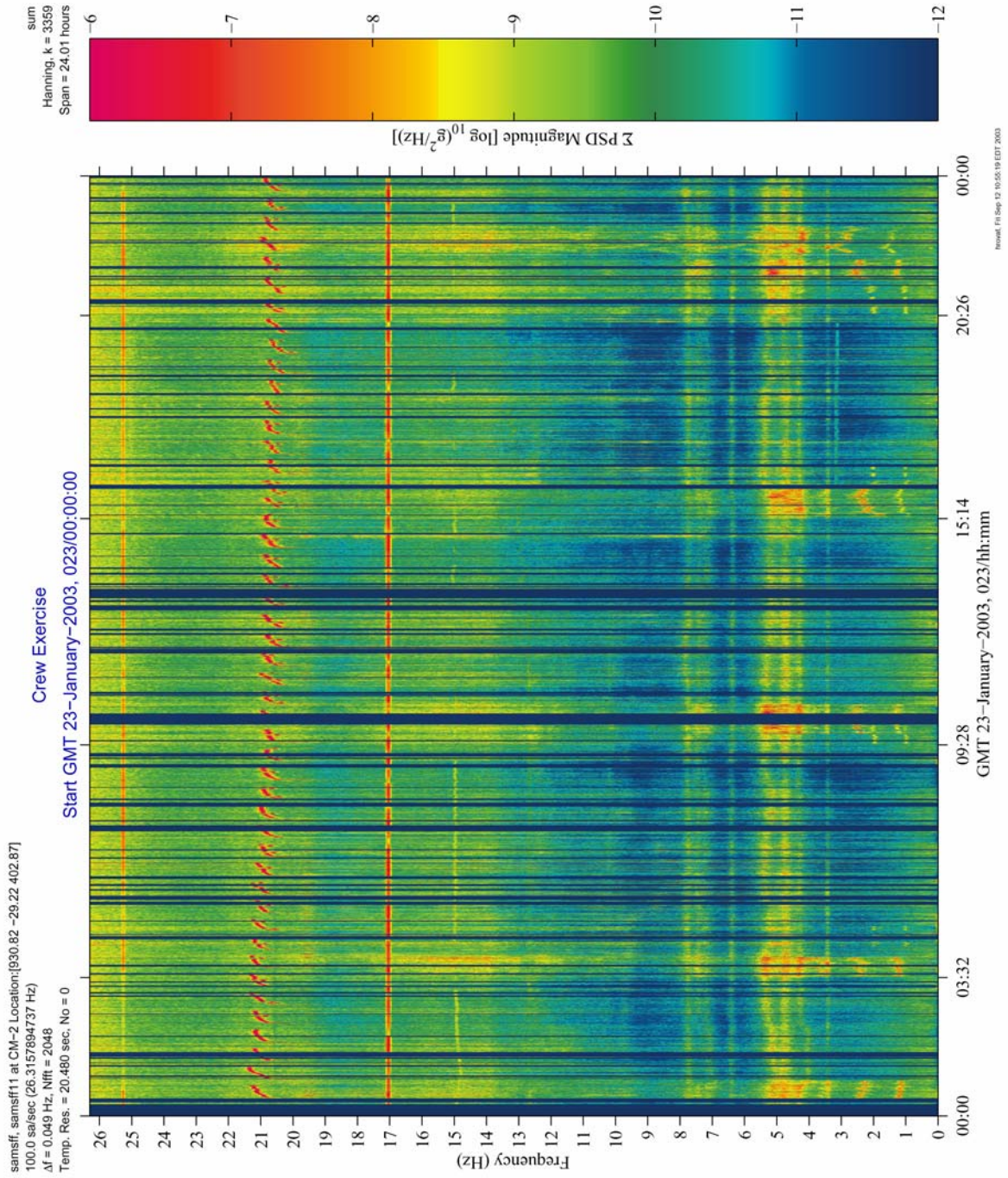


Figure 6.112 Spectrogram of 24-Hour Span with Crew Exercise Periods

**PIMS STS-107 Mission Microgravity Environment Summary Report:
January 16 to February 1, 2003**

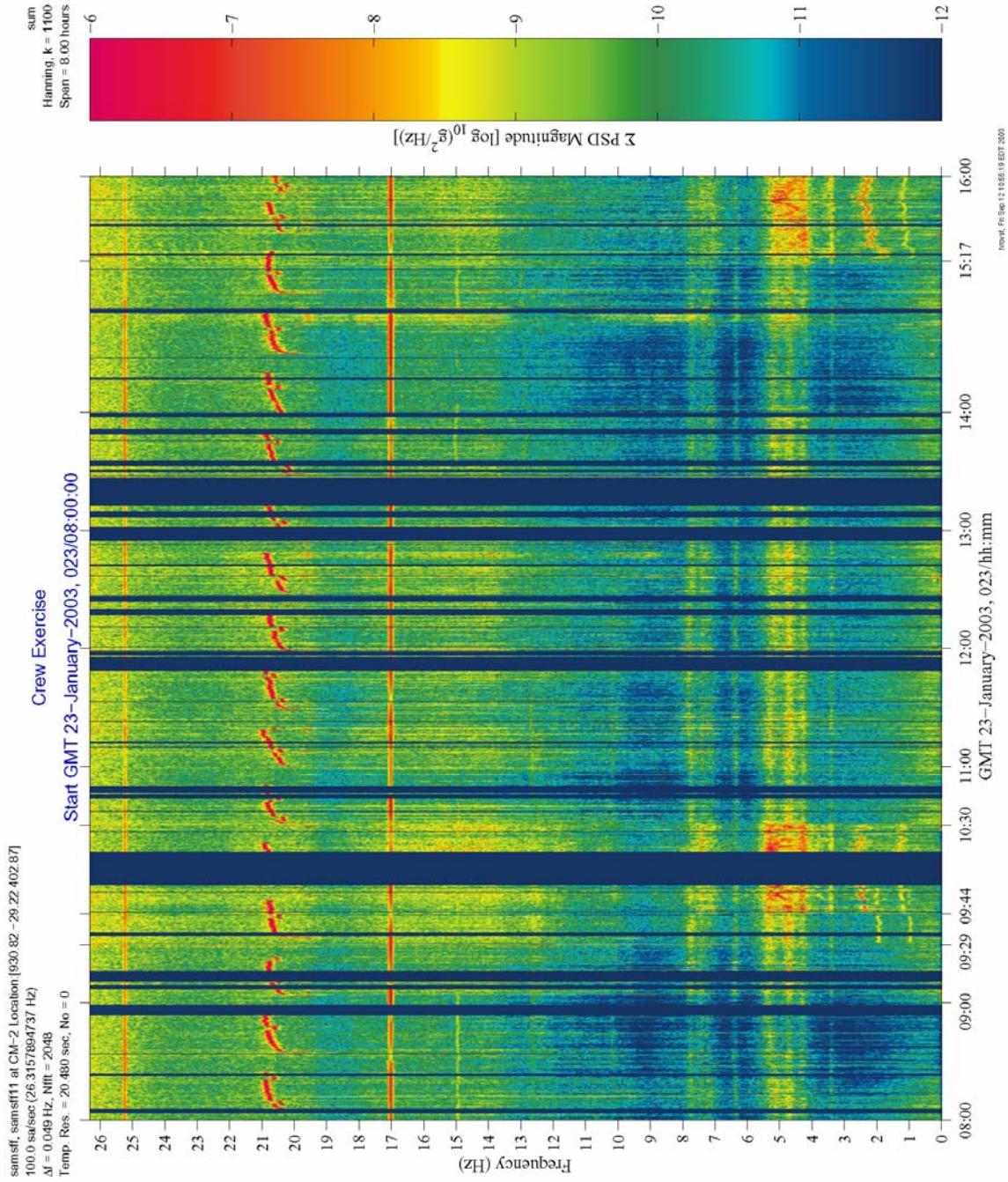


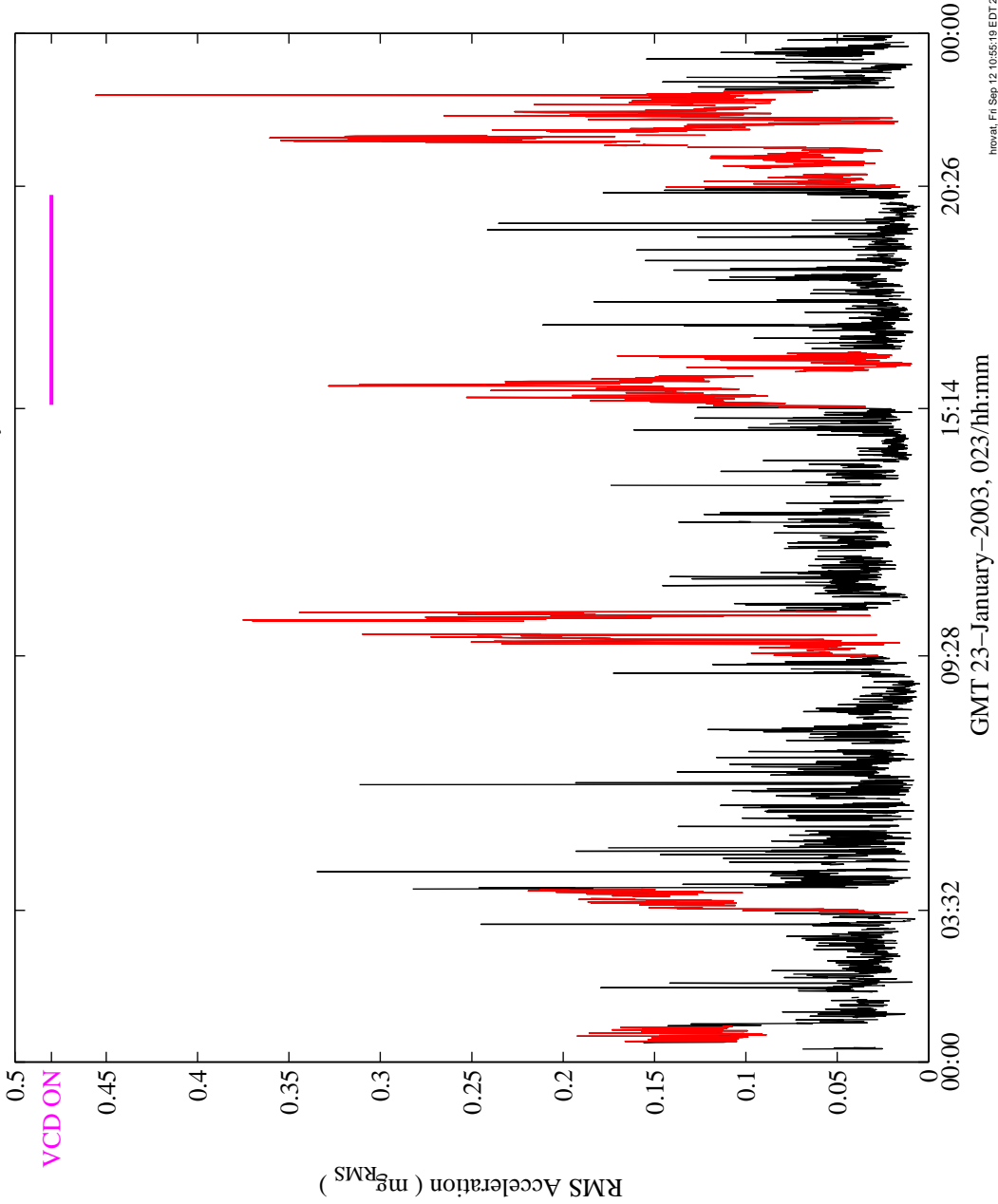
Figure 6.113 Spectrogram of 8-Hour Span with Crew Exercise Periods

**PIMS STS-107 Mission Microgravity Environment Summary Report:
January 16 to February 1, 2003**

STS-107
sum
Hanning, k = 3359
Span = 24.01 hours

samsff, samsff11 at CM-2 Location:[930.82 -29.22 402.87]
100.0 sav/sec (26.3 Hz)
 $\Delta f = 0.049$ Hz; Nfft = 2048
Temp. Res. = 20.480 sec; No = 0

Crew Exercise, 0 < f < 6 Hz
Median RMS: 0.11 mg During Exercise, 0.03 mg Without Exercise
Start GMT 23-January-2003, 023/00:00:00



Novatel, Fri Sep 12 10:55:18 EDT 2003

Figure 6.114 Interval RMS of 24-Hour Span with Crew Exercise Periods

**PIMS STS-107 Mission Microgravity Environment Summary Report:
January 16 to February 1, 2003**

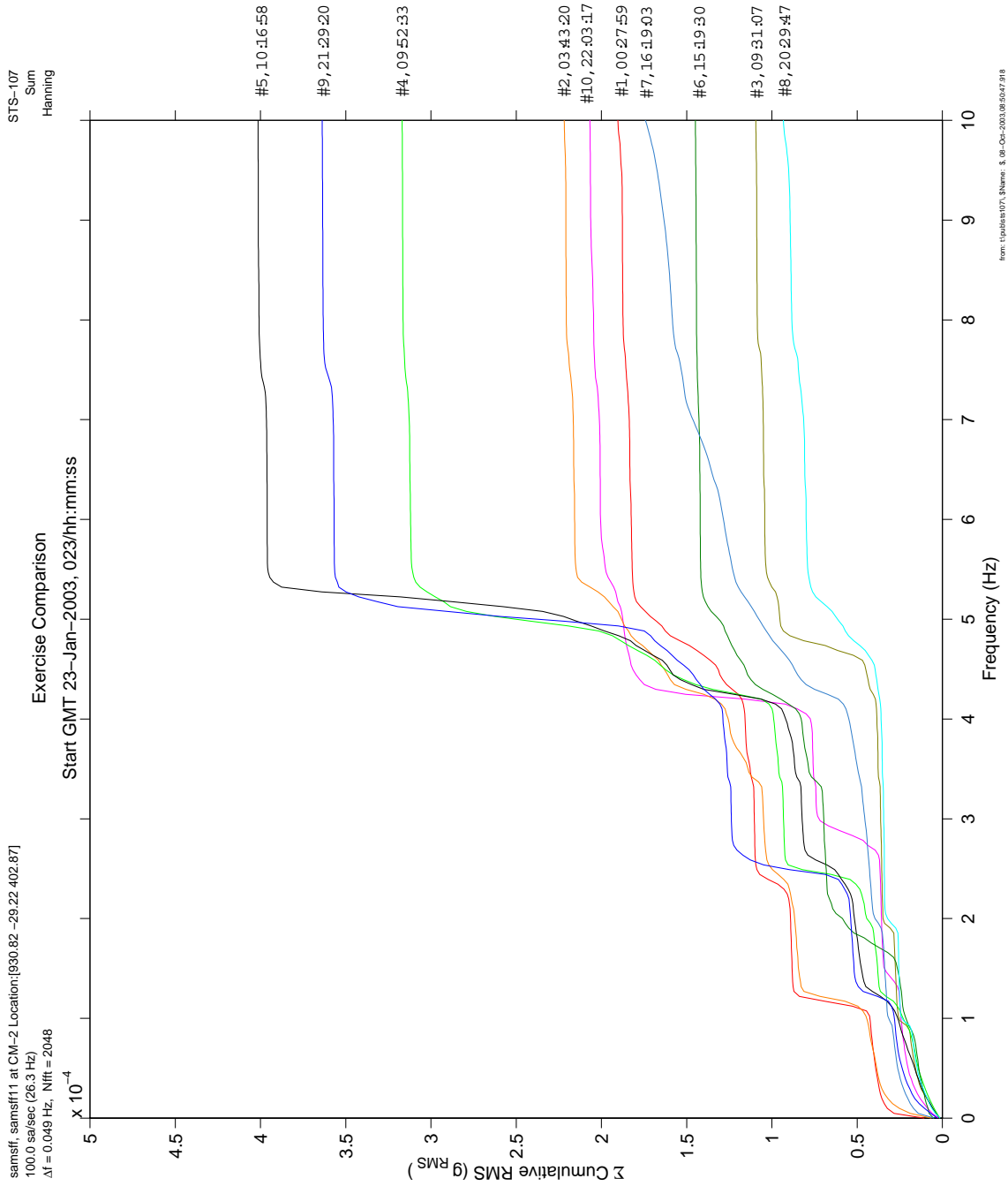


Figure 6.115 Cumulative RMS vs. Frequency Of Crew Exercise Periods In 24-Hour Span

**PIMS STS-107 Mission Microgravity Environment Summary Report:
January 16 to February 1, 2003**

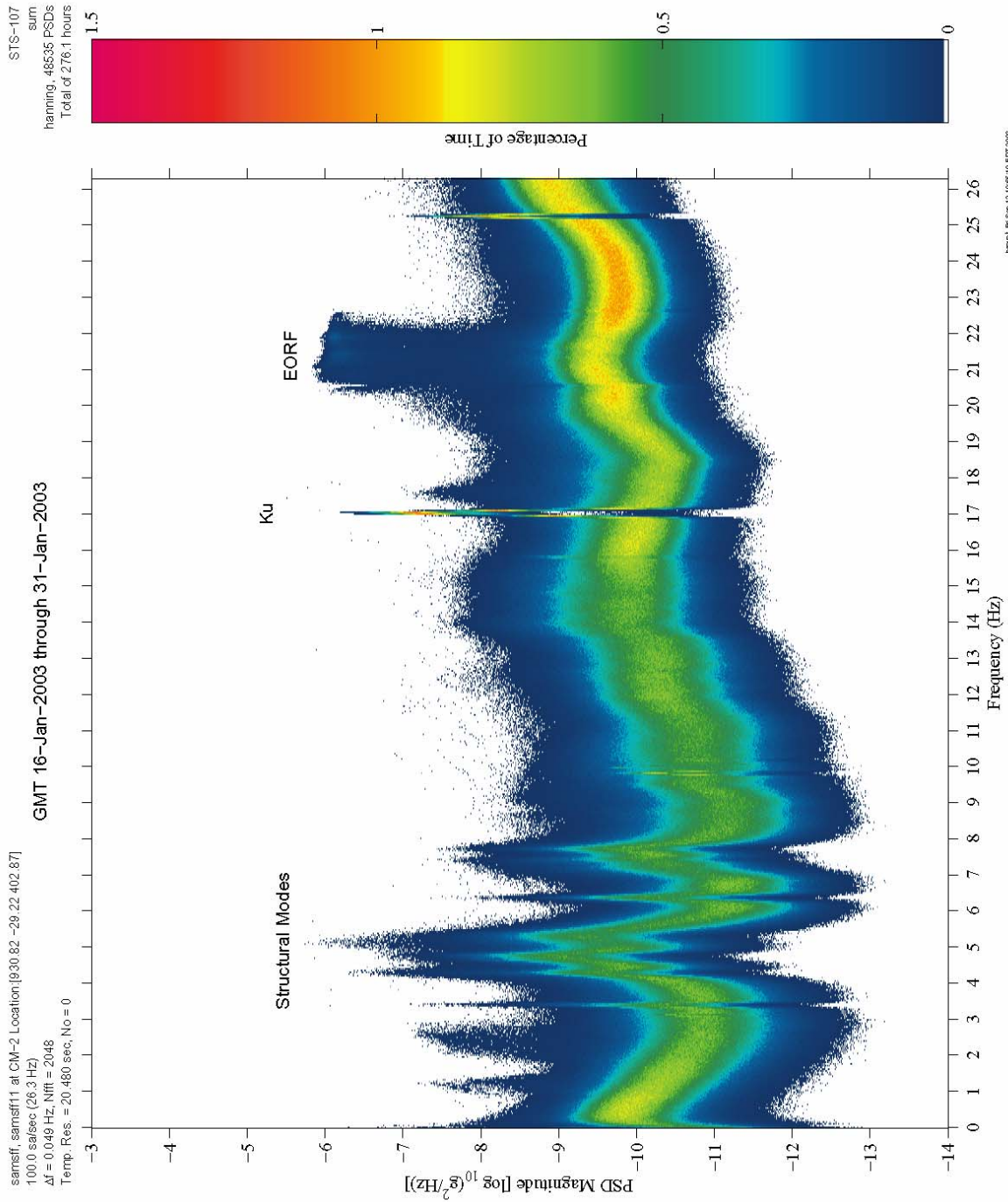


Figure 6.116 Principal Component Spectral Analysis

**PIMS STS-107 Mission Microgravity Environment Summary Report:
January 16 to February 1, 2003**

7 Summary of the STS-107 Mission Analysis

The acceleration data collected during the 16-day span of the STS-107 dual shift mission was analyzed and presented in this report for the two accelerometer systems, SAMS-FF and OARE, that flew onboard the Columbia Orbiter on January 16th 2003 from the Kennedy Space Center, Florida. The analysis was performed by the PIMS project, at NASA Glenn Research Center, Cleveland, Ohio, for two regimes: quasi-steady and vibratory.

The quasi-steady regime was dominated, as expected, by the orbiter attitudes, venting operations and crew activity. The vibratory, on the other hand, was dominated by crew exercise, experiment operations (i.e., start-ups, on-going operations and shutdowns), vehicle subsystem operations and crew life support systems. And, of course, some transient effects were noticeable. They were caused by crew locomotion, crew interaction with some experiments, thruster firings for vehicle attitude control, maintenance and maneuvers.

Specific analyses were performed for the experiments that PIMS directly supported during the 16-day mission in order to characterize the reduced gravity environment in which these experiments were performed. These analyses were performed for SOFBALL, LSP, *Mist*, MGM as well as VCD-FE, even though PIMS did not directly support VCD-FE. In addition to these specific analyses, the overall reduced gravity environment for the STS-107 mission was analyzed for the benefit of the other experiments.

For more detail, see the applicable technical narrative sections of this report. Also, and most importantly, if this report does not include specific analysis for a particular event that could have facilitated the correlation of your science data with the acceleration data, then please contact PIMS via email at pimsops@grc.nasa.gov for further assistance.

**PIMS STS-107 Mission Microgravity Environment Summary Report:
January 16 to February 1, 2003**

8 References

1. Hamacher, H., Fluid Sciences and Materials Science in Space, Springer-Verlag, 1987.
2. STS-107 Shuttle Press Kit: Providing 24/7 Space Science Research—STS-107, Boeing/NASA/United Space Alliance, December 16, 2002
3. STS-107: Space Research and You—Mission Highlights Human Health Experiments: Overview of STS-107 Mission and Key Research, NASA
4. Milton E. Moskowitz et al., Summary Report of Mission Acceleration Measurements for MSL-1: STS-83 and STS-94, NASA/TM-1998-206979, May 1998
5. James E. Rice., OARE STS-94 (MSL-1R) Final Report, OARE Technical Report # 151—Contract NAS3-26556, Canopus Systems, Inc., August 1997
6. SOFBALL-2 Fact Sheet, M-0723-13, NASA Glenn Research Center, June 2002
7. Ronney, P. D., Combustion and Flame, Vol. 82, 1990, pp. 1-14
8. Buckmaster, J. D., Joulin, G., and Ronney, P. D., Combustion and Flame, Vol. 79, 1990, pp. 381-392; Ibid, Combustion and Flame, Vol. 84, 1991, pp. 411-422
9. Ronney, P. D., Wu, M. S., Pearlman, H. G., and Weiland, K. J., AIAA Journal, Vol. 36, 1998, pp. 1361-1368
10. Private conversation with Dr. Ronney – for more information contact Dr. Ronney P. D at ronney@usc.edu
11. K. Hrovat and K. McPherson, “Summary Report of Mission Acceleration Measurements for STS-89”, NASA TM 1999-209084, June 1999, pp. 9-10
12. E. P. Cunningham, *Digital Filtering: An Introduction* (Boston, MA: Houghton Mifflin Company, 1992), Chap. 3
13. M. Rogers, K. Hrovat, K. McPherson, and R. DeLombard, “Summary Report of Mission Acceleration Measurements for STS-87”, NASA TM-1999-208647, January 1999, pp. 9-11.
14. M. Rogers and R. DeLombard, “Summary Report of Mission Acceleration Measurements for STS-65”, NASA TM-106871, March 1995.

**PIMS STS-107 Mission Microgravity Environment Summary Report:
January 16 to February 1, 2003**

15. R. Hakimzadeh, K. Hrovat, K. McPherson, M. Moskowitz, and M. Rogers, "Summary Report of Mission Acceleration Measurements for STS-78", NASA TM-107401, January 1997.
16. M. Rogers, M. Moskowitz, K. Hrovat, and T. Reckart, "Summary Report of Mission Acceleration Measurements for STS-79", NASA CR-202325, March 1997.
17. P. Tschen, K. Hrovat, K. McPherson, M. Moskowitz, M. Nati, and T. Reckart, "A Summary of the Quasi-Steady Acceleration Environment On-Board STS-94", NASA TM-1999-208853, February 1999.
18. R. DeLombard, "Compendium of Information for interpreting the Microgravity Environment of the Orbiter Spacecraft", NASA TM-107032, 1996.
19. Personal e-mail from K. Jules to K Hrovat, June 16, 2003.

**PIMS STS-107 Mission Microgravity Environment Summary Report:
January 16 to February 1, 2003**

9 Appendix A. Acronym List and Definition

ACRONYM	DEFINITION
AM	Ante Meridiem
CCD	Charge-Coupled Device
CDU	Control and Data acquisition Unit
CM	Combustion Module; Center of Mass
CST	Central Standard Time
DA	Distillation Assembly
DC	Direct Current
EMS	Experiment Mounting Structures
EORF	Enhanced Orbiter Refrigerator/Freezer
ESE	Experiment Support Engineer
FCPA	Fluids Control Pump Assembly
FOG	Fiber optic Gyroscope
FREESTAR	Fast Reaction Experiments Enabling Science, Technology, Applications and Research
g	nominal gravitational acceleration at Earth's surface (9.81 m/s ²)
GMT	Greenwich Mean Time
GRC	Glenn Research Center
HRM	High Rate Multiplexer
Hz	Hertz
INCO	Instrumentation and Communications Officer
ISS	International Space Station
JSC	Johnson Space Center
KSC	Kennedy Space Center
LOS	Loss of Signal
LSP	Laminar Soot Processes
LVLH	Local Vertical Local Horizontal
MEP	Microgravity Environment Program
mg	milli-g, 1 x 10 ⁻³ g
<i>Mist</i>	Water Mist Fire-Suppression Experiment
MGM	Mechanics of Granular Materials
MSFC	Marshall Space Flight Center
MSL	Microgravity Science Laboratory
NASA	National Aeronautics and Space Administration
OARE	Orbital Acceleration Research Experiment
OBPR	Office of Biological and Physical Research
ODRC	Operational Data Retrieval Complex
PAD	PIMS Acceleration Data
PAH	Polycyclic Aromatic Hydrocarbons
PAO	Public Affairs Office
PCSA	Principal Component Spectral Analysis
PDR	Payload Data Recorder
PI	Principal Investigator
PIMS	Principal Investigator Microgravity Services

**PIMS STS-107 Mission Microgravity Environment Summary Report:
January 16 to February 1, 2003**

POCC	Payload Operation Control Center
PRCS	Primary Reaction Control System
PSD	Power Spectral Density
RDM	Research Double Module
RMS	Root-Mean-Square
RSS	Root-Sum-of-Squares
SAMS-FF	Space Acceleration Measurement System for Free Flyers
SOFBALL	Structure of Flame Balls at Low Lewis-number
STS	Space Transportation System
TMF	TrimMean Filter
TSH	Triaxial Sensor Head
μg	micro-g, $1 \times 10^{-6}\text{g}$
VCD-FE	Vapor Compression Distillation Flight Experiment
VRCS	Vernier Reaction Control System